

Pharmacokinetic interactions: the effect of herbal extracts and supplements on drug permeation

C. Jacobsz



orcid.org/0000-0001-7857-6489

B.Pharm

Dissertation submitted in fulfilment of the requirements for the degree *Magister Scientiae* in *Pharmaceutics* at the Potchefstroom Campus of the North-West University

Supervisor:

Dr JD Steyn

Co-supervisor:

Prof JH Hamman

Graduation May 2018

Student number: 22743960

ACKNOWLEDGEMENTS

~You must do the things you think you cannot do~ Eleanor Roosevelt

Undertaking this master's degree took a lot of sacrifice and self-discipline. It wasn't only me that felt the pressure that such a mammoth task requires but also my family and friends. But before I thank them I would like to thank my *Heavenly Father* for I would not have been able to even think about finishing without His guidance. I will always be grateful to Him for He has been the answer to so many unanswered questions. Life is complicated enough, simplifying it is the real challenge.

Secondly, I would like to thank my family and friends. I would like to thank my father for making me the person that I am today. I would also like to thank my brothers, Zach and Marnus, for always putting a smile on my face. To my friends that have really become my family and pillar of strength, Carmen, Anja, Zenobia, Chantelle, Alandi, there are simply no words to describe what you mean to me and I will always be grateful to each and every one of you.

I would also like to thank Dr. Steyn and Prof. Sias for always listening to me and being calm when I wasn't. Without your patience and wisdom this project would not have been what it is today. These two years was a rollercoaster but I would not have been able to climb off if it wasn't for your support and for that I will be forever grateful. I would also like to thank the North-West University for my student bursary and helping me to make a dream come true.

Lastly, but not the least, mom I did this for you. I miss you every single day and will never forget your smile and light that you bestowed onto this world. May your soul R.I.P.

ABSTRACT

The surge in popularity to treat illnesses with a more holistic approach is causing growing concern due to the increasing occurrence of adverse reactions, which are the result of interactions due to the concomitant use of herbal medicine and/or supplements with Western medicines. The modulating effects that herbal medicines and/or supplements can have on the pharmacokinetics of concomitantly administered allopathic drugs have recently captured the attention of both researchers and medical practitioners. During this study, emphasis was placed on the investigation of the potential membrane modulating effects of four selected herbal extracts (i.e. *Vitis vinifera* seed, *Hoodia gordonii*, *Harpagophytum procumbens*, *Leonotis leonurus*) and one supplement (i.e. methylsulfonylmethane) on the intestinal epithelial permeation of a model compound. The permeation modulating effects of the selected herbal extracts and supplement were evaluated with Rhodamine 123 (RH-123), which is a known substrate of the active efflux transporter, P-glycoprotein (P-gp).

The bi-directional transport of RH-123 was measured in the presence and absence of the selected herbal extracts/supplement across excised pig jejunum tissues using a Sweetana-Grass diffusion chamber apparatus. Samples of 180 μ l were withdrawn every 20 min over a period of 2 h. A validated fluorescence spectroscopic method on a Spectramax Paradigm[®] plate reader was employed to analyse the experimental samples to determine the RH-123 concentration in each sample. A Lucifer yellow (LY) transport study was performed to prove that the technique employed in mounting the excised pig jejunum tissue was not detrimental to the integrity and viability of the tissue. All transport studies were performed in triplicate at three different concentrations of each selected herbal extract and supplement. The percentage transport and apparent permeability coefficient (P_{app}) values were calculated from the obtained transport data in two directions. The efflux ratio (ER) values were calculated from these P_{app} values. Trans-epithelial electrical resistance (TEER) was measured at the onset and termination of each transport experiment using a Warner Instruments[®] EC-825A epithelial voltage clamp. Decreases in the TEER values were used to confirm compromising effects on the integrity of the membrane and/or to note any potential effects of the selected herbal extracts and supplement on the tight junctions.

Methylsulfonylmethane (MSM) mediated a discernible increase in RH-123 transport in the secretory (i.e. basolateral-to-apical) direction, whilst a decrease in RH-123 transport was observed in the absorptive (i.e. apical-to-basolateral) direction when compared to the negative control group (i.e. RH-123 alone). This verified that MSM is adept to induce P-gp mediated efflux in a concentration dependent manner. *Vitis vinifera* seed extract mediated a concentration dependent increase in RH-123 transport in both directions when compared to the negative control.

Vitis vinifera seed extract also caused the TEER to decrease concentration dependently in both directions, which indicated the opening of tight junctions and consequently also caused an apparent increase in RH-123 transport. *Hoodia gordonii* extract mediated a concentration dependent increase in RH-123 transport in the absorptive direction with a decrease in the secretory direction, which indicated that *Hoodia gordonii* extract may contain molecule(s) that act as P-gp efflux pump inhibitors. *Harpagophytum procumbens* extract demonstrated a non-concentration dependent induction of P-gp mediated efflux. *Leonotis leonurus* extract exhibited a concentration dependent increase in RH-123 transport in the absorptive direction but the secretory direction demonstrated an induction of P-gp related efflux upon reaching a baseline concentration.

These *ex vivo* pharmacokinetic interactions proved that herbal medicines and supplements can have an effect on Western medicine's membrane permeation and therefore also their bioavailability and further *in vivo* studies should be conducted to confirm the clinical significance thereof.

Key words: *Ex vivo*, *Harpagophytum procumbens*, *Hoodia gordonii*, *Leonotis leonurus*, Lucifer yellow, methylsulfonylmethane, pharmacokinetic interactions, P-glycoprotein, Rhodamine 123, *Vitis vinifera*.

UITTREKSEL

Die skielike oplewing in die gewildheid om siektes te behandel deur 'n meer holistiese benadering te volg het groeiende kommer tot gevolg weens die toenemende insidensie van ongewenste reaksies wat bemiddel word deur die gesamentlike toediening van kruie-medisyne/aanvullings tesame met Westerse-medisyne. Dié modulerende effekte van kruie-medisyne en aanvullings op die membraandeurlaatbaarheid van ander geneesmiddels het die aandag van baie navorsers getrek omrede hierdie effekte kan lei tot 'n toename of afname in die biobeskikbaarheid van allopatiese medisyne wat daarmee saam geneem word. Tydens die studie is klem geplaas op die maandelike membraanmodulerende effekte van die vier gekose kruie-ekstrakte (d.i. *Vitis vinifera* saad, *Hoodia gordonii*, *Harpagophytum procumbens*, *Leonotis leonurus*) en een gekose aanvulling (d.i. metielsulfonielmetaan) op die deurlaatbaarheid van intestinale epiteel. Hierdie geselekteerde kruie-ekstrakte en aanvulling is saam met Rodamien 123 (RH-123), 'n substraat vir die aktiewe transporter, P-glikoproteïen (P-gp), ondersoek.

Gedissekteerde vark jejunum weefsel is gemonteer op 'n Sweetana-Grass diffusie apparaat en transportstudies van RH-123 is in tweerigtings hierop uitgevoer. 'n Spectramax Paradigm® plaatleser is gebruik om monsters van 180 µl wat elke 20 min oor 'n tydperk van 2 ure geneem is, met behulp van 'n gevalideerde fluoressensie spektroskopiese metode, vir die hoeveelheid van RH-123 daarin, te ontleed. Om te bewys dat die tegniek wat gebruik is om die gedissekteerde vark jejunum weefsel te monteer nie nadelig vir die weefsel is nie, is 'n weefsel-integriteitstoets uitgevoer met behulp van die "Lucifer yellow" kleurmiddel. Alle transportstudies is in triplikaat uitgevoer en drie verskillende konsentrasies vir elk van die kruie-ekstrakte en aanvulling is getoets. Die persentasie transport en skynbare permeabiliteitskoëffisiënt (P_{app}) waardes is bereken vanaf die transport data. Die effluks verhouding (EV) is vanaf die P_{app} waardes in twee rigtings bereken. Die trans-epiteliale elektriese weerstand (TEEW) is aan die begin en einde van elke transport eksperiment gemeet met behulp van 'n Warner Instruments® EC-825A epiteliale spanningsklamp. Veranderinge in die TEEW waardes is bereken en gebruik om enige kompromieë in die integriteit van die weefsel en/of die effek van die kruie-ekstrakte en aanvulling op die intersellulêre-aansluitings te identifiseer.

Metielsulfonielmetaan (MSM) het 'n waarneembare verhoging in RH-123 transport in die sekretoriese rigting (nl. basolateraal-na-apikaal) veroorsaak, terwyl dit 'n afname in RH-123 transport in die absorptiewe rigting (nl. apikaal-na-basolateraal) tot gevolg gehad het in vergelyking met die negatiewe kontrole (nl. RH-123 alleen). Hierdie resultate bevestig dat MSM oor die vermoë beskik om P-gp bemiddelde effluks op 'n konsentrasie-afhanklike wyse te induseer. Wanneer *Vitis vinifera* saadekstrak se RH-123 transport resultate vergelyk word met die negatiewe kontrole is 'n konsentrasie-afhanklike toename in RH-123 transport in beide rigtings

waargeneem. Die TEEW het afgeneem soos die konsentrasie toegeneem het in beide rigtings, hierdie is aanduidend van die opening van die intersellulêre-aansluitings en gevolglik 'n toename in RH-123 transport. *Hoodia gordonii* ekstrak het 'n konsentrasie-afhanklike toename in die absorptiewe rigting getoon en 'n afname in die sekretoriese rigting tot gevolg gehad. Hierdie is aanduidend dat *Hoodia gordonii* oor molekules beskik wat kan dien as P-gp effluks pomp inhibeerders. *Harpagophytum procumbens* ekstrak het 'n nie-konsentrasie afhanklike induksie van P-gp bemiddelde effluks tot gevolg gehad. *Leonotis leonurus* ekstrak het, in die absorptiewe rigting, 'n konsentrasie-afhanklike toename van RH-123 transport tot gevolg gehad, maar die transport van RH-123 in die sekretoriese rigting verg dat 'n basislyn-konsentrasie eers bereik moet word voordat die induksie van P-gp verwante effluks kon plaasvind.

Hierdie *ex vivo* farmakokinetiese interaksies dien as bewys dat kruiegedisynie en aanvullings 'n effek op die membraandeurlaatbaarheid het, en gevolglik ook die biobeskikbaarheid van allopatiese medisyne en dat verdere *in vivo* studies uitgevoer moet word om die kliniese betekenisvolheid daarvan te bevestig.

Sleuteltermes: *Ex vivo*, farmakokinetiese interaksies, *Harpagophytum procumbens*, *Hoodia gordonii*, *Leonotis leonurus*, "Lucifer yellow", metielsulfoniemetaan, P-glikoproteïene, Rodamien 123, *Vitis vinifera* saadekstrak.

TABLE OF CONTENTS

ACKNOWLEDGEMENTS	I
ABSTRACT	II
UITTREKSEL.....	IV
LIST OF ABBREVIATIONS	XIX
CHAPTER 1: INTRODUCTION.....	1
1.1 Background and justification	1
1.1.1 Pharmacokinetic interactions	1
1.1.2 Selection of herbal and non-herbal supplement products	2
1.1.3 Supplement usage.....	3
1.2 Intestinal absorption models	3
1.3 Problem statement	4
1.4 Goals and objectives	5
1.4.1 General aim.....	5
1.4.2 Specific objectives	5
1.5 Ethics	6
1.6 Dissertation layout	6
CHAPTER 2: THE PHARMACOKINETIC EFFECTS OF HERBAL EXTRACTS AND SUPPLEMENTS ON DRUG PERMEATION	7
2.1 Introduction.....	7
2.1.1 Anatomy of the gastrointestinal tract.....	9
2.1.2 Comparison of the human and pig gastrointestinal tract anatomy	10
2.2 Absorption mechanisms within the gastrointestinal tract	13

2.2.1	Passive paracellular transport.....	14
2.2.2	Passive transcellular transport.....	14
2.2.3	Carrier-mediated transport.....	15
2.2.4	Transcytosis	16
2.2.5	Efflux transport	16
2.3	Herb-drug and supplement-drug pharmacokinetic interactions	17
2.3.1	Effect of herbs and supplements on enzymatic metabolism.....	17
2.3.1.1	Inhibition of CYP450.....	18
2.3.1.2	Induction of CYP450.....	20
2.3.2	Effects of herbal extracts and supplements on efflux transporters	22
2.3.2.1	The ATP-binding cassette (ABC) super-family of transporters.....	22
2.3.2.2	P-glycoprotein (P-gp or ABCB1/MDR1)	22
2.3.2.3	ABCC2/Multi-drug resistance-associated protein-2.....	23
2.3.2.4	ABCG2/Breast cancer resistance protein.....	24
2.3.3	Effects of herbs on uptake carrier proteins.....	24
2.3.4	Effects of herbs on gastrointestinal motility	25
2.3.5	Herb-drug and supplement-drug complex formations	26
2.4	Models to predict drug absorption.....	27
2.4.1	<i>In vivo</i> models.....	27
2.4.2	<i>In vitro</i> models	27
2.4.3	<i>In situ</i> models	32
2.4.4	<i>Ex vivo</i> models	32
2.4.5	<i>In silico</i> models.....	33

2.5	Selected herbal extracts and non-herbal supplements investigated in this study.....	33
2.5.1	Methylsulfonylmethane (MSM)	33
2.5.1.1	Medicinal applications of methylsulfonylmethane (MSM)	34
2.5.1.2	Pharmacokinetics of methylsulfonylmethane	34
2.5.2	<i>Hoodia gordonii</i>	34
2.5.2.1	Botany of <i>Hoodia gordonii</i>	34
2.5.2.2	Chemical composition of <i>Hoodia gordonii</i>	35
2.5.2.3	Medicinal applications of <i>Hoodia gordonii</i>	36
2.5.2.4	Pharmacokinetic interactions of <i>Hoodia gordonii</i>	36
2.5.3	<i>Vitis vinifera</i> seed extract.....	36
2.5.3.1	Botany of <i>Vitis vinifera</i>	36
2.5.3.2	Chemical composition of <i>Vitis vinifera</i>	37
2.5.3.3	Medicinal applications of <i>Vitis vinifera</i>	38
2.5.3.4	Pharmacokinetic interactions of <i>Vitis vinifera</i>	39
2.5.4	<i>Harpagophytum procumbens</i>	39
2.5.4.1	Botany of <i>Harpagophytum procumbens</i>	39
2.5.4.2	Chemical composition of <i>Harpagophytum procumbens</i>	40
2.5.4.3	Medicinal applications of <i>Harpagophytum procumbens</i>	40
2.5.4.4	Pharmacokinetic interactions of <i>Harpagophytum procumbens</i>	41
2.5.5	<i>Leonotis leonurus</i>	41
2.5.5.1	Botany of <i>Leonotis leonurus</i>	41
2.5.5.2	Chemical composition of <i>Leonotis leonurus</i>	42
2.5.5.3	Medicinal applications of <i>Leonotis leonurus</i>	43

2.5.5.4	Pharmacokinetic interactions of <i>Leonotis leonurus</i>	43
2.6	Summary	44
CHAPTER 3: MATERIALS AND METHODS		46
3.1	Introduction.....	46
3.2	Materials.....	46
3.3	Preparation of herbal extracts.....	47
3.4	Chemical fingerprinting of plant extracts	47
3.4.1	<i>Vitis vinifera</i> seed extract.....	47
3.4.2	UPLC-MS analytical method for <i>Vitis vinifera</i> seed extract.....	47
3.4.3	<i>Harpagophytum procumbens</i>	48
3.4.4	UPLC-MS analytical method for <i>Harpagophytum procumbens</i>	48
3.4.5	<i>Hoodia gordonii</i>	48
3.4.6	UPLC-MS analytical method for <i>Hoodia gordonii</i>	48
3.4.7	<i>Leonotis leonurus</i>	49
3.4.8	UPLC-MS analytical method for <i>Leonotis leonurus</i>	49
3.5	Fluorescence spectrometry analytical method validation for Rhodamine 123 and Lucifer yellow	49
3.5.1	Linearity.....	50
3.5.2	Limit of detection (LOD) and limit of quantification (LOQ)	50
3.5.3	Precision.....	51
3.5.3.1	Intra-day precision	51
3.5.3.2	Inter-day precision	51
3.5.4	Specificity	52

3.5.5	Accuracy.....	52
3.6	Buffer preparation for transport studies.....	53
3.7	<i>Ex vivo</i> transport studies.....	53
3.7.1	Preparation of experimental solutions.....	53
3.7.2	Collection and preparation of excised pig intestinal tissues for <i>ex vivo</i> transport studies	55
3.7.3	Bi-directional transport studies.....	59
3.8	Assessment of intestinal tissue integrity.....	60
3.9	Analysis of transport samples	60
3.10	Positive and negative control for RH-123 transport experiments.....	61
3.11	Data processing and statistical analysis.....	61
3.11.1	Percentage transport (% Transport).....	61
3.11.2	Apparent permeability coefficient (P_{app})	61
3.11.3	Efflux ratio (ER)	62
3.11.4	Statistical analysis of results	62
CHAPTER 4: RESULTS AND DISCUSSION.....		63
4.1	Introduction.....	63
4.2	Chemical fingerprinting of the herbal extracts	64
4.2.1	<i>Vitis vinifera</i> seed extract.....	64
4.2.2	<i>Hoodia gordonii</i>	65
4.2.3	<i>Harpagophytum procumbens</i>	66
4.2.4	<i>Leonotis leonurus</i>	66
4.2.5	Methylsfonylmethane (MSM)	67

4.3	Fluorescence spectrometry analytical method validation for Rhodamine 123 and Lucifer yellow	67
4.3.1	Method validation results: Rhodamine 123	68
4.3.1.1	Linearity	68
4.3.1.2	Limit of detection and limit of quantification.....	69
4.3.1.3	Accuracy.....	70
4.3.1.4	Precision.....	71
4.3.1.4.1	Intra-day precision	71
4.3.1.4.2	Inter-day precision	72
4.3.1.5	Specificity	73
4.3.2	Method validation results: Lucifer yellow.....	75
4.3.2.1	Linearity.....	75
4.3.2.2	Limit of detection and limit of quantification.....	76
4.3.2.3	Accuracy.....	77
4.3.2.4	Precision.....	78
4.3.2.4.1	Intra-day precision	78
4.3.2.4.2	Inter-day precision	79
4.3.3	Summary of validation results.....	80
4.4	Bi-directional transport studies.....	80
4.4.1	Methylsulfonylmethane (MSM)	81
4.4.2	<i>Vitis vinifera</i> seed extract.....	83
4.4.3	<i>Hoodia gordonii</i>	87
4.4.4	<i>Harpagophytum procumbens</i>	90
4.4.5	<i>Leonotis leonurus</i>	92

4.5	Evaluation of efflux ratios.....	95
4.6	Comparison and evaluation of TEER.....	97
4.7	Lucifer yellow studies.....	99
4.8	Conclusion.....	100
CHAPTER 5: FINAL CONCLUSIONS AND FUTURE RECOMMENDATIONS.....		101
5.1	Final conclusions	101
5.2	Future recommendations.....	103
REFERENCES.....		104
ADDENDUM A.....		126
ADDENDUM B.....		128
ADDENDUM C.....		134
ADDENDUM D.....		153
ADDENDUM E.....		166
ADDENDUM F.....		172

LIST OF TABLES

Table 2.1:	Comparison of the gastrointestinal tract of humans and pigs with regards to anatomy and physiological parameters	11
Table 2.2:	Examples of pharmacokinetic interactions between certain herbal medicines and the CYP450 family of enzymes.....	21
Table 2.3:	Advantages and limitations of a selection of <i>in vitro</i> models and techniques which are commonly used for permeation studies	29
Table 3.1:	Concentrations (% w/v) of each selected herbal extract and supplement used in the bi-directional transport study (Hellum <i>et al.</i> , 2007b)	54
Table 3.2:	Mass of each herbal extract/supplement used in preparation of the test solutions for the <i>ex vivo</i> transport experiments.....	55
Table 4.1:	Mean fluorescence values of Rhodamine 123 recorded over a defined concentration range	69
Table 4.2:	Blank fluorescence values together with the standard deviation and limit of detection (LOD) as well as limit of quantification (LOQ).....	70
Table 4.3:	Data procured from sample analysis to determine the accuracy of the analytical method for Rhodamine 123 across a specified concentration range.....	71
Table 4.4:	Data used to calculate the intra-day precision of the analytical method.....	72
Table 4.5:	Data used to calculate the inter-day precision of the analytical method.....	73
Table 4.6:	Summary of the specificity validation data for Rhodamine 123 in the presence of methylsulfonylmethane and <i>Vitis vinifera</i> seed extract	74
Table 4.7:	Summary of the linearity data for Rhodamine 123 in the presence of <i>Hoodia gordonii</i> , <i>Harpagophytum procumbens</i> and <i>Leonotis leonurus</i>	74
Table 4.8:	Mean fluorescence values of Lucifer yellow demonstrated over a defined concentration range	76
Table 4.9:	Fluorescence values of the blanks (KRB buffer) together with the standard deviation.....	77

Table 4.10:	Data procured from the Lucifer yellow sample analysis to ascertain accuracy across a specified concentration range	78
Table 4.11:	Data used to calculate intra-day precision of Lucifer yellow.....	79
Table 4.12:	Data used to calculate inter-day precision of Lucifer yellow.....	80
Table 4.13:	Summary of the average P_{app} values and efflux ratio (ER) values for the selected herbal extracts and supplement at the selected concentrations	96
Table 4.14:	Average percentage trans-epithelial electrical resistance (TEER) for excised tissue exposed to each of the selected herbal extracts and supplement over a 2 h period (all values are expressed as average percentage change from the initial T_0 to the T_{120} value).....	98
Table 4.15:	The permeability coefficient values for Lucifer yellow across excised pig intestinal jejunum tissue	99

LIST OF FIGURES

Figure 2.1:	A complementary model combining biomedical and healing paradigms (adapted from Moshabela <i>et al.</i> , 2016).....	8
Figure 2.2:	Lumen of the small intestine (adapted from www.studyblue.com)	10
Figure 2.3:	A schematic illustration of transport pathways across the intestinal epithelium: A) passive paracellular transport; B) passive transcellular transport; B*) intracellular metabolism; C) carrier-mediated transport; D) transcytosis (Flint, 2012).	13
Figure 2.4:	A schematic representation of the ATP cycle, A) , and the formation of ADP and ATP respectively B) . (www.khanacademy.org ; http://general.utpb.edu)	16
Figure 2.5:	Schematic representation of the P-glycoprotein efflux transporter (www.absorption.com)	17
Figure 2.6:	The chemical structure of methylsulfonylmethane	34
Figure 2.7:	Photographs showing <i>Hoodia gordonii</i> plants (Van Wyk <i>et al.</i> , 2000).....	35
Figure 2.8:	The chemical structures of P57, A) and hoodigogenin A, B)	36
Figure 2.9:	Photographs showing leaves and fruit of <i>Vitis vinifera</i> (Kleist, 2016) A) <i>Vitis vinifera</i> seed extract (www.gonutra.com) B) and C) <i>Vitis vinifera</i> seeds (London, 2015)	37
Figure 2.10:	The chemical structures of procyanidins illustrating the position of the different monomeric linkages as demonstrated by the configuration of the OH groups with A) as procyanidin B1, B) as procyanidin B2, C) as procyanidin B3 and D) as procyanidin B4.....	38
Figure 2.11:	Photograph of <i>Harpagophytum procumbens</i> fruit and flowers (Smithies, 2006).....	40
Figure 2.12:	Chemical structures of <i>Harpagophytum procumbens</i> constituents: A) Harpagoside, B) Harpagide, and C) Procumbide	40

Figure 2.13:	<i>Leonotis leonurus</i> inflorescence A) leaves B) <i>Leonotis leonurus</i> plant (Miner, 2012) and C) geographical distribution (dark green) in South Africa (adapted from Nsuala <i>et al.</i> , 2015)	42
Figure 2.14:	The chemical structures of selected phytochemicals of <i>L. leonurus</i> namely premarrubiin A) and marrubiin B)	43
Figure 3.1:	Photographic images of: A) Excised pig intestinal jejunum tissue mounted on a glass tube with mesenteric border visible, B) Careful removal of the serosal layer	56
Figure 3.2:	Photographic images A) and B) illustrating Peyer's patches in the excised pig intestinal jejunum tissue	56
Figure 3.3:	Photographic images of: A) the jejunum is cut along the mesenteric border, B) the jejunum is washed from the glass tube and C) transferred to heavy duty filter paper	57
Figure 3.4:	Photographic images of A) and B) the process of the proximal jejunum being cut into smaller pieces, C) and D) the process of the mounting the jejunum pieces onto the half cells, E) removal of the heavy duty filter paper and F) the assembling of the half cells into a single diffusion chamber	58
Figure 3.5:	Photographic image of a completely assembled Sweetana-Grass diffusion apparatus with excised pig intestinal jejunum tissues mounted between the half-cells	59
Figure 3.6:	The measuring of the TEER in the Sweetana-Grass diffusion chamber apparatus during bi-directional transport studies	60
Figure 4.1:	LC-MS chromatogram of <i>Vitis vinifera</i> seed extract.....	65
Figure 4.2:	LC-MS and LC-UV chromatograms of <i>Hoodia gordonii</i> extract	65
Figure 4.3:	LC-MS and LC-UV chromatograms of <i>Harpagophytum procumbens</i> extract.....	66
Figure 4.4	LC-MS chromatogram of <i>Leonotis leonurus</i> extract.....	67
Figure 4.5:	Linear regression curve for Rhodamine 123 with the straight line equation and correlation coefficient (R^2) value	68

Figure 4.6:	Linear regression curve for Lucifer yellow demonstrated with the straight line equation as well as the correlation coefficient (R^2) value	75
Figure 4.7:	Apical-to-basolateral transport of Rhodamine 123 in the presence of different concentrations of methylsulfonylmethane (MSM) across excised pig jejunum tissue plotted as a function of time	81
Figure 4.8:	Basolateral-to-apical transport of Rhodamine 123 in the presence of different concentrations of methylsulfonylmethane (MSM) across excised pig jejunum tissue plotted as a function of time	82
Figure 4.9:	Average P_{app} values for bi-directional transport of Rhodamine 123 in the presence of different concentrations of methylsulfonylmethane (MSM) across excised pig jejunum tissue (*statistically significant differences, $p \leq 0.05$).....	83
Figure 4.10:	Apical-to-basolateral transport of Rhodamine 123 in the presence of different concentrations of <i>Vitis vinifera</i> seed extract across excised pig jejunum tissue plotted as a function of time	84
Figure 4.11:	Basolateral-to-apical transport of Rhodamine 123 in the presence of different concentrations of <i>Vitis vinifera</i> seed extract across excised pig jejunum tissue plotted as a function of time	84
Figure 4.12:	Average P_{app} values for bi-directional transport of Rhodamine 123 in the presence of <i>Vitis vinifera</i> seed extract across excised pig jejunum tissue (*statistically significant differences, $p \leq 0.05$)	85
Figure 4.13:	Apical-to-basolateral transport of Rhodamine 123 in the presence of different concentrations of <i>Hoodia gordonii</i> extract across excised pig jejunum tissue plotted as a function of time	87
Figure 4.14:	Basolateral-to-apical transport of Rhodamine 123 in the presence of <i>Hoodia gordonii</i> extract across excised pig jejunum tissue plotted as a function of time.....	88
Figure 4.15:	Average P_{app} values for bi-directional transport of Rhodamine 123 in the presence of different concentrations of <i>Hoodia gordonii</i> extract across excised pig jejunum tissue (*statistically significant differences, $p \leq 0.05$)	89

Figure 4.16:	Apical-to-basolateral transport of Rhodamine 123 in the presence of different concentrations of <i>Harpagophytum procumbens</i> extract across excised pig jejunum tissue plotted as a function of time	90
Figure 4.17:	Basolateral-to-apical transport of Rhodamine 123 in the presence of different concentrations of <i>Harpagophytum procumbens</i> extract across excised pig jejunum tissue plotted as a function of time	91
Figure 4.18:	Average P_{app} values for bi-directional transport of Rhodamine 123 in the presence of different concentrations of <i>Harpagophytum procumbens</i> extract across excised pig jejunum tissue	91
Figure 4.19:	Apical-to-basolateral transport of Rhodamine 123 in the presence of different concentrations of <i>Leonotis leonurus</i> extract across excised pig jejunum tissue plotted as a function of time	93
Figure 4.20:	Basolateral-to-apical transport of Rhodamine 123 in the presence of different concentrations of <i>Leonotis leonurus</i> extract across excised pig jejunum tissue plotted as a function of time	94
Figure 4.21:	Average P_{app} values for bi-directional transport of Rhodamine 123 in the presence of <i>Leonotis leonurus</i> extract across excised pig jejunum tissue	94
Figure 4.22:	Efflux ratio values graphically represented for each of the selected herbal extracts and supplement at the three selected concentrations	97
Figure 4.23:	Apical-to-basolateral transport of Lucifer yellow across excised pig intestinal jejunum tissue plotted as a function of time	99

LIST OF ABBREVIATIONS

3 R	Replacement, reduction, refinement
ABC	ATP-binding cassettes
ADMET	Absorption, distribution, metabolism, excretion and toxicity
ANOVA	Analysis of variance
A-B	Apical-to-basolateral
AP-BL	Apical-to-basolateral
ATP	Adenosine triphosphate
BCRP	Breast cancer resistance protein
B-A	Basolateral-to-apical
BL-AP	Basolateral-to-apical
Caco-2	Human colorectal carcinoma cells
CO ₂	Carbon dioxide
CYP450	Cytochrome P450
Da	Dalton
d.i.	Dit is
EGCG	Epigallocatechin gallate
e.g.	<i>Exempli gratia</i> (for example)
EPH	Epoxide hydrolases
ER	Efflux ratio
EV	Effluks verhouding
FD	Functional dyspepsia
GIT	Gastrointestinal tract

GST	Glutathione S-transferases
HIV	Human Immunodeficiency Virus
HSD	Honest Significant Difference
IBS	Irritable bowel syndrome
IC ₅₀	Inhibitory concentration at 50%
i.e.	<i>Id est</i> (in other words)
kDa	Kilo-Dalton
KRB	Krebs-Ringer bicarbonate
LC-MS	Liquid chromatography-Mass spectrometry
LC-UV	Liquid chromatography-Ultra violet
LI	Large intestine
LOD	Limit of detection
LOQ	Limit of quantification
LRP	Lung cancer-associated resistance protein
LY	Lucifer yellow
MDCK	Madin-Darby canine kidney cells
MDR	Multidrug resistance
mRNA	Messenger ribonucleic acid
MRP2	Multi-drug resistance-associated protein-2
MSM	Methylsulfonylmethane
mTor	Millitor
MW	Molecular weight
NADPH	Nicotinamide adenine dinucleotide phosphate

NAT	<i>N</i> -acetyltransferases
NBD	Nucleotide binding domain
NCE	New chemical entity
nl.	Naamlik
NMO	NAD(P)H: menadione
NQO	NAD(P)H: quinone oxidoreductase
N ₂	Nitrogen
OA	Osteoarthritis
OATP	Organic anion transporting polypeptides
OCT	Organic cation transporter
O ₂	Oxygen
PAMPA	Parallel artificial membrane permeability assay
P _{app}	Apparent permeability coefficient/Skynbare permeabiliteitskoëffisiënt
PGE ₂	Prostaglandin E ₂
PDA	Photodiode array
P-gp	P-glycoprotein/P-glikoproteïen
QSAR	Quantitative structure-activity relationships
RH-123	Rhodamine 123/Rodamien 123
ROS	Reactive oxygen species
R ²	Correlation coefficient
RSD	Relative standard deviation
S	Slope
SAR	Structure-activity relationship

SD	Standard deviation
SI	Small intestine
SLC	Solute carriers
SULT	Sulfotransferases
TEER	Trans-epithelial electrical resistance
TEEW	Transepiteliale elektriese weerstand
TMD	Trans-membrane domain
TUT	Tshwane University of Technology
UGT	UDP-glucuronosyltransferases
UPLC-MS	Ultra performance liquid chromatography-tandem mass spectrometry
USP-NF	The United States Pharmacopeia and the National Formulary
V	Volt
WHO	World Health Organisation
w/v	Weight per volume (g/100ml)

CHAPTER 1: INTRODUCTION

1.1 Background and justification

1.1.1 Pharmacokinetic interactions

According to Shargel *et al.* (2005) 'pharmacokinetics' is the science of the kinetics of drug processes in the human body such as absorption, distribution and elimination (elimination comprises of both excretion and metabolism). The term 'drug disposition' is used to describe drug distribution and elimination. Drug absorption is the process of movement of drug molecules from the site of administration, such as the intestinal lumen after oral administration, across biological membranes into blood vessels, which drain into gastrointestinal tract and transports blood via the liver to the systemic circulation and finally to the drug's site of action. Permeation across membranes can be accomplished by means of passive diffusion or carrier mediated transport, which can either be passive or active in nature. The former is responsible for the movement of molecules across membranes from an area of high concentration to an area of low concentration, the latter incongruous can be responsible for the movement of molecules against a concentration gradient. Active transport can occur in the absorptive direction or in the secretory direction (the latter occurs where molecules are moved from within the epithelial cells back into the intestinal lumen by means of active transporters such as P-glycoprotein (P-gp)) (Rowland & Tozer, 2011).

P-gp is a member of the adenosine triphosphate (ATP)-binding cassette (ABC) transporter superfamily and is prominently expressed in the apical membranes of various biologically important epithelial barriers such as in the kidney, liver, intestine, and blood-brain barrier (Thiebaut *et al.*, 1987). P-gp is an energy dependent efflux transporter, which may limit the absorption of substrate molecules and may thereby contribute to poor bioavailability of certain drugs. Another contributing factor to poor bioavailability of certain drugs is pre-systemic metabolism of the drug molecules by the cytochrome P450 (CYP450) family of enzymes. CYP3A4 is the most abundant isoform of the CYP450 enzyme family that contributes to hepatic and intestinal phase I enzyme reactions and is believed to be responsible for the metabolism of more than 50% of prescription drugs (Zhou, 2008).

When herbs and/or other supplements are used concomitantly with Western medicines, pharmacokinetic interactions can occur due to altering of drug pharmacokinetic processes such as absorption, distribution, metabolism or excretion by means of various mechanisms (Tarirai *et al.*, 2010). This can lead to an increase or decrease of pharmacological or toxicological effects, which may influence the long term therapeutic effect of the administered drug. A prerequisite chronic drug therapeutic monitoring program may be paramount in such cases (Fugh-Berman,

2000). In its entirety, there is limited information available with regards to pharmacokinetic interactions between herbal extracts and/or supplements with Western medicines and therefore it is of utmost importance to research this subject to make this important information available to health care workers.

1.1.2 Selection of herbal and non-herbal supplement products

For this study, selections of herbal and non-herbal supplement products were researched to identify potential pharmacokinetic interactions during membrane permeation (simulated process of drug absorption from the gastrointestinal tract). Extracts from the following four commonly used herbal products and one non-herbal supplement product were selected: extract from the *Vitis vinifera* seeds, *Hoodia gordonii*, *Harpagophytum procumbens*, *Leonotis leonurus* and the supplement, methylsulfonylmethane (MSM).

Vitis vinifera seed extract has a high polyphenolic content of which the procyanidins/proanthocyanidins (these terms are used interchangeably and for the purpose of this study procyanidins will be used) are more prominently known for their ability to scavenge for free radicals and manifests itself as anti-oxidants (Madhavan *et al.*, 2016; Monages *et al.*, 2005; Tsang *et al.*, 2005).

The prevalence of obesity has increased and excessive weight puts patients at risk for the development of chronic diseases such as osteoarthritis, diabetes, cardiovascular diseases and high blood pressure. As a result, patients often seek help in the form of weight loss products, especially natural products as it is deemed “safer” and can be acquired without a prescription (Whelan *et al.*, 2010). *Hoodia gordonii* is used to treat obesity by means of appetite suppression and the main active constituent responsible for the anorexic action is the steroidal glycoside namely P57AS3 (Kamsu-Foguem & Foguem, 2014).

Extracts of the roots of *H. procumbens* provides a herbal medicine with various clinical indications. A popular area of usage is demonstrated in the treatment of inflammatory disorders of the musculoskeletal system e.g. osteoarthritis. Furthermore, *H. procumbens* shows pharmacological evidence of analgesic activities utilised for the treatment of lower back pain (McGregor *et al.*, 2005).

Leonotis leonurus is a traditional herbal medicine native to South Africa and is used in various forms such as decoctions, infusions and inhalations (Van Wyk *et al.*, 2000). Every part of the plant is utilised for a specific indication, e.g. decoctions (mainly made from the dried leaves) are used for coughs and constipation, whilst smoking of the dried leaves is utilised for its psychoactive effects (Baudry *et al.*, 2015). Farmers also use this traditional medicine to treat gall sickness (anaplasmosis) in their livestock and prevent worm infestations in their cattle (Nsuala *et al.*, 2015).

Dietary supplements have bombarded the health market with a variety of products in the past few decades. Methylsulfonylmethane (MSM) is a non-herbal supplement and was chosen for this study on account of its ability to act as a sulfur molecule donor. Sulfur is a major component in connective tissue and contributes to the compilation of cartilage. MSM is commonly used to treat inflammation associated with osteoarthritis, a common chronic joint disease defined by focal lesions of articular cartilage (Jacob & Appleton, 2003; Küçükşen & Şahin, 2015).

1.1.3 Supplement usage

Many individuals take herbal health products, often without their physician's knowledge, due to the constantly increasing scientific recognition of these products for the prevention and treatment of diseases. Demographic information signified that patients with a compromised health status, and those that take chronic medication, are more inclined to take herbal supplements in addition to their prescribed medications (Rafferty *et al.*, 2002). Furthermore, there is a general belief that herbal products of natural origin are safer and contributes more to a holistic lifestyle (Cass, 2004; Ingersoll, 2005). Although the use of herbal supplements and health products provided by traditional healers might be seen as beneficial, Colalto (2010) stated that the lack of information supporting the safety and efficacy of these type of treatments as well as the absence of guidelines for manufacturing, adulteration of plants and possible lack of identification of plants may lead to an unwanted reaction between supplements and conventional drugs.

1.2 Intestinal absorption models

Even though we are faced with a number of routes available for the administration of drugs and supplements, the oral route is the most preferred means of drug administration. It is of utmost importance to achieve acceptable bioavailability of any active ingredient after oral administration to provide a successful treatment outcome (Alderborn, 2007; Desai *et al.*, 2016, Liu *et al.*, 2009). Based on this knowledge, Alqahtani *et al.* (2013) noted the importance of having models at our disposal to mimic *in vivo* conditions in order to determine the ability of a marker compound to traverse across biological membranes. Models used for predicting the transport of drugs across the gastrointestinal epithelium can be divided into different categories namely *in situ*, *in silico*, *in vitro*, *ex vivo* and *in vivo*. The initial screenings for prediction of pharmacokinetic parameters are preferably done by means of high throughput methods such as *in vitro* techniques (Honig *et al.*, 1993).

- *In situ* refers to an experimental approach where specific secluded portions of the intestine of an anesthetised living organism are used to determine the compound's absorption and metabolism. However, pre-systemic metabolism (e.g. CYP450) and efflux transport (e.g. P-gp) are not taken into account because only a small volume of the drug solution is

exposed to the gastrointestinal tract and measured rather than the resultant drug concentrations in the blood plasma. Furthermore, to obtain statistically significant data, a large number of animals are required (Hamman, 2007).

- *In silico* refers to computer software programmes that can predict the key pharmacokinetic properties of the test compounds (Alqahtani *et al.*, 2013).
- *In vivo* models are utilised to ascertain a drug's bioavailability and metabolism within a living organism (e.g. animals or humans) (Alqahtani *et al.*, 2013).
- *In vitro* models describe experiments performed outside the body of living organisms in a glass container in a laboratory, e.g. human adenocarcinoma cells of the colon (Caco-2), Madin-Darby canine kidney (MDCK) cells and other immortalised cell lines (Balimane *et al.*, 2000).
- *Ex vivo* models are utilised to perform experiments on excised tissue from living organisms (e.g. animals or humans), which may be mounted in an Ussing-type diffusion apparatus such as the Sweetana-Grass diffusion apparatus (Dahan & Hoffman, 2007).

1.3 Problem statement

Empiric evidence demonstrated that the use of Western medicines together with certain natural health products can pose a risk in the form of potential adverse interactions. These interactions can occur in the form of pharmacokinetic and/or pharmacodynamic interferences. Patients at greatest risk for interactions are those with chronic disease who use multiple medications, particularly those with small therapeutic ranges (Boullata, 2005). It is also apparent that a substantial number of patients in developing countries who are living with chronic illnesses still consult traditional healers often during the same time that medical doctors are consulted. Self-administered herbal products (or prescribed by traditional healers) along with prescribed Western medicines raised concerns of modified therapeutic activity due to possible herb-drug or supplement-drug interactions (Dhananjay & Mitra, 2006).

Various problems, commonly associated with the use of polypharmacy, have been identified in patients. Health care providers are usually unaware of the use of herbal medicines, which may lead to potential interactions. This, together with a lack of pre-clinical and clinical evidence, may often prevent the health care provider from providing sufficient and accurate advice to the patient regarding the concomitant use of supplements with their prescribed medicines. There is no proper surveillance procedure or reporting system for the quality control and monitoring of adverse effects that occurred due to herb-drug combinations (Dhananjay & Mitra, 2006).

The interactions between herbal medicines and conventional medicines have started to draw more and more attention due to the increasing awareness of physicians regarding the adverse effects caused by undisclosed herbal medicine usage. However, a lack of information on interactions between certain herbal medicines and Western medicine makes it difficult for health care providers to provide patients with accurate and up to date advice.

1.4 Goals and objectives

1.4.1 General aim

The main aim of this study was to investigate and identify potential pharmacokinetic interactions during drug absorption between selected supplement/herbal medicines and a model compound (i.e. Rhodamine 123 (RH-123), which is a known P-gp substrate) by using an *in vitro* permeation model (i.e. excised pig intestinal jejunum tissues mounted in a Sweetana-Grass diffusion chamber apparatus).

1.4.2 Specific objectives

The specific objectives of the study were:

- To conduct a literature review and to select herbal and non-herbal supplements/extracts that is commonly used in South Africa concomitantly with prescribed medicine for which limited information is available regarding pharmacokinetic interactions.
- To validate a fluorometric analytical method (SpectraMax® Paradigm Multi-Mode Microplate Reader) for analysis of RH-123, specifically by means of linearity between the analyte concentration and detector response as well as in terms of specificity, precision and accuracy.
- To conduct bi-directional transport studies across excised pig jejunum intestinal tissue on RH-123 in the presence and absence of the selected herbal and non-herbal supplements/extracts. Each supplement/extract will be tested at three experimental concentrations.
- To process and interpret the transport data of the bi-directional transport studies and to calculate trans-epithelial electrical resistance (% TEER), apparent permeability coefficient (P_{app}) and efflux ratio (ER) values in order to determine the effect of the selected herbal and non-herbal extracts/supplements on RH-123 transport and efflux.

1.5 Ethics

Excised pig intestinal jejunum tissues were collected from the Potchefstroom abattoir where pigs are slaughtered solely for meat production purposes and not for research purposes. It therefore complies with the 3 R (Reduce, Replace and Refine) principles (Sjögren *et al.*, 2014). However, a few aspects do involve ethical consideration like the control with regards to the site of tissue collection (e.g. disease control is applied to slaughtered animals) and the correct disposal of the intestinal tissue upon completion of the transport experiments.

An ethics application addressing all the above mentioned ethical considerations for the use of excised pig jejunum intestinal tissue was already approved by the Ethics Committee (AnimCare) of the North-West University (NWU00025-15-A5 – valid from 2015 to 2020) (Addendum A).

1.6 Dissertation layout

In this dissertation, Chapter 1 describes the rationale as well as the aim and objectives of the study, Chapter 2 follows with an in depth look at the literature applicable to this study. Experimental materials and methods that were used and applied are encompassed in Chapter 3. Chapter 4 describes the results of the experiments, along with explanations of P_{app} and ER value changes and % TEER changes obtained. Chapter 4 also contains all statistically analysed data and discussions of relevant results. Chapter 5 contains conclusions and future recommendations based on the results of this study.

CHAPTER 2: THE PHARMACOKINETIC EFFECTS OF HERBAL EXTRACTS AND SUPPLEMENTS ON DRUG PERMEATION

2.1 Introduction

“Herbal medicine(s)” can as a collective on a high-level basis appositely be defined as “medicines including herbs, herbal materials, herbal preparations and finished herbal products that contain as active ingredients parts of plants, or other plant materials, or combinations” (WHO, 2000).

The popularity of herbal extracts and supplements for medicinal use has proliferated substantially over the past three decades. An estimated four billion people (representing approximately 80% of the world’s population) living in developing countries rely on herbal medicine as their primary source of everyday health care (Ekor, 2014).

A wide variety of floras, in various forms and preparations, have been exploited and utilised by mankind for medicinal purposes over the ages. Advocating an indigenous knowledge system and subscribing to the amalgamation of the biomedical and traditional healing paradigms have however proven over time to provide a reciprocal system of diverse health care, which manifest in a more holistic and thorough form of health care for patients.

Previous perceptions of traditional healing in South Africa have to this end shifted from a derogatory ‘witchcraft paradigm’ and narrative demonstrated in legislation as the Witchcraft Suppression Act 3, 1957 (Act 3 of 1957) to that of a forbearing pontification of a ‘healing paradigm’ acknowledged and protected under the Traditional Health Practitioners Act 22, 2007 (Act 22 of 2007) (Moshabela *et al.*, 2016). Figure 2.1 illustrates the primary differences in emphasis between traditional healers and the biomedical sciences.

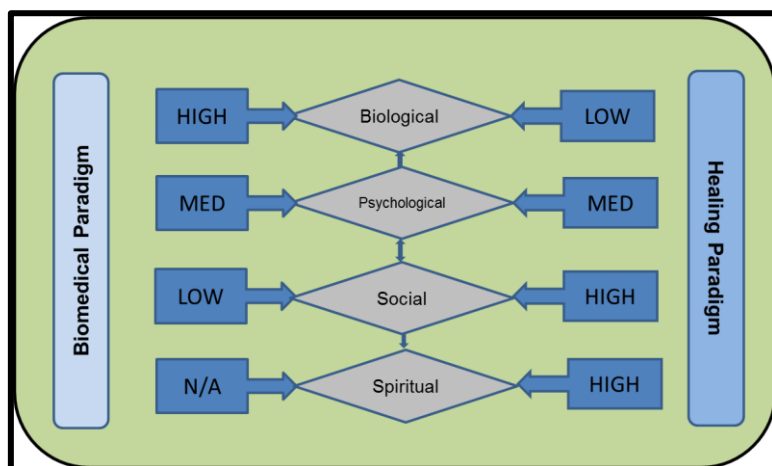


Figure 2.1: A complementary model combining biomedical and healing paradigms (adapted from Moshabela *et al.*, 2016)

There is substantive evidence that natural originating herbal products are often safer and contribute to a healthier lifestyle more than allopathic type medicines (Cass, 2004; Ingersoll, 2005). Raskin *et al.* (2002) expounded on this premise by emphasising that the concept of growing crops for health rather than for food or fibre is slowly changing plant biotechnology and the medicinal industry environments. Raskin *et al.* (2002) further mentioned that the re-discovery of the connection between plants and health played a pivotal part and serve as impetus in the launch of a new generation of botanical therapeutic products. These products amongst others include plant-derived pharmaceuticals, multi-component botanical drugs, dietary supplements and plant-produced recombinant proteins.

Herbs in their unprocessed form embody the primary element of many traditional herbal medicines, and herbal products have become a composite or integral keystone part of the current globally developing tendency to resort to alternative medicine therapy (Itokawa *et al.*, 2008; Zhou, 2006).

Although the benefits of herbal supplements and health products provided by traditional healers are often culturally entrenched and acknowledged, unwanted interactions between herbal extracts and Western medicines may occur in the event of concomitant use (Colalto, 2010). Zhou *et al.* (2007) mentioned that the incidence of herbal extract-drug interactions is higher than that of drug-drug interactions and that it can mainly be attributed to the complex chemical composition of herbal extracts. He also pointed out that the use of multiple medicines will notably increase the likelihood of herb-drug interactions and that this problem especially pertains to geriatric patients and patients on chronic prescribed medicine. A higher number of herbal products consumed increase the risk for the number of drug interactions that can occur. Zhou *et al.* (2007) further expounded on this premise by stating that while the estimated risk for potential interactions

between herbal extracts and Western medicines upon concomitant consumption of two products is 6%; for five products, it increases to 50%, with a risk of 100% on the concomitant intake of eight or more products (Fugh-Berman, 2000).

The gastrointestinal tract (GIT), as part of the digestive systems of humans and most mammals, serves as an acknowledged barrier to drug absorption and is also the primary site for absorption of orally administered drugs. However, orally administered drugs are subjected to metabolism by the major phase I metabolising enzyme cytochrome P450 (CYP450) as well as the multidrug efflux pump proteins, P-glycoprotein (P-gp). Both are present at eminent levels in the villus tip of the enterocytes in the GIT which serves as the dominant site of absorption for orally administered drugs (Zhang & Benet, 2001). This intestinal drug metabolism and anti-transport processes have led to a potential paradigm shift in the delivery of orally administered drugs and by understanding and using it to our advantage will contribute to a significant improvement in drug bioavailability and treatment outcomes (Benet *et al.*, 1996).

2.1.1 Anatomy of the gastrointestinal tract

The pig is often utilised as an animal model for drug pharmacokinetic studies. *In vitro* studies and data acquired from studies on excised pig tissues have been shown to correlate well with data generated in humans, probably due to similarities in the physiology and anatomy of pigs and humans (Guilloteau *et al.*, 2010).

The basic macro-anatomical structure of the GIT can be described as a long muscular tube with areas specifically differentiated for digestion and absorption of nutrients (Figure 2.2). These regions are supplied with blood by a network of arteries and drained by veins and are supported by a blanket of connective tissue known as the mesentery. Functionally, the GIT is segregated into a preparative and primary storage region (mouth and stomach), a secretory and absorptive region (the mid-gastrointestinal tract region), a water reclamation region (ascending colon) and lastly a waste product storage region (descending and sigmoid colon). Due to the nature of the epithelial tissue, the small intestine is structurally capable of maximal absorption of substances and nutrients (Sjögren *et al.*, 2014).

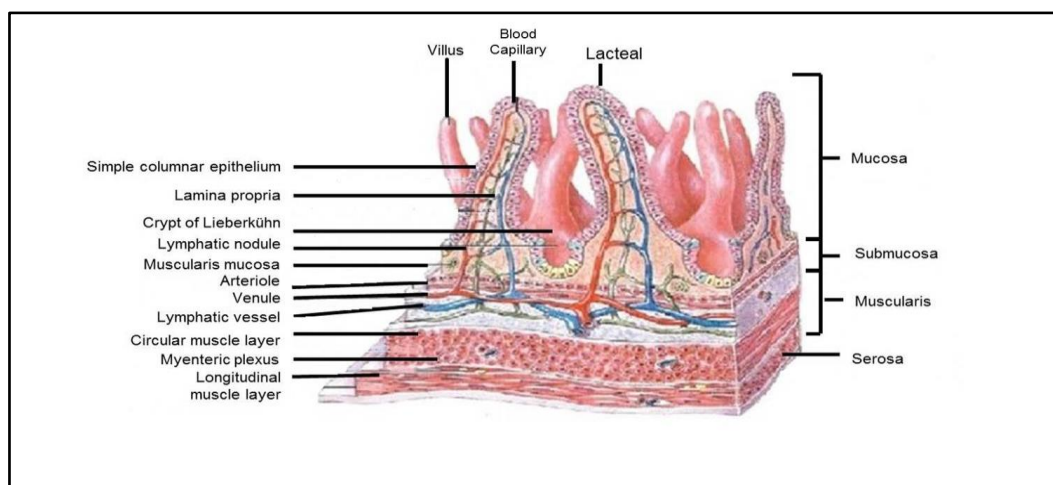


Figure 2.2: Lumen of the small intestine (adapted from www.studyblue.com)

2.1.2 Comparison of the human and pig gastrointestinal tract anatomy

Different species present remarkable differences with regards to the lengths of the GIT regions and absorption surface areas, environmental conditions such as the pH and fluidity of the chyme, intestinal transit time and the amount and origin of the bacterial flora. Even though discrepancies exist with respect to GIT anatomy between different species, certain anatomical (and chemical) characteristics of animals are very similar when comparing them with the human GIT anatomy. All the regions in the GIT are lined with a mucous membrane consisting of a single layer of epithelial cells concerted by tight junctions (DeSesso & Williams, 2008). Due to its similarities on an anatomical, physiological and biochemical platform to the human, the pig is regarded as a translational model for humans in biomedical research (Puccinelli *et al.*, 2011). For this reason, using pigs as an animal model in drug development has become increasingly popular among the scientific community (Helke & Swindle, 2013).

With regards to transport proteins found in the GIT, Sjögren *et al.* (2014) found that P-gp and breast cancer resistance protein (BCRP) levels increase in the direction of the small intestine from the stomach with a relatively high concentration found in the distal jejunum. Multi-drug resistance-associated protein-2 (MRP2) showed the same expression pattern, but a high concentration of this transporter protein was also observed in the large intestine. Sjögren and co-workers further demonstrated a relatively high correlation in P-gp expression within the human and the pig, when taking transcriptional, protein and functional levels into account. This information is particularly important, especially pertaining to this research study where interactions pertaining to both absorptive and secretory transport across the small intestinal epithelium have been investigated. Table 2.1 compares certain physiological and anatomical aspects of the GIT of the human with that of the pig.

Table 2.1: Comparison of the gastrointestinal tract of humans and pigs with regards to anatomy and physiological parameters

Parameter	Anatomical Region	Human	Pig
pH fasted	Stomach	1-3.5(Simonian <i>et al.</i> , 2005)	1.2-4.0 (Hossain <i>et al.</i> , 1990)
	Small intestine (SI)	Duodenum: 6.0-7.0 Jejunum: 6.0-7.7 Ileum: 6.5-8.0(Lennernäs, 2007c)	7.0-8.0 (Oberle & Das, 1994)
	Large intestine (LI)	Cecum: 5.5-6.5 Ascending colon: 5.5-7.5 Descending colon: 7.0-8.0(Sjögren <i>et al.</i> , 2014)	n.a.
pH fed	Stomach	3.0-6.0 (Simonian <i>et al.</i> , 2005)	4.4 (Merchant <i>et al.</i> , 2011)
	SI	Duodenum: 5.0-5.5 Jejunum: 5.0-6.5 Ileum: Akin to fasted (Persson <i>et al.</i> , 2005)	Duodenum: 4.7-6.1 Jejunum: 6.0-6.5 Ileum: 6.3-7.2 (Merchant <i>et al.</i> , 2011)
	LI	n.a.	6.1-6.6 (Merchant <i>et al.</i> , 2011)
Transit time fasted	Stomach	10-15 min (for liquids) & 0-2 h for solids (Davis <i>et al.</i> , 1986)	1-28 days (Hossain <i>et al.</i> , 1990)
	SI	3-4 h (Davis <i>et al.</i> , 1986)	<1-3 days (Hossain <i>et al.</i> , 1990)
	LI	8.0-18.0 h (Davis <i>et al.</i> , 1986)	<1-3 days (Hossain <i>et al.</i> , 1990)
Transit time fed	Stomach	Liquid: rapid but slower than same liquid in fasted state (Brener <i>et al.</i> , 1983). Solids: extremely fast for <2mm particles; >7-10 mm	Pellets 1.4-2.2 h (Davis <i>et al.</i> , 2001); Tablet 1.5-6.0 h (Wilfart <i>et al.</i> , 2007)

		particles retained for hours (DeSesso & Jacobson, 2001)	
	SI	3.0-4.0 h (Davis <i>et al.</i> , 1986)	3-4 h (Davis <i>et al.</i> , 2001; Wilfart <i>et al.</i> , 2007)
	LI	n.a.	24-48 h (Davis <i>et al.</i> , 2001; Wilfart <i>et al.</i> , 2007)
Length	SI	680 cm (DeSesso & Jacobson, 2001; DeSesso & Williams, 2008)	1500-2000 cm (DeSesso & Jacobson, 2001; DeSesso & Williams, 2008)
	LI	150 cm (DeSesso & Jacobson, 2001)	323 cm (Merchant <i>et al.</i> , 2011)

n.a. = not available

2.2 Absorption mechanisms within the gastrointestinal tract

One of the most important pharmacokinetic features of an effective drug is the ability to cross biological membranes in its unchanged form (Sugano *et al.*, 2010). Absorption from the GIT can either be accomplished by means of passive diffusion through the epithelial cells (i.e. transcellular), through the interstitial spaces (i.e. paracellular) or by means of carrier mediated transport, which can either be active or passive by nature (Rowland & Tozer, 2011).

Passive diffusion is the process by which molecules diffuse from a region of higher concentration to a region of lower concentration. This mechanism of transport does not necessitate energy to accomplish movement of molecules across a biological membrane. The main driving force for passive diffusion is the concentration difference, which exists between the mucosal side (i.e. the GIT lumen) of the intestinal membrane and the basolateral side (i.e. the blood), which results in a concentration gradient (Shargel *et al.*, 2012).

Active transport, in contrast, is an energy consuming process, which is characterised by the transport of a compound against a concentration gradient (i.e. from a region of lower concentration to a region of higher concentration). Active transport is regarded as a specialised process that requires a carrier that binds to compounds, which traverse across the intestinal membrane and dissociate on the other side of the membrane, releasing the compound and reactivating the carrier molecule (Shargel *et al.*, 2005). The transport mechanisms for drug molecules across the intestinal epithelium are illustrated in Figure 2.3 and discussed in further detail below.

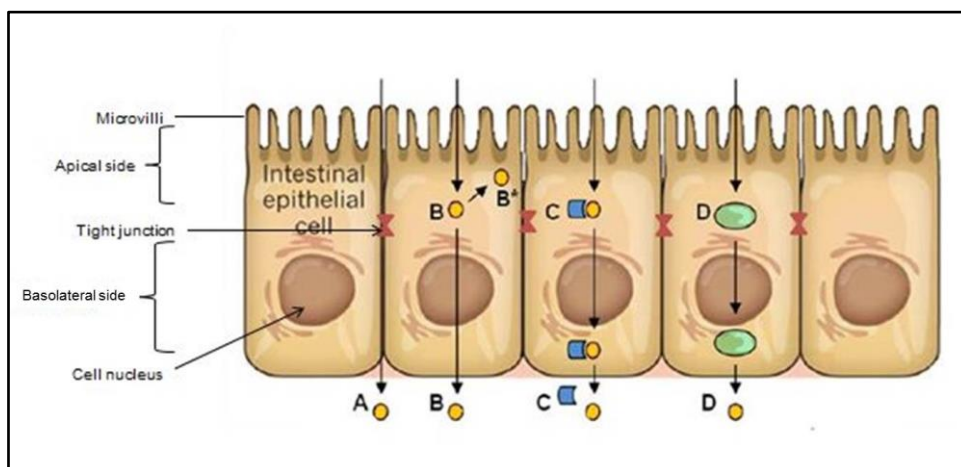


Figure 2.3: A schematic illustration of transport pathways across the intestinal epithelium: **A)** passive paracellular transport; **B)** passive transcellular transport; **B*)** intracellular metabolism; **C)** carrier-mediated transport; **D)** transcytosis (Flint, 2012).

2.2.1 Passive paracellular transport

In order for a drug molecule to traverse the epithelial cell layer, it must be able to penetrate the plasma membrane of the biological cell. This biological cell membrane consists of a double layer of phospholipids and cholesterol with proteins embedded in the bilayer (Sugano *et al.*, 2010).

Passive paracellular transport (Figure 2.3 A) is the transport via water-filled intercellular spaces between the epithelial cells. Compounds that are relatively hydrophilic with molecular weights < 200 Da can permeate the intestinal epithelium via the paracellular route in substantial amounts (Artursson *et al.*, 1993). Hydrophilic compounds will not easily partition into the intestinal membranes because of the charge they carry and these compounds would rather be susceptible to absorption into the systemic circulation by means of other pathways (Kumar *et al.*, 2010; Li, 2001). Drugs that are small hydrophilic compounds are therefore usually transported by means of the paracellular transport pathway. It has been demonstrated that cations permeate with more ease than neutral molecules that will in turn permeate with more ease than anions (Linnankoski *et al.*, 2010). However, the apical and basolateral membrane domains are separated by tight junctions, providing a seal between adjacent epithelial cells with the consequence that free movement of molecules through the paracellular pathway is restricted (Tavelin *et al.*, 2003).

2.2.2 Passive transcellular transport

The passive transcellular pathway (Figure 2.3 B) is the main route by which most compounds are absorbed from the GIT. Although there are variations in the lipid composition of membranes between different cell types, the lipid bilayer portion is present in almost all cell types and the same passive transcellular transport process takes place regardless of cell type (Sugano *et al.*, 2010).

Penetration of the apical membrane by a compound is the first step of passive transcellular transport. The compound molecules intended for absorption must partition into the membrane after which the molecules subsequently move through the lipid bilayer of the cell. Lipophilic compounds intended for absorption from the GIT are exclusively absorbed by this pathway and will rapidly diffuse through the cytoplasm of the cell interior and subsequently permeate the basolateral membrane and enter the blood circulation (Li, 2001; Muranishi, 1990). Furthermore, passive transport is not dependent on the stereo-chemical structure of the compound being transported; it does not adhere to a site-specific binding regime and therefore is not a saturable transport process. The compound intended for transport must carry certain physico-chemical properties that include a favourable molecular charge, partition coefficient, solubility, molecular size and pKa value. These characteristics are compulsory for the compound to pass through

both layers of the cell, which is the hydrophilic outer layers as well as the hydrophobic center (Chan *et al.*, 2004; Sugano *et al.*, 2010).

2.2.3 Carrier-mediated transport

Active carrier-mediated transport (Figure 2.3 C) is a transport mechanism that entails the transport of molecules by means of protein based membrane carriers that can either be directly or indirectly energy dependent. The main membrane transporter families are the ATP (Adenosine triphosphate)-binding cassettes (ABC) and the solute carriers (SLC). The energy required for this transport mechanism is generated from the hydrolysis of adenosine triphosphate (ATP) (Ashford, 2007). ATP presents itself as the primary energy carrier for most energy-requiring biochemical reactions that occur in the cell (Figure 2.4 A). The turnover rate of ATP is very swift and occurs in a rapid manner. Adenosine diphosphate (ADP) can be synthesized into ATP and vice versa (Figure 2.4 B).

Energy dependent carrier mediated transport is prone to saturation at high concentrations of the substrate, which may cause an inimical effect on drug absorption (Artursson *et al.*, 2012). Utilising the energy from ATP, either directly or indirectly, enables the transporter proteins to transport compounds against the concentration gradient. ABC transporters directly utilises the energy obtained from ATP to activate the transport process. The SLC transporter family utilises ion gradients for transport, which in turn are ATP-dependant (Sugano *et al.*, 2010).

Passive carrier mediated transport is not energy dependent and may also be defined as facilitated diffusion. Facilitated diffusion involves binding of molecules to carriers, which move them across the membrane. It requires a concentration gradient as its driving force. This process is saturable as the transporters are fixed proteins and stereo-specific and can be blocked by compounds other than a drug e.g. inhibition due to a competitive inhibitor (Ashford, 2007).

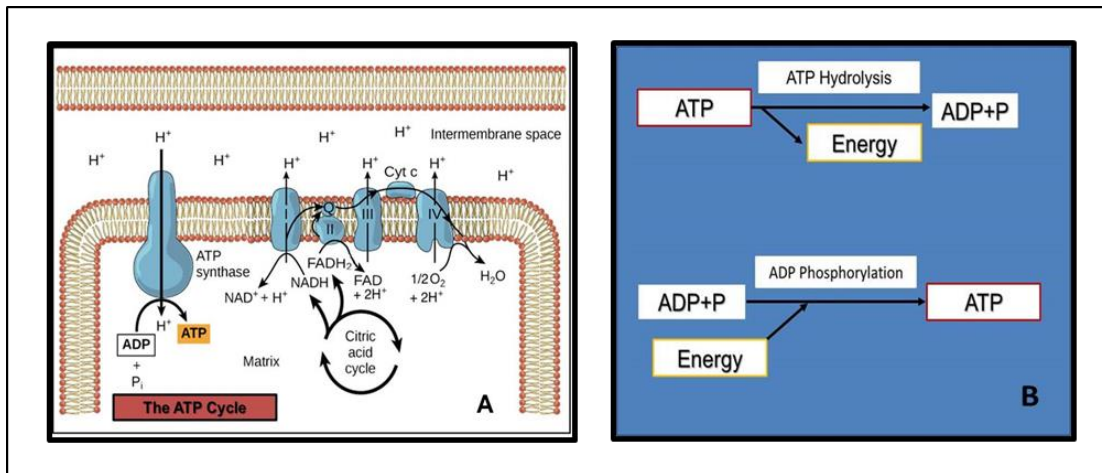


Figure 2.4: A schematic representation of the ATP cycle, **A**), and the formation of ADP and ATP respectively **B**). (www.khanacademy.org; http://general.utpb.edu)

2.2.4 Transcytosis

Transcytosis (Figure 2.3 D) represents another passive process by which molecules are transported across cells. The mechanism by which transcytosis operate can be explained and simplified by a few steps. Firstly, an engulfment of the molecules by the plasma membrane occurs; this is followed by pinching off the material internalized by the membrane to form a material filled intra-cellular vesicle. This process is termed 'endocytosis' and can be subdivided into pinocytosis and phagocytosis. The former is the engulfment of small droplets of extracellular fluid by a membrane vesicle and the latter is the engulfment of particles larger than 500 nm by the cell membrane (Ashford, 2007). Upon completion of endocytosis the material is relocated to other vesicles or lysosomes, representing the end-stage of the endocytic pathway. Lysosomes are responsible for the digestion of materials; however, some materials abscond from digestion and move through the cell to be released at the basolateral side, and this is known as exocytosis (Ashford, 2007; Di Pasquale & Chiorini, 2006).

2.2.5 Efflux transport

Efflux transport, also classifiable as active transport, is the transport of compounds mediated by ATP-dependent efflux transporters namely P-gp, BCRP and MRP2 in the secretory direction, thus from within the cells to the apical side of the intestinal epithelium (i.e. the lumen of the GIT). P-gp is a member of the ABC super-family of transporters and is one of the most significant counter-transport proteins that is prominently expressed in the apical membrane of various pharmacokinetically important epithelial barriers such as the kidney, liver, intestine and blood-brain barrier (Figure 2.5) (Takano *et al.*, 2006).

Due to the nature of the efflux transport mechanism, certain limitations exist regarding the absorption of substrate molecules into certain cells (Berggren *et al.*, 2007; Takano *et al.*, 2006). Efflux transporters may also be classified as a type of defence mechanism which reduces/prevents the uptake of potentially toxic substances in the cells. This character trait of efflux mechanisms may also in some instances be considered as a nuisance because it can have a negative effect on the bioavailability of orally administered drugs, which are substrates of these efflux proteins (Chan *et al.*, 2004; Varma *et al.*, 2003).

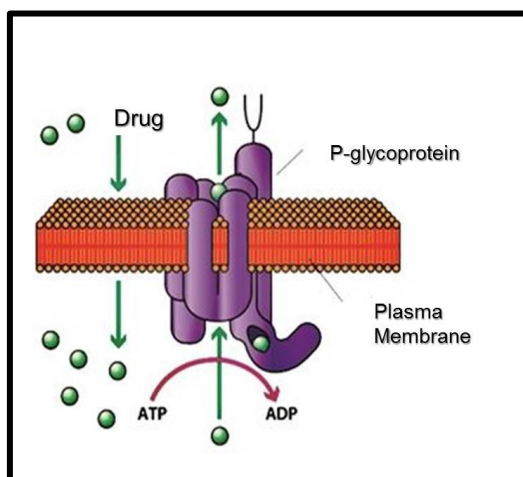


Figure 2.5: Schematic representation of the P-glycoprotein efflux transporter (www.absorption.com)

2.3 Herb-drug and supplement-drug pharmacokinetic interactions

Pharmacokinetic interactions can occur due to modulation of metabolizing enzymes as well as active transporters. Pharmacokinetic interactions are also apparent with regards to uptake carrier proteins and the modulation thereof as a result of the herbal extract or supplement used. Furthermore, changes in the gastrointestinal motility and complex formation with other substances present in the gut will lead to an alteration in the absorption of the herbal extract or supplement used. Comprehensive literature studies encompassing each of these aspects are described in more detail below.

2.3.1 Effect of herbs and supplements on enzymatic metabolism

Exogenous compounds entering the body can be chemically modified by means of either phase I or phase II metabolic reactions. Phase I metabolism involves modifications primarily mediated by the CYP450 enzyme family and the reactions include changes such as oxidation, reduction and hydrolysis. Phase II drug-metabolizing or conjugating enzymes consist of enzyme super-families that include *N*-acetyltransferases (NAT), glutathione S-transferases (GST), sulfotransferases (SULT), epoxide hydrolases (EPH), UDP-glucuronosyltransferases (UGT) and

DT-diaphorase or NAD(P)H:quinone oxidoreductase (NQO) or NAD(P)H: menadione reductase (NMO) (Iyanagi, 2007). During phase II reactions, an endogenous compound such as sulfate, glucuronic acid or glutathione are required to conjugate with the exogenous compound or its phase I-derived metabolite to generate a more polar compound, thus increasing the hydrophilicity and thereby promoting excretion in the bile and/or urine (Iyanagi, 2007; Rushmore & Kong, 2002).

The CYP450 system is a super-family of heme-containing enzymes and is responsible for phase I metabolism of various xenobiotics that include chemical drugs, herbal constituents, toxic substances and some endogenous compounds such as steroids (Zhou *et al.*, 2003). CYP450 enzymes are distributed throughout miscellaneous tissue in the body and are primarily expressed in the liver and intracellularly in the endoplasmic reticulum, however, it can also be found in the respiratory tract, lungs, brain and the small intestine (Ding & Kaminsky, 2003).

The CYP450 super-family is divided into 18 families and 42 sub-families in humans. This is based on the nucleotide sequence homology that covers 57 different human CYP450 genes (Singh *et al.*, 2011). Although a relatively large number of CYP450 isozymes participate in drug metabolism, the more prominent CYP1A2, CYP2C9, CYP2C19, CYP2D6 and CYP3A4 genes are responsible for the CYP-dependant metabolism of more than 90% of marketed drugs. CYP1A2 is exclusively expressed in the liver and contributes 13-15% to the total hepatic CYP content (Martignoni *et al.*, 2006). CYP2C (mainly 9 and 19) accounts for approximately 20% of the total human hepatic CYP450 (Gerbal-Chaloin *et al.*, 2001; Martignoni *et al.*, 2006). CYP2C is the second most abundant CYP450 after CYP3A; the latter is expressed in the liver and extra-hepatic tissues and accounts for almost 80% of intestinal CYP450 and is primarily responsible for pre-systemic drug metabolism (Paine *et al.*, 2006). CYP3A4 is the most significant drug-metabolizing CYP450 and is accountable for almost 40% of the total hepatic CYP450 and 50% of all CYP450-mediated drug metabolizing reactions (Ferguson & Tyndale., 2011; Rendic, 2002; Singh *et al.*, 2011).

It has been proven in previous studies that the inhibition and/or induction of both intestinal and liver based CYP450 enzymes are responsible for the majority of pharmacokinetic herb-drug and/or supplement-drug interactions (Fasinu *et al.*, 2014; Galetin *et al.*, 2007).

2.3.1.1 Inhibition of CYP450

Inhibition of CYP450 is either reversible or irreversible (mechanism-based inhibition). The most typical type of enzyme inhibition is reversible inhibition which can further be divided into subsections that include competitive, uncompetitive, non-competitive and mixed-type forms of inhibition. Reversible inhibitors act rapidly, are bound to the enzyme with weak bonds and do not dismantle the enzyme. Competitive inhibition is the result of competition between the enzyme

substrate and the inhibitor compound for binding to the same region on the active site of the enzyme, whereas uncompetitive inhibition is the result of the inhibitor compound binding to the enzyme-substrate complex and not the free enzyme. Non-competitive inhibition is the result of the substrate and inhibitor molecule that bind to distinct divergent regions on the enzyme, while elements of both competitive and non-competitive inhibition may also be present (Hellum *et al.*, 2007b; Nekvindova, *et al.*, 2006).

Mechanism-based inhibition, also known as suicide inhibition, entails the biotransformation of the inhibitor and occurs either via a metabolite intermediate complex or by the formation of strong covalent bonds between the reactive intermediates and specific regions of the enzyme (Hellum *et al.*, 2007b). Mechanism-based inhibition is set apart from other inhibition mechanisms due to the nicotinamide adenine dinucleotide phosphate (NADPH)-, time- and concentration-dependent enzyme inactivation, which can transpire when some herbs are modified to reactive metabolites during metabolism (Zhou *et al.*, 2004b). Irreversible inactivation of CYP450 isoforms in the presence of certain herbal constituents, may be attributed to the chemical alteration of either the heme or the CYP450 enzyme protein itself or both, which lead to the formation of covalent bonds between the heme and the CYP450 protein (Zhou *et al.*, 2004a).

A well-known pharmacokinetic interaction that demonstrates the inhibition of CYP3A4 is that of *Citrus paradisi* (grapefruit) juice, which in most cases leads to increased bioavailability of co-administered drugs. Bressler (2006) demonstrated that grapefruit juice had a significant inhibitory effect on the intestinal CYP450 system, especially pertaining to CYP3A4, with an insignificant effect on the hepatic CYP3A4 level. Kim *et al.* (2006) further expounded on this premise by proving that the intake of grapefruit juice abates CYP3A4 mRNA activity through post transcriptional activity allegedly by facilitating degradation of the enzyme. Another example of a CYP inhibitor is *Silybum marianum* (milk thistle) extract, which is a commonly used traditional medicine and is believed to promote liver health. Silimarin, the extract of milk thistle, is traditionally used for the treatment of a variety of liver disorders, dyspepsia and diabetes and has also been investigated for the potential treatment of prostate cancer (Singh *et al.*, 2004). Silimarin non-competitively inhibits CYP3A4 and CYP2C9 activity and it has been demonstrated that this inhibition may result from irreversible binding of the reactive intermediate to the heme component of both CYP3A4 and CYP2C9 (Beckmann-Knopp *et al.*, 2000; Sridar, *et al.*, 2004; Zuber *et al.*, 2002).

Prediction of the clinical outcomes as a result of the irreversible inactivation of enzymes is a challenging endeavour due to a number of drug, herb and/or patient related factors (Zhou *et al.*, 2007). Drug related factors encompass product formulation, constituent solubility, dose, dosing regimen and administration route. Herb related factors include the complexity and solubility of constituents, quality of the plant material, method of extraction, product formulation, dose, dosing

regimen and route of administration (Zhou, 2006; Zhou *et al.*, 2007). Furthermore, patient factors include genetic variations, environmental factors, age, gender and pathological conditions (Tomlinson *et al.*, 2008; Zhou, 2006).

2.3.1.2 Induction of CYP450

Induction of CYP450 enzymes is a relatively slow process that involves nuclear receptors and usually requires multiple dosing of the inducing compound. It has been demonstrated through various studies that the pregnane X receptor plays an important role in CYP3A4 induction (Geick *et al.*, 2001; Moore *et al.*, 2000; Synold *et al.*, 2001). Many of the CYP450 enzymes are inducible, e.g. CYP3A4, CYP2E1 and CYP1A2 (Xu *et al.*, 2005). Upon induction an increased amount of CYP450 enzymes are produced which will, from a biological point of view, serve as a defensive response by increasing the detoxification activity. However, from a clinical perspective, induction of CYP450 enzymes may lead to a decrease in the bioavailability of co-administered drugs with the probability of therapeutic failure due to sub-therapeutic drug plasma levels (Farkas *et al.*, 2008; Zhou *et al.*, 2004b).

Hypericum perforatum (St. John's Wort) is a popular herbal product that is commonly used for the treatment of mild, moderate and major depression (Izzo & Ernst, 2009). This herbal product has been shown to decrease the oral bioavailability of several concomitantly administered drugs by means of induction of CYP3A4 (Dürr *et al.*, 2000; Hellum & Nilsen, 2008; Ho *et al.*, 2009; Lundahl *et al.*, 2009; Mills *et al.*, 2005; Moore *et al.*, 2000). It has been demonstrated that St. John's Wort interacts with various Western medicines such as immunosuppressants, anti-depressants, anti-retrovirals, anti-cancer drugs, anxiolytics, contraceptives, anti-microbials and cardiovascular medicines (Izzo & Ernst, 2009). Examples of herbal medicines that are known to cause pharmacokinetic interactions by means of enzyme modulation with concomitantly administered drugs are listed in Table 2.2.

Table 2.2: Examples of pharmacokinetic interactions between certain herbal medicines and the CYP450 family of enzymes

Species Name	Common Name	CYP 450 Subtype	Induction/Inhibition	Reference
<i>Allium sativum</i>	Garlic extract	CYP3A4	Induction	Qiu <i>et al.</i> , 2010
<i>Echinacea angustifolia</i> & <i>E. purpurea</i>	Echinacea	CYP3A4	Hepatic induction	Hellum & Nilsen, 2008
<i>Ginkgo biloba</i>	Ginkgo	CYP3A4	Induction	Liu <i>et al.</i> , 2011
<i>Hypericum perforatum</i>	St. John's Wort	CYP3A4	Induction	Liu <i>et al.</i> , 2011
<i>Panax ginseng</i>	Ginseng	CYP450 (3A4, 2D6, 2C19, 2C9)	Inhibition	Qiu <i>et al.</i> , 2010
<i>Glycyrrhiza glabra</i>	Liquorice	CYP3A4	Induction	Colalto, 2010
<i>Serenoa repens</i>	Saw palmetto	CYP450 (3A4, 2D6,2C9)	Inhibition	Colalto, 2010
<i>Silybum marianum</i>	Milk thistle	CYP3A4	Induction	Colalto, 2010
<i>Piper methysticum</i>	Kava	CYP450 (1A2, 2C9, 2C19, 2D6, 3A4, 4A9/11, 2A6)	Inhibition	Singh, 2005
<i>Camellia sinensis</i>	Green tea	CYP3A4	Induction	Zhou <i>et al.</i> , 2003
<i>Hydrastis canadensis</i>	Goldenseal (tea)	CYP450 (2D6, 3A4)	Inhibition	Gurley <i>et al.</i> , 2008; Nowack, 2003.

2.3.2 Effects of herbal extracts and supplements on efflux transporters

2.3.2.1 The ATP-binding cassette (ABC) super-family of transporters

Most human drug transporters can be assigned to two super-families, which include the ABC efflux transporters and SLC uptake transporters that are expressed on the apical or basal surfaces of epithelial cells in various organs (Takano *et al.*, 2006). The human genome accommodates 48 ABC genes, which are responsible for many processes that occur within the cell. Any mutations in these genes are coupled with defined human diseases such as cystic fibrosis and anaemia (Borst & Elferink, 2002; Dean *et al.*, 2001). Furthermore, Borst and Elferink (2002) demonstrated that multi-drug resistance (MDR) transporter proteins play a vital role in guarding cells against cytotoxic drugs.

Modulation of ABC transporters can readily take place in the presence of exogenous compounds such as herbal medicines, foods, beverages and Western medicines. Toxic blood concentrations of the co-administered drug may develop in some cases of transporter inhibition due to the limiting nature of these transporters in terms of drug influx. Conversely, drug treatment failure may occur upon induction of the transporters resulting in sub-therapeutic plasma levels of the drug (Takano *et al.*, 2006).

P-gp (also referred to as ABCB1/MDR1), Multi-drug resistance-associated protein-2 (ABCC2/MRP2) and breast cancer resistance protein (ABCG2/BCRP) presents itself as barriers in the cellular uptake of some Western medicines (Schinkel & Jonker, 2003). P-gp recognises various structurally and pharmacologically diverse compounds as substrates. On the other hand, ABCC2/MRP2 tends to transport more hydrophilic compounds, which include glucuronide, glutathione and sulphate and will export a range of conjugated and unconjugated exogenous and endogenous compounds into the bile (Chan *et al.*, 2004). Additionally, BCRP is responsible for efflux of relatively hydrophilic anti-cancer drugs (Doyle & Ross, 2003).

2.3.2.2 P-glycoprotein (P-gp or ABCB1/MDR1)

P-gp is a product of the multi-drug resistance 1 gene also known as ABC sub-family B member 1 (ABCB1). It is a membrane bound efflux pump, which has the ability to export various substances across the cell membrane and is the leading cause of multi-drug resistance in cancerous cells (Boullata, 2005; Ho *et al.*, 2003).

Takano *et al.* (2006) determined that P-gp is a 170 000 g/mol protein consisting of 1280 amino acids. It has 12 hydrophobic transmembrane domains (TMD's) and 2 nucleotide-binding domains (NBD) and exists in the form of two homologous halves (Takano *et al.*, 2006). P-gp is expressed in an extensive range of tissues that comprise of the adrenals, kidney, liver, blood-brain barrier,

pancreas, stomach, oesophagus, colon and jejunum. P-gp is very prevalent within the intestinal brush border on the apical surface of mature enterocytes and is known to restrict the oral absorption of exogenous compounds considerably (Dhananjay & Mitra, 2006).

P-gp modulation can be allocated to three pre-dominant mechanisms, which include i) modification of the drug-membrane interaction by means of interaction with the lipid membrane of the cell thus agitating the membrane surroundings; ii) inhibition of ATP binding, hydrolysis or integrating of ATP hydrolysis to the conversion of substrates; iii) competitive or non-competitive inhibition and thus blocking transport through direct interaction with one or more binding sites on the P-gp transporter protein (Ambudkar *et al.*, 1999; Salama *et al.*, 2004).

Ginkgo biloba (ginkgo) is a commonly used herbal extract that has been shown to inhibit P-gp (Hellum & Nilsen, 2008). The dried roots of *Glycyrrhiza glabra* or *G. uralensis* (liquorice) contains active constituents such as glycyrrhetic acid, glabridin, isoliquiritigenin and the main constituent glycyrrhizin (Choi *et al.*, 2011). Glycyrrhetic acid and glycyrrhizin have demonstrated the ability to inhibit P-gp while glabridin had failed to elicit any inhibitory effect on P-gp (Nabekura *et al.*, 2008; Najjar *et al.*, 2010).

As mentioned before, certain constituents of *C. paradisi* (grapefruit) juice, prenylated furanocoumarins and bergamottin, have the ability to inhibit CYP3A4, but is also known to irreversibly inhibit intestinal P-gp related efflux (Bressler, 2006). As mentioned above, *H. perforatum* (St. John's Wort) a commonly used herbal product is known to initially inhibit human CYP3A4 and P-gp, but this inhibition is then followed by an induction of human CYP3A4 and P-gp by means of the pregnane X receptor (Dürr *et al.*, 2000). *Allium sativum* (garlic) has been used as a herbal medicine for more than five thousand years and it has been reported to have immune-enhancing, anti-platelet, anti-microbial, anti-tumour and hypolipidemic characteristics (Choi *et al.*, 2011). Constituents contained in garlic comprises of a high-level of sulphur-containing compounds such as allicin and alliin, various flavonoids/isoflavonoids like nobiletin, quercetin, rutoside and tangeretin. Further constituents include prostaglandins, polysaccharides, saponins and terpenes (Singh *et al.*, 2001). Lee *et al.* (2006) demonstrated that garlic extract induced intestinal P-gp in clinical studies. A 21 day usage of garlic extract showed an induced expression of intestinal P-gp by 31%. Garlic is a known supplement used by patients infected with HIV and it is of utmost importance to advise patients on the effect that garlic may have when co-administered with protease inhibitors such as saquinavir and ritonavir (Chen *et al.*, 2012).

2.3.2.3 ABCC2/Multi-drug resistance-associated protein-2

MRP2 or ABC subfamily C member 2 (ABCC2) is part of the 9-member human sub-family of multi-drug resistance-associated proteins (MRP1-MRP9) and consists of a 145-amino-acid, 190 kDa

protein with two ATP-binding domains and 17 TM regions (Mandava *et al.*, 2010; Takano *et al.*, 2006). The ABCG2 was also as a collective on a high level basis appositely identified as a multi-specific organic anion-excreting transporter situated across the hepatocyte canalicular membrane (Wada, 2006), but also presents itself at the brush-border membrane of renal proximal tubule cells and absorptive enterocytes. Furthermore, it can be found at the apical membrane of the gallbladder epithelial cells (Borst *et al.*, 2000; Keppler *et al.*, 1997; Mottino *et al.*, 2001; Rost *et al.*, 2002).

The use of St. John's Wort for medicinal purposes has been shown to mediate an increase in MRP2 levels through trans-activating the pregnane X receptor. Other natural products like carotenoids and their metabolites have also shown a tendency to increase MRP2 expression. Genipin, a component present in various herbal medicines, has demonstrated a potent choleric effect by enhancing MRP2 levels in the bile canaluculi by means of increased MRP2 expression (Fardel *et al.*, 2005).

2.3.2.4 ABCG2/Breast cancer resistance protein

BCRP is associated with the ABC White (ABCG) sub-family that contain 'half-transporters' (Venkataramanan *et al.*, 2006). BCRP is a 655-amino-acid, 72 kDa protein which is expressed in high levels in the placental syncytiotrophoblasts and in lower levels in the breast, ovaries, small intestine, colon and liver. BCRP differs from other ABC transporters, which as a rule usually have 2 ATP-binding regions and 2 TM regions, while BCRP has only one nucleotide binding domain (Chan *et al.*, 2004; Takano *et al.*, 2006).

Previous studies have shown that BCRP activity may be inhibited by the consumption of food and herbal extracts which contain certain flavonoids such as apigenin, chrysin, biochanin A, kaempferol, genistein, naringenin, sillimarin and hesperetin (Yang *et al.*, 2004).

2.3.3 Effects of herbs on uptake carrier proteins

The SLC superfamily of transporters is the biggest collection of transporters, which consist of approximately 225 proteins such as organic anion transporting polypeptides 1B1 (OATP1B1), OAT1B3, and organic cation transporter 1 (OCT1). OATP's are responsible for facilitating the transmembrane transport of various substrates such as metabolic products, drugs and xenobiotics (Beringer & Slaughter, 2005). These transporters are situated on the basolateral membrane of hepatocytes and mediate uptake into the hepatocytes (Mandery *et al.*, 2012). Naringin, a flavanone glycoside which is a component in grapefruit juice has the ability to inhibit the uptake active transporter organic anion transporting polypeptide (OATP) 1A2 and thereby decreasing the bioavailability of certain co-administered drugs (Farkas & Greenblatt, 2008). Kobayashi *et al.* (2003) demonstrated that *Camellia sinensis* (green tea) contains a polyphenolic

catechin namely (-)-epigallocatechin gallate (EGCG) that has the propensity to inhibit OATP-B and thus reducing drug carrier-mediated transport. On the other hand, Okamura *et al.* (1993) proposed that induction of OATP may under certain circumstances increase drug uptake and have toxic plasma drug levels as a result.

2.3.4 Effects of herbs on gastrointestinal motility

Gastrointestinal motility describes the process where the ingested compounds and food products move from the stomach to the rectum. Gastrointestinal motility can be altered after the consumption of certain herbal products, which can either slow down or increase the rate of motility. Both scenarios can have a pronounced impact on the therapeutic outcome of concomitantly administered drugs. Herbally-induced diarrhoea will reduce the transit time of the drug in the GIT and will result in an abridged contact time with the gastrointestinal epithelium and thus lower drug absorption. *Capsicum sp.* (Chilli pepper) known for its spicy taste contains capsaicin (8-methyl-N-vanillyl-6-ninemamide), the main phytochemical in its extract. Debreceni (1999) found that capsaicin increases gastric emptying in humans, possibly by means of stimulating the sensitive afferent nerves. The rhizomes of *Zingiber officinale* (ginger) contains gingerols (zingerone, zingerberol) and shogaols that have a “pro-kinetic” pharmacological effect and therefore enhances gastric emptying and affects drug absorption (Borrelli *et al.*, 2004; Hu *et al.*, 2011). *G. biloba* (ginkgo) leaf extracts (main pharmacologically active phytochemicals: terpene lactones, ginkgolides A, B and C, and bilobabides) and *Piper methysticum* (kava) extracts were shown to increase gastrointestinal motility in *in vivo* studies (Colalto, 2010; Dubey *et al.*, 2004). Induced diarrhoea as side effect of *Echinacea purpurea* (Echinacea) and *H. perforatum* (St. John’s Wort) was also shown to influence drug absorption in a similar manner (Colalto, 2010).

Functional gastrointestinal disorders like functional dyspepsia (FD) and motility associated dysfunctions like irritable bowel syndrome (IBS) or slow transit are treated symptomatically due to multifactorial pathogenesis. As a result of this a multifactorial pathogenesis therapy with multi-target action is the optimum approach in treatment of the aforementioned syndromes (Heinle *et al.*, 2006). STW 5 (Iberogast®) is a fixed combination product used as gastrointestinal phytotherapeutic medicine that consist of nine different herbal product extracts e.g. bitter candy tuft (15%), angelica root (10%), *Citrus limonum* (lemon balm) leaves (10%), *Glycyrrhiza glabra* (liquorice) root (10%), caraway fruit (10%), greater celadine herb (10%), *Matricaria recutita* (chamomile) flower (20%), *Silybum marianum* (milk thistle) fruit (10%) and *Mentha piperita* (peppermint) leaves (5%) with a final concentration of 31% ethanol (Reichling & Saller, 2002). This preparation has demonstrated modulating effects on different regions of the intestinal muscle causing relaxation of the circular and longitudinal muscle strips and contraction of the antral muscle strips of mouse intestines (Hohenester *et al.*, 2004). These are both desired effects in

patients suffering from dyspepsia and impeded gastric emptying as it enhances the relaxation of the fundus and corpus and increases antral activity (Sibaev *et al.*, 2006).

Epigallocatechin-3-gallate (EGCG) is a well-documented polyphenol that is derived from *C. sinensis* (green tea) and previous studies have shown that the use of green tea extracts may cause a delay in the gastric emptying time (Jang *et al.*, 2005).

2.3.5 Herb-drug and supplement-drug complex formations

The co-administration of herbal medicines or supplements and Western medicines can lead to the formation of insoluble herb-drug complexes in the GIT that can significantly reduce the bioavailability of the drug. Herbs that contain hydrocolloidal carbohydrate components such as gums and mucilages are soluble in water and poorly absorbable (i.e. membrane permeable). Fibres like psyllium and alginates are prime examples of herbs that are prone to binding to other drugs, especially when consumed in powder form. Psyllium, for example, inhibits the absorption of lithium; it also reduces the clinical efficacy of drugs such as metformin and glibenclamide (Chiesare *et al.*, 1995; Kuhn, 2002). Drugs such as cholestyramine (Questran[®]), colestipol (Colestid[®]), sucralfate (Carafate[®]) and orlistat (Xenical[®]) may form insoluble complexes with certain herbal extracts resulting in decreased absorption of both substances (Chen, 2006). Antibiotics like fluoroquinolones and tetracyclines bind to iron, calcium and calcium-enriched foods and supplements (Leigh, 2008). Zinc on the other hand, administered in the form of zinc lozenges and taken for a common cold, will chelate fluoroquinolones and tetracyclines resulting in lower serum concentration levels of the antibiotics (Scott & Elmer, 2002). Furthermore, iron supplements may impede the absorption of angiotensin-converting enzyme inhibitors by means of complex formation within the GIT (Boullata, 2005). Due to this potential chelating and complexation effects of certain antibiotics and mineral components in herbal preparations, it is considered good practice to administer the problematic herbal products either two hours before or two hours after the dose of potentially interacting medicine to prevent exiguous absorption of the drug (Kuhn, 2002).

2.4 Models to predict drug absorption

2.4.1 *In vivo* models

In vivo animal models are extensively used to investigate intestinal drug absorption and metabolism (Alqahtani *et al.*, 2013). The anatomy of mammals such as rats, dogs, monkeys and pigs exhibit functional correlation with that of humans and as a result, the characteristics of drug absorption in animals can in most cases be used as a trustworthy indicator of the biological factors that can impede intestinal drug absorption in humans (Hidalgo, 2001). However, differences regarding anatomical and physiological facets between human and animal models do exist such as transporter proteins, metabolizing enzymes, pH, gastric emptying rate and gastrointestinal motility (Alqahtani *et al.*, 2013).

One of the main amenities of using *in vivo* models to examine drug absorption is the interplay of the dynamic components that include the mesenteric blood circulation, the mucous layer and all other biological factors which influence drug absorption (Le Ferrec *et al.*, 2001). Another amenity displayed by *in vivo* models is the fact that it delivers multi-factorial results, it provides an integrated effect of absorption, distribution, metabolism and excretion, and can yield a quantitative set of pharmacokinetic parameters and toxicological properties (ADMET) (Zhang *et al.*, 2012).

However, limitations associated with *in vivo* models include the difficulty of differentiation between relevant variables such as the individual rate-limiting factors that influence drug absorption and bioavailability (Le Ferrec *et al.*, 2001). Furthermore, ethical issues comes into play as a large number of animals are required and analysis of the drug in the blood plasma can render itself invasive and the 3 R principle (replacement, reduction and refinement needs to be taken into account (Sjögren *et al.*, 2014)). Lastly, this model can only provide restricted insight into the specific mechanism of absorption and renders itself as an expensive procedure (Hidalgo, 2001). These factors render *in vivo* animal models impractical for high-throughput screening and could be the cause of failure to progress to the next phase of development. *In vivo* models need to be replaced by high-throughput screening techniques to ameliorate the process (Balimane *et al.*, 2000; Spalding *et al.*, 2004).

2.4.2 *In vitro* models

The use of animals in experimental research has led to an ethical dilemma and the increased interest in and the concern for animal welfare prompted the sanction of legislative regulations in numerous countries and the inauguration of animal ethics committees (Baumans, 2004). Furthermore, modern drug development is confronted with numerous obstacles regarding the discovery and development of new chemical entities (NCE). This process delineates a highly complex, inefficient and costly process, but the implementation of novel predictive absorption

models can lead to faster and more efficient development of effective NCE's and will shorten the time-to-market period (Cunha *et al.*, 2014; Lipsky & Sharp, 2001).

The concept of *in vitro* models involves any experiment conducted in a controlled environment external from a living organism e.g. cell cultures, artificial membranes and excised tissue (Dixit *et al.*, 2012; Reis *et al.*, 2013; Volpe, 2010). *In vitro* models, which are used to predict intestinal absorption, can be divided into cell-based models (Caco-2 cells, Mardin-Darby canine kidney [MDCK]), tissue-based models where excised tissues from animals are used or membrane-based (e.g. parallel artificial membrane permeability assay [PAMPA]). These models are described in more detail in Table 2.3.

Researchers have developed *in vitro* models to gain a thorough understanding of membrane permeation and metabolism and also for assessing drug disposition, pharmacokinetics, drug efficacy and disease mechanisms (Mudra *et al.*, 2001). Furthermore, *in vitro* models can be utilised to assess a large amount of different combinations of experimental parameters and such high-throughput testing are generally not attainable with animal-based models (Nelita & Yuan, 2011).

A controlled environment implies that various factors pertaining to pharmacokinetics and drug metabolism can each be analysed as single components (Spalding *et al.*, 2000). A major advantage associated with the use of *in vitro* models is the identification with regards to the permeability and metabolic profile of the NCE amid the precocious stages of drug development. Furthermore, data arising from these methods are more pertinent and relevant to conclude human *in vivo* situations in comparison to other models used (Baranczewski *et al.*, 2006).

However, Balimane *et al.* (2000) demonstrated that the use of *in vitro* models encompass certain limitations and that the effects of physiological factors such as gastrointestinal transit rate, gastric emptying and the gastrointestinal pH cannot be desegregated in the data analysis.

Table 2.3: Advantages and limitations of a selection of *in vitro* models and techniques which are commonly used for permeation studies

Model	Technique	Advantages	Limitations	Reference
<u>Excised tissue-based models</u>				
Ussing Chambers	Isolation and dissection of tissue into strips of appropriate size. Clamping of sample onto acceptable device where after the rate of drug transport across the membrane is measured.	<p>Possibility of drug absorption and passage at specific intestinal regions.</p> <p>Both apical and basolateral sides can be tested.</p> <p>Metabolism studies are feasible.</p>	<p>Viability, the sample can only be used up to 2-3 h after isolation; integrity of the intestinal cells decreases with time.</p> <p>Drugs are diluted in the diffusion chamber thus the analytical technique must be sensitive.</p> <p>Absence of blood supply and end nerve innervation.</p>	<p>Balimane <i>et al.</i>, 2000</p> <p>Alqahtani <i>et al.</i>, 2013</p> <p>Le Ferrec <i>et al.</i>, 2001</p>
Everted gut	Isolation of intestine is followed by flushing of the sac with cleaning solution, everted with a glass rod and subsequently filled with oxygenated medium. Each sac is submerged in a drug containing medium for a calculated time period and is followed by the measuring of the drug concentration within the sac.	<p>Fast, cheap and utilised to study substrates of carrier-mediated and efflux transport systems.</p> <p>Isolated intestinal regions can be tested during drug absorption studies.</p>	<p>Small closed serosal compartment reduces sink conditions due to the absence of blood perfusion.</p> <p>Compound must cross entire intestinal wall including the muscle layer.</p>	<p>Alqahtani <i>et al.</i>, 2013</p> <p>Bohets <i>et al.</i>, 2001</p> <p>Dixit <i>et al.</i>, 2012</p>

Cell-based models

Caco-2 cells	Isolated human colon adenocarcinoma cells. In culture these cells grow and manifests as a polarized monolayer. This displays similar morphological and functional characteristics as the human intestinal enterocytes. Tight junctions are formed and enzymes and transporter proteins are expressed.	A flexible, relatively fast and easy method. Can be utilised for drug screening testing. Test drug can be introduced to either apical or basolateral side.	Physiological factors that improve transport (e.g. cholesterol, mucous, bile salts). Long time period required to form tight junctions. Low amount of CYP3A4 is expressed. A model with only one cell type. P-gp influence is arduous to determine.	Abuasal <i>et al.</i> , 2012 Alqahtani <i>et al.</i> , 2013 Gundogdu <i>et al.</i> , 2011 Le Ferrec <i>et al.</i> , 2001
MDCK cells	Cells derived from the distal tubular part of the dog kidney. Cells grow to form a polarized monolayer with completed tight junctions. A culture time of 3-5 days is required.	Fast and simple method utilised for drug screening testing. Passive diffusion can be measured.	Not an intestinal model, its origin is from a canine kidney.	Alqahtani <i>et al.</i> , 2013 Bohets <i>et al.</i> , 2001 Le Ferrec <i>et al.</i> , 2001

Membrane based models

PAMPA	A hydrophobic filter material is coated with a mixture of lecithin/phospholipids. It is further dissolved in an inert organic solvent (e.g. dodecane). This leads to the creation of an artificial membrane known to mimic the endothelial membrane of the human.	Low cost, high throughput method. Less labour intensive than cell culture models.	Cannot predict absorption for compounds actively absorbed by drug transporters.	Balimane <i>et al.</i> , 2000 Reis <i>et al.</i> , 2013
-------	-------------------------------------------------------------------------------------------------------------------------------------------------------------------------------------------------------------------------------------------------------------------	-----------------------------------------------------------------------------------	---------------------------------------------------------------------------------	----------------------------------------------------------------

2.4.3 *In situ* models

In situ refers to an experiment conducted on a body part that has not been completely removed from the living organism, e.g. the intestinal segment into which a drug solution is introduced can either be a single pass perfusion, recirculating perfusion, closed-loop and/or oscillating perfusion through parts of the intestinal tract. The development of these stable, vascularly perfused models has provided a powerful exploration device for the examination of intestinal transport and metabolism. *In situ* models have various advantages, such as bypassing the stomach, which means the precipitation of acidic compounds are not conceivable, thus dissolution rate does not perplex intestinal drug concentrations and therefore plasma levels. This model also makes it possible to assess compound secretion into the intestinal lumen after intravenous administration, i.e. it is possible to inspect the effect of transport of xenobiotics into the intestinal lumen by means of P-gp, multidrug resistance-associated protein (MRP) and lung cancer-associated resistance protein (LRP) from the systemic circulation (Le Ferrec *et al.*, 2001). Further desirable attributes of the *in situ* model include the presence of an intact mucosal layer, good blood perfusion, an intact nerve system as well as the expression of enzymes (Holmstock *et al.*, 2012). However, this model requires the use of highly sophisticated instruments and expert surgical procedures to be performed by trained personnel. Furthermore, to obtain statistically significant data, a large number of animals are required, which make this a less suitable option for screening of large numbers of compounds (Hamman, 2007; Luo *et al.*, 2013).

2.4.4 *Ex vivo* models

Ex vivo pharmacokinetic studies pertain to methods where a drug is applied to one side of excised animal/human tissues and samples are collected on the other side over time (Zhang *et al.*, 2012). This involves techniques such as everted sacs and excised tissue pieces mounted in Ussing chambers that overlap with the “*in vitro*” experimental model (Dahan & Hoffman, 2007). *Ex vivo* models differ to some degree with *in vitro* models and are distinguished by various unique features such as the existence of a mucous layer, the presence of transporter proteins and paracellular transport pathways as well as drug metabolising enzymes (Luo *et al.*, 2013).

The advantages of this technique entails that it is rapid, inexpensive and can be utilised to study substrates of efflux and carrier-mediated transporter systems. Furthermore, it can also be employed for the study of region specific intestinal drug absorption. Drug metabolism studies can be performed in conjunction with bi-directional transport studies (Antunes *et al.*, 2013). However, limitations regarding this model, especially pertaining to everted sacs, include the relatively small volume inside the sac, rendering this model useless for well absorbed compounds due to the abridgement of the sink conditions (Alqahtani *et al.*, 2013). *Ex vivo* techniques are arduous to master, which can lead to damage of tissue and fluctuations in the resultant transport of the drug.

Furthermore, inter-experimental variations may occur due to variations in tissue sample preparation and setup times (Antunes *et al.*, 2013).

2.4.5 In silico models

In silico refers to computational models with the ability to assess the ADME properties of most compounds. The major amenity of these models is their ability to reduce the cost during the early stages of drug discovery and therefore the use of these models will increase in the future (Alqahtani *et al.*, 2013). The rapid development of computer technology in the past decade has led to extensive progress in the development of drug permeability prediction software (Stenberg *et al.*, 2000).

In silico models includes simple rule-based modelling (e.g. Lipinski's rule of five), structure-activity relationships (SAR), three-dimensional quantitative structure-activity relationships (QSAR), and the recognition of pharmacophores (Hutter, 2009; Krejsa *et al.*, 2003). A drawback regarding this method is its inability to study herb-drug interactions due to various uncertainties regarding the constituents of herbal extracts and their activity *in vivo* and the acquisition of the correct parameters may be difficult to obtain (Hellum, 2007a).

2.5 Selected herbal extracts and non-herbal supplements investigated in this study

2.5.1 Methylsulfonylmethane (MSM)

Methylsulfonylmethane (MSM) is an organic sulfur containing substance also known as dimethyl-sulfone (DMSO₂) or methyl sulfone, the oxidised form of dimethyl-sulfoxide (DMSO) (Usha & Naido, 2004) (Figure 2.6). Approximately 15% of the total amount of DMSO that is metabolised is converted to MSM (Pagonis *et al.*, 2014). MSM is present in a wide variety of human foods and is naturally prevalent in an array of fruits, vegetables, grains and the most abundant source of MSM, namely cow's milk, contains a generous 3.3 parts per million (ppm) of this compound. MSM forms an integral part of proteins, connective tissues, hormones and enzymes (Jacob & Appleton, 2003; Parcell, 2002). Usha and Naido (2004) demonstrated that MSM is exceedingly more stable than DMSO₂, but still demonstrates pharmacotherapeutic qualities equal to DMSO₂ without the slightly bitter taste and skin irritation that has been reported with the use of DMSO₂.

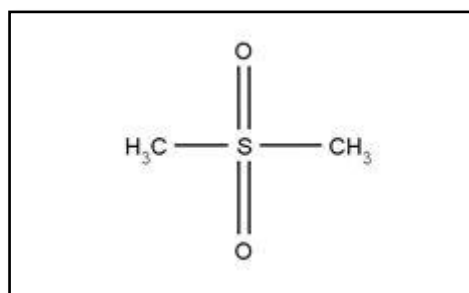


Figure 2.6: The chemical structure of methylsulfonylmethane

2.5.1.1 Medicinal applications of methylsulfonylmethane (MSM)

Jacob and co-worker demonstrated in 2003 that the primary mechanism of action of MSM is through the donation of sulfur, which is a major component in connective tissue and strengthens it by forming cross-linkages called disulphide bonds (these are the links in the chains of glycosaminoglycan that build cartilage). MSM is therefore primarily used for its anti-inflammatory properties in the treatment of osteoarthritis (OA). Other clinical indications for MSM include the treatment of interstitial cystitis, scleroderma, fibromyalgia, systemic lupus erythematosus and repetitive stress injuries (Jacob & Appleton, 2003).

2.5.1.2 Pharmacokinetics of methylsulfonylmethane

A study performed on the metabolism and excretion of DMSO indicated that the primary metabolite, namely DMSO₂, is discernable in the blood serum at approximately two hours after ingestion. Upon stopping the therapy, the DMSO₂ blood concentration declined over the following 96 hours until only a fragment remained after 5 days. The extent of absorption in animals was showed to be similar as in humans, but elimination of the supplement was more rapid in animals than in humans (Jacob & Appleton, 2003). Studies regarding potential MSM-drug interactions are of paramount importance due to the high frequency of consumption of this supplement by geriatric patients. Varied co-morbid conditions suggested that the best therapy for OA is the concomitant use of various drug compounds. MSM in combination with other Western medicines was reported to give better pharmacological outcomes than other combinations (Pagonis *et al.*, 2014).

2.5.2 Hoodia gordonii

2.5.2.1 Botany of *Hoodia gordonii*

The World Health Organisation (WHO, 2015) estimated in 2014 that globally more than 1.9 billion adults, 18 years and older, were overweight of which an astounding 600 million were obese.

Hoodia gordonii forms part of the genus *Hoodia* that is classified as stapeliads within the tribe Ceropegieae of the subfamily Asclepiadoideae relating to the Apocynaceae family. The complete botanical name is *Hoodia gordonii* (Masson) Sweet ex Decne (Vermaak *et al.*, 2011a). *H. gordonii* is a spiny succulent plant with small rows of thorns along the grey-green to grey-brown stems (Figure 2.7). The height and length of the plant is usually congruent with a height of up to approximately one meter. The large flowers, usually flesh coloured, are borne on or near the terminal apex. Flower size varies (typically 50-100 mm) depending on the flowering period. Pollination is achieved by means of flies and blowflies that are attracted by an unpleasant smell resembling decaying flesh (Van Wyk & Wink, 2004). As a result of the plant's limited growth area and slow cycle of maturation, *H. gordonii* is limited in its supply. Due to this reason, *H. gordonii* is listed on the endangered species list as conservation concern and export out of South Africa is strictly regulated (Rader *et al.*, 2007).



Figure 2.7: Photographs showing *Hoodia gordonii* plants (Van Wyk *et al.*, 2000)

2.5.2.2 Chemical composition of *Hoodia gordonii*

Previous studies have indicated that two steroidal glycosides have been isolated from *H. gordonii* namely P57AS3 glycoside, more commonly referred to as P57, and hoodigogenin A (see Figure 2.8). Many other structural analogues were later identified and isolated from *H. gordonii* namely

eleven oxypregnane glycosides-hoodigoside A-K; ten pregnane glycosides-hoodigoside; ten steroidal glycosides-gordonoside A-I, L; seven pregnane glycosides-hoodigoside V-Z and hoodistanaloside A-B (Dall'Acqua & Innocenti, 2007; Pawar *et al.*, 2007). The corner stone chemical structures of these compounds are hoodigogenin A, calogenin, hoodistanal, dehydrohoodistanal and isoramanone (Avula *et al.*, 2008).

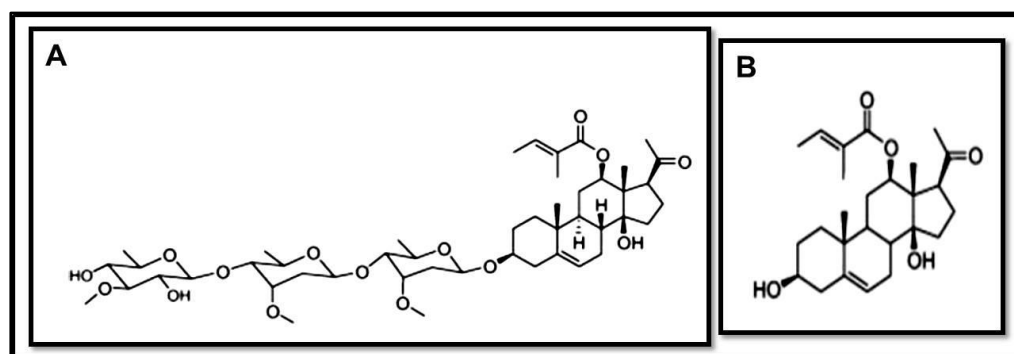


Figure 2.8: The chemical structures of P57, **A)** and hoodigogenin A, **B)**

2.5.2.3 Medicinal applications of *Hoodia gordonii*

H. gordonii is a commercially important medicinal plant with anti-obesity potential that is believed to suppress appetite and have anorexic action (Kamsu-Foguem & Foguem, 2014). According to African folklore *Hoodia* was utilised as treatment in a wide variety of ailments such as abdominal cramps, haemorrhoids and tuberculosis. The Xhmani San Bushmen in the Kalahari Desert would consume fresh *H.gordonii* with the sole purpose of aiding in hydration and suppression of their appetites when undertaking long hunting trips (Avula *et al.*, 2007).

2.5.2.4 Pharmacokinetic interactions of *Hoodia gordonii*

In 2008, Madgula and co-workers demonstrated that P57 inhibited CYP3A4 activity with an IC_{50} value of 45 μ M, however, the activity of CYP1A2, CYP2C9, and CYP2D6 was not inhibited. It was also demonstrated that intestinal transport of P57 is mediated by P-gp efflux transporters, which resulted in the efflux of the compound (Vermaak *et al.*, 2011b). However, the effect of *H. gordonii* extract or pure P57 on drug pharmacokinetics has not yet been investigated.

2.5.3 *Vitis vinifera* seed extract

2.5.3.1 Botany of *Vitis vinifera*

Vitis vinifera seed extract is derived from the seeds of grapes (*Vitis vinifera* L.). *Vitis vinifera* L. is a type of woody perennial vine that belong to the Vitaceae family. The grape vine is a woody climber that can, during the pruning stage, reach a height of 1-3 m. The leaves can be described as circular or oval, thin, toothed or vaguely dented on the edges, with a diameter of 5-23 cm. The

leaves consist of 4-5 lobes and the colour varies from the upper face to the lower face, the former having a dull green colour and the latter a stormy grey tone. Unostentatious flowers are grouped in clusters. Bunches of green, reddish or dark red fruit with a diameter of 6-12 mm may be present in various forms (Van Wyk & Wink, 2004; http://www.botanical-online.com/english/grape_vine.htm).

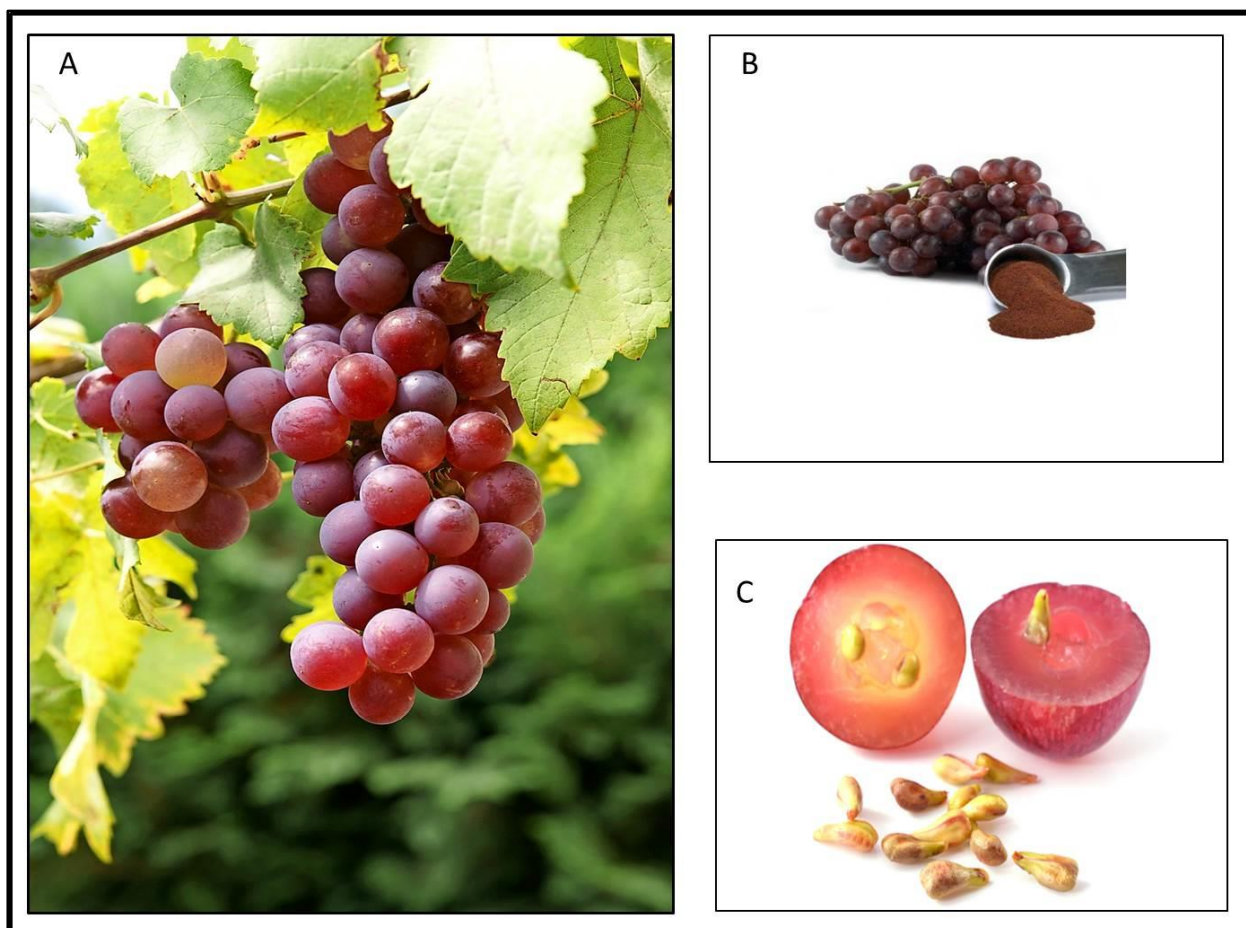


Figure 2.9: Photographs showing leaves and fruit of *Vitis vinifera* (Kleist, 2016) **A)** *Vitis vinifera* seed extract (www.gonutra.com) **B)** and **C)** *Vitis vinifera* seeds (London, 2015)

2.5.3.2 Chemical composition of *Vitis vinifera*

Vitis vinifera seed extract is known for its high polyphenolic content (Madhavan *et al.*, 2016). These polyphenolic derivatives include bioactive compounds such as phenolics, flavonoids, anthocyanins, stilbenes and vitamin E (Ali *et al.*, 2010; Ananga *et al.*, 2013, Nassiri-Asl & Hosseinzadeh, 2009). Flavan-3-ols form an intricate sub-class of flavonoids that are composed of monomeric flavan-3-ols [(+)-catechin, (-)-epicatechin, and (-)-epicatechin-3-O-gallate], oligomeric (2-5 units) and polymeric (6-20 units) procyanidins. Procyanidins/proanthocyanidins (these two terms are used interchangeably) consist of flavan-3-ol monomeric units, which are

linked at C4-C8 and C4-C6 by interflavanic bonds (Monages & Hernández-Ledesma, 2005; Tsang *et al.*, 2005).

The formation of procyanidins can be attributed to the condensation of monomeric units. Two to five units will result in the formation of oligomers and the condensation of more than five units will form polymers. Procyanidins can differ due to the position and configuration of its monomeric linkages. The dimers B1, B2, B3 and B4 are the most abundant (see Figure 2.10) (Tsang *et al.*, 2005). Flavanols (flavan-3-ols) and flavanol oligomers and polymers (procyanidins) are considered to be important flavonoids due to their inherent anti-oxidant properties (Pannala *et al.*, 2001).

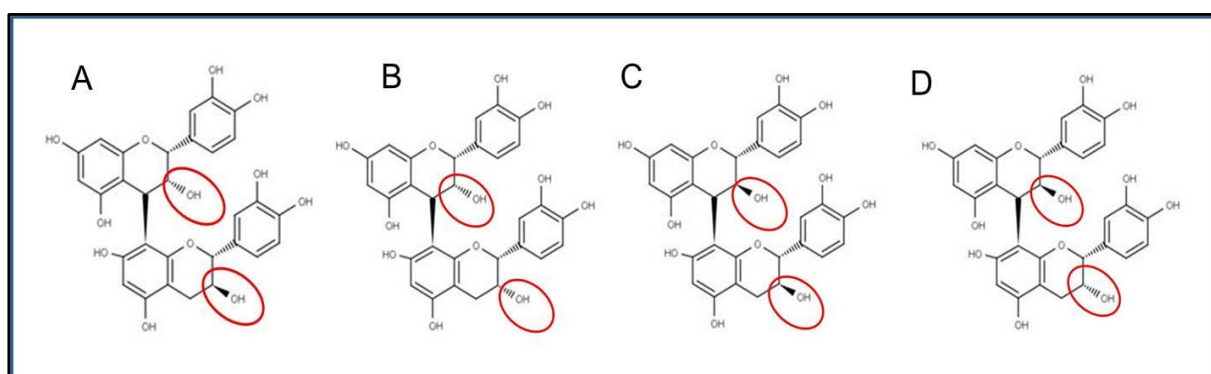


Figure 2.10: The chemical structures of procyanidins illustrating the position of the different monomeric linkages as demonstrated by the configuration of the OH groups with **A)** as procyanidin B1, **B)** as procyanidin B2, **C)** as procyanidin B3 and **D)** as procyanidin B4

2.5.3.3 Medicinal applications of *Vitis vinifera*

V. vinifera has been used for its medicinal properties for well over thousands of years, which has not only been used for its enormous therapeutic contribution, but also for its nutritional value. The vines, leaves, stem and seeds contain procyanidins, which were used to treat conditions such as blood clotting, cancer, nausea, inflammation, cholera, smallpox, eye infections and also skin, kidney and liver diseases. Many pathological conditions such as metabolic disorders, cell ageing, atherosclerosis, carcinogenesis and inflammation are associated with the presence of free radicals, reactive oxygen species (ROS) and reactive nitrogen species (Madhavan *et al.*, 2016).

Traditionally, the anti-oxidative ability of polyphenols has been attributed to their potential of scavenging free radicals. Bagchi *et al.* (2002) demonstrated that phenolic procyanidins originating from *V. vinifera* seed extract have a far more superior ability to scavenge for free radicals than Vitamin E, C and β -carotene. It is also a blood thinner due to the action of procyanidins on limiting platelet adhesion making it a blood anti-coagulant that increases clot

time. It was also reported that *V. vinifera* seed extract had exhibited anti-ulcer activity on stomach lesions and this anti-ulcer activity can be attributed to the presence of procyanidin oligomers. A study conducted by Saito *et al.* (1998) showed that oligomers, which are longer than three catechin units, had a notable protective effect on a stomach mucosal injury.

2.5.3.4 Pharmacokinetic interactions of *Vitis vinifera*

Resveratrol, an electron-rich molecule with two aromatic benzene rings linked by an ethylene bridge, is an important constituent in *V. vinifera* seed extract (Choi *et al.*, 2011; Rodríguez-Fragoso *et al.*, 2011). Chan and Delucchi demonstrated in 2000 that resveratrol is an irreversible inhibitor of CYP3A4 and a non-competitive reversible inhibitor of CYP2E1. Rodríguez-Fragoso and colleagues expounded on this by proving that aromatic hydroxylation and epoxidation of resveratrol, mediated by CYP3A4, conceivably produced a reactive metabolite namely *p*-benzoquinonemethide. This reactive metabolite was reported to bind covalently to the CYP3A4 enzyme, which consequently inactivated the enzyme (Rodríguez-Fragoso *et al.*, 2011).

2.5.4 Harpagophytum procumbens

2.5.4.1 Botany of *Harpagophytum procumbens*

Harpagophytum procumbens (Pedaliceae) is a weedy, perennial tuberous plant that presents distinctive fruit. The fruits have abundant, strikingly long, protrusions with sharp, grapple-like hooks and two straight thorns on the upper surface. This characteristic leads to its name commonly known as Devil's Claw (Mncwangi *et al.*, 2012). The flowers are tubular and present with a purplish-pink colour with a yellow and white throat set against sea-green leaves divided into lobes (Stewart & Cole, 2005). The creeping stems (up to 2 m long), will periodically sprout from the perpetual primary tubers, which can reach up to 2 m in length. The stems provide a number of secondary storage tubers (up to 25 cm long with a diameter of 6 cm). The secondary tubers are usually harvested and used because of their medicinal properties (Stewart & Cole, 2005).



Figure 2.11: Photograph of *Harpagophytum procumbens* fruit and flowers (Smithies, 2006)

2.5.4.2 Chemical composition of *Harpagophytum procumbens*

Constituents of *H. procumbens* include iridoids, harpagoquinones, amino acids, flavonoids (kaempferol), phytosterols (β -sitosterol and stigmasterol) and carbohydrates. Harpagoside is the primary iridoid glycoside isolated from *H. procumbens*, and is considered to be the primary active constituent together with harpagide and procumbide (Mncwangi *et al.*, 2012).

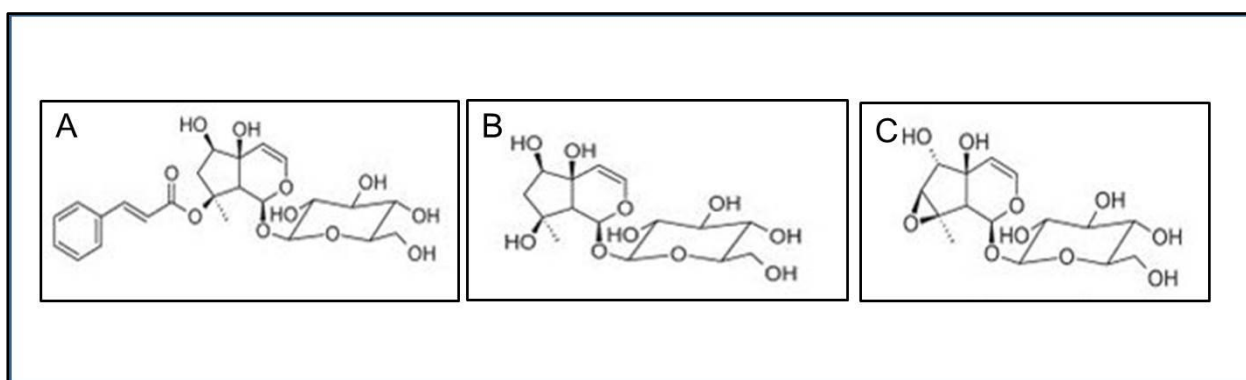


Figure 2.12: Chemical structures of *Harpagophytum procumbens* constituents: **A)** Harpagoside, **B)** Harpagide, and **C)** Procumbide

2.5.4.3 Medicinal applications of *Harpagophytum procumbens*

H. procumbens is used for the treatment and prevention of a wide variety of medical conditions. It is utilised for its anti-inflammatory activity, analgesic activity, anti-oxidant activity, anti-diabetic, anti-microbial, anti-malaria and anti-cancer activity (Mncwangi *et al.*, 2012). It is administered to patients in the form of infusions, decoctions, tinctures, powders and extracts to treat conditions like dyspepsia, wounds and skin rashes, appetite stimulation, blood diseases, fever, urinary tract

infections, postpartum pain, sores, ulcers, boils and liver and kidney disorders (Akhtar & Haqqi, 2012).

H. procumbens was shown to be beneficial in pain alleviation and the improvement of movement in musculoskeletal conditions such as OA. The mechanism of pain relief is rooted from the ability of *H. procumbens* to block the production of inflammatory mediators like PGE₂ and therefore relieves inflammation and pain. It can either be used as a single or combination therapy (Akhtar & Haqqi, 2012; Street & Prinsloo, 2012). Even though *H. procumbens* is indicated for the treatment of osteoarthritic and lower back pain, Vlachoianis *et al.* (2008) demonstrated that adverse reactions (mainly gastrointestinal) may occur during the course of treatment. No negative interactions have been reported in the event of concomitant use of *H. procumbens* and conventional medicines used for rheumatoid arthritis, which supports the theory that *H. procumbens* can be used as adjunct therapy for these conditions (Grant *et al.*, 2007). Furthermore, due to its reported cardiac activity, treatment with *H. procumbens* is not recommended for chronic treatments and pertaining to the lack of data with regards to pregnancy and lactation treatment should also be avoided by these patients (Barnes, 2009). Additional data pertaining to the effects of chronic use of *H. procumbens* is crucial to ensure patient safety, especially during long term use (Vlachoianis *et al.*, 2008).

2.5.4.4 Pharmacokinetic interactions of *Harpagophytum procumbens*

Romiti *et al.* (2009) have proven that commercial preparations of *H. procumbens* inhibit P-gp activity, while pure harpagoside, a derivative of harpagide, was virtually ineffective. It was also shown that extracts of *H. procumbens* can modulate P-gp activity and P-gp expression, which suggests that it may cause potential herb-drug interactions (Nair *et al.*, 2007; Romiti *et al.*, 2009). Furthermore, *H. procumbens* was shown to be a feeble inhibitor of CYP1A2 and CYP2D and showed moderate inhibition of CYP3A4 (Unger & Frank, 2004).

2.5.5 Leonotis leonurus

2.5.5.1 Botany of *Leonotis leonurus*

Leonotis leonurus (L.) R. Br. is a shrub that is affiliated with the Lamiaceae (mint) family. These perennial shrubs, with red-orange flowers that grow in spikes are found on rocky hillsides, grasslands and swamplands. The spikes are clustered umbels of intersperse flowers that coincide with the image of a lion's ear. This image led to the more commonly named and general identification of *Leonotis leonurus* as "lion's ear, lion's tail, Wilde dagga, Dacha, Daggha (Arica), Wild Hemp, Minaret Flower, Flor de Mundo and Mota (Mexico)" (Mazimba, 2015).

This drought-tolerant plant is frost hardy and is easily cultivated, especially in late summer and early autumn. The leaves have a distinct pungent smell, consist of a bright yellow-green colour and are texturally rough. Flowers raising above the shrubby mass makes this plant easily identifiable and it can be procured in the Eastern and Western Cape, KwaZulu-Natal and Mpumalanga throughout the summer season (Nsuala *et al.*, 2015).



Figure 2.13: *Leonotis leonurus* inflorescence **A)** leaves **B)** *Leonotis leonurus* plant (Miner, 2012) and **C)** geographical distribution (dark green) in South Africa (adapted from Nsuala *et al.*, 2015)

2.5.5.2 Chemical composition of *Leonotis leonurus*

Due to the large number of biological activities that have been reported with the utilisation of *L. leonurus*, extensive research has been done on the phytochemical characterization of all biologically active compounds. These studies demonstrated that terpenoids (mono-, sesqui and diterpenoids) are the main biologically active compounds present in the plant. Labdane diterpenes namely marrubiin and premarrubiin, however, are the most bountiful compounds that can be extracted from the leaves (Narukawa *et al.*, 2015; Nsuala *et al.*, 2015).

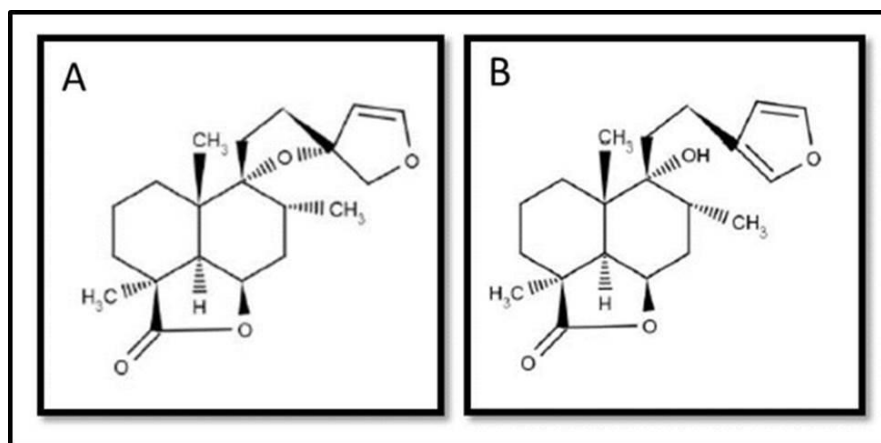


Figure 2.14: The chemical structures of selected phytochemicals of *L. leonurus* namely premarrubiin **A**) and marrubiin **B**)

2.5.5.3 Medicinal applications of *Leonotis leonurus*

L. leonurus is used in various forms to treat a cornucopia of health related illnesses, both internally as well as externally. Traditionally, a decoction was prepared where one tablespoon of chopped dried leaves are added to three cups of boiling water and boiled for 10 min. This decoction is left to cool overnight and is subsequently strained to deliver a clear liquid (Nsuala *et al.*, 2015). Taking this decoction orally contributed to the relief of coughs, colds and bronchitis. The Khoisan people utilised this decoction in the treatment of constipation and nausea. The aerial parts (leaves and flowers) have often been used for the treatment of chest infection, flu, intestinal worms, dysentery, influenza, constipation, and headache (Stafford *et al.*, 2008; Van Wyk *et al.*, 2000). The extracts of *L. leonurus* that contain the diterpenoid marrubiin was shown to restrain the hypercoagulable and inflammatory state often associated with diabetes and cardiac conditions such as hypertension and is thus known to alleviate symptoms associated with diabetes and has an inherent cardioprotective activity (Popoola *et al.*, 2013).

Upon smoking of the dried leaves and flowers a mild euphoric effect has been reported and this effect has been relatable to that of cannabis but less potent (Wu *et al.*, 2013). Externally, the powdered leaves can be mixed into a lotion and applied topically to relieve pain above to the eyes (Nsuala *et al.*, 2015). Furthermore, the leaves and stems are often used in decoctions, which are topically applied to the skin in the event of eczema, pruritus and infections (Mazimba, 2015).

2.5.5.4 Pharmacokinetic interactions of *Leonotis leonurus*

Even though a substantial amount of medicinal applications for *L. leonurus* have been reported, there is still paucity in the amount of information available regarding the pharmacokinetic interactions of this herbal extract. However, Ojewole (2005) identified that *L. leonurus* has the ability to induce enzymes.

2.6 Summary

Recognition of the significance of the use of traditional medicine in health care has led to the surge in the practice of herbalism throughout the world. In the Western world, there is a developing perception that 'natural' is better than 'synthetic' or 'chemical'. This perception has led to the evolution of "Neo-Western" type of herbalism which forms the foundation of this ever expanding industry (Elvin-Lewis, 2001). This trend has, instead of being killed off by medical science and pharmaceutical chemistry, been promoted and encouraged by medical practitioners and the role of herbal medicines that have been successful in healing have been acknowledged (Pal & Shukla, 2003).

Due to the surge in popularity, there is a growing concern of the potential interactions between herbal medicines as well as supplements on Western medicines, especially interactions pertaining to potential pharmacokinetic alterations. From the literature study, it was evident that some herbal medicines and supplements can present modulating effects on the membrane permeation characteristics of Western medicines. It is also evident that there is a lack of scientific evidence regarding the pharmacokinetic interactions of certain herbal extracts and supplements with prescribed medicines. Research in this regard is needed that will lead to improved vigilance regarding the prescribing of medicine with herbal extracts and supplements. It can also make a contribution to the health of patients by identifying potential interactions with concomitant use of medicine and avoiding the adverse effects that occur as a result of it.

The worldwide scientific community has been confronted with the responsibility to replace animal testing with a more ethical approach to scientific testing. Surrogate experimental models such as *in vitro* and *ex vivo* models are good alternatives that provide the answer to our moral and ethical responsibility. By using excised pig intestinal jejunum tissue in the *ex vivo* model, permeation studies can be performed to screen for potential pharmacokinetic interactions. This intestinal tissue is easily accessible from an abattoir, the anatomy resembles that of a human intestine and all ethics are taken into consideration.

It is evident that the effect of the use of herbal extracts and supplements cannot be exemplified and need to be regarded as a significant stepping stone in the advancement of modern medicine. As seen in the literature certain herb-drug interactions can have a significant impact on the efficacy of prescribed medicine which begs the question "are people who use "natural drugs" informed about the potentially harmful side effects?"(Giveon *et al.*, 2004).

One of the most common interactions are that of St. John's Wort (*Hypericum perforatum*) used in the treatment of depression and the effect it may exert on prescribed medicines such as warfarin, digoxin and oral contraceptives. These interactions include a decrease in the concentration or

efficacy of the medicine. This is a result of CYP450 induction, especially CYP3A4, CYP2C9 and CYP1A2 as well as the induction of P-gp (Henderson *et al.*, 2002). Another herbal medicine commonly used by patients to prevent and treat upper respiratory infections is *Echinacea* (i.e. *E. purpurea*, *E. angustifolia* and *E. pallida*). This herbal medicine has been found to modulate the catalytic ability of CYP3A4 (Izzo & Ernst, 2009).

In conclusion, it is evident that due to the heterogeneous nature of herbal medicine it is of great importance to impose the necessary trials with regards to the clinical aspects of each herbal extract and supplement chosen for this study. To promote the selected herbal extracts and supplement used in this study, data should be reliable and concrete. Examples regarding the data of the chosen herbal extracts and supplement in this study exist but are vague, obtuse or even contrived. This study forms an integral part in the determining of the possible effects the chosen herbal extracts and supplement may have on other concomitantly administered medicinal products.

CHAPTER 3: MATERIALS AND METHODS

3.1 Introduction

Working with materials that inherently contain a diverse mixture of constituents as in the case of crude herbal extracts, often creates more challenges than when working with pure single chemical entities as found in Western drug products. Interferences by certain herbal constituents, which may be present in experimental solutions, are often encountered during the development and/or validation of suitable analytical methods to analyse experimental samples. Validation forms an integral part of an analytical method to prove that it is scientifically acceptable and can be defined as ‘the process where it is demonstrated that the performance characteristics of said analytical procedure being performed meet certain criteria’ (Shabir, 2003). The performance characteristics that are usually measured during validation include: linearity, precision, accuracy, quantification limits, specificity, detection limits, range and robustness (USP-NF, 2017a).

Pertaining to this study, a Sweetana-Grass diffusion apparatus was utilised to investigate if selected herbal extracts and a supplement could alter the transport and efflux characteristics of a known P-gp substrate, Rhodamine 123 (RH-123) (Pavek *et al.*, 2003). Excised pig intestinal jejunum tissue was used as an appropriate *ex vivo* model because of the ease of accessibility of the intestines (obtained from the local abattoir) and the anatomical as well as the physiological resemblance to that of human intestinal tissue (Nolte *et al.*, 2000; Pietzonka *et al.*, 2002).

Bi-directional transport studies were performed in the absence and presence of the selected extracts and compounds across excised intestinal jejunum tissues by using RH-123 as a marker compound. Transport across the membrane in the apical-to-basolateral (AP-BL) direction represented RH-123 absorption (i.e. absorptive transport), while transport in the basolateral-to-apical (BL-AP) direction represented secretion of RH-123 (i.e. secretory transport).

3.2 Materials

RH-123, Krebs-Ringer bicarbonate (KRB) buffer, sodium bicarbonate and Lucifer yellow (LY) CH dilithium salt were purchased from Sigma-Aldrich (Johannesburg, South Africa). Herbal extracts were purchased from Parceval Pharmaceuticals (Cape Town, South Africa) including *Hoodia gordonii*, *Harpagophytum procumbens* and *Vitis vinifera* seed extract. *Leonotis leonurus* plant material was donated by Professor Alvaro Viljoen at Tshwane University of Technology (TUT) in Pretoria. Methylsulfonylmethane (MSM) was obtained from Warren Chem Specialities in Johannesburg, South Africa. Verapamil was donated by Novartis, South Africa. Costar® 96-well plates were purchased from The Scientific Group (Randburg, South Africa). Excised pig intestinal

jejunum was collected from the local abattoir in Potchefstroom, South Africa. State the ethical clearance permit number as well.

3.3 Preparation of herbal extracts

Extracts of *Hoodia gordonii*, *Harpagophytum procumbens* and *Vitis vinifera* (seed) were purchased in liquid form (i.e. ethanol based infusions). The ethanol was removed from these extract solutions under reduced pressure by means of evaporation (Rotavapor® R-100) with the temperature set at 40 °C to prevent degradation of the active constituents in the extracts (Djeridane *et al.*, 2006). After evaporation of the ethanol, the remaining solid fraction was diluted with distilled water and frozen in ice trays at -80 °C.

Leonotis leonurus was obtained in the form of dried plant leaf material. Two extracts were prepared from the leaf material. An ethanol based extract was prepared by adding 100 g of the leaf material to 150 ml ethanol while the second extract was prepared by adding the same amount of leaf material to 150 ml distilled water at a temperature of 4 °C (Oyedemi & Afolayan, 2011). These mixtures were constantly agitated using a mechanical shaker for a period of 48 hours after which the mixtures were centrifuged and then filtered through a Buchner funnel using Whatman No.1 filter paper. The filtrate was then frozen at -80 °C.

For the process of lyophilisation (freeze drying), all frozen plant extract materials (without containing any ethanol) were crushed into smaller fragments using a mortar and pestle. The crushed ice fragments were then transferred to conical glass flasks and the contents were then freeze dried using a Virtis Benchtop Freeze dryer (United Scientific, Gauteng, South Africa) for at least 72h. The dry products were then transferred to air-tight glass containers and stored in a desiccator until required for experimental purposes (Lebitsa *et al.*, 2012).

3.4 Chemical fingerprinting of plant extracts

3.4.1 *Vitis vinifera* seed extract

A solution was prepared by adding 2 ml methanol to 2 mg of the freeze dried powder of *V. vinifera* seed extract. The resultant solution was sonicated for 10 min and filtered through a 0.2 µm syringe filter before UPLC-MS analysis.

3.4.2 UPLC-MS analytical method for *Vitis vinifera* seed extract

UPLC analyses were performed using a Waters Acquity Ultra Performance Liquid Chromatographic system with PDA (photodiode array) detector (Waters, Milford, MA, USA). LC-MS separation was achieved on an Acquity UPLC BEH C₁₈ column (150 mm × 2.1 mm, i.d., 1.7 µm particle sizes, Waters) maintained at 40 °C. The mobile phase consisted of 0.1% formic

acid in water (solvent A) and acetonitrile (solvent B) at a flow rate of 0.3 ml/min; a gradient elution was followed: 95% A: 5% B, to 25% A: 75% B in 8 min, to 22% A: 78% B in 2 min, to 10% A: 90% B in 5 min, and back to initial ratio in 0.5 min. The samples were injected in the mobile phase with an injection volume of 4.0 μ l (full-loop injection). Mass spectrometry was operated in negative ion electrospray mode. Nitrogen (N₂) was used as the desolvation gas. The desolvation temperature was set to 350 °C at a flow rate of 500 l/hr and the source temperature was 100 °C. The capillary and cone voltages were set to 2500 and 45 V, respectively. Data were collected between 80 and 1200 *m/z*.

3.4.3 Harpagophytum procumbens

A solution was prepared by adding 2 ml methanol to 2 mg of the freeze dried powder of the *H. procumbens* extract. The resultant solution was sonicated for 10 min and filtered through a 0.2 μ m syringe filter before UPLC-MS analysis.

3.4.4 UPLC-MS analytical method for *Harpagophytum procumbens*

UPLC-MS analyses were performed using a Waters Acquity Ultra Performance Liquid Chromatographic system with PDA detector (Waters, Milford, MA, USA). UPLC-MS separation was achieved on an Acquity UPLC BEH C₁₈ column (150 mm x 2.1 mm, i.d., 1.7 μ m particle size, Waters) maintained at 40° C. The mobile phase consisted of 0.1% formic acid in water (solvent A) and acetonitrile (solvent B) at a flow rate of 0.4 ml/min. A gradient elution was followed: 85% A: 15% B, to 65% A: 35% B in 4 min, to 50% A: 50% B in 2 min, to 20% A: 80% B in 1 min, holding for 1 min and back to initial ratio in 0.5 min. The samples were injected in the mobile phase with an injection volume of 2.0 μ l (full-loop injection). Mass spectrometry was operated in negative ion electrospray mode. N₂ was used as the desolvation gas. The desolvation temperature was set to 400 °C at a flow rate of 600 l/hr and the source temperature was 100 °C. The capillary and cone voltages were set to 2450 and 46 V, respectively. Data were collected between 100 and 1500 *m/z*.

3.4.5 Hoodia gordonii

A solution was prepared by adding 2 ml methanol to 2 mg of the freeze-dried *H. gordonii* extract. The resultant solution was sonicated for 10 min and filtered through a 0.2 μ m syringe filter before UPLC-MS analysis.

3.4.6 UPLC-MS analytical method for *Hoodia gordonii*

UPLC-MS analyses were performed using a Waters Acquity Ultra Performance Liquid Chromatographic system with PDA detector (Waters, Milford, MA, USA). UPLC-MS separation was achieved on an Acquity UPLC BEH C₁₈ column (150 mm x 2.1 mm, i.d., 1.7 μ m particle sizes,

Waters) maintained at 40° C. The mobile phase consisted of 0.1% formic acid in water (solvent A) and acetonitrile (solvent B) at a flow rate of 0.3 ml/min. A gradient elution was followed: 85% A: 15% B, to 50% A: 50% B in 4 min, to 25% A: 75% B in 2min, to 10% A: 90% B in 3 min, holding for 2 min and back to initial ratio in 0.5 min. The samples were injected in the mobile phase with an injection volume of 2.0 µl (full-loop injection). Mass spectrometry was operated in negative ion electrospray mode. N₂ was used as the desolvation gas. The desolvation temperature was set to 450 °C at a flow rate of 550 l/hr and the source temperature was 100 °C. The capillary and cone voltages were set to 3500 and 45 V, respectively. Data were collected between 100 and 1500 *m/z*.

3.4.7 Leonotis leonurus

A solution was prepared by adding 2 ml methanol to 2 mg of the freeze dried *L. leonurus* extract. The resultant solution was sonicated for 10 min and filtered through a 0.2 µm syringe filter before UPLC-MS analysis.

3.4.8 UPLC-MS analytical method for *Leonotis leonurus*

UPLC-MS analyses were performed using a Waters Acquity Ultra Performance Liquid Chromatographic system with PDA detector (Waters, Milford, MA, USA). UPLC separation was achieved on an Acquity UPLC BEH C₁₈ column (150 mm × 2.1 mm, i.d., 1.7 µm particle size, Waters) maintained at 40 °C. The mobile phase consisted of 0.1% formic acid in water (solvent A) and acetonitrile (solvent B) at a flow rate of 0.4 ml/min; a gradient elution was followed: 90% A: 10% B, to 60% A: 40% B in 2 min, to 30% A: 70% B in 10 min, to 5% A: 95% B in 2 min, holding for 0.5 min and back to initial ratio in 0.5 min. The samples were injected in the mobile phase with an injection volume of 5.0 µl (full-loop injection). Mass spectrometry was operated in negative ion electrospray mode. N₂ was used as the desolvation gas. The desolvation temperature was set to 350 °C at a flow rate of 500 l/hr and the source temperature was 100°C. The capillary and cone voltages were set to 2450 and 46 V, respectively. Data were collected between 100 and 1200 *m/z*.

3.5 Fluorescence spectrometry analytical method validation for Rhodamine 123 and Lucifer yellow

The *ex vivo* experimental samples were transferred to a Costar[®] 96-well plate to determine the RH-123 and LY concentration in each sample by means of fluorescence spectrometry. Fluorescence spectroscopic analysis of the samples were performed with a Spectramax Paradigm[®] multi-mode detection platform plate reader with the excitation and emission wavelengths set to 480 nm and 520 nm, respectively for RH-123 and emission and excitation wavelengths of 485 nm and 530 nm for LY (Irvine *et al.*, 1999; Kageyama *et al.*, 2006; Kapreylyants & Kell, 1992).

3.5.1 Linearity

Linearity encompasses the ability of an analytical method to elicit test results which are directly proportionate to the concentration of an analyte in the test samples over a specific range. The concentration range selected for use in the determination of linearity should be in the same value range as the sample concentrations expected to be encountered during the experimental procedure (USP-NF, 2017a). For an analytical method to be considered acceptable in terms of linearity, a correlation coefficient (R^2) of more than 0.995 should be achieved. The correlation coefficient should be determined by a series of three to nine tests over a minimum of five concentrations (Shabir, 2003; Singh, 2013).

To determine the linearity for the fluorescence spectrometry method, two stock solutions containing RH-123 at a concentration of 5 μM and 2.5 μM were prepared. The 5 μM solution was diluted four times by a factor of ten and the 2.5 μM solution was diluted three times by the same factor. To calculate the regression of the calibration curve, samples over the entire concentration range (i.e. 5 μM , 2.5 μM , 0.5 μM , 0.25 μM , 0.05 μM , 0.025 μM , 0.005 μM , 0.0025 μM and 0.0005 μM) were analysed. Samples were analysed in how many replicates?

For LY, the regression of the concentration curve was determined by preparing a stock solution of 50 $\mu\text{g/ml}$ LY and preparing serial dilutions from it (i.e. 50 $\mu\text{g/ml}$; 16.667 $\mu\text{g/ml}$; 5.556 $\mu\text{g/ml}$; 1.852 $\mu\text{g/ml}$; 0.617 $\mu\text{g/ml}$; 0.206 $\mu\text{g/ml}$; 0.069 $\mu\text{g/ml}$; 0.023 $\mu\text{g/ml}$; 0.008 $\mu\text{g/ml}$; 0.003 $\mu\text{g/ml}$; 0.001 $\mu\text{g/ml}$ and 0.0003 $\mu\text{g/ml}$). These concentrations were used to plot the standard curve (fluorescence value as a function of concentration) in order to perform a regression analysis to obtain the R^2 value.

3.5.2 Limit of detection (LOD) and limit of quantification (LOQ)

Limit of detection (LOD) is defined as “the lowest concentration at which an analyte can be detected using a specific analytical method for any given sample under specific experimental conditions”. It can be calculated using Equation 1 (Shabir, 2003).

$$\text{Limit of Detection (LOD)} = 3.3 \times \left(\frac{\text{SD}}{\text{S}} \right) \quad (\text{Eq. 1})$$

The limit of quantification (LOQ) describes “the lowest concentration at which an analyte can be quantified in any given sample containing the said analyte with optimal precision and accuracy”. LOQ can be calculated using Equation 2 (Shabir, 2003).

$$\text{Limit of Quantification (LOQ)} = 10 \times \left(\frac{\text{SD}}{\text{S}} \right) \quad (\text{Eq. 2})$$

Where the factor constants, 3.3 for LOD and 10 for LOQ, as seen in Equation 1 and 2 represent the signal-to-noise ratio, SD represents the standard deviation of the plate blanks (background noise) and S represents the slope of the standard curve (regression line).

3.5.3 Precision

The precision of an analytical method is the degree to which individual test sample results agree within a series of measurements obtained at different times. Precision thus measures the degree of repeatability and reliability of the analytical method under normal operating conditions. Precision can be categorised into two categories namely intra-day precision and inter-day precision (Shabir, 2003).

3.5.3.1 Intra-day precision

When results of the analytical method are tested for repeatability over a short time interval, i.e. on the same day, it is referred to as intra-day precision testing. Intra-day precision testing entails that three concentrations of the analyte are analysed three times at three separate time intervals during a 24-hour period. To confirm the precision of the analytical method, a percentage relative standard deviation (% RSD) of $\leq 2\%$ should be achieved (Shabir, 2003).

Three solutions with three different RH-123 concentrations (5 μM , 2.5 μM and 0.125 μM) were analysed three times at three separate times during a 24-hour period and subsequently the % RSD values were calculated for each concentration.

To determine the intra-day precision of LY three solutions of three different LY concentrations (50 $\mu\text{g/ml}$; 25 $\mu\text{g/ml}$ and 12.5 $\mu\text{g/ml}$) were analysed three times at three different occasions during a 24 h period after which the % RSD values were calculated for each concentration.

3.5.3.2 Inter-day precision

The inter-day precision of the analytical method was determined by using the same three RH-123 solutions (5 μM , 2.5 μM and 0.125 μM) and analysing them at the same time over three consecutive days. A % RSD value of $\leq 2\%$ should be achieved during the inter-day precision evaluation in order for the analytical method to be considered acceptable (Shabir, 2003).

For the inter-day precision of LY, the same three concentrations of LY (50 $\mu\text{g/ml}$; 25 $\mu\text{g/ml}$ and 12.5 $\mu\text{g/ml}$) were used to determine the inter-day precision. These solutions were analysed at the same time over three consecutive days. For the analytical method to be deemed acceptable a % RSD value of $\leq 2\%$ should be achieved (Shabir, 2003).

3.5.4 Specificity

The specificity of an analytical method describes the ability of the method and equipment to unmistakably assess and accurately detect the analyte in the presence of other components that may be present in the solution and therefore may influence the detection of the specific analyte (USP-NF, 2017a).

To determine the specificity of the analytical method, solutions of RH-123 alone (control) and in the presence of the selected herb extracts and supplement (test solutions) were prepared in Costar® 96-well plates. Control solutions consisted of 5 µM RH-123 alone and test solutions consisted of 5 µM RH-123 mixed with the MSM and *V. Vinifera* seed extract. The prepared solutions were measured for fluorescence detection (Spectramax Paradigm® plate reader) and after analysis, the mean fluorescence values of each test solution were compared to that of the RH-123 alone (control) solution. To determine if the MSM and *V. Vinifera* seed extract had interfered with the fluorescence yield of RH-123, the actual concentration of RH-123 in the test solutions could be compared to the RH-123 concentration in the control solutions. Acceptable specificity of an analytical method is achieved when the analyte recovery is $100 \pm 2\%$ in the presence of the other component (Shabir, 2003; USP-NF, 2017a).

An alternative method was employed to overcome the lack of specificity of RH-123 in the presence of *H. gordonii*, *H. procumbens* and *L. leonurus* extracts. It is not always conceivable to prove that an analytical method is specific for a particular analyte in the presence of certain excipients. The R^2 values of RH-123 in the presence of the mentioned herbal extracts were calculated as described in 3.5.1 “Linearity”. The highest concentration of the herbal extracts was included in the RH-123 solutions, which were then subjected to the test for linearity (Patel *et al.*, 2017).

3.5.5 Accuracy

The accuracy of an analytical method refers to the “closeness” of the measured concentration of a test analyte compared to the true concentration of the analyte. To determine the accuracy of an analytical method, at least nine readings are required over a range of at least three concentrations. Low, medium and high concentrations within the working range of concentrations of the specific analyte should be selected and individually analysed in triplicate. To determine the accuracy of the analytical method, the concentration values of the test solutions are calculated as a percentage of the theoretical (‘true’) concentration (USP-NF, 2017a). The accuracy of the analytical method may be considered to be acceptable if the mean recovery is $100 \pm 2\%$ at each of the test concentrations (Shabir, 2003).

Pertaining to this experiment ten samples from each solution containing RH-123 at concentrations of 5 μ M, 2.5 μ M and 0.125 μ M were used to determine the percentage recovery.

With regards to the accuracy of LY ten samples from each solution containing LY at concentrations 50 μ g/ml; 25 μ g/ml and 12.5 μ g/ml were used to determine the percentage recovery.

3.6 Buffer preparation for transport studies

Sodium bicarbonate powder (1.2 g) was added to the standard KRB buffer powder mixture (Sigma-Aldrich, Johannesburg, SA). This powder mixture was made up to the desired volume of 1000 ml with distilled water. A magnetic stirrer was used to stir the mixture for approximately 5 min until all powder had dissolved. This solution was then stored in the fridge where it was kept until needed for the transport experiments.

3.7 Ex vivo transport studies

3.7.1 Preparation of experimental solutions

The herbal/supplement concentrations that were chosen for use in this study were based on the total recommended daily intake of the different herbal extracts and supplements as commonly reported in the literature (Chapter 2 of this dissertation). The chosen concentrations were then used in the calculations (based on a publication by Hellum *et al.*, 2007b) to determine the concentrations which should be evaluated. The total recommended daily intake of the different herbal extracts and supplement that were used in the calculations are listed in Table 3.1. Hellum *et al.* (2007b) recommended the use of three test concentrations based on the daily dose values where the specific herbal extract/supplement dose is dissolved in three different fluid volumes (i.e. 53 l, 5.3 l and 0.53 l). The respective fluid volumes represent the herbal extract/supplement concentration in the extracellular fluid (and plasma), and also a superlative concentration anticipated to appear in the small intestine (i.e. to cover both the lowest and highest range of concentration values that may occur in the GIT).

Table 3.1 shows the anticipated concentrations of each herbal extract and supplement when dissolved in specific fluid volumes as would be encountered in the different compartments of the GIT as well as in the extracellular fluid based on the recommendations of Hellum *et al.* (2007b).

Table 3.1: Concentrations (% w/v) of each selected herbal extract and supplement used in the bi-directional transport study (Hellum *et al.*, 2007b)

Herbal extracts/supplement (Trade name)	Recommended Daily Allowance	Concentration of herbal extract/supplement (% w/v)		
		53 l	5.3 l	0.53 l
<i>Vitis vinifera</i> Seed Extract (Procydin®)	140 mg (2 capsules)	0.000264	0.00264	0.0264
<i>Harpagophytum procumbens</i> (Flora Force® Products)	1000 mg (2 tablets)	0.00188	0.0188	0.188
<i>Hoodia gordonii</i> (Holistix®)	1350 mg (3 capsules)	0.00255	0.0255	0.255
<i>Leonotis leonurus</i>	400 mg	0.000755	0.00755	0.0755
Methylsulfonylmethane (MSM) (MSM-90 Solal Technologies®)	2100 mg (3 capsules)	0.003962	0.03962	0.3962

RH-123, a highly selective P-gp substrate, was used as the model compound at a concentration of 5 μ M in the bi-directional transport studies. It was used to determine the extent of P-gp related efflux transport and to determine if the selected herbal extracts/supplement has any effect on the P-gp related efflux transport (Pavek *et al.*, 2003).

To conduct the transport experiments, a sufficient amount of RH-123 was mixed with KRB to render a 50 ml solution with a final concentration of 5 μ M. For transport experiments conducted in the apical-to-basolateral direction a double strength concentration was prepared for a 10 μ M RH-123 solution which was subsequently mixed with the appropriate herbal extract/supplement concentration rendering a 5 μ M RH-123 solution. A volume of 7 ml of this RH-123 and herbal extract/supplement mixture was added to the apical side (donor chamber) of the excised intestinal tissue mounted in the Sweetana-Grass diffusion chamber.

Transport experiments conducted in the basolateral-to-apical direction required two different solutions. A 50 ml solution of pure RH-123 was prepared in KRB with a final concentration of 5 μ M from which a volume of 7 ml was added to the basolateral side (donor chamber) of the

excised intestinal tissue mounted in the Sweetana-Grass diffusion chamber. For the apical side (acceptor chamber), a solution was prepared by weighing the correct amount of herbal extract/supplement and making it up to a volume of 50 ml with KRB buffer. A volume of 7 ml of this solution was then added to the apical side (acceptor chamber).

Application of the solutions in the manner described above was designed specifically to mimic normal physiological processes and conditions in the body. All herbal extracts/supplement were always added to the apical side of the intestine where the constituents being tested will be available in the lumen of the GIT after oral administration. Table 3.2 indicates the mass of each herbal extract/supplement that was used to prepare a volume of 50 ml of each test solution (to produce the concentrations listed in Table 3.1) required for the *ex vivo* permeation experiments.

Table 3.2: Mass of each herbal extract/supplement used in preparation of the test solutions for the *ex vivo* transport experiments

Herbal extracts/supplement	Mass of herbal extract/supplement (g)		
	53 l	5.3 l	0.53 l
<i>Vitis vinifera</i> seed extract	0.000132	0.00132	0.0132
<i>Harpagophytum procumbens</i>	0.000944	0.00944	0.0944
<i>Hoodia gordonii</i>	0.001275	0.01275	0.1275
<i>Leonotis leonurus</i>	0.000375	0.00375	0.0375
Methylsulfonylmethane (MSM)	0.001981	0.01981	0.1981

3.7.2 Collection and preparation of excised pig intestinal tissues for *ex vivo* transport studies

On the day of the transport experiment, a piece of pig intestinal jejunum was collected from the local abattoir located in Potchefstroom, South Africa. Promptly upon slaughtering of the pigs, the proximal jejunum was identified and a segment (\pm 30 cm) was excised and the inside was rinsed thoroughly with ice-cold KRB buffer. The excised pig intestinal jejunum segment was then submerged in ice-cold KRB buffer, placed in a cooler box, and immediately transferred to the transport study laboratory. The entire process from obtaining the intestinal tissue, identifying the

region required for the experiment and transferring it to the laboratory did not exceed 30 min from the time of slaughtering.

In the laboratory, the intestine was hauled over a wetted glass tube (Figure 3.1 A). The serosal layer was cautiously removed from the small intestine by making a superficial incision along the mesenteric border. Subsequently, the serosal layer was pulled off (Figure 3.1 B) and separated from the intestinal tissue (Aucamp *et al.*, 2014; Legen *et al.*, 2005; Pietzonka *et al.*, 2002).

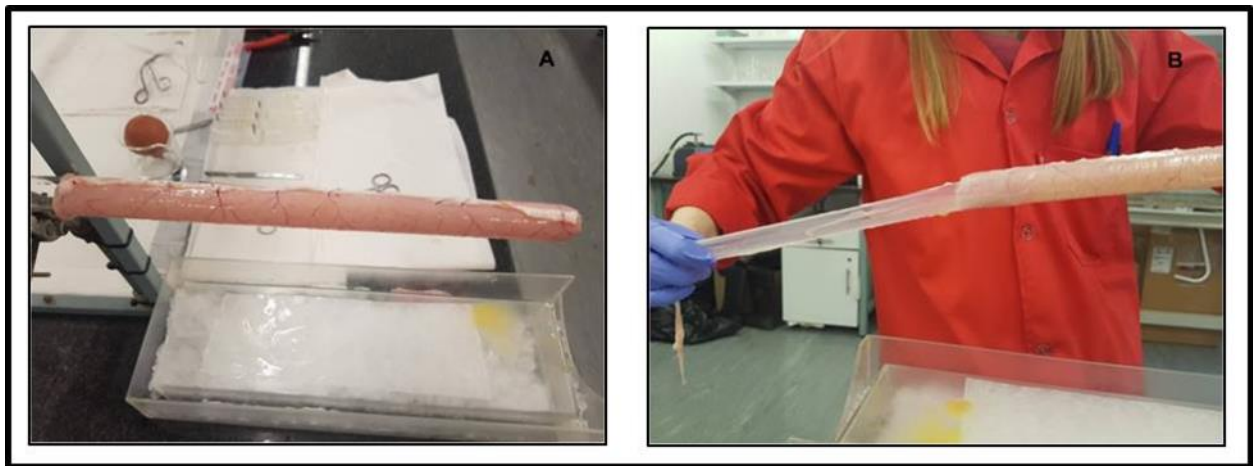


Figure 3.1: Photographic images of: **A)** Excised pig intestinal jejunum tissue mounted on a glass tube with mesenteric border visible, **B)** Careful removal of the serosal layer

The tissue remaining on the glass rod was inspected for Peyer's Patches (Figure 3.2). Peyer's patches are areas of lymphoid tissue in the wall of the small intestine that can affect drug absorption and may negatively influence the transport results. These patches were not included in the intestinal tissue that was used for the transport studies.

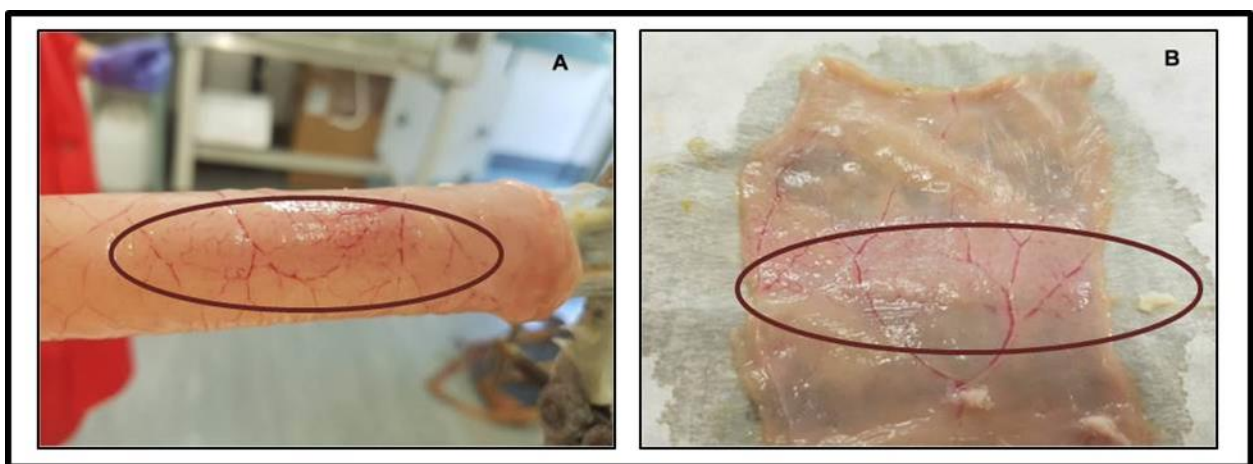


Figure 3.2: Photographic images **A)** and **B)** illustrating Peyer's patches in the excised pig intestinal jejunum tissue

Following this, the mesenteric border was used as a guide to dissect the segment of intestinal tissue to produce a flat sheet of tissue. The dissected tissue was rinsed off with cold KRB buffer in order to remove it from the glass tube onto a piece of heavy duty filter paper (Figure 3.3).

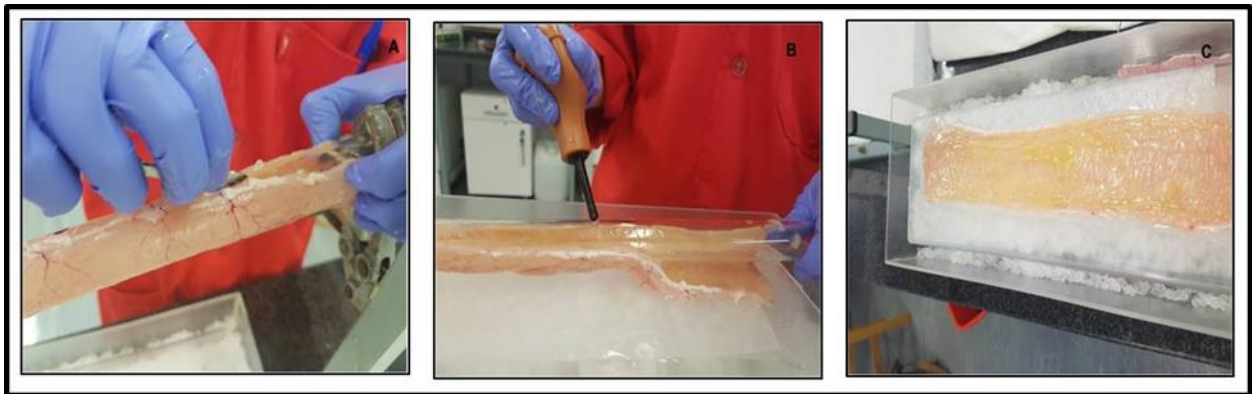


Figure 3.3: Photographic images of: **A)** the jejunum is cut along the mesenteric border, **B)** the jejunum is washed from the glass tube and **C)** transferred to heavy duty filter paper

The jejunum tissue was subsequently cut into smaller segments of ± 2 cm wide, which were intended for mounting between two half cells of the Sweetana-Grass diffusion (Ussing-type diffusion) apparatus. All segments were kept moist with KRB buffer throughout the procedure. After mounting, a tissue surface area of 1.78 cm^2 was available in each chamber for transport of the model compound (Figure 3.4).

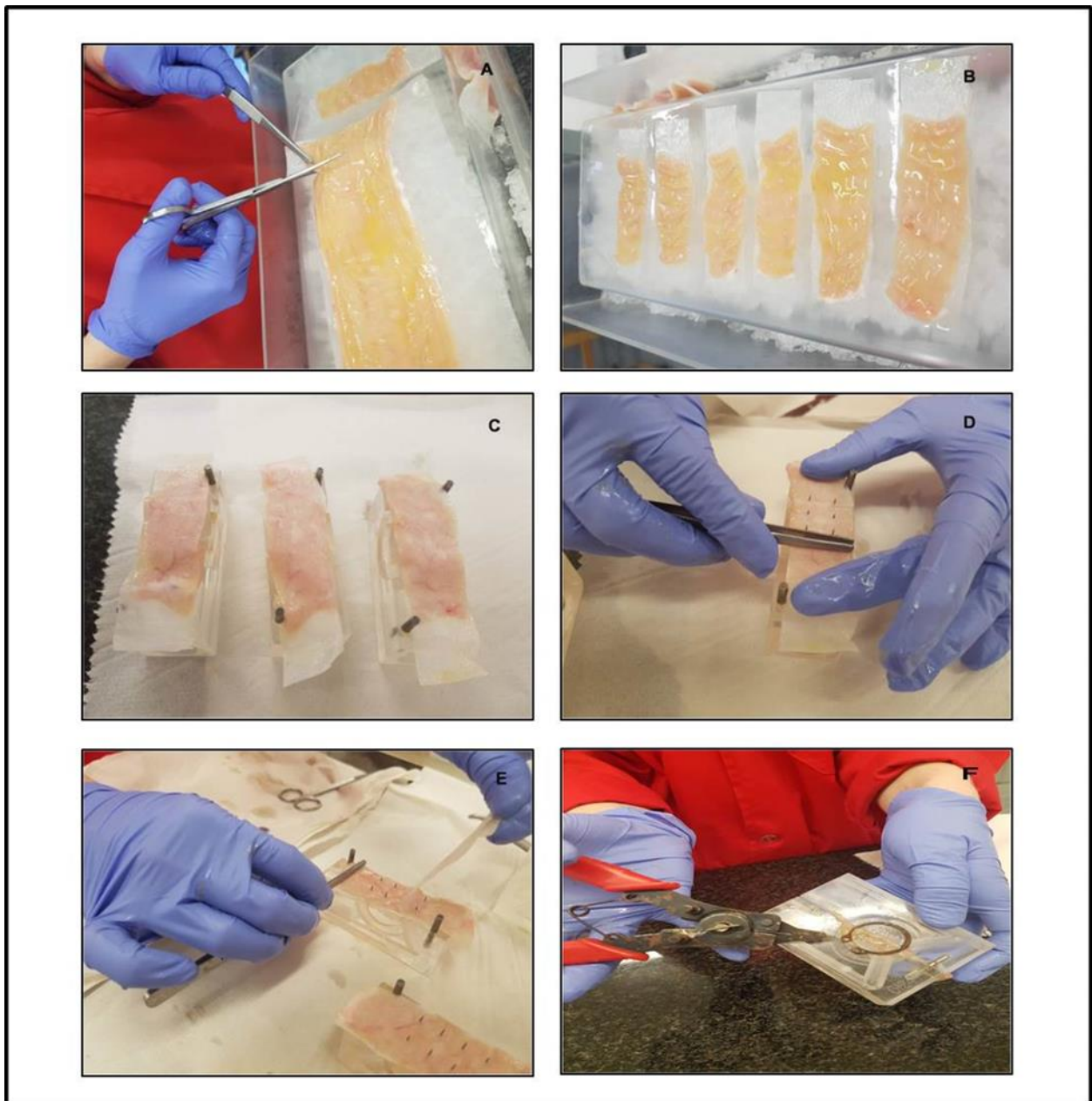


Figure 3.4: Photographic images of **A)** and **B)** the process of the proximal jejunum being cut into smaller pieces, **C)** and **D)** the process of mounting the jejunum pieces onto the half cells, **E)** removal of the heavy duty filter paper and **F)** the assembling of the half cells into a single diffusion chamber

The six assembled diffusion chambers were placed in the diffusion apparatus linked to a heating block (37°C) and a carbogen (95% O₂: 5% CO₂) supply (Figure 3.5) (Aucamp *et al.*, 2014).

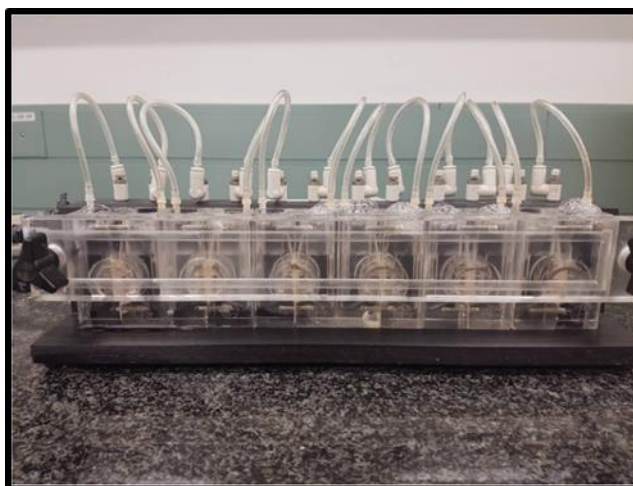


Figure 3.5: Photographic image of a completely assembled Sweetana-Grass diffusion apparatus with excised pig intestinal jejunum tissues mounted between the half-cells

3.7.3 Bi-directional transport studies

The transport studies conducted on RH-123 were performed in triplicate in two directions namely in the AP-BL direction and BL-AP direction. Pre-heated (37°C) KRB buffer (7 ml) was added to both sides of the intestinal membrane mounted in the diffusion chamber and left to incubate for 15 min to allow the tissue to adapt to its new environment. The 7 ml KRB buffer was then removed from the chambers and the intestinal tissue was incubated with a RH-123 solution in the presence of the herbal extracts and supplement being tested and absence (control groups) of the herbal extracts and supplement. The trans-epithelial electrical resistance (TEER) was measured at the beginning and at the end of each study and served as an indication of the integrity of the excised intestinal tissue over the duration of the transport study (Figure 3.6). TEER was measured using a Warner Instruments® EC-825A epithelial voltage clamp (Serial nr 211). Samples (180 µl) were withdrawn from the acceptor chamber at 20, 40, 60, 80, 100 and 120 min after application of the experimental solutions to the donor chamber. Each sample withdrawn was replaced by 180 µl pre-heated KRB buffer (in the case of AP-BL transport) or 180 µl of the experimental solution (in the case of BL-AP transport).

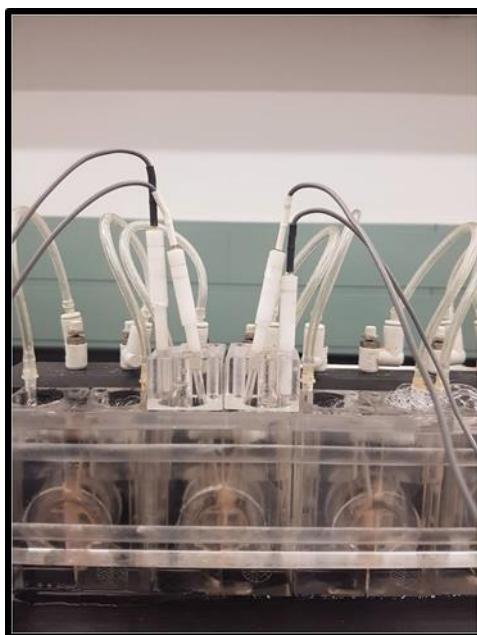


Figure 3.6: The measuring of the TEER in the Sweetana-Grass diffusion chamber apparatus during bi-directional transport studies

3.8 Assessment of intestinal tissue integrity

Lucifer yellow (LY), a fluorescent stain (MW: 457.25 g/mol) was employed as a paracellular transport marker to assess the integrity of the mounted intestinal jejunum tissue over the period of the transport study. A solution of 50 ml was prepared, which contained 2.5 mg LY in KRB buffer. Transport studies were conducted on this LY solution in the AP-BL direction. Fluorescence of the transported LY was measured at an excitation wavelength of 485 nm and an emission wavelength of 535 nm by means of a fluorescence microplate reader (Spectramax Paradigm® multi-mode detection platform reader). The fluorescence data were processed and the permeability coefficient (P_{app}) of LY was calculated to determine if the integrity of the intestinal tissue was maintained for the duration of the transport experiment (Nguyen *et al.*, 2013; Zhang *et al.*, 2004). Irvine *et al.* (1999) determined that in order to verify the integrity of the intestine the P_{app} values should be approximately 1 to 7 nm/sec ($1 \text{ nm/sec} = 1 \times 10^{-7} \text{ cm/s}$).

3.9 Analysis of transport samples

A Spectramax Paradigm® (Serial nr 33270-1142) multi-mode detection platform reader was used to determine the RH-123 concentration in each of the experimental transport samples. This was achieved by means of a validated fluorescence spectroscopic method as described in section 3.5 “Fluorescence spectrometry analytical method validation for Rhodamine 123” of this chapter.

3.10 Positive and negative control for RH-123 transport experiments

Two control groups were included in the design of the experiment, namely a negative and positive control. The negative control group consisted of RH -123 alone (5 μ M), the transport of which was measured in two directions across the excised pig intestinal jejunum tissue. The positive control group included verapamil (100 μ M), which is a known P-gp inhibitor (Nabekura *et al.*, 2015). The bi-directional transport of RH -123 was measured in the presence of verapamil to serve as a reference value against which the efflux related effects of the herbal extracts/supplement could be compared. The control experiments were performed to indicate that any effects observed was a result of the modulators' ability to cause a modulation and that the outcome was not a result of external factors or any arbitrary interference.

3.11 Data processing and statistical analysis

3.11.1 Percentage transport (% Transport)

The percentage transport was calculated at each designated time set out for withdrawal using Equation 3 after the fluorescence values (that were used to determine RH-123 concentration) were corrected for dilution. The correction factor was determined firstly to compensate for the amount of RH-123 and buffer lost during the withdrawal of samples and secondly to compensate for the remainder of the RH-123 which will further be diluted as the experiment proceeds. The sample volume was 180 μ l, and the total volume of each chamber's well was 7 ml. Thus, $0.18/7 = 0.0257$ ml was used as the correction factor for each dilution. A percentage transport versus time curve was then constructed to illustrate the transport of RH-123 over the transport period of 2 h in both directions obtained from each individual transport study.

$$\% \text{ Transport} = \frac{\text{Mean fluorescence value at specific time}}{\text{Mean value fluorescence of donor solution}} \times 100 \quad (\text{Eq. 3})$$

3.11.2 Apparent permeability coefficient (P_{app})

The apparent permeability coefficient (P_{app}) is defined as “the rate of drug accumulation in the receiver chamber normalized for tissue surface area” (Volpe, 2010). The P_{app} values for the herbal extracts and supplement used are from the samples withdrawn from the receiver compartment (i.e. apical or basolateral side) (Thanou *et al.*, 2000). Equation 4 indicates how the P_{app} values for RH-123 in the presence and absence of the selected herbal extracts and supplement were calculated.

$$P_{app} = \frac{dC}{dt} \left(\frac{1}{A \cdot 60 \cdot C_0} \right) \quad (\text{Eq. 4})$$

Where P_{app} is the apparent permeability coefficient ($\text{cm} \cdot \text{s}^{-1}$), $\frac{dQ}{dt}$ is the permeability rate (thus the amount of RH-123 permeated per minute), A is the diffusion area of the membrane (excised pig intestinal jejunum) and C_0 is the initial concentration (μM) of RH-123 (Legen *et al.*, 2005).

3.11.3 Efflux ratio (ER)

The efflux ratio values were calculated using Equation 5 (Wempe *et al.*, 2009). The ER values generated by the use of this equation give an indication of the extent to which RH-123 underwent efflux.

$$\text{ER} = \frac{P_{app(B-A)}}{P_{app(A-B)}} \quad (\text{Eq. 5})$$

P_{app} (B-A) represents the apparent permeability coefficient value for RH-123 permeation in the basolateral to the apical direction and P_{app} (A-B) is representative of the RH-123 permeation in the apical-to-basolateral direction.

3.11.4 Statistical analysis of results

Statistical analysis was performed on all experimental data obtained from the bi-directional transport studies. The Tukey's Honest Significant Difference (HSD) post hoc test was performed to determine the statistical significance between the transport values of the control group (RH-123 alone) and the experimental groups (herbal extracts and supplement used). It also presents the statistical significance between the experimental groups when compared to each other's concentration within the designated group. Differences between the control and experimental groups were considered to be statistically significant if $p \leq 0.05000$.

Furthermore, an analysis of variance test (ANOVA) together with a 2-Way Table of Descriptive Statistics and the Brown-Forsythe Test of Homogeneity of Variances were performed to identify any statistical differences among the data generated from the transport experiments. All statistical analyses data can be found in Addendum F of this dissertation.

CHAPTER 4: RESULTS AND DISCUSSION

4.1 Introduction

The potential for herbal extract/supplement-drug pharmacokinetic interactions were investigated following concomitant application of selected extracts/supplement with a P-gp substrate to excised pig intestinal jejunum tissues. For this study, herbal extracts (including *Vitis vinifera* seed extract, *Hoodia gordonii*, *Harpagophytum procumbens*, *Leonotis leonurus*) and a supplement (methylsulfonylmethane (MSM)) were selected and concomitantly applied with Rhodamine 123 (RH-123) to excised pig intestinal jejunum in order to investigate potential interactions during absorption. All the selected herbal extracts were chemically fingerprinted by means of Liquid chromatography-Mass spectrometry (LC-MS) and Liquid chromatography-Ultra violet (LC-UV) analytical methods. *Ex vivo* transport studies were conducted bi-directionally, in triplicate, using excised pig intestinal jejunum tissues mounted between the half-cells of a Sweetana-Grass diffusion apparatus. The effects of the selected herbal extracts and supplement on the absorption and P-gp related efflux of RH-123 were investigated. All data generated from the transport studies were expressed as cumulative RH-123 transport over a 2 h period followed by calculations of the apparent permeability coefficient (P_{app}) values as well as efflux ratio (ER) values.

The fluorometric analytical method was validated to confirm the capability of the analytical method to analyse samples accurately and invariably to ensure that all experimental results are reliable. The validation process of the analytical method was conducted foremost to ensure compliance with all applicable analytical parameters.

A transport study with Lucifer yellow (LY) was performed prior to commencement with the transport experiments to verify that the technique that was used to prepare and mount the excised pig intestinal jejunum onto the half-cells of the diffusion chambers was adequate and to ensure that the tissue was intact and viable before commencing with the transport studies. The transport results of the LY study indicated that the mounting technique of the excised pig intestinal tissue was adequate and did not damage the excised intestinal jejunum tissue and could therefore not have any negative effect on the outcome of the RH-123 transport results.

The trans-epithelial electrical resistance (TEER) was also measured at pre-determined time intervals during all transport experiments. Changes in the measured TEER values may be indicative of changes in tight junction integrity, which may have been mediated by the addition of the herbal extracts or supplement. Reduced tight junction integrity (indicated by lower TEER values) may serve as an indicator that the transport of RH-123 may potentially increase via paracellular transport mechanisms.

Control groups were included in the experimental design to serve as a baseline against which all other transport results could be compared. Furthermore, the inclusion of control groups in the bi-directional transport studies of RH-123 were essential to gauge whether any changes in transport may be attributed to the presence of the herbal extracts/supplement instead of chance interferences. As discussed in Chapter 3, a RH-123 solution (no extract or supplement added) served as a negative control for the bi-directional transport studies, whereas verapamil (100 μ M), a known P-gp inhibitor, served as a positive control (Nabekura *et al.*, 2015).

Statistical analysis was performed on all P_{app} values where the transport of RH-123 in the apical-to-basolateral (AP-BL) direction and in the basolateral-to-apical (BL-AP) direction was compared to the respective control groups. Changes in the percentage TEER were also calculated to aid in the interpretation of the transport results and to help explain which transport mechanisms may potentially be involved in the altered transport of RH-123.

4.2 Chemical fingerprinting of the herbal extracts

4.2.1 Vitis vinifera seed extract

The results of the LC-MS chemical fingerprinting were indicative of the presence of certain active constituents, which are known to be found in *V. vinifera* seed extract. The presence of procyanidin B1 and procyanidin B2 was confirmed in the extract by the peak indicated by an arrow on the LC-MS chromatogram (Figure 4.1) of a molecule with a molecular weight of 564.3246 g/mol (Monages & Hernández-Ledesma, 2005).

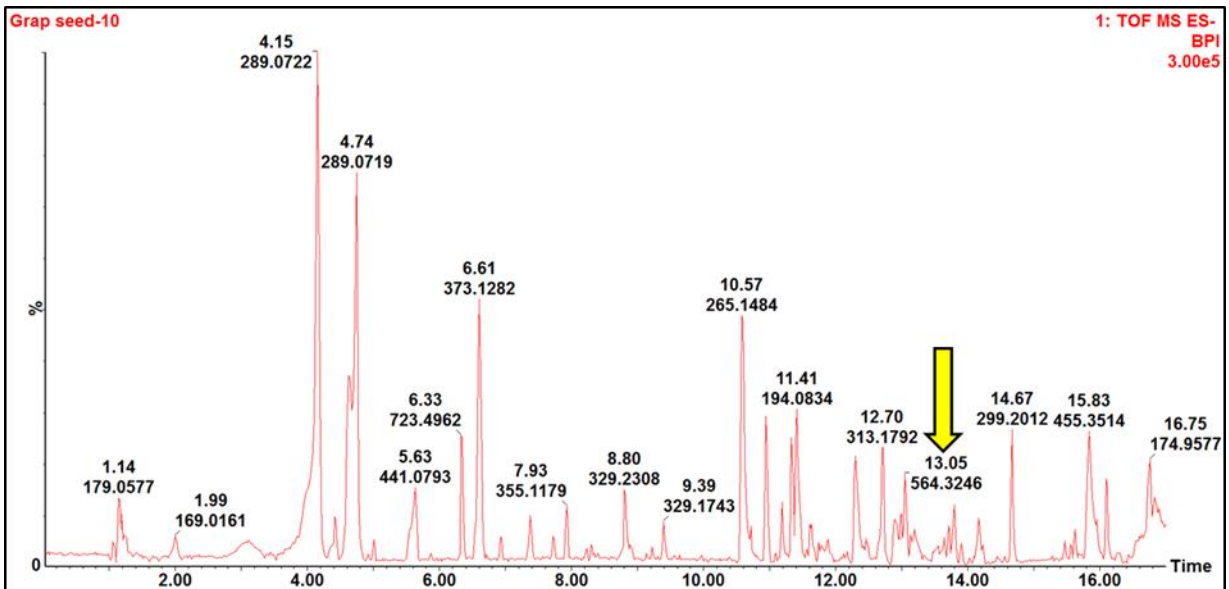


Figure 4.1: LC-MS chromatogram of *Vitis vinifera* seed extract

4.2.2 Hoodia gordonii

Figure 4.2 indicates the results of the chemical fingerprinting of the *H. gordonii* extract by means of LC-MS and LC-UV chromatograms. The active constituent of *H. gordonii* extract, namely an oxypregnane steroidal glycoside called P57AS3 (P57) (295.204 g/mol), was identified in the extract and quantified to be present in a concentration of 6.2 µg/mg (n=2).

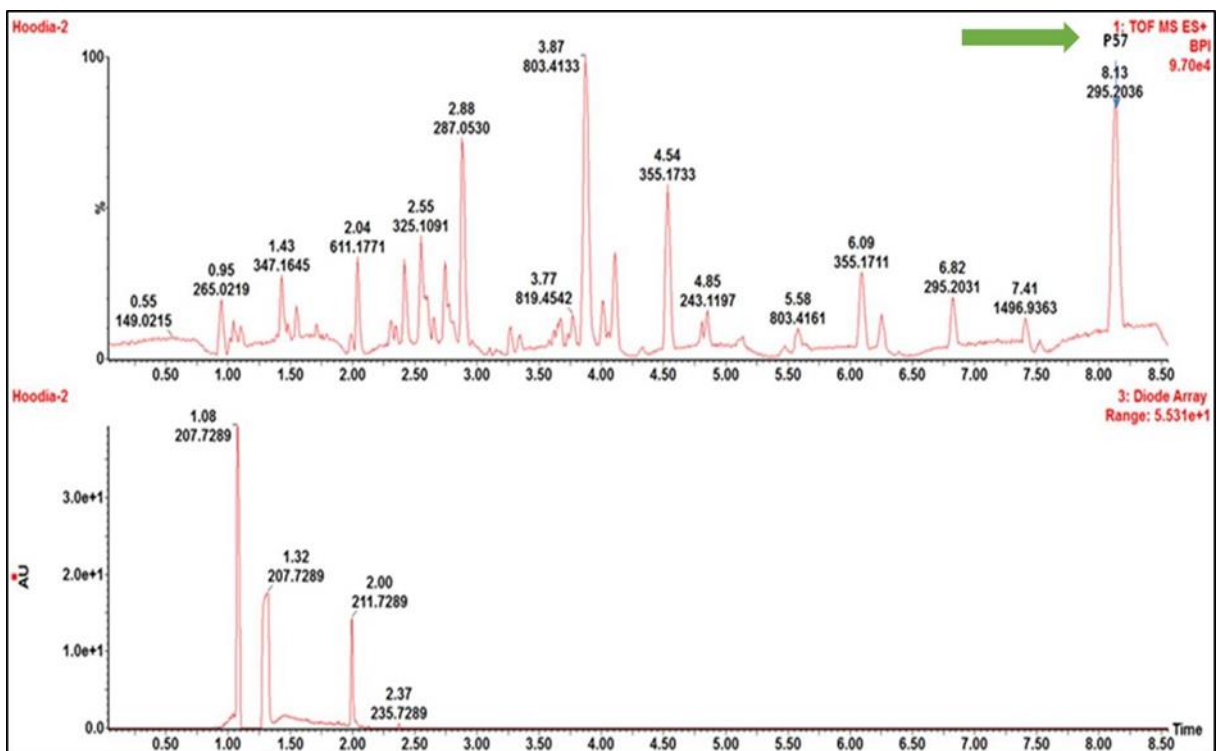


Figure 4.2: LC-MS and LC-UV chromatograms of *Hoodia gordonii* extract

4.2.3 Harpagophytum procumbens

The LC-MS and LC-UV chromatograms of *H. procumbens* extract are shown in Figure 4.3 and indicate the presence of harpagoside (493.146 g/mol), which was quantified to be present in a concentration of 17.5 µg/mg in the extract (n=2).

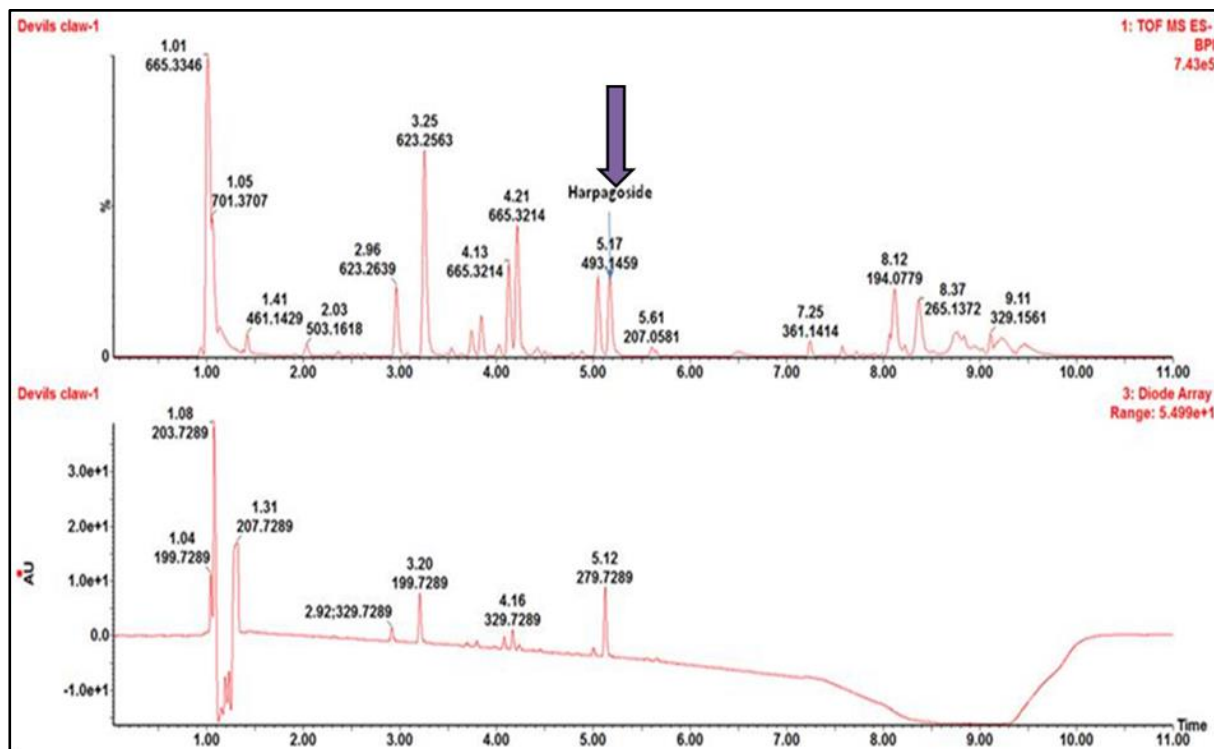


Figure 4.3: LC-MS and LC-UV chromatograms of *Harpagophytum procumbens* extract

4.2.4 Leonotis leonurus

Figure 4.4 shows the LC-MS chromatogram of *L. leonurus* extract. It is clear from the chromatogram that the extract contained narrulibanoside in a concentration of 35.4 µg/mg (n=2).

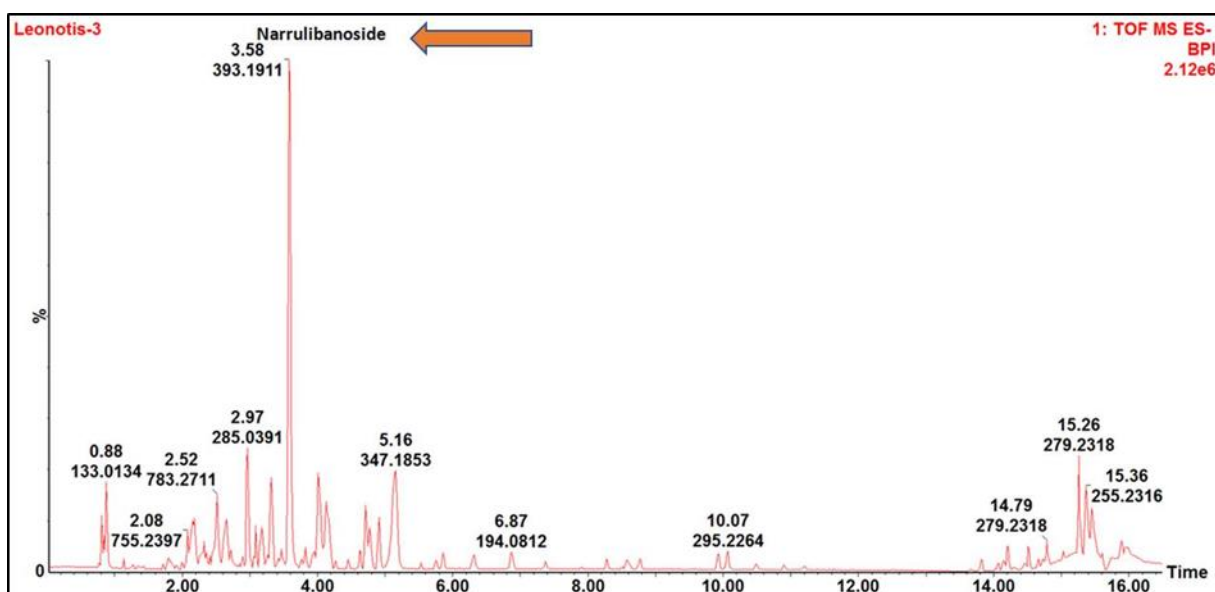


Figure 4.4 LC-MS chromatogram of *Leonotis leonurus* extract

4.2.5 Methylsulfonylmethane (MSM)

Even though no UPLC-MS analytical assays were done on the MSM material used in this study, a certificate of analysis was provided by the supplier, which can be found in Addendum B. The chemical analysis which was performed by the supplier proved that the material used did comply with all specifications with regards to purity and identity.

4.3 Fluorescence spectrometry analytical method validation for Rhodamine 123 and Lucifer yellow

The RH-123 concentration in all the transport samples, as well as the LY concentration in samples from the membrane integrity evaluation, were analysed by means of fluorescence spectrometry and were performed with a Spectramax Paradigm® plate reader. The excitation and emission wavelengths for RH-123 were set at 480 nm and 520 nm respectively, and the excitation wavelength for LY was set at 485 nm with the emission wavelength set at 530 nm (Colabufo *et al.*, 2008; Irvine *et al.*, 1999; Kaprelyants & Kell, 1992). Validation of these analytic methods was corroborated by the determination of the linearity, accuracy, precision, specificity, limit of detection and limit of quantification.

4.3.1 Method validation results: Rhodamine 123

4.3.1.1 Linearity

Linearity was determined by using the results obtained from a standard curve following the analysis of a series of RH-123 solutions with varying concentrations (Table 4.1). The fluorescence values were used to construct a regression curve of fluorescence plotted as a function of RH-123 concentration, which is demonstrated in Figure 4.5.

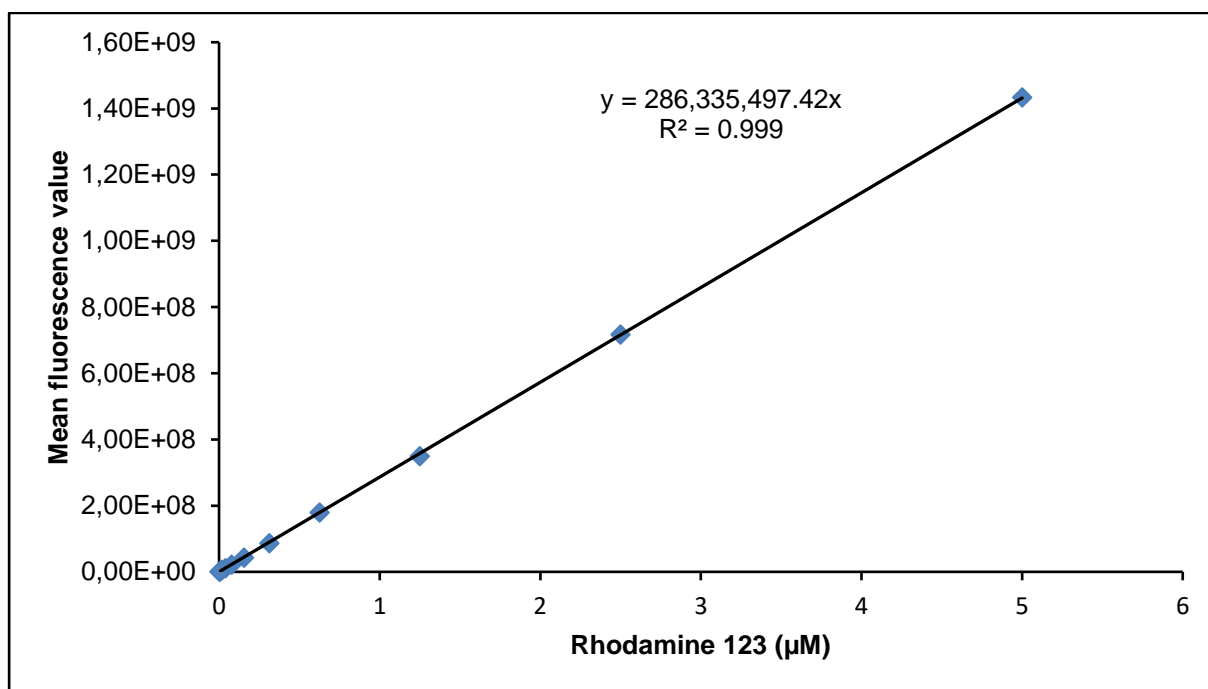


Figure 4.5: Linear regression curve for Rhodamine 123 with the straight line equation and correlation coefficient (R^2) value

Table 4.1: Mean fluorescence values of Rhodamine 123 recorded over a defined concentration range

RH-123 Concentration (μM)	Mean fluorescence value
5	1433323663.00
2.5	717025742.70
1.25	349761582.70
0.625	179303214.70
0.313	86806302.70
0.156	42770286.70
0.078	21801618.70
0.039	11174713.70
0.020	5741531.70
0.010	3021214.70
0.005	1572144.70
0.002	844865.70
Slope	286335497.42
R²	0.999

According to published requirements, the acceptable value for the correlation coefficient value of a standard curve is $R^2 > 0.995$ (Shabir, 2003; Singh, 2013). It is evident from the collected data (Figure 4.5 and Table 4.1) that the analytical method used for RH-123 did meet the specified criterium for linearity with a correlation coefficient value of 0.999.

4.3.1.2 Limit of detection and limit of quantification

The standard deviation values of the blank test samples (KRB buffer), also known as the background noise (Table 4.2) were used to mathematically calculate the limit of detection (LOD) and limit of quantification (LOQ). The slope of the regression curve shown in Figure 4.5 was also used.

Table 4.2: Blank fluorescence values together with the standard deviation and limit of detection (LOD) as well as limit of quantification (LOQ)

Blank fluorescence values	Average	Standard deviation	LOD (μM)	LOQ (μM)
189024	189041.30	6042.52	6.96×10^{-5}	2.11×10^{-4}
193518				
194067				
194760				
193142				
189262				
182287				
186355				
193125				
174873				

The experimental RH-123 concentrations in the transport samples were much higher than the calculated LOD and LOQ and it could therefore accurately quantify the RH-123 concentration in the experimental samples.

4.3.1.3 Accuracy

Table 4.3 provides information regarding the accuracy (% recovery) achieved with the fluorometric analytical method based on the analysis of three different RH-123 test concentrations. The analytical method achieved acceptable accuracy and complied with the specified recovery requirements of $100 \pm 2\%$ as disclosed in the literature (Shabir, 2003).

Table 4.3: Data procured from sample analysis to determine the accuracy of the analytical method for Rhodamine 123 across a specified concentration range

Theoretical concentration (μM)	5	2.5	0.125
Fluorescence values	1374304768	714863744	35190200
	1413897472	730335232	36293648
	1423600000	719642944	41629624
	1380864640	722737984	41513688
	1381045120	714502720	40831920
	1409393152	714556608	41481164
	1403218688	718679872	41243024
	1385916672	723542080	40687368
	1372816768	728484736	41529164
	1372593280	717087232	40282364
Average fluorescence values	1391765056.00	720443315.20	40068216.40
Actual concentration (μM)	5.01	2.52	0.125
Accuracy (% recovery)	100.27	100.64	100.13

4.3.1.4 Precision

4.3.1.4.1 Intra-day precision

Three RH-123 solutions with varying concentrations (i.e. 5 μM , 2.5 μM and 0.125 μM) were analysed in triplicate during a 24 h period to obtain standard deviation and percentage relative standard deviation (% RSD) values in order to determine the intra-day precision of the analytical method. Table 4.4 provides a summary of the data used to calculate the intra-day precision of the analytical method.

Table 4.4: Data used to calculate the intra-day precision of the analytical method

Concentration (μM)	Repeat	Mean fluorescence value	Standard deviation	% RSD
5	1	1394082419.00	9514583.36	0.68
	2	1391765056.00		
	3	1413007194.00		
2.5	1	727881670.40	2426166.36	0.33
	2	726199859.20		
	3	722104480.00		
0.125	1	40751802.80	453466.97	1.12
	2	40068216.40		
	3	41168216.40		

Shabir (2003) stated that all % RSD values should be $< 2\%$ and the data in Table 4.4 indicate that the analytical method did comply with this requirement as stated in the literature to confirm intra-day precision.

4.3.1.4.2 Inter-day precision

Three RH-123 solutions with varying concentrations (i.e. $5 \mu\text{M}$, $2.5 \mu\text{M}$ and $0.125 \mu\text{M}$) were analysed in triplicate to obtain standard deviation and % RSD values in order to determine the inter-day precision of the analytical method. The inter-day precision of the analytical method was determined by measuring the fluorescence of each test concentration in triplicate over a period of three days. The standard deviation and % RSD were subsequently calculated from the data presented in Table 4.5.

Table 4.5: Data used to calculate the inter-day precision of the analytical method

Concentration (μM)	Day	Mean fluorescence value	Standard deviation	% RSD
5	1	1399618223.00	6043036.96	0.43
	2	1408277594.00		
	3	1393551091.00		
2.5	1	725395336.50	2222755.68	0.31
	2	720443315.20		
	3	724879174.40		
0.125	1	40662745.20	531782.59	1.29
	2	41950603.20		
	3	41475888.80		

All % RSD values were in accordance with the requirements stated in the literature (% RSD < 2%) and thus the fluorescence spectrometry analytical method did comply with this requirement to confirm inter-day precision of the method (Shabir, 2003).

4.3.1.5 Specificity

The analytical method was able to accurately quantify the RH-123 content ($100 \pm 2\%$) in the experimental samples in the presence of one of the selected herbal extracts and the supplement. *V. vinifera* seed extract and MSM did not show any interference with regards to the accuracy and Table 4.6 shows the concentrations and percentage accuracy of RH-123 achieved during the validation of this analytical method. To determine the specificity of RH-123 in the presence of the remaining extracts namely *H. gordonii*, *H. procumbens* and *L. leonurus* the method described in section 3.5.4 “Specificity” was employed to determine the specificity and achieving an R^2 value of above 0.995 as depicted in Table 4.7.

Table 4.6: Summary of the specificity validation data for Rhodamine 123 in the presence of methylsulfonylmethane and *Vitis vinifera* seed extract

Analyte	Theoretical concentration (µM)	Mean fluorescence value	Actual concentration (µM)	Accuracy (%)
Rhodamine 123 alone	5.00	1391765056	5.01	100.27
Methylsulfonylmethane	5.00	1412433302	4.89	100.21
<i>Vitis vinifera</i> seed extract	5.00	1336343837	4.79	98.33

The analytical method yielded acceptable recovery of RH-123 in the presence of MSM and *V. vinifera* seed extract and the analytical method therefore did comply with the required specificity criteria in the presence of these two substances.

In order to overcome interferences of the remaining extracts with RH-123 fluorometric analysis, standard curves of RH-123 in the presence of these extracts were constructed and subjected to linear regression. The regression results obtained from these curves are shown in Table 4.7.

Table 4.7: Summary of the linearity data for Rhodamine 123 in the presence of *Hoodia gordonii*, *Harpagophytum procumbens* and *Leonotis leonurus*

Herbal extract	R ²
<i>Hoodia gordonii</i>	0.998
<i>Harpagophytum procumbens</i>	0.996
<i>Leonotis leonurus</i>	0.999

The linearity results correlated with the specific criteria of R² with a value of more than 0.995 and the method yielded acceptable specificity.

4.3.2 Method validation results: Lucifer yellow

4.3.2.1 Linearity

Linearity was determined by using the results obtained from a standard curve following the analysis of a series of LY solutions with varying concentrations (Table 4.8). The fluorescence values were then used to construct a regression curve of fluorescence versus LY concentration, which is depicted in Figure 4.6. The curve consists of the fluorescence values that were plotted as a function of the LY concentration.

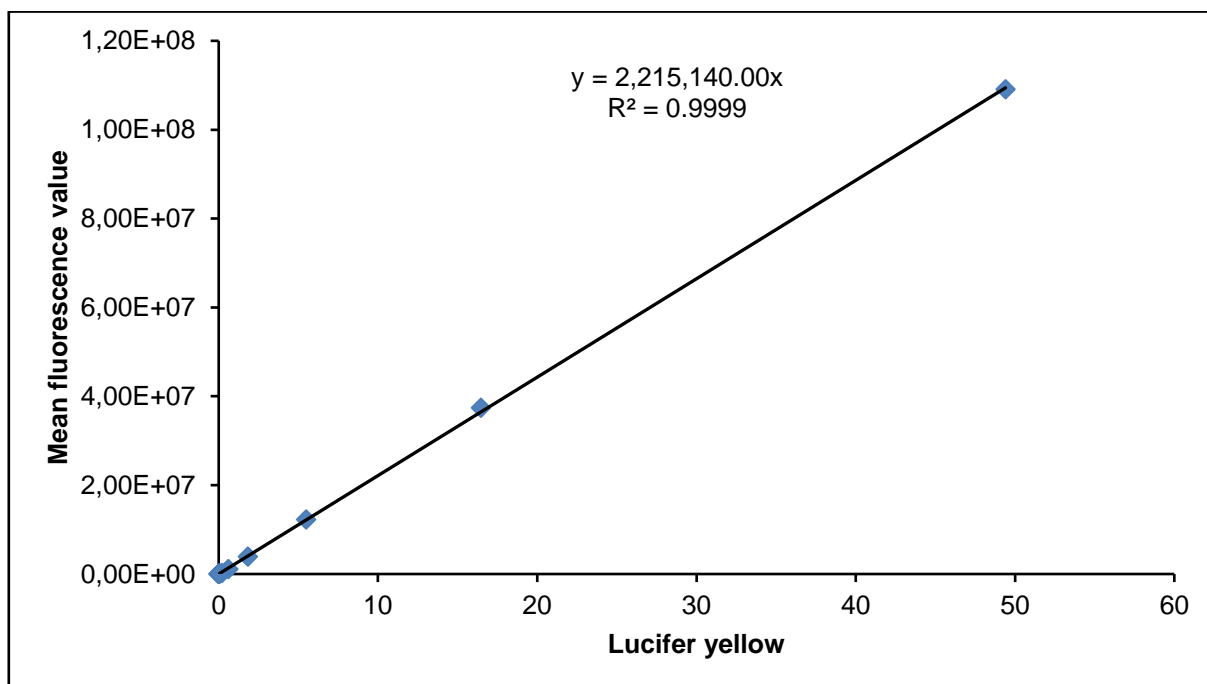


Figure 4.6: Linear regression curve for Lucifer yellow demonstrated with the straight line equation as well as the correlation coefficient (R^2) value

Table 4.8: Mean fluorescence values of Lucifer yellow demonstrated over a defined concentration range

Lucifer yellow concentration ($\mu\text{g/ml}$)	Mean fluorescence value
50	109099528
16.667	37448948
5.556	12272638
1.852	3914932
0.617	1146500
0.206	301366
0.069	105170
0.023	51697
0.008	40986
0.003	30474
0.001	23466
0.0003	29489
Slope	2233762.89
R²	0.9999

4.3.2.2 Limit of detection and limit of quantification

The standard deviation of the blank (KRB buffer) readings, also known as the background noise (Table 4.9) as well as the slope of the regression curve shown in Figure 4.6 and Table 4.8 were used to mathematically calculate the limit of detection (LOD) and limit of quantification (LOQ).

Table 4.9: Fluorescence values of the blanks (KRB buffer) together with the standard deviation

Blanks fluorescent values	Average	Standard deviation	LOD (µg/ml)	LOQ (µg/ml)
23186	24465.50	1249.47	1.75×10^{-3}	5.31×10^{-3}
25794				
23434				
24669				
23210				
27021				
24849				
23054				
24115				
25323				

The concentrations used of LY in the experiments were higher than the concentration values obtained for the LOD and LOQ. This is thus indicative that the analytical method used was able to detect and quantify the amount of LY used in the experiments pertaining to the integrity of the intestinal membrane.

4.3.2.3 Accuracy

Table 4.10 presents information concerning the accuracy (% recovery) of all three concentrations of LY. The analytical method used to determine the accuracy was satisfactory as it complied with the specification of $100 \pm 2\%$ recovery as disclosed in the literature (Shabir, 2003).

Table 4.10: Data procured from the Lucifer yellow sample analysis to ascertain accuracy across a specified concentration range

Theoretical concentration (µg/ml)	50	25	12.5
Fluorescence values	111388024	58994780	27960306
	111148736	57311556	27695060
	107838672	58675744	27419306
	107816904	56950012	27340096
	106026184	57504668	27189250
	106022088	57372532	27157480
	109583344	57249632	27459234
	108442264	57813600	27704446
	106831008	59289612	27065400
	107019608	57419092	27126692
Average fluorescence values	108211683.20	57858122.80	27411727.00
Actual concentration (µg/ml)	48.85	24.56	12.27
Accuracy (% recovery)	98.29	98.83	100.03

4.3.2.4 Precision

4.3.2.4.1 Intra-day precision

Three LY concentrations (i.e. 50 µg/ml, 25 µg/ml and 12.5 µg/ml) were analysed and the fluorescence values were used to obtain the standard deviation and % RSD. Table 4.11 shows a summary of the data used to determine intra-day precision.

Table 4.11: Data used to calculate intra-day precision of Lucifer yellow

Concentration ($\mu\text{g/ml}$)	Repeat	Mean fluorescence value	Standard deviation	% RSD
50	1	108211683.20	712457.88	0.66
	2	107644265.60		
	3	106498740.00		
25	1	57785951.00	56932862.70	1.07
	2	56594358.00		
	3	56418279.11		
12.5	1	27496753.60	279879.41	1.03
	2	27039436.20		
	3	26825780.80		

It is evident from Table 4.11 that the data obtained by using the analytical method complied with the precision standards as set out by Shabir (2003) and that the % RSD value was $\leq 2\%$.

4.3.2.4.2 Inter-day precision

Aforementioned concentrations of LY (i.e. 50 $\mu\text{g/ml}$, 25 $\mu\text{g/ml}$ and 12.5 $\mu\text{g/ml}$) were used to calculate the average fluorescence value of each of the concentrations over a period of three days. The standard deviation and % RSD were subsequently calculated from the data procured in Table 4.12.

Table 4.12: Data used to calculate inter-day precision of Lucifer yellow

Concentration ($\mu\text{g/ml}$)	Day	Mean fluorescence value	Standard deviation	% RSD
50	1	108211683.20	1175431.73	1.07
	2	110514439.33		
	3	110859846.00		
25	1	57785951.00	127871.34	0.22
	2	57647100.86		
	3	57959672.67		
12.5	1	27496753.60	115074.96	0.42
	2	27560700.00		
	3	27766473.00		

It is evident from Table 4.12 that the analytical method used complied with the precision standard of % RSD \leq 2% (Shabir, 2003).

4.3.3 Summary of validation results

Each validation test performed and all the data obtained for RH-123 and LY during the orchestration of the analytical method validation procedure have proved that the analysis methods that were used on the Spectramax Paradigm[®] plate reader did comply with all the stated validation criteria as mentioned above.

4.4 Bi-directional transport studies

In vitro transport studies were conducted bi-directionally across excised pig intestinal jejunum tissue to determine the effects of the selected herbal extracts and supplement on the transport of RH-123. Each individual transport study yielded its own P_{app} value for RH-123. As discussed in Chapter 3, a RH-123 solution (no extract or supplement added) served as a negative control for the bi-directional transport studies whereas verapamil (100 μM), a known P-gp inhibitor, served as a positive control (Nabekura *et al.*, 2015).

4.4.1 Methylsulfonylmethane (MSM)

Figure 4.7 exhibits the average percentage transport of RH-123 in the apical-to-basolateral (AP-BL) direction, while Figure 4.8 represents the average percentage transport in the basolateral-to-apical (BL-AP) direction in the presence of different concentrations of MSM.

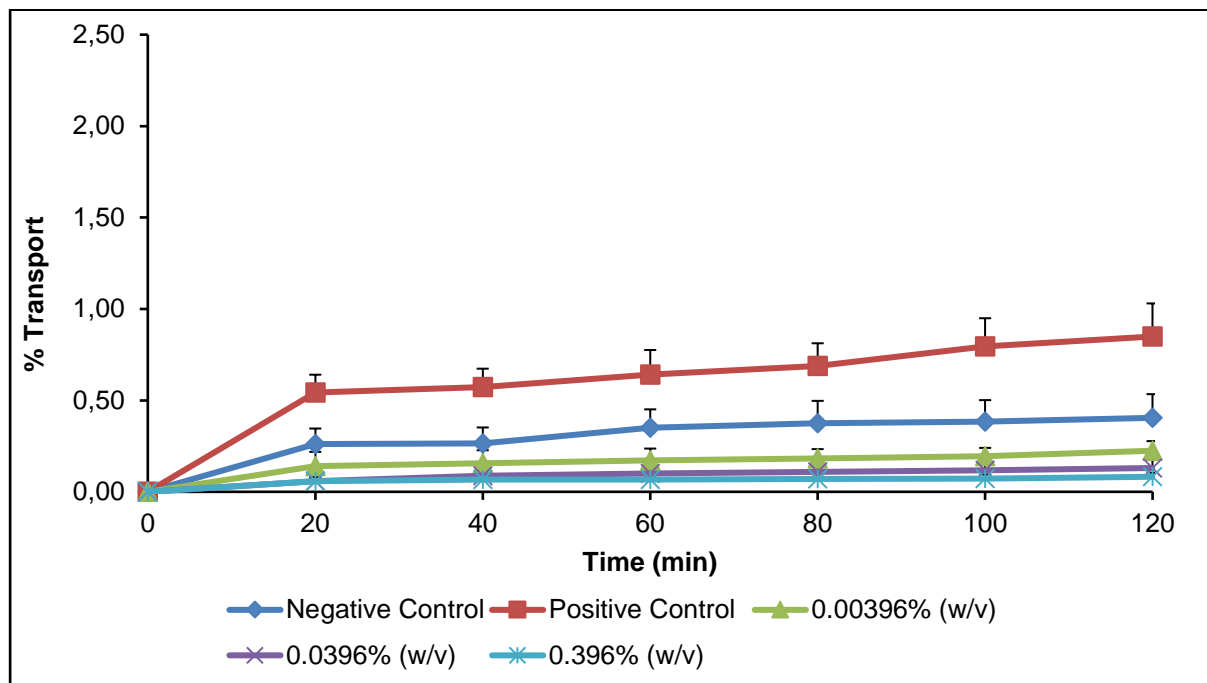


Figure 4.7: Apical-to-basolateral transport of Rhodamine 123 in the presence of different concentrations of methylsulfonylmethane (MSM) across excised pig jejunum tissue plotted as a function of time

From Figure 4.7 it can be observed that addition of verapamil, a known P-gp inhibitor (i.e. positive control group), mediated an increase in the uptake of RH-123 in the AP-BL direction. MSM mediated a concentration dependent decrease in the transport of RH-123 in the AP-BL direction. Upon comparing the percentage transport of RH-123 in the presence of the selected MSM concentrations to that of RH-123 alone (i.e. negative control group), it is evident that the highest concentration (0.396% (w/v)) had the most pronounced decreasing effect on RH-123 transport. Furthermore, Skrovanek *et al.* (2007) noted that the presence of sulfur molecules within the molecular structure of some compounds can lead to alterations in the claudin composition in the gastrointestinal tract (GIT), which in turn may improve the barrier function of tight junctions. This effect was supported by the data from this study, which showed that the higher MSM concentration and therefore higher sulfur content caused the most pronounced reduction in RH-123 uptake. An increase in the recorded TEER values (as discussed in section 4.5, Table 4.14) also confirmed that the tight junction integrity had increased with an increase in the MSM concentration and the highest MSM concentration that was tested yielded a change in percentage

TEER to 104.68%. Another contributing factor to decreased AP-BL transport of RH-123 in the presence of MSM may be due to stimulation of efflux as shown in Figure 4.8.

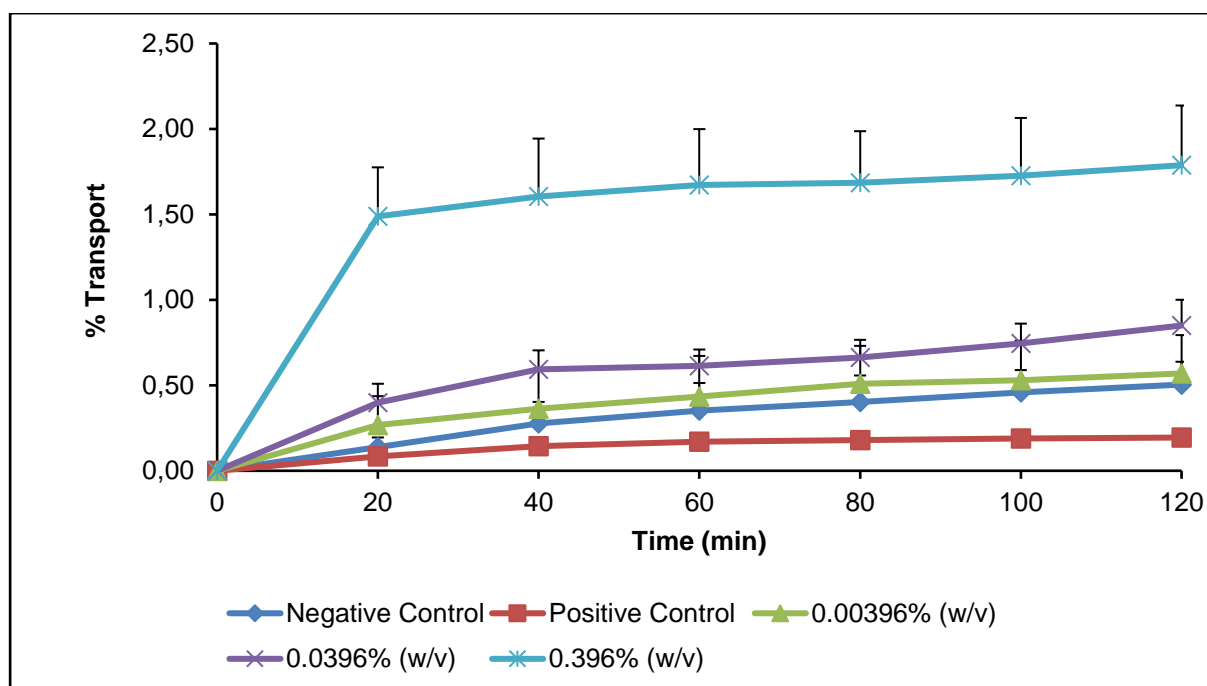


Figure 4.8: Basolateral-to-apical transport of Rhodamine 123 in the presence of different concentrations of methylsulfonylmethane (MSM) across excised pig jejunum tissue plotted as a function of time

MSM yielded a concentration dependent increase in RH-123 transport in the BL-AP or secretory direction (Figure 4.8). During the BL-AP transport studies, MSM mediated an increase in RH-123 transport by as much as 3.5 and 9.2 fold in relation to the negative and positive control groups, respectively. An efflux ratio (ER) $\gg 1$ indicates that a compound is susceptible to active efflux transport (Section 4.4 “Evaluation of efflux ratios”). It is clear from the efflux ratio data procured from this study (i.e. ER = 2.94 for the 0.00396% (w/v) MSM group, ER = 6.22 for the 0.0396% (w/v) MSM group and ER = 21.2 for the 0.396% (w/v) MSM group) that the mechanism of transport for RH-123 in the secretory direction was by means of stimulation or induction of P-gp related efflux transport. This increased efflux of RH-123 in the BL-AP direction modulated by MSM is therefore also partly responsible for the decrease in AP-BL transport.

A summary of the calculated P_{app} values in the AP-BL and BL-AP directions is presented in Figure 4.9. These values are indicative of the diffusion rate of the compound normalised for the surface area of the excised intestinal jejunum tissue and the drug concentration on the donor side of the membrane (Tarirai *et al.*, 2010). In Figure 4.9, it can be seen that MSM had mediated a pronounced increase in the BL-AP transport of RH-123, which contributed to the reduction of RH-

123 transport in the AP-BL direction compared to that of the negative control group (RH-123 alone). The increase in the P-gp related efflux was concentration dependent and the highest MSM concentration (0.396% (w/v) rendered a secretory P_{app} value of 9.902×10^{-7} cm/s as opposed to the negative control (i.e. RH-123 alone) with a secretory P_{app} value of 3.811×10^{-7} cm/s. All MSM concentrations demonstrated a consistency with respect to the change in the percentage transport in both the AP-BL and BL-AP directions. Statistically significant differences ($p \leq 0.05$) were evident when the average P_{app} value of the negative control in the BL-AP direction, was compared to the P_{app} values in the presence of MSM concentrations of 0.0396% (w/v) and 0.396% (w/v).

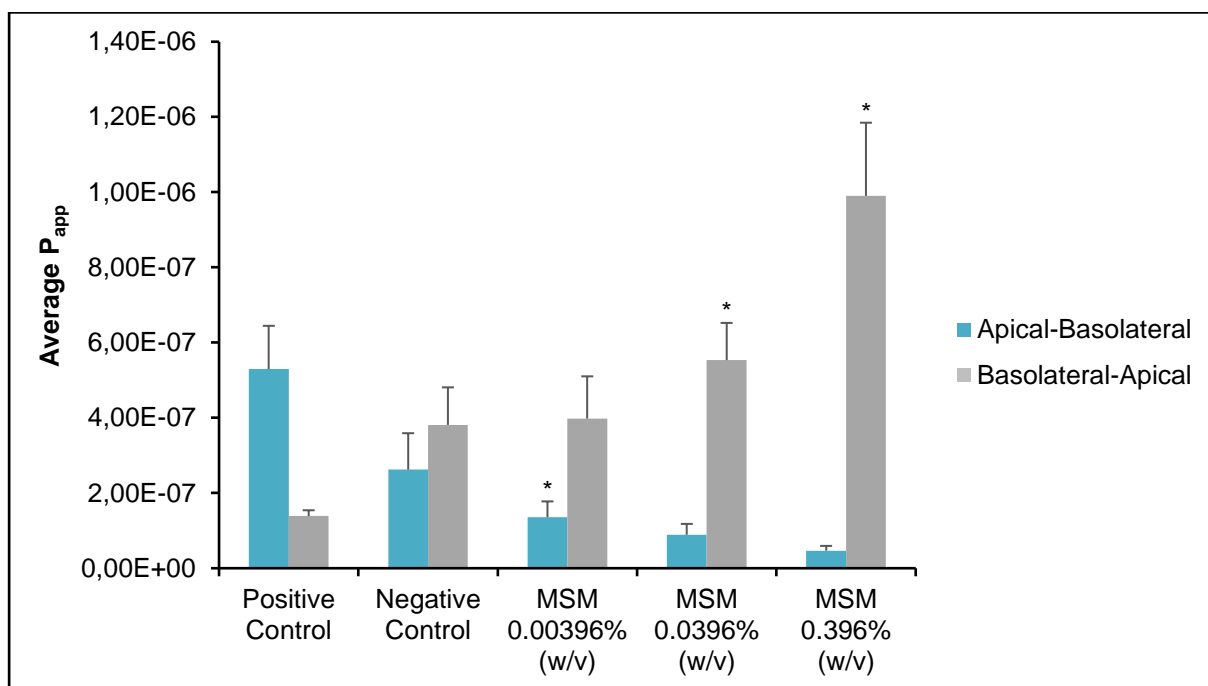


Figure 4.9: Average P_{app} values for bi-directional transport of Rhodamine 123 in the presence of different concentrations of methylsulfonylmethane (MSM) across excised pig jejunum tissue (*statistically significant differences, $p \leq 0.05$)

4.4.2 Vitis vinifera seed extract

It has been reported in the literature that *V. vinifera* seed extract contains procyanidin (a polyphenol), which is commonly used for its anti-inflammatory properties (Zhao *et al.*, 2013). Figure 4.10 exhibits the average percentage transport of RH-123 in the AP-BL direction, while Figure 4.11 represents the average percentage transport in the BL-AP direction.

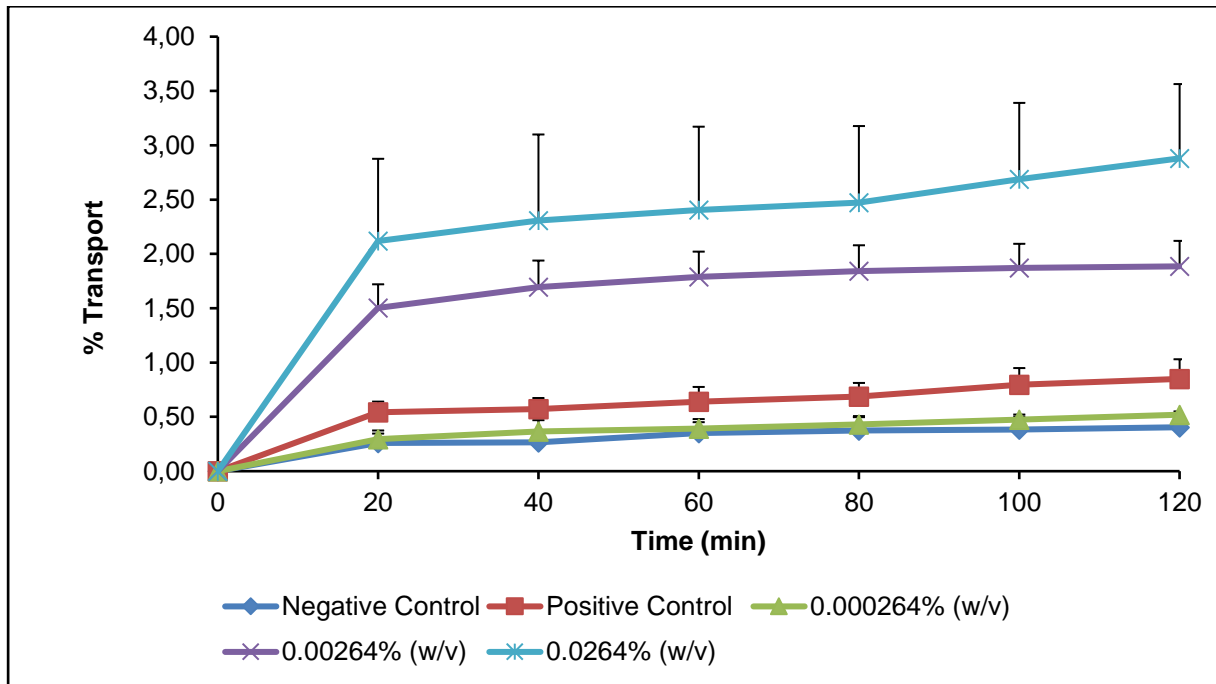


Figure 4.10: Apical-to-basolateral transport of Rhodamine 123 in the presence of different concentrations of *Vitis vinifera* seed extract across excised pig jejunum tissue plotted as a function of time

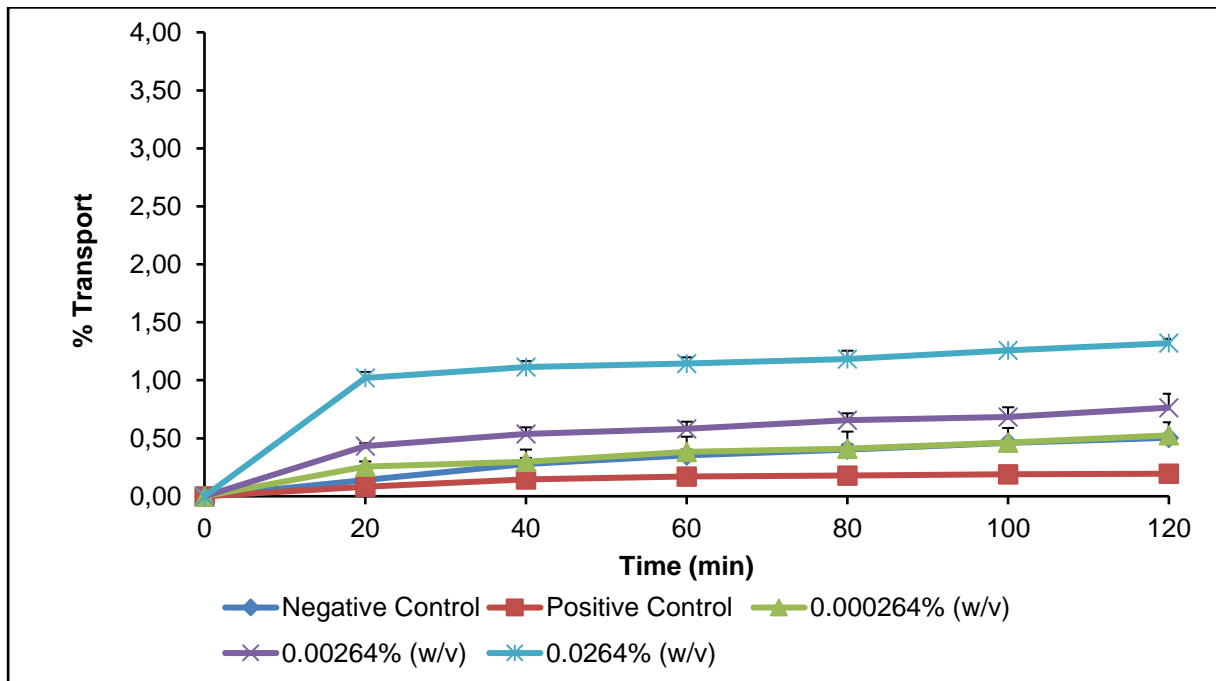


Figure 4.11: Basolateral-to-apical transport of Rhodamine 123 in the presence of different concentrations of *Vitis vinifera* seed extract across excised pig jejunum tissue plotted as a function of time

Figures 4.10 and 4.11 shows that *V. vinifera* seed extract mediated a concentration dependent increase in both the uptake (in the AP-BL direction) and the secretory transport (in the BL-AP direction) of RH-123. This phenomenon may be explained by changes in the TEER values. An overall decrease in the TEER values (Table 4.14) of the excised jejunum tissues during the transport study in the AP-BL direction indicated that a pronounced opening of the tight junctions was mediated by the addition of increasing concentrations of *V. vinifera* seed extract. A study conducted by Takizawa *et al.* (2013) illustrated that RH-123 can be transported by means of paracellular diffusion across membranes and it may be possible that the decrease in TEER may, in this instance, also have mediated an increase in the diffusion of RH-123 across the membrane.

The transport results in the BL-AP direction (Figure 4.11) have also shown a concentration dependent increase in RH-123 transport and this increase may again be attributed to a decrease in TEER values (Table 4.14). In a study performed by Zhao *et al.* (2013), it was found that *V. vinifera* seed extract had the ability to inhibit P-gp activity by blocking the MDR1 gene transcription with a resultant increase in the intracellular accumulation of RH-123. Results obtained in this study were in accordance with the study by Zhao *et al.* (2013).

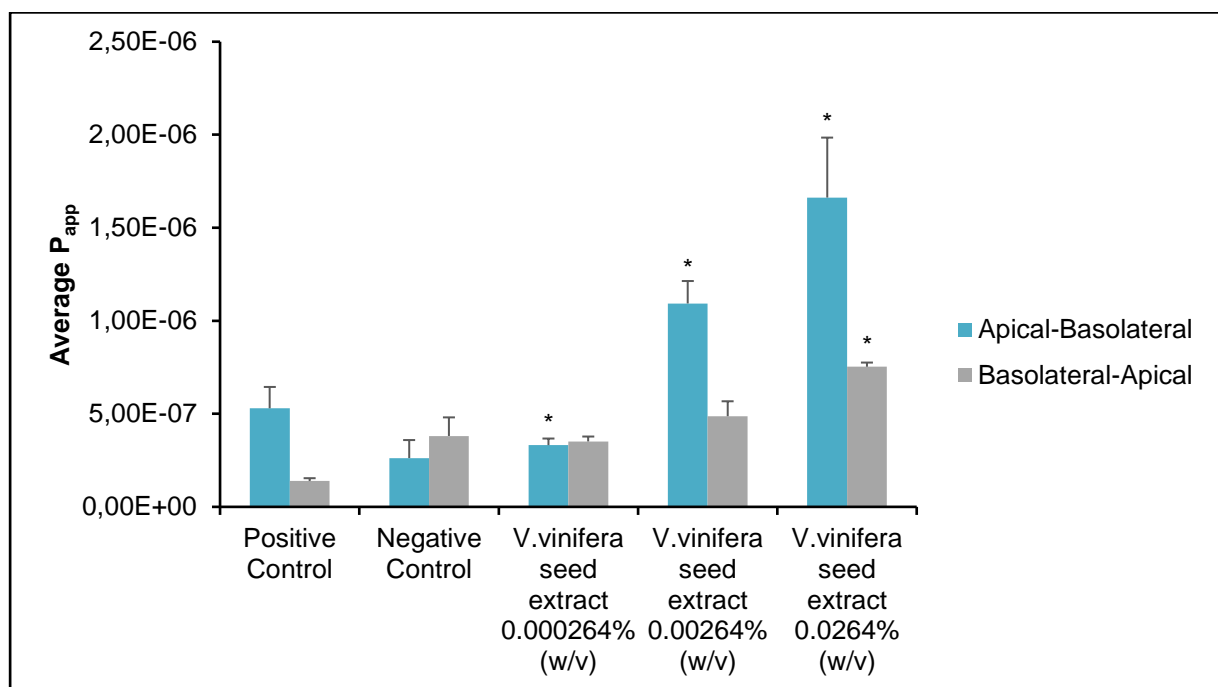


Figure 4.12: Average P_{app} values for bi-directional transport of Rhodamine 123 in the presence of *Vitis vinifera* seed extract across excised pig jejunum tissue (*statistically significant differences, p ≤ 0.05)

A summary of the calculated average P_{app} values is presented in Figure 4.12. A concentration dependent increase in the P_{app} values is evident for the uptake of RH-123 (i.e. transport AP-BL) when compared to the negative control (RH-123 alone). A concentration dependent increase can also be observed for the secretory transport of RH-123 (i.e. transport BL-AP) even though the lowest concentration (0.000264% (w/v)) has a lower average P_{app} value than the negative control. With regards to the ER value of each concentration, it is observed that these values are $\ll 1$, which is indicative that the transport was subjected to active absorptive uptake (Bock *et al.*, 2003). The ER value for the 0.000264% (w/v) *V. vinifera* seed extract solution was 0.96, for the 0.00264% (w/v) *V. vinifera* seed extract solution, 0.45 and for the 0.0264% (w/v) *V. vinifera* seed extract solution, 0.45. These values cannot, however, be interpreted on their own and the TEER, which have decreased must also be taken into consideration. Statistically significant differences in the extent of RH-123 transport compared to the control were evident at all three *V. vinifera* seed extract concentrations that were evaluated in the AP-BL direction as well as for the highest concentration in the BL-AP direction.

V. vinifera seed extract may have had effects on transport mechanisms other than P-gp related efflux, but it could not be confirmed from the results of this study and additional studies are required to elucidate the experimental results. It was previously reported by Varma *et al.* (2003) that P-gp modulation can occur through either direct blocking of the drug binding site, interference with ATP hydrolysis or altering the cell membrane integrity; this in conjunction with the decrease in TEER values can serve as another explanation that can contribute to an alteration in the membrane integrity.

4.4.3 Hoodia gordonii

Figure 4.13 exhibits the average percentage transport of RH-123 in the AP-BL direction.

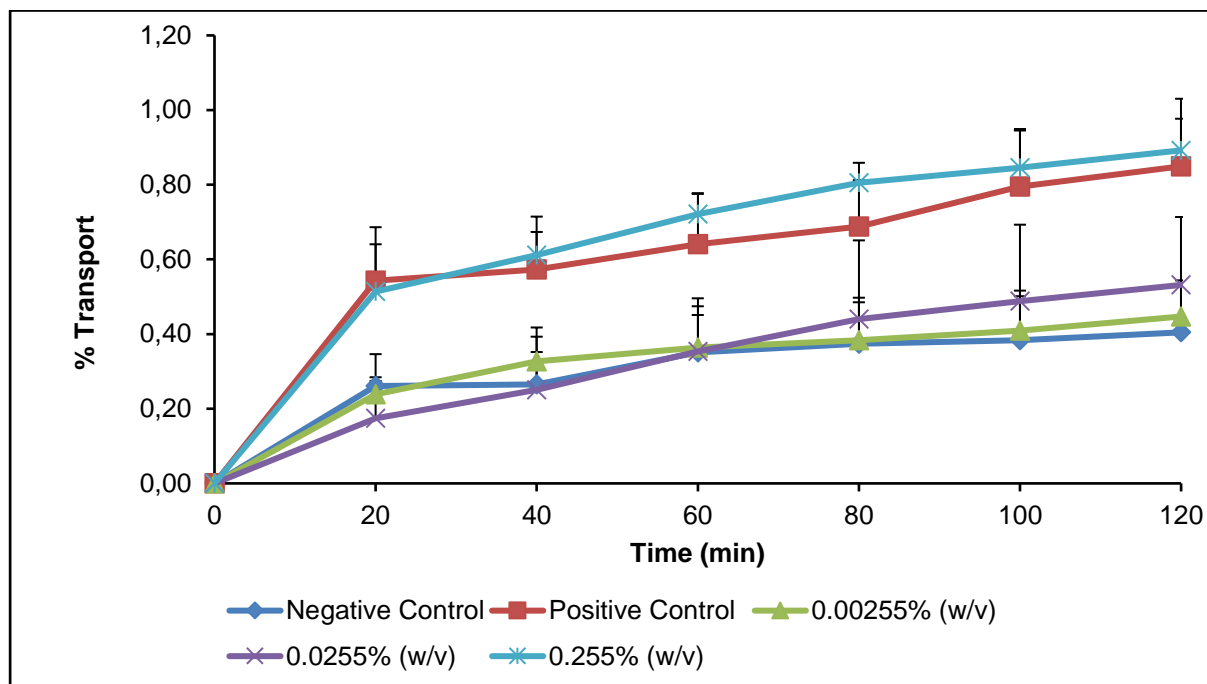


Figure 4.13: Apical-to-basolateral transport of Rhodamine 123 in the presence of different concentrations of *Hoodia gordonii* extract across excised pig jejunum tissue plotted as a function of time

Figure 4.13 shows that the cumulative amount of RH-123 that was transported across the excised tissues had increased linearly over time in a concentration dependent manner in the absorptive direction. The lower concentration (0.00255% (w/v)) and medium concentration (0.0255% (w/v)) of *H. gordonii* extract did not increase the uptake of RH-123 statistically significantly compared to the negative control. Incongruently, the highest concentration of *H. gordonii* extract (0.255% (w/v)) increased the uptake of RH-123 by 2.2-fold compared to the negative control. The TEER of the excised tissue at the highest concentration of *H. gordonii* extract applied showed a decrease of 38.1% over the 2 h period. This indicated that paracellular uptake via opened tight junctions may also have contributed to the increased uptake of RH-123. The ER values were calculated and found to be 0.80, 0.52 and 0.27 for the low, medium and high concentrations of *H. gordonii* extract, respectively. Bock *et al.* (2003) reported that an ER \ll 1 is indicative of absorptive uptake due to decreased efflux and the ER values calculated from the experimental results suggest that RH-123 transport was increased.

The BL-AP percentage transport is depicted in Figure 4.14.

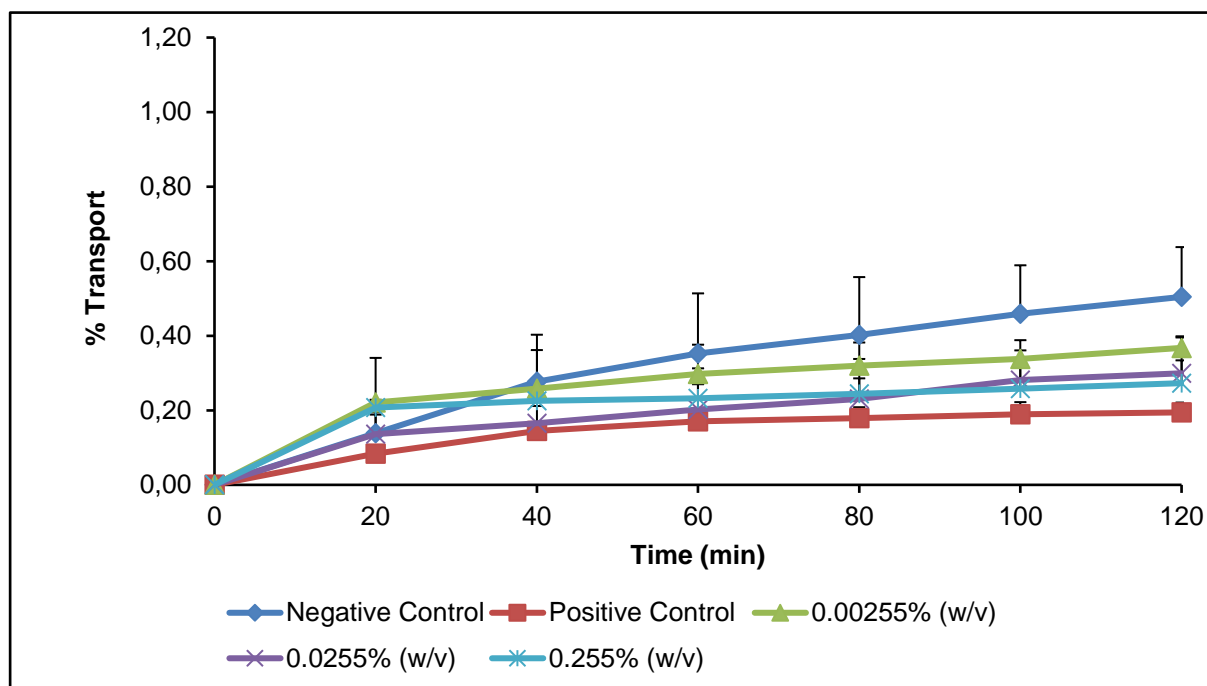


Figure 4.14: Basolateral-to-apical transport of Rhodamine 123 in the presence of *Hoodia gordonii* extract across excised pig jejunum tissue plotted as a function of time

A concentration dependent decrease in the secretory direction of RH-123 is observed in the presence of *H. gordonii* extract. With regards to the negative control (i.e. RH-123 alone) the highest concentration of *H. gordonii* extract (0.225% (w/v) decreased the transport of RH-123 by 1.8-fold. The highest concentration of *H. gordonii* extract (0.225% (w/v) showed a decrease in RH-123 efflux similar to that of the positive control group (i.e. RH-123 and verapamil combination).

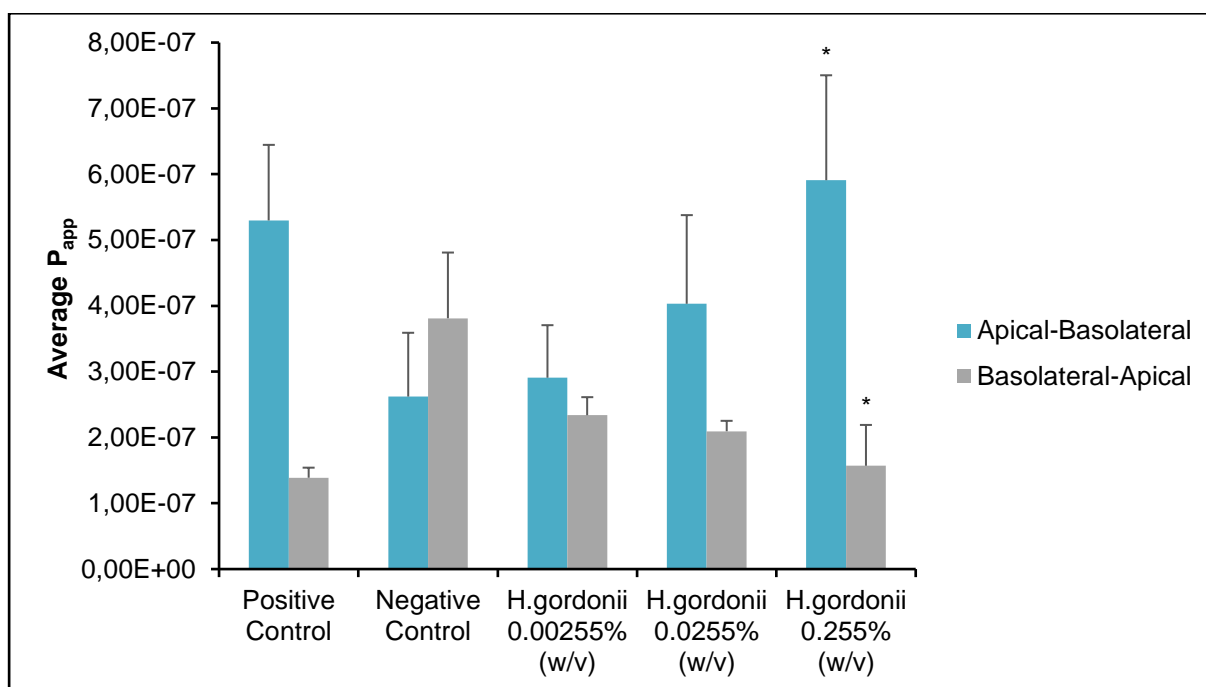


Figure 4.15: Average P_{app} values for bi-directional transport of Rhodamine 123 in the presence of different concentrations of *Hoodia gordonii* extract across excised pig jejunum tissue (*statistically significant differences, $p \leq 0.05$)

Figure 4.15 confirms a decrease in the secretory transport of RH-123 in the BL-AP direction in the presence of *H. gordonii* extract. This indicates that *H. gordonii* extract contains molecule(s) that act as efflux pump inhibitor(s) in a concentration dependent way. The decrease in TEER values of the excised jejunum tissues for the highest concentration of *H. gordonii* extract in the AP-BL direction could explain the surge in the transport increase of RH-123 in this group. A relatively slight decrease in the TEER values could be observed for the rest of the concentrations that were tested in the AP-BL and BL-AP directions. Taking this into consideration, the change in TEER values and the resultant modulation of the paracellular transport of RH-123 as a result therefore, may have been negligibly small (Table 4.14). Furthermore, transport of RH-123, with regards to the P_{app} values were significantly higher in the absorptive than in the secretory direction (Table 4.13). These results correspond to findings which were reported by Vermaak *et al.* (2011b) and Madgula *et al.* (2008) where they also found that *H. gordonii* extracts were able to inhibit P-gp related efflux.

4.4.4 Harpagophytum procumbens

Herbal preparations containing *H. procumbens* constituents are taken by a large number of individuals as an alternative to conventional anti-inflammatory drugs (Grant *et al.*, 2007; Warnock *et al.*, 2007). Figures 4.16 and 4.17 depict the percentage transport of RH-123 in the AP-BL and BL-AP directions for the different concentrations of *H. procumbens* extract, namely low (0.00188% (w/v)), medium (0.0188% (w/v)) and high (0.188% (w/v)), respectively.

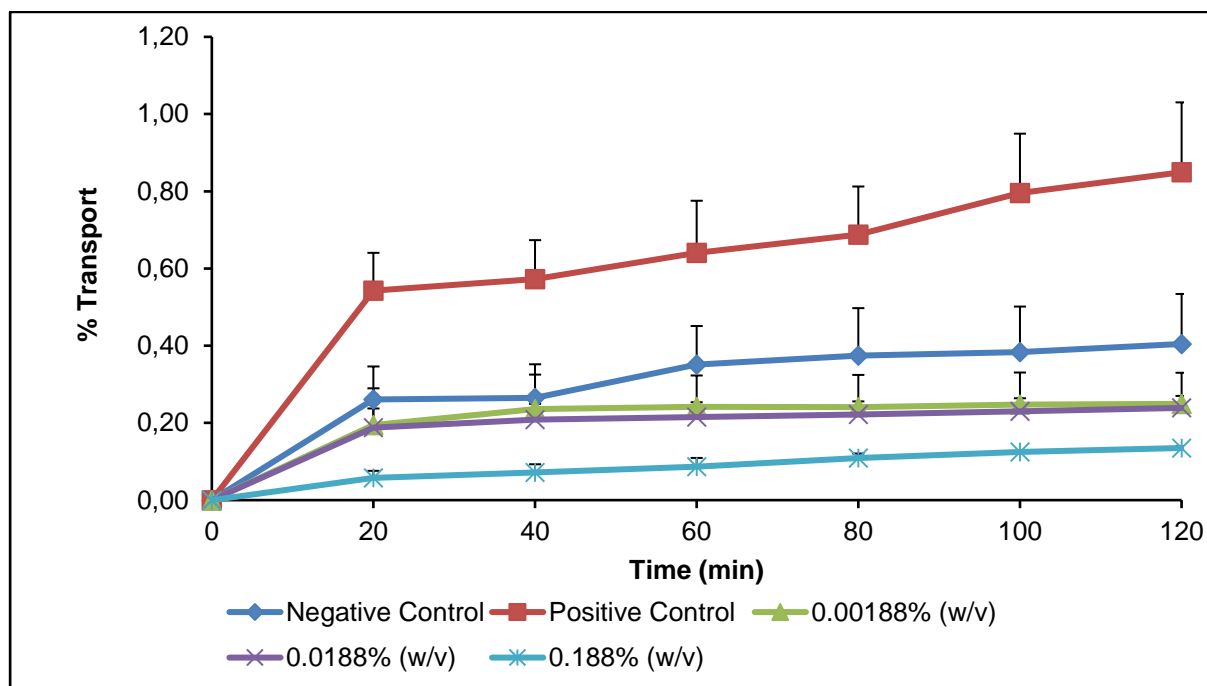


Figure 4.16: Apical-to-basolateral transport of Rhodamine 123 in the presence of different concentrations of *Harpagophytum procumbens* extract across excised pig jejunum tissue plotted as a function of time

Figure 4.16 shows that *H. procumbens* extract mediated a concentration dependent (i.e. from highest to lowest) decrease in the percentage transport of RH-123 in the AP-BL direction in comparison to the negative control. The low *H. procumbens* extract concentration yielded a percentage transport value of 0.249% and the medium concentration a percentage transport value of 0.239 % as calculated from the initial RH-123 concentration of 5 μ M. The highest concentration of the *H. procumbens* extract (0.188% (w/v)) mediated the most significant reduction in RH-123 transport by reducing the uptake by 3-fold in comparison to the negative control.

From the results depicted in Figure 4.17, it is evident that only a relatively slight concentration dependent increase in P-gp related efflux of RH-123 had occurred (when compared to the negative control) between the lowest (0.00188% (w/v)) and the highest (0.188% (w/v)) *H. procumbens* extract concentrations that were tested.

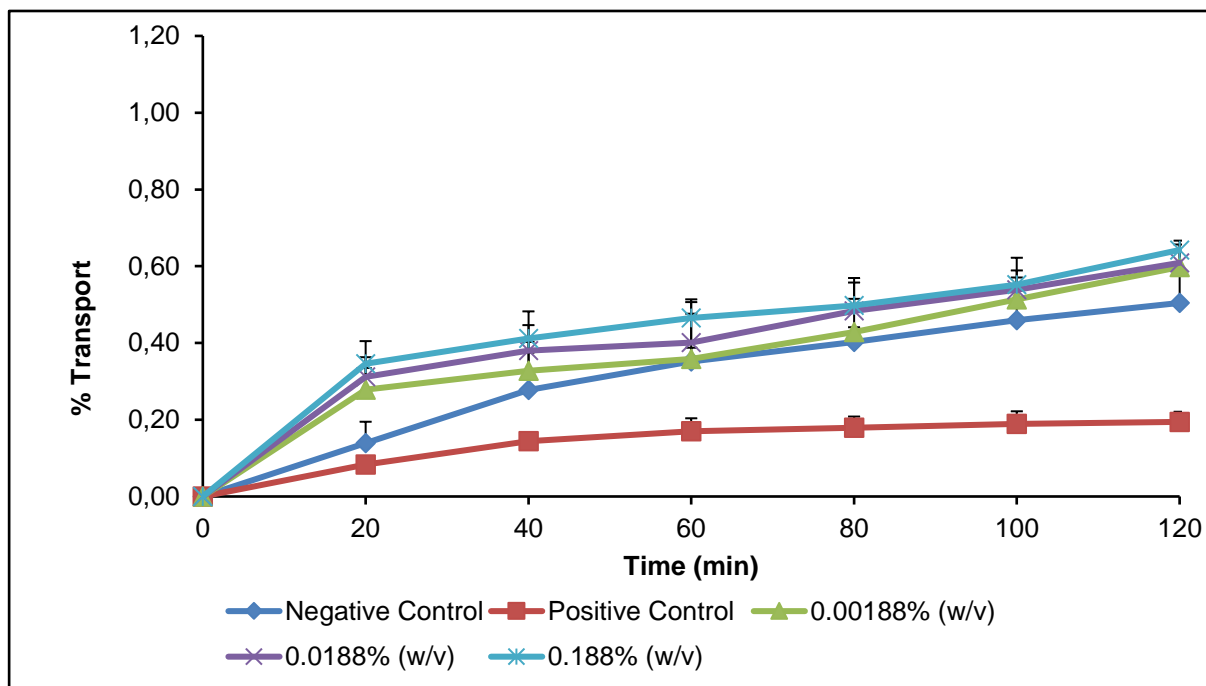


Figure 4.17: Basolateral-to-apical transport of Rhodamine 123 in the presence of different concentrations of *Harpagophytum procumbens* extract across excised pig jejunum tissue plotted as a function of time

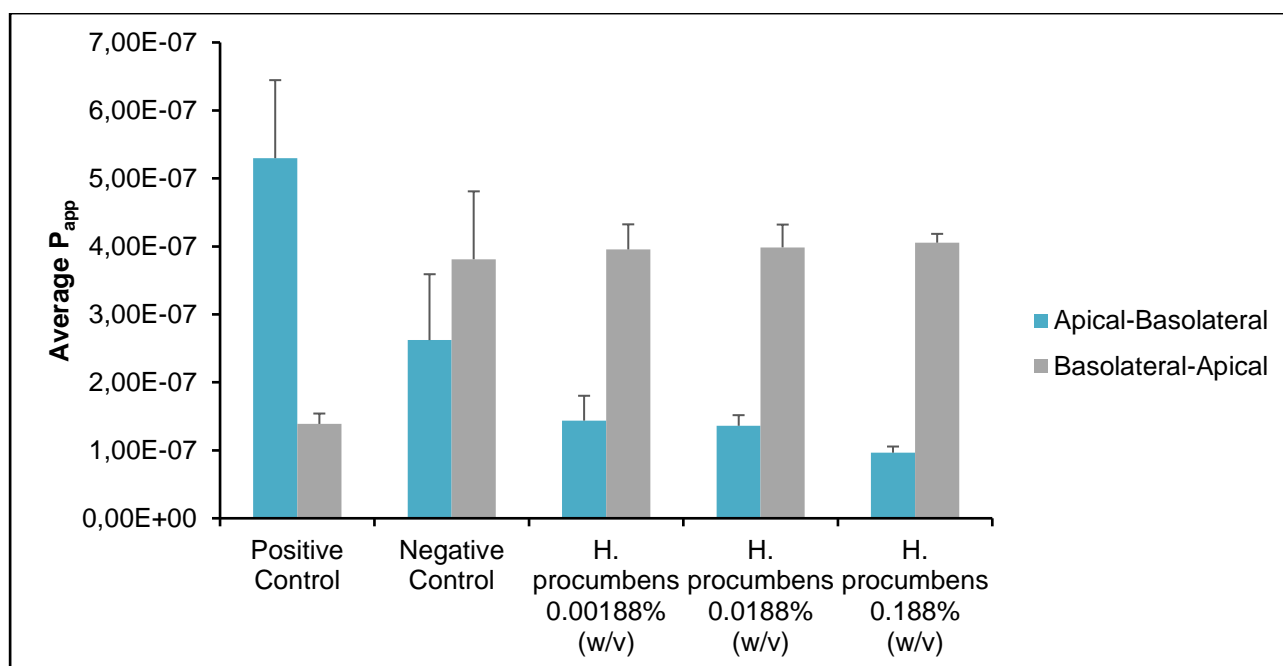


Figure 4.18: Average P_{app} values for bi-directional transport of Rhodamine 123 in the presence of different concentrations of *Harpagophytum procumbens* extract across excised pig jejunum tissue

The calculated P_{app} values are shown in Figure 4.18 and it can be seen that a concentration dependent decrease in RH-123 transport (AP-BL) had occurred when the P_{app} values of RH-123 in the presence of the three *H. procumbens* extract solutions are compared to the P_{app} value of the negative control. An increase, albeit not concentration dependent, can be noticed when the P_{app} data acquired from the transport studies in the BL-AP (secretory) direction are compared to that of the control group. This phenomenon can possibly be explained by a concentration independent stimulation/induction of efflux that caused an increase in the BL-AP RH-123 transport. The ER values established for each concentration were well above 1, with ER = 2.75 for the 0.00188 % (w/v) *H. procumbens* extract solution, ER = 2.93 for the 0.0188% (w/v) *H. procumbens* extract solution and ER = 4.20 for the 0.188% (w/v) *H. procumbens* extract solution. The TEER values that were recorded during all of these transport studies (Table 4.14) showed only negligible fluctuations in both directions of transport (AP-BL and BL-AP) and it can be concluded that the observed changes in RH-123 transport were mediated by the presence of the *H. procumbens* extracts and not due to altered membrane integrity.

4.4.5 Leonotis leonurus

L. leonurus, a shrub also known as “wilde dagga” has many traditional applications and consists of over 37 phytochemicals (Mazimba, 2015). The transport studies were performed on three different concentrations of *L. leonurus* extract namely low (0.000755% (w/v)), medium (0.00755% (w/v)) and high (0.0755% (w/v)). Figure 4.19 exhibits the average percentage transport of RH-123 in the AP-BL direction, while Figure 4.20 represents the average percentage transport in the BL-AP direction.

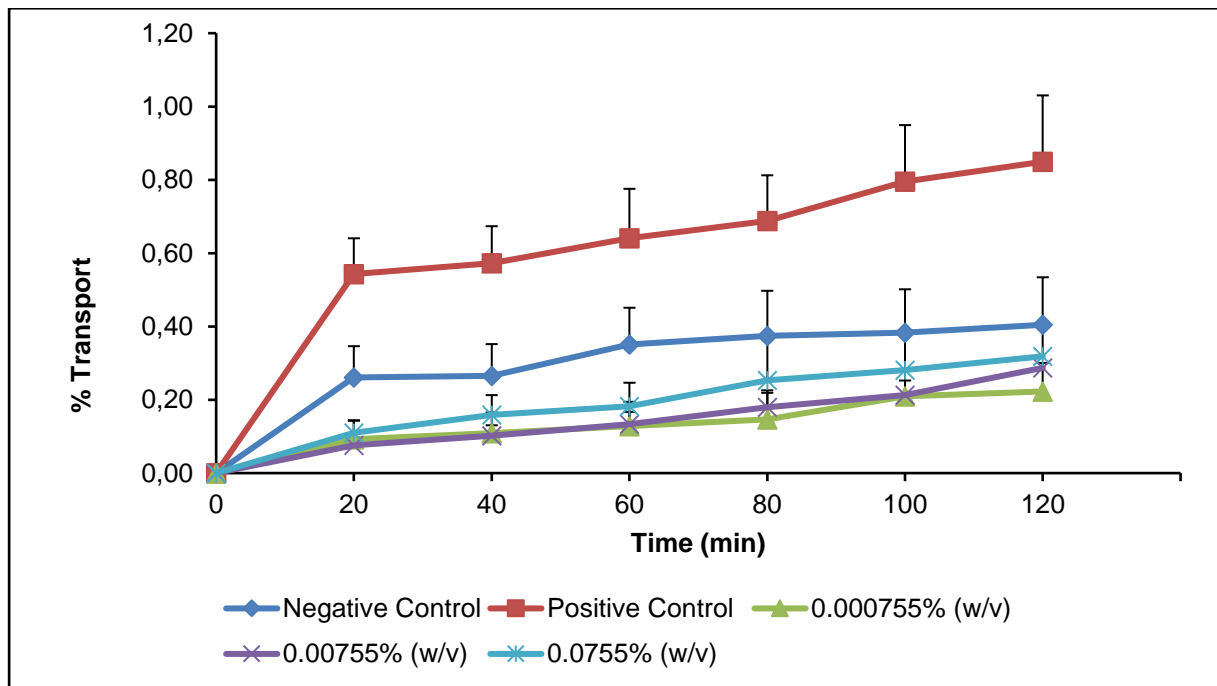


Figure 4.19: Apical-to-basolateral transport of Rhodamine 123 in the presence of different concentrations of *Leonotis leonurus* extract across excised pig jejunum tissue plotted as a function of time

Figure 4.19 exhibits a concentration dependent decrease in RH-123 transport mediated by the *L. leonurus* extracts in the AP-BL direction when compared to the negative control (i.e. RH-123 alone). Figure 4.20 shows an increase in the secretory transport of RH-123 for the highest concentration of *L. leonurus* extract (0.0755% (w/v)) when compared to the negative control. The medium (0.00755% (w/v)) and low concentrations (0.000755% (w/v)) of *L. leonurus* extract did not show any significant effects on RH-123 transport in the BL-AP direction when compared to the negative control.

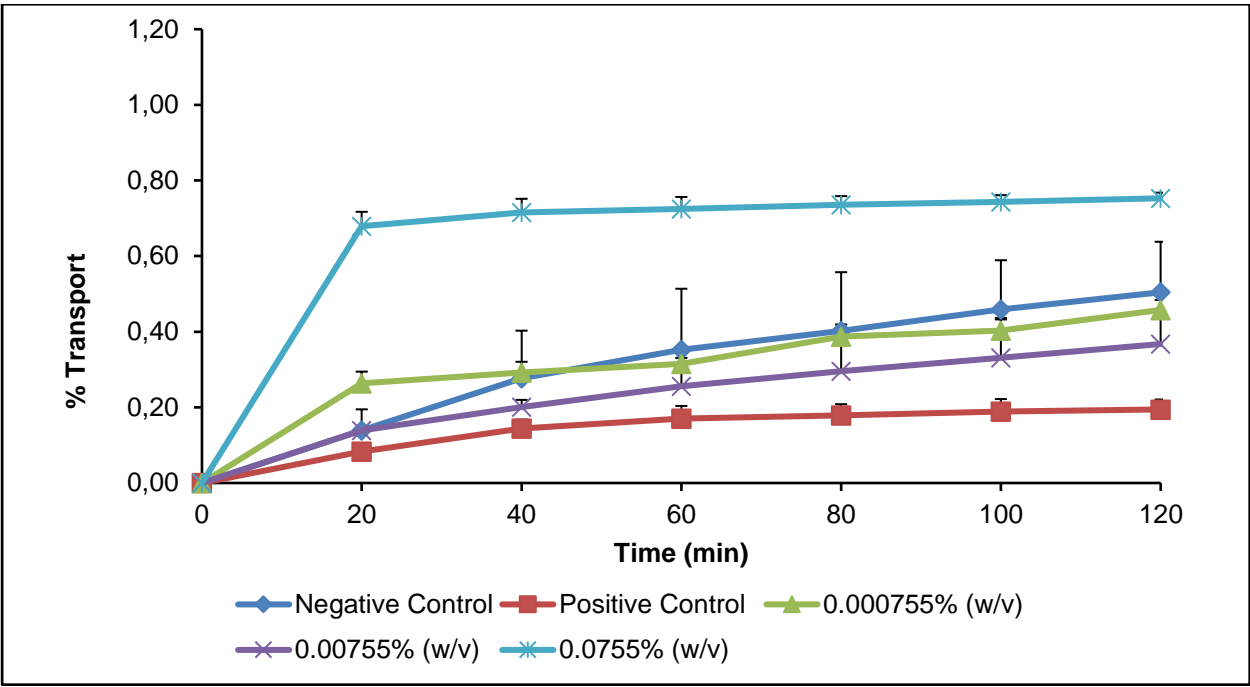


Figure 4.20: Basolateral-to-apical transport of Rhodamine 123 in the presence of different concentrations of *Leonotis leonurus* extract across excised pig jejunum tissue plotted as a function of time

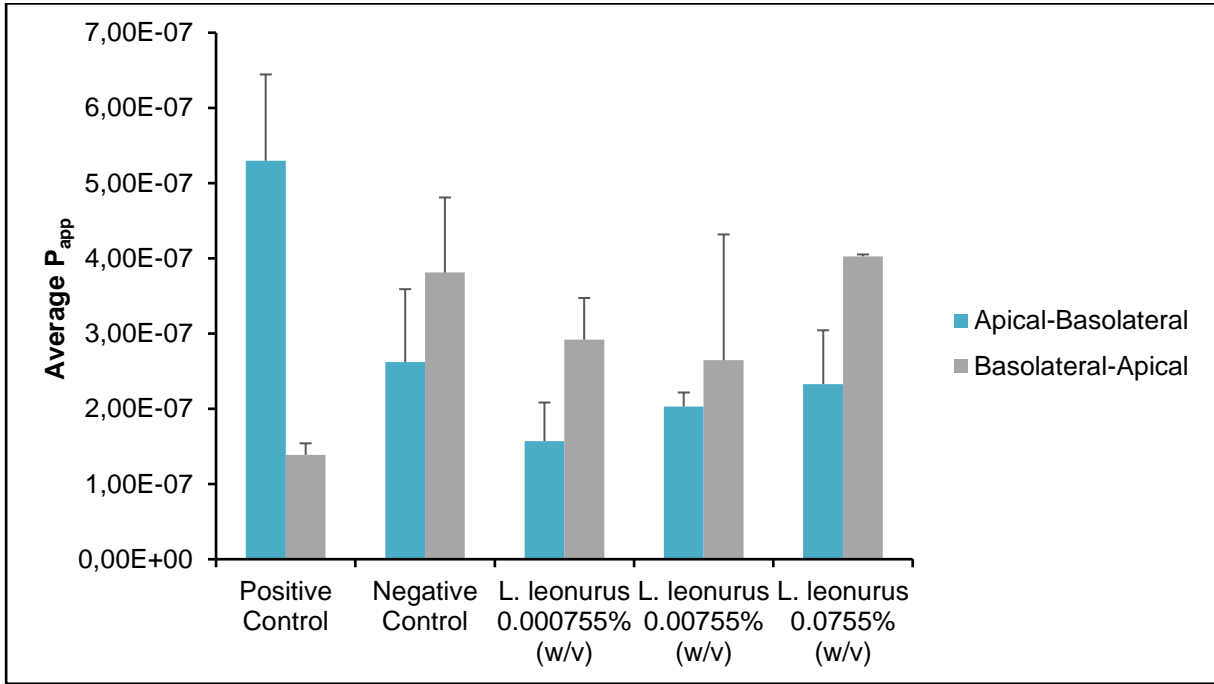


Figure 4.21: Average P_{app} values for bi-directional transport of Rhodamine 123 in the presence of *Leonotis leonurus* extract across excised pig jejunum tissue

Figure 4.21 shows that the uptake of RH-123 in the AP-BL direction had increased in relation to each other in a concentration dependent manner in the presence of increasing concentrations of the *L. leonurus* extract. These P_{app} values are, however, still lower than the P_{app} value of the negative control. The TEER values in the presence of the lowest *L. leonurus* extract concentration showed a small to negligible increase in trans-membrane resistance while the medium and higher concentrations mediated a slight decrease in trans-membrane resistance (Table 4.14). These changes in the TEER values are in accordance with the slight increase in RH-123 transport that was evident. A slight increase in the P_{app} value suggests that an apparent induction of P-gp related efflux of RH-123 occurred in the presence of the highest *L. leonurus* extract concentration (0.0755% (w/v)). The low and medium concentrations of *L. leonurus* extract (0.000755% (w/v) and 0.00755% (w/v) respectively) had apparently inhibited efflux based on the calculated P_{app} values, which were lower than that of the negative control. The calculated ER values were 1.86, 1.30 and 1.73 in the presence of the respective *L. leonurus* extract concentrations (0.000755% (w/v), 0.00755% (w/v) and 0.0755% (w/v)). Therefore, the probability exists that the *L. leonurus* extract had mediated an induction of P-gp related efflux upon reaching a specific baseline concentration as was evident in the presence of the highest *L. leonurus* extract concentration of (0.0755% (w/v)). It is, however, necessary to conduct additional studies in the future with regards to the different transport mechanisms which are involved to determine exactly at which critical *L. leonurus* concentration the turning point in transport mechanisms occur.

4.5 Evaluation of efflux ratios

Efflux ratio values (ER's as described in section 3.11.3 "*Efflux ratio (ER)*") of this dissertation) are indicative of the extent of transport in both AP-BL and BL-AP directions and serves as an indication of the possible main mechanism of transport. Table 4.13 represents the ER values which were calculated for RH-123 in the presence of the selected herbal extracts and supplement.

Table 4.13: Summary of the average P_{app} values and efflux ratio (ER) values for the selected herbal extracts and supplement at the selected concentrations

	Methylsulfonylmethane		
	0.00396% (w/v)	0.0396% (w/v)	0.396% (w/v)
Mean P_{app} (BL-AP)	3.98E-07	5.53E-07	9.90E-07
Mean P_{app} (AP-BL)	1.36E-07	8.90E-08	4.67E-08
Efflux Ratio (ER)	2.94	6.22	21.20
	<i>Vitis vinifera</i> seed extract		
	0.000264% (w/v)	0.00264% (w/v)	0.0264% (w/v)
Mean P_{app} (BL-AP)	3.178E-07	4.87E-07	7.53E-07
Mean P_{app} (AP-BL)	3.32E-07	1.10E-06	1.66E-06
Efflux Ratio (ER)	0.96	0.45	0.45
	<i>Hoodia gordonii</i>		
	0.00255% (w/v)	0.0255% (w/v)	0.255% (w/v)
Mean P_{app} (BL-AP)	2.34E-07	2.10E-07	1.57E-07
Mean P_{app} (AP-BL)	2.91E-07	4.03E-07	5.91E-07
Efflux Ratio (ER)	0.80	0.52	0.27
	<i>Harpagophytum procumbens</i>		
	0.00188% (w/v)	0.0188% (w/v)	0.188% (w/v)
Mean P_{app} (BL-AP)	3.95E-07	3.99E-07	4.05E-07
Mean P_{app} (AP-BL)	1.44E-07	1.36E-07	9.65E-08
Efflux Ratio (ER)	2.75	2.93	4.20
	<i>Leonotis leonurus</i>		
	0.000755% (w/v)	0.00755% (w/v)	0.0755% (w/v)
Mean P_{app} (BL-AP)	2.92E-07	2.65E-07	4.03E-07
Mean P_{app} (AP-BL)	1.57E-07	2.03E-07	2.33E-07
Efflux Ratio (ER)	1.86	1.30	1.73

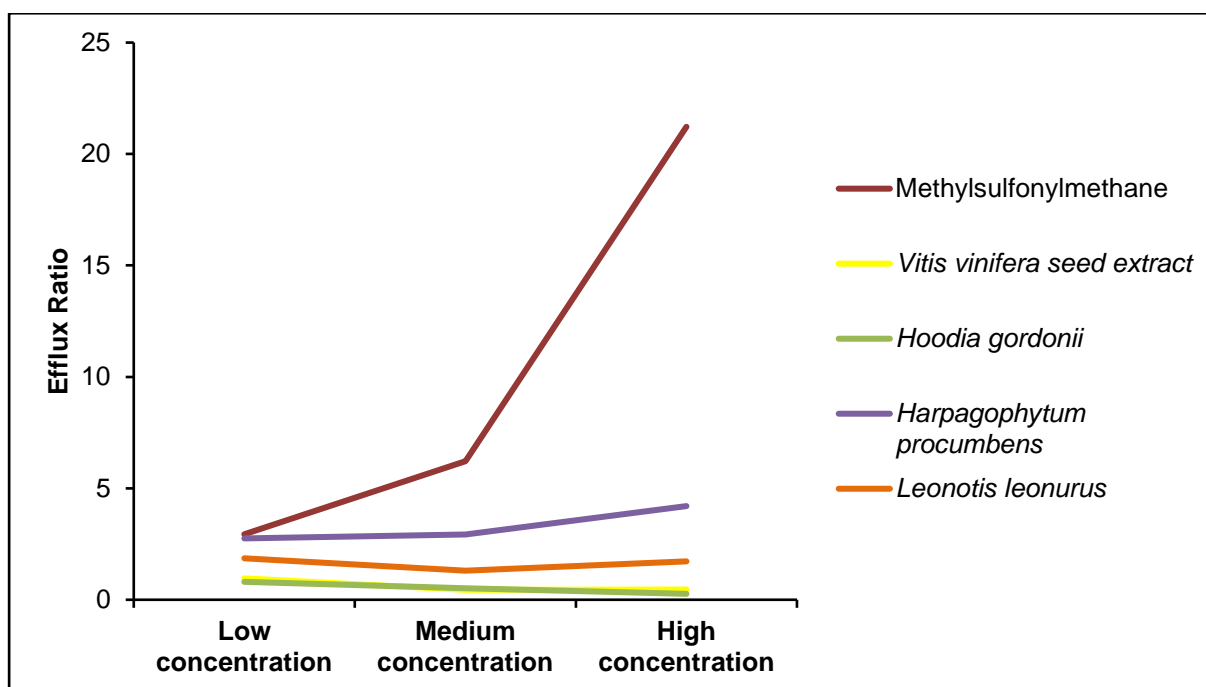


Figure 4.22: Efflux ratio values graphically represented for each of the selected herbal extracts and supplement at the three selected concentrations

Figure 4.22 portrays the resultant ER values of each of the selected herbal extracts and supplement. It is evident from the results depicted in Figure 4.22 that a difference in the directional transport of RH-123 had occurred when it was combined with the selected herbal extracts and/or supplement. When efflux occurs, a lesser amount of the drug is expected to traverse the epithelium through absorption due to the active pumping of the molecules from within the cells to the initial apical side. This increase in efflux will thus lead to a reduction in the bioavailability of any drug when administered concomitantly with an efflux inducing compound. This phenomenon was observed during the evaluation of MSM and *H. procumbens* extract. However, a reduction in P-gp related efflux on the other hand (as a result of P-gp inhibition) may lead to an increase in the bioavailability of co-administered compounds as was evident with the transport of RH-123 in the presence of the *H. gordonii* extracts that were used in this study.

4.6 Comparison and evaluation of TEER

Trans-epithelial electrical resistance (TEER) readings are widely used as an indication of membrane integrity and may serve as a quality control assay when performing transport experiments (Henry *et al.*, 2017). The TEER readings can be influenced by a number of factors and in this instance changes in the TEER readings could most likely have been attributed to the presence of the selected herbal extracts and/or supplement which mediated a modulation of the intercellular tight junctions.

The effects of the selected herbal extracts and supplement were monitored at the beginning and the end of each study by measuring the TEER. The average percentage change in the TEER readings were then calculated between the times T_0 and T_{120} and are reported in Table 4.14.

Table 4.14: Average percentage trans-epithelial electrical resistance (TEER) for excised tissue exposed to each of the selected herbal extracts and supplement over a 2 h period (all values are expressed as average percentage change from the initial T_0 to the T_{120} value)

	Methylsulfonylmethane		
	0.00396% (w/v)	0.0396% (w/v)	0.396% (w/v)
Apical-basolateral	88.16	95.29	104.68
Basolateral-apical	99.71	86.45	92.36
	<i>Vitis vinifera</i> seed extract		
	0.000264% (w/v)	0.00264% (w/v)	0.0264% (w/v)
Apical-basolateral	63.44	75.08	64.46
Basolateral-apical	66.47	74.57	75.00
	<i>Hoodia gordonii</i>		
	0.00255% (w/v)	0.0255% (w/v)	0.255% (w/v)
Apical-basolateral	93.50	82.96	61.90
Basolateral-apical	84.51	95.50	93.47
	<i>Harpagophytum procumbens</i>		
	0.00188% (w/v)	0.0188% (w/v)	0.188% (w/v)
Apical-basolateral	93.92	95.82	98.48
Basolateral-apical	100.33	98.34	99.70
	<i>Leonotis leonurus</i>		
	0.000755% (w/v)	0.00755% (w/v)	0.0755% (w/v)
Apical-basolateral	100.00	98.82	99.39
Basolateral-apical	91.46	84.38	80.57

The small fluctuations in the TEER values indicate that this was a suitable model to use for the purpose of this study. A slight additional decrease in the TEER values could be explained by the modulation effect of herbal extracts and supplement on the tight junctions between the adjacent cells.

4.7 Lucifer yellow studies

As discussed in section 3.9 “Assessment of intestinal tissue integrity” of this dissertation, to prove that the integrity of the intestine was maintained for the duration of the experimental process, the P_{app} value should be approximately 1 to 7 nm/sec (1 nm/sec = 1×10^{-7} cm/s). The P_{app} value obtained during the experiment was 3.097×10^{-7} cm/s, thus indicating that the method used to mount the intestine did not in any way influence the integrity of the excised tissues and therefore also the outcome of the transport studies conducted (Irvine *et al.*, 1999).

Table 4.15: The permeability coefficient values for Lucifer yellow across excised pig intestinal jejunum tissue

Chamber	P_{app} ($\times 10^{-7}$)
Chamber 1	2.133
Chamber 2	2.693
Chamber 3	4.465
Average	3.097

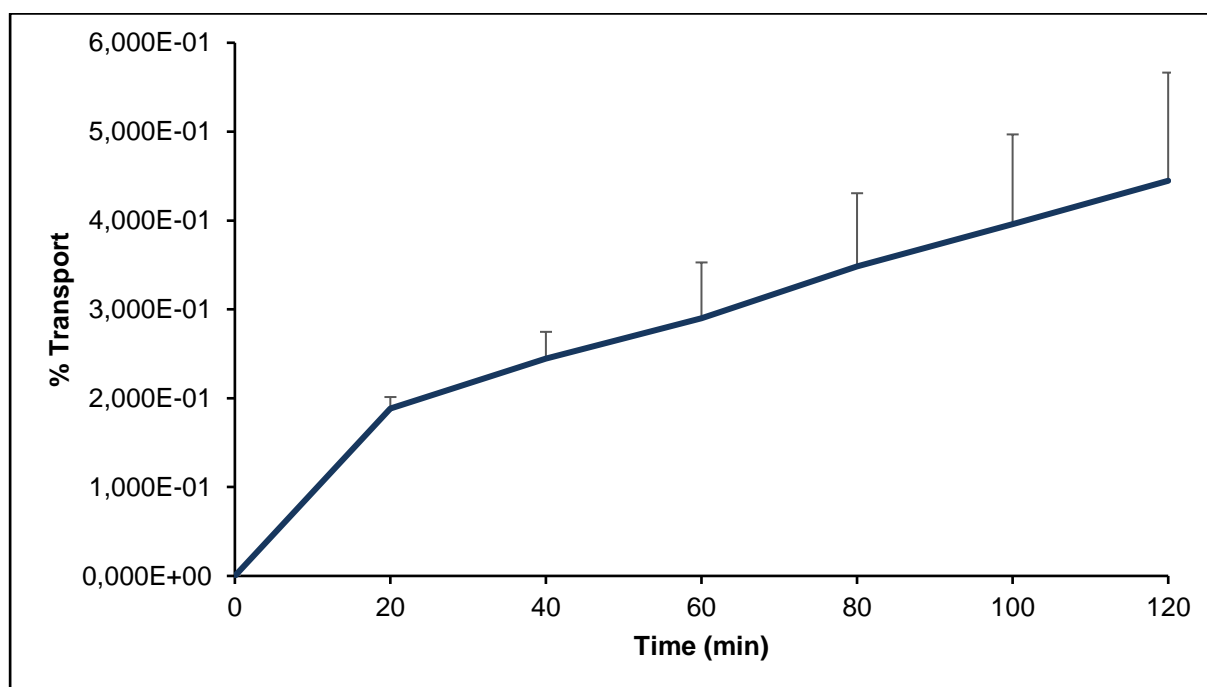


Figure 4.23: Apical-to-basolateral transport of Lucifer yellow across excised pig intestinal jejunum tissue plotted as a function of time

4.8 Conclusion

The analytical methods that were used to measure and quantify the RH-123 and LY content in the test samples complied with all the validation specifications with regards to linearity, selectivity, accuracy and precision. The study conducted with RH-123 in the presence of MSM showed that this supplement had statistically significant transport altering effects on the P-gp related efflux of RH-123, which may possibly be attributed to P-gp induction. *V. vinifera* seed extract showed statistically significant transport altering effects in both the AP-BL and BL-AP directions, which were concentration dependent. With regards to the decrease in TEER values, the notion that RH-123 is transported via the paracellular route supports the increase in RH-123 transport in the AP-BL direction. Furthermore, *H. gordonii* extract inhibited P-gp related efflux transport in the BL-AP direction, which led to a statistically significant increase in RH-123 transport in the AP-BL direction. *H. procumbens* and *L. leonurus* extracts did not show any statistically significant transport altering effects of RH-123, but a slight induction of P-gp related efflux transport was evident in the presence of *H. procumbens* extracts, while the results were inconclusive for the *L. leonurus* extracts.

CHAPTER 5: FINAL CONCLUSIONS AND FUTURE RECOMMENDATIONS

5.1 Final conclusions

The main goal of this study was to investigate and identify potential pharmacokinetic interactions that may occur between four selected herbal extracts and one supplement when concomitantly administered with a model compound which is a known P-gp substrate. The four herbal extracts chosen were *Vitis vinifera* seed extract, *Hoodia gordonii*, *Harpagophytum procumbens* and *Leonotis leonurus* and one supplement namely methylsulfonylmethane (MSM). A model compound for the transport studies namely Rhodamine 123 (RH-123) was chosen due to its distinguishing characteristic of being a substrate for the P-glycoprotein (P-gp) transporter. Its bi-directional transport was evaluated across excised pig jejunum tissues mounted between the half-cells of a Sweetana-Grass diffusion chamber apparatus.

At the beginning of this study, four objectives were aimed at. The first objective was to perform a comprehensive literature study and to identify a lack in scientific knowledge regarding the effects of the concomitant use of herbal extracts and supplements with Western drug products. This lack of knowledge and scientific evidence may place a considerable burden on the pharmaceutical industry in future with regards to the modification of medicine to such an extent that it will appeal to each individual's need. To assuage this burden an amalgamation of indigenous knowledge and biomedical interventions will in the long run contribute to a more thorough form of health care for patients.

The second objective stated that the fluorometric analysis of the model compound, RH-123, should be validated specifically with regards to linearity, specificity, precision and accuracy. The validation of RH-123 analysis with a fluorometric method showed that this method met all the requirements and specifications as reported in the literature to such an extent that all RH-123 concentration data acquired from the experimental transport samples could be deemed reliable.

Thirdly, bi-directional transport studies were conducted across excised pig intestinal jejunum tissue using RH-123 as model compound in the presence and absence of the selected herbal extracts and supplement. For the *in vitro* pharmacokinetic interaction studies, three concentrations for each of the herbal extracts and three concentrations for the supplement were chosen based on the information published before by Hellum *et al.* (2007b). Chapter 3 of this dissertation provided a thorough explanation of methods employed to conduct the transport studies. All the data collected from the transport studies were processed and interpreted including

calculation of the percentage change in the trans-epithelial electrical resistance (% TEER), apparent permeability coefficient (P_{app}) and efflux ratio (ER) values.

This study yielded results that indicated that MSM has the ability to modulate efflux of RH-123 in the BL-AP (i.e. secretory) direction by means of a concentration dependent stimulation/induction effect. A concentration independent stimulation/induction of P-gp related efflux of RH-123 was also observed for *H. procumbens* in the BL-AP direction. *V. vinifera* seed extract showed a concentration dependent increase in the transport of RH-123 in both the AP-BL (i.e. absorptive) and BL-AP (i.e. secretory) directions. *H. gordonii* decreased the secretory transport of RH-123 in the BL-AP direction indicating the presence of molecules that can act as efflux pump inhibitors in a concentration dependent manner. The transport experiments with *L. leonurus* provided results that suggested that P-gp related efflux may have been induced upon reaching a specific baseline concentration. However, further investigation with regards to different transport mechanisms involved and the critical concentration of *L. leonurus* extract where the turning point in the transport mechanism occurs should be investigated in future studies.

With regards to tight junction modulation, the results showed that the presence of MSM may have improved the barrier function of the intestinal membrane due to the presence of sulfur molecules contained within the molecular structure of MSM. *V. vinifera* seed extracts showed a decrease in the tightness of the tight junctions which may have contributed to the increased uptake of RH-123 in the AP-BL direction as well as in the BL-AP direction. The minimum fluctuations in the TEER values for *H. gordonii* and *H. procumbens* showed that these extracts had little to no effect on tight junction modulation. *L. leonurus* had effects on the tight junctions, with the lower concentration exhibiting a slight increase in TEER, whilst the medium and high concentrations demonstrated a decrease in TEER. These TEER results were therefore inconclusive and also showed differing/contradictory transport results.

The results generated from this study confirmed that the selected herbal extracts and supplement taken concomitantly with other Western medicine may lead to interferences with regards to drug absorption from the gastrointestinal tract. The concomitant use of the selected herbal extracts and/or supplement can either lead to an increase or decrease in the permeability of absorbed compounds which may result in unwanted pharmacokinetic interactions. This study design and the experimental results may serve as a baseline/reference platform to aid in the design and improvement of follow-up studies.

5.2 Future recommendations

When working with biological materials, e.g. the excised pig intestinal jejunum tissue model, it is important to consider inter-individual variation between the animals. It is recommended that pigs of approximately the same weight and age should be used to minimise the possibility of variation during the transport studies due to the influence of physiological differences between the animal subjects from which the intestinal jejunum tissues were obtained.

Future transport studies should also be conducted on different regional segments of the gastrointestinal tract other than the proximal jejunum, e.g. the duodenum, medial jejunum, distal jejunum and the ileum. Each region is unique with regards to the thickness of the mucosa, pH, enzyme activity, transporter expression and surface area. All these factors may cause variation in the extent of drug absorption and should be investigated thoroughly (Kompella & Lee, 2001).

It is highly recommended that *in vivo* bioavailability studies should be conducted in conjunction with *in vitro* studies to verify the clinical significance of the results obtained. In addition, a study should be carried out on the CYP450 enzymes to determine if any of the selected herbal extracts or supplement could influence the metabolic enzyme activity and thus the bioavailability of co-administered substrate drugs by modulation of enzymatic degradation.

With regards to the plant extracts, additional studies should be performed with extracts that are derived from different parts of the plants, e.g. leaves, bark or flowers. All potential active constituents should be extracted as pure, single compounds and should be individually characterised. Studies can also be performed by using different methods of preparation of the herbal extract, e.g. infusions in different solvents, decoctions and teas. However, special emphasis should be placed on the traditional method of preparation as well as the administration thereof, e.g. the preparation of a decoction of *L. leonurus* and the maceration thereof overnight before taken orally as a liquid extract.

The vast global consumption of herbal/supplemental products which are taken in conjunction with Western medicine necessitates the need for the development of a pharmacovigilance system where patients can report adverse events. This system may be a valuable tool to help minimize the risk of potential pharmacokinetic interactions between concomitantly administered medicines and supplements, which in turn may improve the treatment outcome of patients (Ekor, 2014).

REFERENCES

- Absorption Systems. 2016. Efflux transporters. www.absorption.com/kc/efflux-transporters/
Date of access: 15 March 2017.
- Abuasal, B.S., Bolger, M.B., Walker, D.K. & Kaddoumi, A. 2012. *In silico* modelling for the nonlinear absorption kinetics of UK-343,664: a P-gp and CYP3A4 substrate. *Molecular pharmaceutics*, 9:492-504.
- Akhtar, N. & Haqqi, T.M. 2012. Current nutraceuticals in the management of osteoarthritis: a review. *Therapeutic advances in musculoskeletal disease*, 4:181-207.
- Alderborn, G. 2007. Tablets and compaction. (In: Aulton, M.E., ed. *Aulton's pharmaceutics. The design and manufacture of medicines*. 3rd ed. Edinburgh: Churchill Livingstone. p. 441-482.)
- Ali, K., Maltese, F., Choi, Y. & Verpoorte, R. 2010. Metabolic constituents of grape vine and grape-derived products. *Phytochemical revolution*, 9:357-378.
- Alqahtani, S., Mohamed, L.A. & Kaddoumi, A. 2013. Experimental models for predicting drug absorption and metabolism. *Expert opinion drug metabolism*, 9(10):1-14.
- Ambudkar, S.V., Dey, S., Hrycyna, C.A., Ramachandra, M., Pastan, I. & Gottesman, M.M. 1999. Biochemical, cellular, and pharmacological aspects of multidrug transporter. *Annual review of pharmacology and toxicology*, 39:361-398.
- Ananga, A., Georgie, V. & Tsoleva, V. 2013. Manipulation and engineering of metabolic and biosynthetic pathway of plant polyphenols. *Current pharmacology*, 19:6186-6206.
- Antioxidants. Grape seed powder. 2015. <https://www.gonutra.com/antioxidants/60-grape-seed-extract-powder.html> Date of access: 5 May 2017.
- Antunes, F., Andrade, F., Ferreira, D., Nielsen, H.M. & Sarmiento, B. 2013. Models to predict intestinal absorption of therapeutic peptides and proteins. *Current drug metabolism*, 14(1):4-20.
- Artursson, P., Ungell, A.L. & Lofroth, J.E. 1993. Selective paracellular permeability in two models of intestinal absorption: cultured monolayers of human intestinal epithelial cells and rat intestinal segments. *Pharmacy research*, 10:1123-1129.
- Artursson, P., Palm, K., & Luthman, K. 2012. Caco-2 monolayers in experimental and theoretical predictions of drug transport. *Advanced drug delivery reviews*, 64:280-289.

Ashford, M. 2007. The gastrointestinal physiology and drug absorption. (*In*: Aulton, M.E., ed. Aulton's pharmaceuticals. The design and manufacture of medicines 3rd ed. New York: Churchill Livingstone. p. 270-285).

Aucamp, M., Odendaal, R., Liebenberg, W. & Hamman, J. 2014. Amorphous azithromycin with improved aqueous solubility and intestinal membrane permeability. *Drug development and industrial pharmacy*, 41(7):1100-1108.

Avula, B., Wang, Y.H. & Pawar, R.S. 2007. Chemical fingerprinting *Hoodia* species and related genera: chemical analysis of oxypregnane glycosides using high-performance liquid chromatography with UV detection in *Hoodia gordonii*. *Journal of the Association of Official Analytical Chemists*, 90(6):1526-1531.

Avula, B., Wang, Y.H., Pawar, R.S., Shukla, Y.J., Smillie, T.J. & Khan, I.A. 2008. A rapid method for chemical fingerprint analysis of *Hoodia* species, related genera, and dietary supplements using UPLC-UV-MS. *Journal of pharmaceutical and biomedical analysis*, 48:722-731.

Bagchi, D., Bagchi, M., Stohs, S.J., Ray, S.D., Sen, C.K. & Preuss, H.G. 2002. Cellular protection with proanthocyanidins derived from grape seeds. *Annals of the New York academy of sciences*, 957:260-270.

Balimane, P.V., Chong., S. & Morrison, R.A. 2000. Current methodologies used for evaluation of intestinal permeability and absorption. *Journal of pharmacological and toxicological methods*, 44:301-312.

Baranczewski, P., Stanczak, A., Sundberg, K., Svensson, R., Wallin, A., Jansson, J. & Postlind, H. 2006. Introduction to *in vitro* estimation of metabolic stability and drug interactions of new chemical entities in drug discovery and development. *Pharmacology reports*, 58:453-472.

Barnes, J. 2009. "Devil's claw" (*Harpagophytum procumbens*). Also known as "grapple plant" or "wood spider". *Journal of primary health care*, 1(3):238-239.

Baudry, N.N., Enslin, G. & Viljoen, A. 2015. "Wild cannabis": a review of the traditional use and phytochemistry of *Leonotis leonurus*. *Journal of ethnopharmacology*, 174:520-539.

Baumans, V. 2004. Use of animals in experimental research: an ethical dilemma? *Gene therapy*, 11:S64-S66.

Beckmann-Knopp, S., Rietbrock, S., Weyhenmeyer, R., Bocker, R.H., Beckurts, K.T., Lang, W., Hunz, M. & Fuhr, U. 2000. Inhibitory effects of silibinin on cytochrome P450 enzymes in human liver microsomes. *Pharmacology toxicology*, 86:250-256.

- Benet, L.Z., Wu, C.Y., Hebert, M.F. & Wacher, V.J. 1996. Intestinal drug metabolism and anti-transport processes: a potential paradigm shift in oral drug delivery. *Journal of controlled release*, 39:139-143.
- Berggren, S., Gail, C., Wollnitz, N., Ekelund, M., Karlbom, U., Hoogstraate, J. & Lennernäs, H. 2007. Gene and protein expression of P-glycoprotein, MRP1, MRP2, and CYP3A4 in the small and large human intestine. *Molecular pharmaceuticals*, 4:252-257.
- Beringer, P.M. & Slaughter, R.L. 2005. Transporters and their impact in drug disposition. *The annals of pharmacotherapy*, 39:1097-1108.
- Bock, U., Kottke, T., Gindorf, C. & Haltner, E. 2003. Validation of caco-2 cell monolayer system for determining the permeability of drug substances according to the Biopharmaceutics Classification System (BCS). (Unpublished)
- Bohets, H., Annaert, P., Mannens, G., van Beijsterveldt, L., Anciaux, K., Verboven, P., Meuldermans, W. & Lavrijsen, K. 2001. Strategies for absorption screening in drug discovery and development. *Current topics in medicinal chemistry*, 1:367-383.
- Borrelli, F., Capasso, R., Pinto, A. & Izzo, A.A. 2004. Inhibitory effect of ginger (*Zingiber officinale*) on rat ileal motility *in vitro*. *Life sciences*, 74:2889-2896.
- Borst, P., Evers, R., Kool, M. & Wijnholds, J. 2000. A family of drug transporters: the multidrug resistance-associated proteins. *Journal of the natural cancer institute*, 92:1295-1302.
- Borst, P. & Elferink, R.O. 2002. Mammalian ABC transporters in health and disease. *Annual review of biochemistry*, 71:537-592.
- Botanical-online.com. 2016. Grape vine properties. http://www.botanical-online.com/english/grape_vine.htm Date of access: 4 Oct. 2016.
- Boullata, J. 2005. Natural health product interactions with medications. *Nutrition in clinical practice*, 20:33-51.
- Brener, W., Hendrix, T.R. & McHugh, P.R. 1983. Regulation of the gastric emptying of glucose. *Gastroenterology*, 85:76-82.
- Bressler, R. 2006. Grapefruit juice and drug interactions: exploring mechanisms of this interaction and potential toxicity for certain drugs. *Geriatrics*, 61:12-18.
- Cass, H. 2004. Herbs for the nervous system: ginkgo, kava, valerian, passionflower. *Seminars in integrated medicine*, 2:82-88.

Chan, W.K. & Delucchi, A.B. 2000. Resveratrol, a red wine constituent, is a mechanism-based inactivator of cytochrome P450 3A4. *Life sciences*, 67(25):3103-3112.

Chan, L.M.S., Lowes, S. & Hirst, B.H. 2004. The ABC's of drug transport in intestine and liver: efflux proteins limiting drug absorption and bioavailability. *European journal of pharmaceutical sciences*, 21(1):25-51.

Chen, J. 2006. Recognition and prevention of herb-drug interactions. <http://www.acupuncturetoday.com/mpacms/at/article.php?id=31417> Date of access: 5 Aug. 2016.

Chen, X.W., Sneed, K.B., Pan, S.Y., Cao, C., Kanwar, J.R., Chew, H. & Zhou, S.F. 2012. Herb-drug interactions and mechanistic and clinical considerations. *Current drug metabolism*, 13:640-651.

Chiesara, T., Borghini, R. & Marabini, L. 1995. Dietary fibre and drug interactions. *European journal of clinical nutrition*, 49(3):S123-S128.

Choi, Y.H., Chin, Y.W. & Kim, Y.G. 2011. Herb-drug interactions: focus on metabolic enzymes and transporters. *Archives of pharmaceutical research*, 34(11):1843-1863.

Colabufo, N.A., Berardi, F., Contino, M., Inglese, C., Niso, M. & Perrone, R. 2008. Effect of some P-glycoprotein modulators on Rhodamine-123 absorption in guinea-pig ileum. *Bioorganic and medicinal chemistry letters*, 18:3741-3744.

Colalto, C. 2010. Herbal interactions on absorption of drugs: mechanisms of action and clinical risk assessment. *Pharmacological research*, 62:207-227.

Cunha, L., Szigetim K., Mathè, D. & Metello, L.F. 2014. The role of molecular imaging in modern drug development. *Drug discovery today*, 19:936-948.

Dahan, A. & Hoffman, A. 2007. The effects of different lipid based formulations on the oral absorption of lipophilic drugs: the ability of *in vitro* lipolysis and consecutive *ex vivo* intestinal permeability data to predict *in vivo* bioavailability in rats. *European journal of pharmaceuticals and biopharmaceutics*, 67:96-105.

Dall'Aqua S. & Innocenti, G. 2007. Steroidal glycosides from *Hoodia gordonii*. *Steroids*, 72:559-568.

Davis, S.S., Hardy, J.G. & Fara, J.W. 1986. Transit of pharmaceutical dosage forms through the small intestine. *Gut*, 27:886-892.

- Davis, S.S., Illum, L. & Hinchcliffe, M. 2001. Gastrointestinal transit of dosage forms in the pig. *Journal of pharmacy and pharmacology*, 53:33-39.
- Dean, M., Hamon, Y. & Chimini, G. 2001. The human ATP-binding cassette (ABC) transporter superfamily. *Journal of lipid research*, 42:1007-1017.
- Debreceeni, A., Abdel-Salam, O.M.E., Fingler, M., Juricskay, I., Szolcsányi, J. & Mòzsik, G. 1999. Capsaicin increases gastric emptying rate in healthy human subjects measured by ¹³C-labelled octanoic acid breath test. *Journal of physiology*, 93:455-460.
- Desai, P.M., Liew, C.V. & Heng, P.W.S. 2016. Review of disintegrates and the disintegration phenomena. *Journal of pharmaceutical sciences*, 105(9):2545-2555.
- DeSesso, J.M. & Jacobson, C.F. 2001. Anatomical and physiological parameters affecting gastrointestinal absorption in humans and rats. *Food and chemical toxicology*, 39:209-228.
- DeSesso, J.M. & Williams, A.L. 2008. Contrasting the gastrointestinal tract of mammals: factors that influence absorption. *Annual reports in medicinal chemistry*, 43:353-371.
- Dhananjay, P. & Mitra, A.K. 2006. MDR-and CYP3A4-mediated drug-herbal interactions. *Life sciences*, 78:2131-2145.
- Di Pasquale, G & Chiorini, J.A. 2006. AVV transcytosis through barrier epithelia and endothelium. *Molecular therapy*, 13:506-515.
- Ding, X. & Kaminsky, L.S. 2003. Human extrahepatic cytochromes P450: function in xenobiotic metabolism and tissue-selective chemical toxicity in the respiratory and gastrointestinal tracts. *Annual review of pharmacology and toxicology*, 43:149-173.
- Dixit, P., Jain, D.K. & Dumbwani, J. 2012. Standardization of an *ex vivo* method for determination of intestinal permeability of drugs using everted rat intestine apparatus. *Journal of pharmacological and toxicological methods*, 65:13-17.
- Djeridane, A., Yousfi, M., Nadjemi, B., Boutassouna, D., Stocker, P. & Vidal, N. 2006. Antioxidant activity of some Algerian medicinal plants extracts containing phenolic compounds. *Food chemistry*, 97:654-660.
- Doyle, L.A. & Ross, D.D. 2003. Multidrug resistance mediated by the breast cancer resistance protein BCRP (ABCG2). *Oncogene*, 22(47):7340-7358.
- Dubey, A.K., Shankar, P.R., Upadhvava, D. & Deshpande, V.Y. 2004. *Ginkgo biloba*: an appraisal. *Kathmandu University medicinal journal*, 2(3):225-229.

- Dürr, D., Stieger, B., Kullak-Ublick, G.A., Rentsch, K.M., Steinert, H.C., Meier, P.J., & Fattinger, K. 2000. St. John's Wort induces intestinal P-glycoprotein/MDR1 and intestinal hepatic CYP3A4. *Clinical pharmacology and therapeutics*, 68(6):598-604.
- Ekor, M. 2014. The growing use of herbal medicines: issues relating to adverse reactions and challenges in monitoring safety. *Frontiers in pharmacology*, 4(177):1-10.
- Eldrige, J. 2016. Energy metabolism. http://general.utpb.edu/FAC/eldrige_j/Kine360 Date of access: 7 March 2017.
- Elvin-Lewis, M. 2001. Should we be concerned about herbal remedies? *Journal of ethnopharmacology*, 75:141-164.
- Fardel, O., Jigorel, E., Le Vee, M. & Payen, L. 2005. Physiological, pharmacological and clinical features of the multidrug resistance protein 2. *Biomedicine and pharmacotherapy*, 59:104-114.
- Farkas, D. & Greenblatt, D.J. 2008. Influence of fruit juices on drug disposition: discrepancies between *in vitro* and clinical studies. *Expert opinion in drug metabolism and toxicology*, 4(4):381-393.
- Fasinu, P.S., Bouic, P.J. & Rosenkranz, B. 2014. The inhibitory activity of the extracts of popular medicinal herbs on CYP1A2, 2C9, 2C19 and 3A4 and the implications for herb-drug interaction. *African journal of traditional, complementary and alternative medicines*, 11(4):54-61.
- Ferguson, C.S & Tyndale, R.F. 2011. Cytochrome P450 enzymes in the brain: emerging evidence of biological significance. *Trends in pharmacological sciences*, 32:708-714.
- Flint, H.J. 2012. Microbiology: antibiotics and adiposity. *Nature*, 488:601-602.
- Fugh-Berman, A. 2000. Herb-drug interactions. *Lancet*, 355:134-138.
- Galetin, A., Hinton, L.K., Burt, H., Obach, R.S. & Houston, J.B. 2007. Maximal inhibition of intestinal first-pass metabolism as a pragmatic indicator of intestinal contribution to the drug-drug interactions for CYP3A4 cleared drugs. *Current drug metabolism*, 8(7):685-693.
- Geick, A., Eichelbaum, M. & Burk, O. 2001. Nuclear receptor response elements mediate induction of intestinal MDR1 by rifampin. *The journal of biological chemistry*, 276(18):14581-14587.
- Gerbal-Chaloin, S., Pascussi, J.M., Pichard-Garcia, L., Daujat, M., Waechter, F., Fabre, J.M., Carrère, N. & Maurel, P. 2001. Induction of CYP2C genes in human hepatocytes in primary culture. *Drug metabolism disposition*, 29(3):242-251.

- Giveon, S.M., Liberman, N., Klang, S. & Kahan, E. 2004. Are people who use “natural drugs” aware of their potentially harmful side effects and reporting to family physician? *Patient education and counselling*, 53:5-11.
- Grant, L., McBean, D.E., Fyfe, L. & Warnock, A.M. 2007. A review of the biological and potential therapeutic actions of *Harpagophytum procumbens*. *Phytotherapy research*, 21(3):199-209.
- Guilloteau, P., Zabielski, R., Hammon, H.M. & Metges, C.C. 2010. Nutritional programming of gastrointestinal tract development. Is the pig a good model for man? *Nutrition research reviews*, 23:4-22.
- Gundogdu, E., Alvarez, I.G. & Karasulu, E. 2011. Improvement of effect of water-in-oil micro-emulsion as an oral delivery system for fexofenadine: *in vitro* and *in vivo* studies. *International journal of nanomedicine*, 6:1631-1640.
- Gurley, B.J., Swain, A., Hubbard, M.A., Williams, D.K., Barone, G., Hartsfield, F., Tong, Y., Carrier, D.J., Cheboyina, S. & Battu, S.K. 2008a. Clinical assessment of CYP2D6-mediated herb-drug interactions in humans: effect of milk thistle, black cohosh, goldenseal, kava kava, St. John's Wort, and Echinacea. *Molecular nutrition and food research*, 52(7):755-763.
- Hamman, J.H. 2007. Oral drug delivery: biopharmaceutical principles, evaluation and optimisation. 2nd ed. Pretoria: Content Solutions.
- Heinle, H., Hagelauer, D., Pascht, U., Kelber, O. & Weiser, D. 2006. Intestinal spasmolytic effects of STW 5 (Iberogast®) and its components. *Phytomedicine*, 13:75-79.
- Helke, K.L. & Swindle, M.M. 2013. Animal models of toxicology: the role of pigs. *Expert opinion on drug metabolism and toxicology*, 9:127-139.
- Hellum, B.H. 2007a. *In vitro* interactions between medicinal drugs and herbs on cytochrome P-450 metabolism and P-glycoprotein transport. Trondheim: Norwegian University of Science and Technology (Thesis-PhD).
- Hellum, B.H., Hu, Z. & Nilsen, O.G. 2007b. The induction of CYP1A2, CYP2D6 and CYP3A4 by six trade herbal products in cultured primary human hepatocytes. *Basic & clinical pharmacology and toxicology*, 100:23-30.
- Hellum, B.H. & Nilsen, O.G. 2008. *In vitro* inhibition of CYP3A4 metabolism and P-glycoprotein mediated transport by trade herbal products. *Basic and clinical pharmacology and toxicology*, 102(5):462-475.

- Henderson, L., Yue, Q.Y., Bergquist, C., Gerden, B. & Arlett, P. 2002. St. John's Wort (*Hypericum perforatum*): drug interactions and clinical outcome. *Journal of clinical pharmacology*, 54:349-356.
- Henry, O.F., Villenave, R., Cronce, M.J., Leineweber, W.D., Benz, M.A. & Ingber, D.E. 2017. Organs-on-chips with integrated electrodes for trans-epithelial resistance (TEER) measurements of human epithelial barrier function. *Lab on a chip*, 13:2141-2336.
- Hidalgo, I.J. 2001. Assessing the absorption of new pharmaceuticals. *Current topics in medicinal chemistry*, 1:385-401.
- Ho, G.T., Moodie, F.M. & Satsangi, J. 2003. Multidrug resistance 1 gene (P-glycoprotein 170): an important determinant in gastrointestinal disease? *Gut*, 52(5):759-766.
- Ho, Y.F., Haung, O.K., Hsueh, W.C., Lui, M.Y., Yu, H.Y. & Tsai, T.H. 2009. Effects of St. John's Wort extract on indinavir pharmacokinetics in rats: differentiation of intestinal and hepatic impacts. *Life sciences*, 85(7-8):296-302.
- Hohonester, B., Rühl, A., Kelber, O. & Schemann, M. 2004. The herbal preparation STW5 (Iberogast®) has potent and region-specific effects on gastric motility. *Neurogastroenterology*, 16(6):765-773.
- Holmstock, N., Annaert, P. & Augustjins, P. 2012. Boosting of HIV protease inhibitors by ritonavir in the intestine: the relative role of cytochrome P450 and P-glycoprotein inhibition based on Caco-2 monolayers versus *in situ* intestinal perfusion in mice. *Drug metabolism and disposition*, 40:1473-1477.
- Honig, P.K., Wortham, D.D., Zamani, K., Conner, D.P., Mullin, J.C. & Cantilena, L.R. 1993. *Journal of the American Medical Association*, 269:1513-1518.
- Hossain, M., Abramowitz, W., Watrous, B.J., Szpunar, G.J. & Ayres, J.W. 1990. Gastrointestinal transit of non-disintegrating, non-erodible oral dosage forms in pigs. *Pharmaceutical research*, 7:1163-1166.
- Hu, M., Rayner, C.K., Wu, K., Chuah, S., Tai, W., Chou, Y., Chiu, Y., Chiu, K. & Hu, T. 2011. Effect of ginger on gastric motility and symptoms of functional dyspepsia. *World journal of gastroenterology*, 17:105-110.
- Hutter, M.C. 2009. *In silico* prediction of drug properties. *Current medicinal chemistry*, 16:189-202.

Ingersoll, R.E. 2005. Herbaceuticals: an overview for counsellors. *Journal of counselling and development*, 83:434-443.

Irvine, J.D., Takahashi, L., Lockhart, K., Cheong, J., Tolan, J.W., Selick, H.E. & Grove, J.R. 1999. MDCK (Madin-Darby Canin Kidney) Cells: a tool for membrane permeability screening. *Journal of pharmaceutical sciences*, 88(1):28-33.

Itokawa, H., Morris-Natshke, S.L., Akiyama, T. & Lee, K.H. 2008. Plant-derived natural product research aimed at new drug discovery. *Journal of natural medicine*, 62(3):263-280.

Iyanagi, T. 2007. Molecular mechanism of phase I and phase II drug-metabolizing enzymes: implications for detoxification. *International review of cytology*, 260:35-112.

Izzo, A.A. & Ernst, E. 2009. Interactions between herbal medicines and prescribed drugs. *Drugs*, 69(13):1777-1798.

Jacob, S.W. & Appleton, J. 2003. MSM: The definitive guide. A comprehensive review of the science and therapeutics of methylsulfonylmethane. *Alternative medicine review*, 8(4):438-441.

Jang, E.H., Choi, J.Y., Park, C.S., Lee, S.K., Kim, C.E., Park, H.J., Kang, J.S., Lee, J.W. & Kang, J.H. 2005. Effects of green tea extract administration on the pharmacokinetics of clozapine in rats. *Journal of pharmacy and pharmacology*, 57(3):311-316.

Kageyama, M., Fukushima, K., Togawa, T., Fujimoto, K., Taki, M., Nishimura, A., Ito, Y., Sugioka, N., Shibata, N. & Takada, K. 2006. Relationship between excretion clearance of Rhodamine 123 and P-glycoprotein (P-gp) expression induced by representative P-gp inducers. *Biological and pharmaceutical bulletin*, 29(4):779-784.

Kahn Academy. 2016. Oxidative phosphorylation. <https://kahnacademy.org/science/biology/cellular-respiration-and-fermentation/oxidative-phosphorylation> Date of access: 7 May 2017.

Kamsu-Foguem, B. & Foguem, C. 2014. Adverse drug reactions in some African herbal medicine: literature review and stakeholders' interview. *Integrative medicine research*, 3:126-132.

Kaprelyants, A.S. & Kell, D.B. 1992. Rapid assessment of bacterial viability and vitality by Rhodamine 123 and flow cytometry. *Journal of applied bacteriology*, 72:410-422.

Keppler, D., Konig, J. & Buchler, M. 1997. The canalicular multidrug resistance protein, cMRP/MRP2, a novel conjugate export pump expressed in the apical membrane of hepatocytes. *Advances in enzyme regulation*, 37:321-333.

Kim, H., Yoon, Y.J., Shon, J.H., Cha, I.J., Shin, J.G. & Liu, K.H. 2006. Inhibitory effects of fruit juices on CYP3A4. *Drug metabolism disposition*, 34:521-530.

Kleist, M.K. 2016. Grape seed extract: a new tool to fight high blood pressure. napervillemagazine.com/2016/grape-seed-extract-a-new-tool-to-fight-high-blood-pressure Date of access; 5 May 2017.

Kobayashi, D., Nozawa, T., Imai, K., Nezu, J., Tsuji, A. & Tamai, I. 2003. Involvement of human organic anion transporting polypeptide OATP-B (SLC21A9) in pH-dependant transport across intestinal apical membrane. *Journal of pharmacology and experimental therapeutics*, 306(2):703-708.

Kompella, U.B. & Lee, V.H. 2001. Delivery systems for penetration enhancement of peptide and protein drugs: design considerations. *Advanced drug delivery reviews*, 46:211-245.

Kresja, C.M., Horvath, D., Rogalski, S.L., Penzotti, J.E., Mao, B., Barbosa, F. & Migeon, J.C. 2003. Predicting ADME properties and side effects: the BioPoint approach. *Current opinion in drug discovery and development*, 6:470-480.

Küçükşen, S. & Şahin, M. 2015. Osteoarthritis prevention. *European journal of general medicine*, 12(1):96-100.

Kuhn, M.A. 2002. Herbal remedies: drug-herb interactions. *Critical care nurse*, 22:22-32.

Kumar, K. K., Karnati, S., Reddy, M.B. & Chandramouli, R. 2010. Caco-2 cell lines in drug discovery: an updated perspective. *Journal of basic and clinical pharmacy*, 1:63-72.

Lebitsa, T., Viljoen, A.M., Lu, Z. & Hamman, J.H. 2012. *In vitro* drug permeation enhancement of aloe gel materials. *Current drug delivery*, 9(3):297-304.

Le Ferrec, E., Chesne, C., Artusson, P., Brayden, D., Fabre, G., Gires, P., Guillou, F., Rousset, M., Rubas, W. & Scarino, M.L. 2001. *In vitro* models of the intestinal barrier. *Alternatives to laboratory animals*, 29:649-668.

Lee, L.S., Andrade, A.S. & Flexner, C. 2006. Interactions between natural health products and antiretroviral drugs: pharmacokinetic and pharmacodynamic effects. *Clinical infectious diseases*, 43:1052-1059.

Legen, I., Salobir, M. & Kerč, J. 2005. Comparison of different intestinal epithelia as models for absorption enhancement studies. *International journal of pharmaceutics*, 291:183-188.

Leigh, E. 2008. Nutrient-drug interactions. *Natural foods merchandiser*, 26(2):42-44.

Lennernas, H. 2007c. Modelling gastrointestinal drug absorption requires more *in vivo* biopharmaceutical data: experience from *in vivo* dissolution and permeability studies in humans. *Current drug metabolism*, 8:645-657.

Li, A.P. 2001. Screening for human ADME/Tox drug properties in drug discovery. *Drug discovery today*, 6:357-366.

Linnankoski, J., Mäkelä, J., Palmgren, J., Mauriala, T., Vedin, C., Ungell, A.L., Lazorova, L., Artursson, P., Urtti, A. & Yliperttula, M. 2010. Paracellular porosity and pore size of the human intestinal epithelium in tissue and cell culture models. *Journal of pharmaceutical sciences*, 99(4):2166-2175.

Lipsky, M.S. & Sharp, L.K. 2001. From idea to market: the drug approval process. *Journal of American board of family medicine*, 14(5):362-367.

Liu, Z., Wang, S. & Hu, M. 2009. Oral absorption basics: Pathways, physico-chemical and biological factors affecting absorption. (In: Qiu, Y., Chen, Y., Zhang, G.G.Z., Liu, L. & Porter, W.R., ed. *Developing solid oral dosage forms*. 1st ed. London: Elsevier. p. 264-288).

Liu, C.X., Yi, X.L., Si, D.Y., Xiao, X.F., He, X & Li, Y.Z. 2011. Herb-drug interactions involving drug metabolizing enzymes and transporters. *Current drug metabolism*, 12:835-849.

London, C. 2015. Polyphenolics. Grape seeds-www.polyphenolics.com/consumer/ Date of access: 5 May 2017.

Lundahl, A., Hedeland, M., Bondesson, U., Knutson, L. & Lennernas, H. 2009. The effect of St. John's Wort on the pharmacokinetics, metabolism and biliary excretion of finasteride and its metabolites in healthy men. *European journal of pharmaceutical sciences*, 36(4-5):433-443.

Luo, Z., Liu, Y., Zhao, B., Tang, M., Dong, H., Zhang, L. & Wei, L. 2013. *Ex vivo* and *in situ* approaches used to study intestinal absorption. *Journal of pharmacological and toxicological methods*, 68:208-216.

Madgula, V.L.M., Avula B., Pawar, R.S., Shukla, Y.J., Khan, I.A., Walker, L.A. & Khan, S.I. 2008. *In vitro* metabolic stability and intestinal transport of P57AS3 (P57) from *Hoodia gordonii* and its interaction with drug metabolizing enzymes. *Plant medicine*, 74:1269-1275.

Madhavan, V., Emelda, J. & Santhanakrishnan, T. 2016. Effects of solvents on phytochemicals, antioxidant and antimicrobial activity of grape seed extract (*Vitis vinifera*). *Photon*, 143:440-445.

Mandava, N., Oberol, R.K., Minocha, M. & Mitra, A.K. 2010. Transporter targeted drug delivery. *Journal of drug delivery science and technology*, 20(2):89-99.

- Mandery, K., Balk, B., Bujok, K., Schmidt, I., Fromm, M.F. & Glaeser, H. 2012. Inhibition of hepatic uptake transporters by flavonoids. *European journal of pharmaceutical sciences*, 46:79-85.
- Martignoni, M., Groothuis, G.M. & de Kanter, R. 2006. Species differences between mouse, rat, dog, monkey and human CYP-mediated drug metabolism, inhibition and induction. *Expert opinion on drug metabolism and toxicology*, 2(6):875-894.
- Mazimba, O. 2015. *Leonotis leonurus*: an herbal medicine review. *Journal of pharmacognosy and phytochemistry*, 3(6):39-42.
- McGregor, G., Fiebich, B., Wartenberg, A., Brien, S., Lewith, G. & Wegener. 2005. Devil's claw (*Harpagophytum procumbens*): an anti-inflammatory herb with therapeutic potential. *Phytochemistry reviews*, 4:47-53.
- Merchant, H.A., McConnell, E.L., Liu, F., Ramaswamy, C., Kulkarni, R.P., Basit, A.W. & Murdan, S. 2011. Assessment of gastrointestinal pH, fluid and lymphoid tissue in the guinea pig, rabbit and pig, and implications for their use in drug development. *European journal of pharmaceutical science*. 42:3-10.
- Mills, E., Foster, B.C., Van Heeswijk, R., Phillips, E., Wilson, K., Leonard, B., Kosuge, K. & Kanfer, I. 2005. Impact of African herbal medicines on antiretroviral metabolism. *AIDS*, 19(1):95-97.
- Miner, L. 2012. Plantilus. plantilus.com/plantdb/LeonLeon/Newly_planted.html Date of access: 15 May 2017.
- Mncwangi, N., Chen, W., Vermaak, I., Viljoen, A.M. & Gericke, N. 2012. Devil's Claw: a review of the ethnobotany, phytochemistry and biological activity of *Harpagophytum procumbens*. *Journal of ethnopharmacology*, 143:755-771.
- Monages, M. & Hernández-Ledesma, B. 2005. Quality assessment of commercial dietary antioxidant products from *Vitis vinifera* L. grape seeds. *Nutrition and cancer*, 53(2):244-254.
- Monages, M., Hernández-Ledesma, B., Garrido, I., Martín-Álvarez, P.J., Gómez-Cordovés. & Bartolomé, B. 2005. Quality assessment of commercial dietary antioxidant products from *Vitis vinifera* L. grape seeds. *Nutrition and cancer*, 53(2):244-254.
- Moore, L.B., Goodwin, B., Jones, S.A., Wisely, G.B., Serabjitsingh, C.J., Willson, T.M., Collins, J.L. & Kliewer, S.A. 2000. St. John's Wort induces hepatic drug metabolism through activation of the pregnane X receptor. *Proceedings of the National Academy of Sciences of the United States of America*, 97(13):7500-7502.

- Moshabela, M., Zuma, T. & Gaede, B. 2016. Bridging the gap between biomedical and traditional health practitioners in South Africa. *South African health review*. p. 83-91.
- Mottino, A.D., Hoffman, T., Jennes, L., Cao, J. & Vore, M. 2001. Expression of multidrug resistance-associated protein 2 in small intestine from pregnant and postpartum rats. *American journal of physiology-gastrointestinal and liver physiology*, 280:G1261-G1273.
- Mudra, D.R., Desinoan, K.E. Desai, P.V. 2001. *In silico, in vitro* and *in situ* models to assess interplay between CYP3A4 and P-gp. *Current drug metabolism*, 12:750-773.
- Muranishi, S. 1990. Absorption enhancers. *Critical review of therapeutic drug carrier systems*, 7:1-33.
- Nabekura, T., Yamaki, T., Ueno, K. & Kitagawa, S. 2008. Inhibition of P-glycoprotein and multidrug resistance protein 1 by dietary phytochemicals. *Cancer chemotherapy and pharmacology*, 62:867-873.
- Nabekura, T., Hiroi, T., Kawasaki, T. & Uwai, Y. 2015. Effects of natural nuclear factor-kappa B inhibitors on anticancer drug efflux transporter human P-glycoprotein. *Biomedicine and pharmacotherapy*, 70:140-145.
- Nair, V.D., Foster, B.C., Arnason, J.T., Mills, E.J. & Kanfer I. 2007. *In vitro* evaluation of human cytochrome P450 and P-glycoprotein-mediated metabolism of some phytochemicals and extracts and formulations of African potato. *Phytomedicine*, 14:498-507.
- Najar, I.A., Sachin, B.S., Sharma, S.C., Satti, N.K., Suri, K.A. & Johri, R.K. 2010. Modulation of P-glycoprotein ATPase activity by some phytoconstituents. *Phytotherapy research*, 24:454-458.
- Narukawa, Y., Komori, M., Niimura, A., Noguchi, H. & Kiuchi, F. 2015. Two new diterpenoids from *Leonotis leonurus* R. Br. *Journal of natural medicines*, 69:130-134.
- Nassiri-Asl, M. & Hosseinzadeh, H. 2009. Review of the pharmacological effects of *Vitis vinifera* and its bioactive compounds. *Phytotherapy research*, 23:1197-1204.
- Nekvindova, J., Masek, V., Veilichova, A., Anzenbacherova, E., Anzenbacher, P. & Zidek, Z. 2006. Inhibition of human liver microsomal cytochrome P450 activities by adefovir and tenofovir. *Xenobiotica*, 36(12):1165-1177.
- Nelita, T.E. & Yuan, F. 2011. A review of three-dimensional *in vitro* tissue models for drug discovery and transport studies. *Journal of pharmaceutical sciences*, 100:59-74.

- Nguyen, D.H., Sinchaipanid, N. & Mitrevej, A. 2013. *In vitro* intestinal transport of phyllanthin across Caco-2 cell monolayers. *Journal of drug delivery science and technology*, 23(3):207-214.
- Nolte, K., Backfisch, G. & Neidlein, R. 2002. *In vitro* studies of poorly absorbed drugs using porcine intestine in the ring model RIMO. *Arzneimittel-Forschung*, 50:664-668.
- Nowack, R. 2003. Cytochrome P450 enzyme, and transport protein mediated herb-drug interactions in renal transplant patients: grapefruit juice, St. John's Wort and beyond! *Nephrology*, 13(4):337-347.
- Nsuala, B.N., Kamatou, G.P., Sandasi, M., Enslin, G. & Viljoen, A. 2015. Variation in essential oil of *Leonotis leonurus*, an important medicinal plant in South Africa. *Biochemical systematics and ecology*, 70:155-161.
- Oberle, R.L. & Das, H. 1994. Variability in gastric pH and delayed gastric emptying in Yucatan miniature pigs. *Pharmaceutical research*, 11:592-594.
- Ojewole, J.A. 2005. Antinociceptive, anti-inflammatory and anti-diabetic effects of *Leonotis leonurus* (L.) R. BR. (Lamiaceae) leaf aqueous extract in mice and rats. *Methods and findings in experimental and clinical pharmacology*, 27:257-264.
- Okamura, N., Hirai, M., Tanigawara, Y., Tanaka, K., Yasuhara, M., ueda, K., Komano, T. & Hori, R. 1993. Digoxin-cyclosporin A interaction: modulation of multidrug transporter in kidney. *Journal of pharmacology and experimental pharmaceutics*, 266(3):1614-1619.
- Oyedemi, S. & Afolayan, A.J. 2011. *In vitro* and *in vivo* antioxidant activity of aqueous leaves extract of *Leonotis leonurus* (L.) R.Br. *International journal of pharmacology*, 7(2):248-256.
- Pagonis, T.A., Givissis, P.A., Kritis, A.C. & Christodoulou, A.C. 2014. The effect of methylsulfonylmethane on osteoarthritic large joints and mobility. *International journal of orthopaedics*, 1(1):19-24.
- Paine, M.F., Hart, H.L., Ludington, S.S., Hainting, R.L., Rettie, A.E. & Zeldin, D.C. 2006. The human intestinal cytochrome P450 'pie'. *Drug metabolism disposition*, 34:880-886.
- Pal, S.K. & Shukla, Y. 2003. Herbal medicine: current status and the future. *Asian pacific journal of cancer prevention*, 4:281-288.
- Pannala, A.S., Chan, T.S., O'Brien, P.J. & Rice-Evans, C.A. 2001. Flavonoid B-ring chemistry and antioxidant activity: fast reaction kinetics. *Biochemical and biophysical research communications*, 282:1161-1168.

Parcell, S. 2002. Sulfur in human nutrition and applications in medicine. *Alternative medicine review*, 7(1):22-24.

Patel, J., Patil, S. & Pawar, S. 2017. A review on method development and validation. *World journal of pharmacy and pharmaceutical sciences*, 6(3):245-259.

Pavek, P., Staud, F., Fendrich, Z., Sklenarova, H., Libra, A., Novotna, M., Kopecky, M., Nobilis, M. & Semecky, V. 2003. Examination of the functional activity of P-glycoprotein in the rat placental barrier using Rhodamine 123. *The journal of pharmacology and experimental therapeutics*, 305(5):1239-1250.

Pawar, R.S., Shukla, Y.J. & Khan, I.A. 2007. New calogenin glycoside from *Hoodia gordonii*. *Steroids*, 72:881-891.

Persson, E.M., Gustafsson, A.S., Carlsson, A.S., Nilsson, R.G., Knutson, L., Forsell, P., Hanisch, G., Lennernäs, H. & Abrahamsson, B. 2005. The effects of food on the dissolution of poorly soluble drugs in human and in model small intestinal fluids. *Pharmaceutical research*, 22:2141-2151.

Pietzonka, P., Walter, E., Duda-Johner, S., Langguth, P. & Merkle, H.P. Compromised integrity of excised porcine intestinal epithelium obtained from the abattoir affects the outcome of *in vitro* particle uptake studies. *European journal of pharmaceutical sciences*, 15:39-47.

Popoola, O.K., Elbagory, A.M., Ameer, F. & Hussein, A.A. 2013. Marrubiin. *Molecules*, 18:9049-9060.

Puccinelli, E., Gervasi, P.G. & Longo, V. 2011. Xenobiotic metabolising cytochrome P450 in pig, a promising animal model. *Current drug metabolism*, 12:507-525.

Qiu, W., Liu, C.X., Ju, Y. & Zhang, H.Y. 2010. Pharmacokinetic interaction of plant preparations with chemical drugs. *Chinese journal of natural medicines*, 8(2):137-144.

Rader, J.I., Delmonte, P. & Trucksess, M.W. 2007. Recent studies on selected botanical dietary supplement ingredients. *Analytical and bioanalytical chemistry*, 289:27-35.

Rafferty, A.P., McGee, H.B., Miller, C.E. & Reyes, M. 2002. Prevalence of complementary and alternative medicine use: State-specific estimates from the 2001 behavioural risk factor surveillance system. *American journal of public health*, 92(10):1598-1600.

Raskin, I., Ribnicky, D.M., Komarnytsky, S., Ilic, N., Poulev, A., Borisjuk, N., Brinker, A., Moreno, A.B., Ripoll, C., Yakoby, N., O'Neal, J.M., Cornwell, T., Pastor, I. & Fridlender, B. 2002. Plants and human health in the twenty-first century. *Trends in biotechnology*, 20:522-531.

- Reichling, W. & Saller, R. 2002. *Iberis amara* L. (bitter candytuft) : profile of a medicinal plant. *Research in complementary and natural classical medicine*, 9(1):21-33.
- Reis, J.M., Dezani, A.B., Pereira, T.M., Avdeef, A. & Serra, C.H.R. 2013. Lamivudine permeability study: a comparison between PAMPA, *ex vivo* and *in situ* Single-Pass Intestinal Perfusion (SPIP) in rat jejunum. *European journal of pharmaceutical sciences*, 48:781-789.
- Rendic, S. 2002. Summary of information on human CYP enzymes: human P450 metabolism data. *Drug metabolism reviews*, 34:83-448.
- Rodríguez-Fragoso, L., Martínez-Arismendi, J.L., Orozco-Bustos, D., Reyes-Esparza, J., Torres, E. & Burchiel, S.W. 2011. Potential risks resulting from fruit/vegetable drug interactions: effects on drug-metabolizing enzymes on drug transporters. *Journal of food sciences*, 79:112-124.
- Romiti, N., Tramonti, G., Corti, A. & Chieli, E. 2009. Effects of Devil's Claw (*Harpagophytum procumbens*) on the multidrug transporter ABCB1/P-glycoprotein. *Phytomedicine*, 16:1095-1100.
- Rost, D., König, J., Weiss, G., Klar, E., Stremmel, W. & Keppler, D. 2001. Expression and localization of the multidrug resistance proteins MRP2 and MRP3 in human gallbladder epithelia. *Gastroenterology*, 121:1203-1208.
- Rowland, M. & Tozer, T.N. 2011. Clinical pharmacokinetics and pharmacodynamics. 4th ed. Philadelphia: Lippincott Williams & Wilkins.
- Rushmore, T.H. & Kong, A.N. 2002. Pharmacogenomics, regulation and signalling pathways of phase I and II drug metabolizing enzymes. *Current drug metabolism*, 3:381-390.
- Saito, M., Hosoyama, H., Ariga, T., Kataoka, S. & Yamaji, N. 1998. Antiulcer activity of grape seed extract and procyanidins. *Journal of agriculture and food chemistry*, 46:1460-1464.
- Salama, N.N., Scott, K.R. & Eddington, N.D. 2004. The influence of enaminones on the transport and oral bioavailability of P-glycoprotein substrate therapeutic agents. *International journal of pharmaceuticals*, 273(1-2):135-147.
- Schinkel, A.H. & Jonker, J.W. 2003. Mammalian drug efflux transporters of the ATP binding cassette (ABC) family: an overview. *Advanced drug delivery reviews*, 55:3-29.
- Scott, G.N. & Elmer, G.W. 2002. Update on natural-product drug interactions. *Therapy update*, 59:339-447.

Shabir, G.A. 2003. Validation of high-performance liquid chromatography methods for pharmaceutical analysis understanding the differences and similarities between validation requirements of the US Food and Drug Administration, the US Pharmacopeia and the International Conference on Harmonization. *Journal of chromatography A*, 987:57-66.

Shargel, L., Wu-Pong, S. & Yu, A.B.C. 2005. Physiological factors related to drug absorption. (In: Shargel, L., Wu-Pong, S. & Yu, A.B.C. ed. Applied biopharmaceutics & pharmacokinetics. 5th ed. New York: McGraw Hill, p. 371-408.)

Shargel, L., Wu-Pong, S. & Yu, A.B.C. 2012. Targeted drug delivery systems and biotechnological products. (In: Shargel, L., Wu-Pong, S. & Yu, A.B.C. ed. Applied biopharmaceutics & pharmacokinetics. 6th ed. Boston: McGraw-Hill, p. 514-515.)

Sibaev, A., Yucece, B., Kelber, O., Weiser, Schirra, J., Göke, B., Allescher, H.D. & Storr, M. 2006. STW (Iberogast®) and its individual herbal components modulate intestinal electrophysiology of mice. *Phytomedicine*, SV:80-89.

Simonian, H.P., Vo, L., Doma, S., Fisher, R.S. & Parkman, H.P. 2005. Regional postprandial differences in pH within the stomach and gastroesophageal junction. *Digestive diseases and sciences*, 50:2276-2285.

Singh, U.P., Prithviraj, B., Sarma, B.K., Singh, M. & Ray, A.B. 2001. Role of garlic (*Allium sativum* L.) in human and plant diseases. *Indian journal of experimental biology*, 39:310-322.

Singh, R.P. & Agarwal, R. 2004. Prostate cancer prevention by silibinin. *Current cancer targets*, 4:1-11.

Singh, Y.N. 2005. Potential for interaction of kava and St. John's wort with drugs. *Journal of ethnopharmacology*, 100:108-113.

Singh, D., Kashyap, A., Pandey, R.V. & Saini, K.S. 2011. Novel advances in cytochrome P450 research. *Drug discovery today*, 16:793-799.

Singh, R. 2013. HPLC method development and validation: an overview. *Indian journal of pharmaceutical education and research*, 4(1):26-33.

Sjögren, E., Abrahamsson, B., Augustijns, P., Becker, D., Bolger, M.B., Brewster, M., Brouwers, J., Flanagan, T., Harwood, M., Heinen, C., Holm, R., Juretschke, H.P., Kubbinga, M., Lindahl, A., Lukacova, V., Münster, U., Neuhoff, S., van Peer, A., Reppas, C., Hodjegan, A.R., Tennergren, C., Weitschies, W., Wilson, C., Zane, P., Lannernäs, H. & Langguth, P. 2014. *In vivo* methods for drug absorption-comparative physiologies, model selection, correlations with *in vitro* methods (IVIVC), and applications for formulation/API/excipient characterization including food effects. *European journal of pharmaceutical sciences*, 57:99-151.

Skrovanek, S., Valenzano, M.C. & Mullin, J.M. 2007. Restriction of sulfur containing amino-acids alters claudin composition and improves tight junction barrier function. *American journal of physiology, regulatory, integrative and comparative physiology*, 293:R1046-R1055.

Smithies, S. 2006. *Harpagophytum procumbens*. <http://www.plantzafrica.com> Date of access: 14 March 2017.

Spalding, D.J., Harker, A.J. & Bayliss, M.K. 2004. Combining high-throughput pharmacokinetic screens at the hits-to-leads stage of drug discovery. *Drug discovery today*, 5:70-76.

Sridar, C., Goosen, T.C., Kent, U.M., Williams, J.A. & Hollenberg, P.F. 2004. Silybin inactivates cytochromes P450 3A4 and 2C9 and inhibits major hepatic glucuronosyltransferases. *Drug metabolism disposition*, 32:587-594.

Stafford, G.I., Pedersen, M.E., van Staden, J. & Jäger, A.K. 2008. Review on plants with CNS-effects used in traditional South African medicine against mental diseases. *Journal of ethnopharmacology*, 119:513-537.

Stenberg, P., Luthman, K. & Artursson, P. 2000. Virtual screening of intestinal drug permeability. *Journal of controlled release*, 65:231-243.

Stewart, K.M. & Cole, D. 2005. The commercial harvest of Devil's Claw (*Harpagophytum procumbens*) in southern Africa: the devil's in the details. *Journal of ethnopharmacology*, 100:225-236.

Street R.A. & Prinsloo, G. 2012. Commercially important medicinal plants of South Africa: a review. *Journal of chemistry*, 2013:1-16.

Study Blue. 2017. Digestive system. <https://www.studyblue.com/#flashcard/view/15514089> Date of access: 2 March 2017.

- Sugano, K., Kansy, M., Artursson, P., Avdeef, A., Bendels, S., Di, L., Ecker, G.F., Faller, B., Fischer, H., Gerebtzoff, G., Lennernaes, H. & Senner, F. 2010. Coexistence of passive and carrier-mediated processes in drug transport. *Perspectives*, 9:597-614.
- Synold, T.W., Dussault, I. & Forman, B.M. 2001. The orphan nuclear receptor SXR co-ordinately regulates drug metabolism and efflux. *Nature medicine*, 7(5):584-590.
- Takano, M., Yumoto, R. & Murakami, T. 2006. Expression and function of efflux drug transporters in the intestine. *Pharmacology & therapeutics*, 109:137-161.
- Takizawa, Y., Kitazato, T., Ishizaka, H., Kamiya, N., Ito, Y., Kishimoto, H., Tomita, M. & Hayashi, M. 2013. Changes in absorption and excretion of Rhodamine 123 by sodium nitroprusside. *International journal of pharmaceutics*, 450:31-35.
- Tarirai, C., Vlijoen, A.M. & Hamman, J.H. 2010. Herb-drug pharmacokinetic interactions reviewed. *Expert opinion on drug metabolism and toxicology*, 6:1515-1538.
- Tavelin, S., Hashimoto, K., Malkinson, J., Lazarova, L., Toth, I. & Artusson, P. 2003. A new principle for tight junction modulation based on occludin peptides. *Molecular pharmacology*, 64(6):1530-1540.
- Thanou, M.M., Kotzé, A.F., Scharringhausen, T., Leußen, H.L., de Boer, A.G., Verhoef, J.C. & Junginger, H.E. 2000. Effect of degree of quaternization of *N*-trimethyl chitosan chloride for enhanced transport of hydrophilic compounds across intestinal Caco-2 cell monolayers. *Journal of controlled release*, 64:15-25.
- Thiebaut, F., Tsuru, T., Hamada, H., Gottesman, M.M., Pastan, I. & Willingham, M.C. 1987. Cellular localization of the multidrug-resistance gene product P-glycoprotein in normal human tissues. *Proceedings of the National Academy of Sciences of the United States*, 84:7735-7738.
- Tomlinson, B., Hu, M. & Lee, V.W.Y. 2008. *In vivo* assessment of herb-drug interactions possible: utility of a pharmacogenetic approach? *Molecular nutrition and food research*, 52(7):799-809.
- Tsang, C., Auger, C., Mullen, W., Bornet, A., Rouanet, J.M., Crozier, A. & Teissedre, P.L. 2005. The absorption, metabolism and excretion of flavan-3-ols and procyanidins following the ingestion of grape seed extract in rats. *British journal of nutrition*, 94:170-181.
- Unger, M. & Frank, A. 2004. Simultaneous determination of the inhibitory potential of herbal extracts on the activity of six major cytochrome P450 enzymes using liquid chromatography/mass spectrometry and automated online extraction. *Rapid communications in mass spectrometry*, 18:2273-2281.

- United States Pharmacopeial Convention. 2017a. Validation of compendial procedures. <http://www.uspnf.com/uspnf/pub/index?usp=40&nf=35&s=0&officialOn=May%201,%202017>
Date of access: 13 June 2017.
- Usha, P.R. & Naidu, M.U.R. 2004. Randomised, double-blind, parallel, placebo-controlled study of oral glucosamine, methylsulfonylmethane and their combination in osteoarthritis. *Clinical drug investigation*, 24(6):353-363.
- Van Wyk, B.E., Van Outdshoorn, B. & Gericke, N. 2000. Medicinal Plants of South Africa, 2nd edition. Pretoria: Briza Publications.
- Van Wyk., B.E. & Wink, M. 2004. Medicinal Plants of the World. Pretoria: Briza Publications. p. 171.
- Varma, M.V.S., Ashokraj, Y., Dey, C.S. & Panchagnula, R. 2003. P-glycoprotein inhibitors and their screening: a perspective from bioavailability enhancement. *Pharmacological research*, 48:374-359.
- Vermaak, I., Hamman, J.H. & Viljoen, A.M. 2011a. *Hoodia gordonii*: an up-to-date review of a commercially important anti-obesity plant. *Planta medica*, 77:1149-1160.
- Vermaak, I., Viljoen, A.M., Chen, W. & Hamman, J.H. 2011b. *In vitro* transport of steroidal glycoside P57 from *Hoodia gordonii* across excised porcine intestinal and buccal tissue. *Phytomedicine*, 18:783-787.
- Venkataramanan, R., Komoroski, B. & Strom, S. 2006. *In vitro* and *in vivo* assessment of herb-drug interactions. *Life sciences*, 78(18):2105-2115.
- Vlachoianis, J., Roufaglis, B.D., Chrubasik, S. & Chrubasik, J. 2008. Systematic review on the safety of *Harpagophytum* preparations for osteoarthritic and low back pain. *Phytotherapy research*, 22(2):149-152.
- Volpe, D.A. 2010. Application of method suitability for drug permeability classification. *The American Association of Pharmaceutical Sciences journal*, 12:670-678.
- Wada, M. 2006. Single nucleotide polymorphisms in ABCC2 and ABCB1 genes and their clinical impact in physiology and drug response. *Cancer letters*, 234:40-50.
- Warnock, M., McBean, D., Suter, A., Tan, J. & Whittaker, P. 2007. Effectiveness and safety of Devil's Claw tablets in patients with general rheumatic disorders. *Phytotherapy research*, 21:1228-1233.

Wempe, A.F., Wright, C., Little, J.L., Lightner, J.W., Large, S.E., Caflich, G.B., Buchanan, C.M., Rice, P.J., Wachter, V.J., Ruble, K.M. & Edgae, K.J. 2009. Inhibiting efflux with novel non-ionic surfactants: rational design based on vitamin E TPGS. *International journal of pharmaceutics*, 370:93-102.

Whelan, A.M., Jurgens, T.M. & Szeto, V. 2010. Efficacy of *Hoodia* for weight loss: is there evidence to support the efficacy claims? *Journal of clinical pharmacy and therapeutics*, 35(5):609-612.

Wilfart, A., Montagne, L., Simmins, H., Noblet, J. & Milgen, J. 2007. Digesta transit in different segments of the gastrointestinal tract of pigs as affected by insoluble fibre supplied by wheat bran. *British journal of nutrition*, 98:54-62.

World Health Organisation (WHO). 2000. Traditional Medicine: Definitions. Geneva: <http://www.who.int/medicines/areas/traditional/definitions/en/> Date of access: 23 June 2016.

World Health Organisation (WHO). 2015. Obesity and overweight. Geneva: <http://www.who.int/mediacentre/factsheets/fs311/en/> Date of access: 15 Feb. 2016.

Wu, H., Li, J., Fronczek, F.R., Ferreira, D., Burandt Jr, C.L., Setola, V., Roth, B.L.K. & Zjawiony, J.K. 2013. Labdane diterpenoids from *Leonotis leonurus*. *Phytochemistry*, 91:229-235.

Xu, C., Li, C.Y. & Kong, A.N. 2005. Induction of phase I, II and III drug metabolism/transport by xenobiotics. *Archives of pharmacal research*. 28(3):249-268.

Zhao, B.X., Sun, Y.B., Wang, S.Q., Duan, L., Huo, Q.L., Ren, F. & Li, G.F. 2013. Grape seed procyanidin of P-glycoprotein associated multi-drug resistanc via down-regulation of NF- κ B and MAPK/ERK mediated YB-1 activity of A2780/T cells. *Plos one*, 8(8):1-11.

Zhang, Y. & Benet, L.Z. 2001. The gut as a barrier to drug absorption. *Clinical pharmacokinetics*, 40(3):159-168.

Zhang, Y., Bachmeier, C. & Miller, D.W. 2003. *In vitro* and *in vivo* models for assessing drug efflux transporter activity. *Advanced drug delivery reviews*, 55:31-51.

Zhang, S., Yang, X. & Morris, M.E. 2004. Combined effects of multiple flavonoids on breast cancer resistance protein (ABCG2)-mediated transport. *Pharmaceutical research*, 21(7):1263-1273.

Zhang, L., Zheng, Y., Chow, M.S.S. Zuo, Z. 2004. Investigation of intestinal absorption and disposition of green tea catechins by Caco-2 monolayer model. *International journal of pharmaceutics*, 287:1-12.

- Zhang, D., Luo, G., Ding, X. & Chuang, L. 2012. Preclinical experimental models of drug metabolism and disposition in drug discovery and development. *Acta pharmaceutica sinica B*, 2(6):549-561.
- Zhou, S., Gao, Y., Jiang, W., Huang, M., Xu, A. & Paxton, J.W. 2003. Interactions of herbs with cytochrome P450. *Drug metabolism reviews*, 35(1):35-98.
- Zhou, S., Chan, E., Lim, L.Y., Boelsterli, U.A., Li, S.C., Wang, J., Zhang, Q., Huang, M. & Xu, A. 2004a. Therapeutic drugs that behave as mechanism-based inhibitors of cytochrome P450 3A4. *Current drug metabolism*, 5(5):415-442.
- Zhou, S., Lim, L.Y. & Chowbay, B. 2004b. Herbal modulation of P-glycoprotein. *Drug metabolism reviews*, 36(1):57-104.
- Zhou, S. 2006. Herbal medicine and drug interactions. *Innovation*, 6(2):44-45.
- Zhou, S.F., Xue, C.C., Yu, X.Q. & Wanf, G. 2007. Clinically important interactions potentially involving mechanism-based inhibition of cytochrome P450 and the role of therapeutic drug monitoring. *Therapeutic drug monitoring*, 29(6):687-710.
- Zhou, S.F. 2008. Structure, function and regulation of P-glycoprotein and its clinical relevance in drug disposition. *Xenobiotica*, 38:802-832.
- Zuber, R., Modriansky, M., Dvorak, Z., Rohocsky, P., Ulrichova, J., Simanek, V. & Anzenbacher, P. 2002. Effect of silybin and its congeners on human liver microsomal cytochrome P450 activities. *Phytotherapy research*, 16:632-638.

ADDENDUM A

ETHICAL APPROVAL



NORTH-WEST UNIVERSITY
YUNIBESITI YA BOKONE-BOPHIRIMA
NOORDWES-UNIVERSITEIT

Private Bag X6001, Potchefstroom
South Africa 2520

Tel: (018) 299-4900
Faks: (018) 299-4910
Web: <http://www.nwu.ac.za>

Ethics Committee

Tel +27 18 299 4849
Email Ethics@nwu.ac.za

ETHICS APPROVAL OF PROJECT

The North-West University Research Ethics Regulatory Committee (NWU-RERC) hereby approves your project as indicated below. This implies that the NWU-RERC grants its permission that provided the special conditions specified below are met and pending any other authorisation that may be necessary, the project may be initiated, using the ethics number below.

Project title: Excised pig buccal and intestinal tissues as in vitro models for pharmacokinetic studies																															
Project Leader: Prof Sias Hamman																															
Ethics number:	<table border="1"><tr><td>N</td><td>W</td><td>U</td><td>-</td><td>0</td><td>0</td><td>0</td><td>2</td><td>5</td><td>-</td><td>1</td><td>5</td><td>-</td><td>A</td><td>5</td></tr><tr><td colspan="3">Institution</td><td></td><td colspan="5">Project Number</td><td colspan="2">Year</td><td colspan="4">Status</td></tr></table> <small>Status: S = Submission; R = Re-Submission; P = Provisional Authorisation; A = Authorisation</small>	N	W	U	-	0	0	0	2	5	-	1	5	-	A	5	Institution				Project Number					Year		Status			
N	W	U	-	0	0	0	2	5	-	1	5	-	A	5																	
Institution				Project Number					Year		Status																				
Approval date: 2015-04-16	Expiry date: 2020-04-15																														

Special conditions of the approval (if any): None

General conditions:

While this ethics approval is subject to all declarations, undertakings and agreements incorporated and signed in the application form, please note the following:

- The project leader (principle investigator) must report in the prescribed format to the NWU-RERC:
 - annually (or as otherwise requested) on the progress of the project,
 - without any delay in case of any adverse event (or any matter that interrupts sound ethical principles) during the course of the project.
- The approval applies strictly to the protocol as stipulated in the application form. Would any changes to the protocol be deemed necessary during the course of the project, the project leader must apply for approval of these changes at the NWU-RERC. Would there be deviated from the project protocol without the necessary approval of such changes, the ethics approval is immediately and automatically forfeited.
- The date of approval indicates the first date that the project may be started. Would the project have to continue after the expiry date, a new application must be made to the NWU-RERC and new approval received before or on the expiry date.
- In the interest of ethical responsibility the NWU-RERC retains the right to:
 - request access to any information or data at any time during the course or after completion of the project;
 - withdraw or postpone approval if:
 - any unethical principles or practices of the project are revealed or suspected,
 - it becomes apparent that any relevant information was withheld from the NWU-RERC or that information has been false or misrepresented,
 - the required annual report and reporting of adverse events was not done timely and accurately,
 - new institutional rules, national legislation or international conventions deem it necessary.

The Ethics Committee would like to remain at your service as scientist and researcher, and wishes you well with your project. Please do not hesitate to contact the Ethics Committee for any further enquiries or requests for assistance.

Yours sincerely

Linda du Plessis

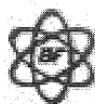
Digitally signed by Linda du Plessis
DN: cn=Linda du Plessis, o=NWU,
Vaal Triangle Campus, ou=Vice-
Rector: Academic,
email=linda.duplessis@nwu.ac.za,
c=US
Date: 2015.04.20 20:35:13 +02'00'

Prof Linda du Plessis

Chair NWU Research Ethics Regulatory Committee (RERC)

ADDENDUM B

CERTIFICATES OF ANALYSIS



Tianjin BaoFeng Chemical Co., Ltd.



Add: Dawanggu economic zone, Wuging, Tianjin, China
Tel: 0086-22-2219 3878 Fax: 0086-22-2219 3877
Http://www.bf-chem.com Email: baofeng@bf-chem.com

CERTIFICATE OF ANALYSIS

Product Name : MethylSulfonylMethane(MSM)	Batch No.160109
Main Date: JAN.09, 2016	Expiry Date: JAN.08, 2018
Test Date: JAN.10, 2016	Report Date: JAN.11, 2016
Test Standard: Enterprise Standard	Quantity: 3900kgs
Package: In 25kg net cardboard drum with two plastic bags	

Test Item	Standard	Test Result
Appearance: 外观	White crystalline powder	White crystalline powder
Residue on ignition: 灼烧残留	0.10%Max	0.02%
Heavy metals: 重金属	5ppmMax	0.0005%
Lead(Pb): 铅	1ppmMax	<1ppm
Cadmium(Cd): 镉	1ppmMax	<1ppm
Arsenic(As): 砷	1ppmMax	<1ppm
Mercury(Hg): 汞	0.1ppmMax	<0.1ppm
Melting point: 熔点	108.0-110.0°C	108.5°C
Boiling point: 沸点	238 °C	238 °C
Water Content: 水分	0.20%Max	0.15%
DMSO Content: 亚砷残留	Free	Free
Mesh size: 目数	About 90% pass 40mesh (60-80 mesh)	Conform
Silicon Dioxide: 二氧化硅	0.3% max	Conform
Assay: 含量	99.90%Min	99.93%
Total plate count: 需氧菌总量	<1000cfu/g	<10cfu/g
Yeast/Mold: 酵母菌/霉菌	<100cfu/g	<10cfu/g
Coliform: 大肠菌	Negative	Negative
E.Coli: 大肠杆菌	Negative	Negative
Salmonella: 沙门氏菌	Negative	Negative
Staphylococcus: 葡萄球菌	Negative	Negative
Conclusion: Pass test according to the Enterprise standard		

Inspector:

Signature:

CHECKED

WCI.2417



CERTIFICATE OF ANALYSIS

GRAPE SEED EXTRACT Ø HAB 4A

Packing code: 09G0108 PHAR001

Packing code: 04G0029

Bulk batch nr: 0316017

Bulk Part no: 04G0029

Manufacturing Date: March 2016

Expiry Date: 03/2021

Specification: Parceval v.003

	Parameters	Results
Appearance	A reddish brown, clear liquid.	Complies
Odour & Taste (Ph. Eur. 2.3.4)	A fruity odour with a dry bitter taste.	Complies
Relative Density (Ph. Eur. 2.2.5)	0.9100 - 0.9700	0.9628
Ethanol Content (Ph. Eur. 2.9.10)	40% - 45%	38.5%*
Dry Residue (Ph. Eur. 2.8.16)	Not less than 5% m/m	8.589%
Microbiology (Ph. Eur. 2.6.12 and 2.6.13)	Total count max 10 000cfu/g Coliforms 100cfu/g Yeasts and Fungi 100cfu/g E.coli absent <i>Salmonella</i> absent	None detected None detected None detected Absent Absent
Thin Layer Chromatography (Ph. Eur. 2.2.27)	Compare to reference run at the same time under the same conditions	Complies

***QA APPROVED**

I have conducted the necessary tests as outlined in this document :

Sue-Ann Engelbrecht
Quality Control

5th April 2016

Date

DIRECTORS HU Feiter

Parceval (Pty) Ltd
PO Box 158 Wellington 7654
South Africa
Phone 021 8733895
Fax 021 8735955
e-mail info@parceval.co.za



PARCEVAL

CERTIFICATE OF ANALYSIS

HOODIA GORDONII HERBA Ø 0.2G/ML

Packing Code: 09H0154 PHAR001

Packing No: 0316053

Bulk Part no: 04C0104

Bulk Batch no: 0316053

Manufacturing Date: May 2021

Expiry Date: 06/2021

Specification: Parceval v.004

Alcohol content: 30% m/m

	Parameters	Results
Appearance	Clear, orange brown liquid no visible impurities or sedimentation.	Complies
Odour & Taste (Ph. Eur. 2.3.4)	Aromatic odour with a sharp, bitter taste.	Complies
Ethanol Content (Ph. Eur. 2.9.10)	Between 27% - 32% m/m	26.3%*
Relative density (Ph. Eur. 2.2.5)	Between 0.9000 - 1.000	0.9799
Dry residue (Ph. Eur. 2.2.32d)	No less than 2.0% m/m	4.870%
Microbiology (Ph. Eur. 2.6.12 and 2.6.13)	Total count max 10 000 cfu/g Coliforms 100 cfu/g Yeasts and Fungi 100 cfu/g E.Coli absent <i>Salmonella</i> absent	580cfu/ml None detected 50cfu/ml Absent Absent
Thin Layer Chromatography (Ph. Eur. 2.2.27)	Compares to reference run at the same time under the same conditions	Complies

***QA APPROVED**

I have conducted the necessary tests as outlined in this document :

Sue-Ann Engelbrecht
Quality Control

27th May 2016

Date

DIRECTOR HU Feiter

| Parceval (Pty) Ltd Pharmaceuticals
 | PO Box 158 Wellington 7654
 | South Africa
 | Phone 021 8733895
 | Fax 021 8735955
 | e-mail info@parceval.co.za



PARCEVAL

CERTIFICATE OF ANALYSIS

HARPAGOPHYTUM PROCUMBENS TUBER Ø HAB 4A

Packing Code. 09H0153 PHAR001

Packing No: 0715048

Bulk Batch no: 0715048

Bulk part no: 04H0009

Manufacturing Date: July 2015

Expiry Date: 07/2020

Specification: Parceval v.003

Alcohol content: 62%*m/m*

	Parameters	Results
Appearance	A brownish yellow clear liquid.	Complies
Odour & Taste (Ph. Eur. 2.3.4)	Aromatic odour and a slightly bitter taste.	Complies
Relative density (Ph. Eur. 2.2.5)	Between 0.900 - 0.920	0.9130
Ethanol Content (Ph. Eur. 2.9.10)	Between 58 - 64% <i>m/m</i>	57.8%*
Dry Residue (Ph. Eur. 2.8.16)	No less than 3.8% <i>m/m</i>	5.751%
Microbiology (Ph. Eur. 2.6.12 and 2.6.13)	Total count max 10 000 cfu/ml Coliforms 100 cfu/ml Yeasts and Fungi 100 cfu/ml E.coli Absent Salmonella Absent	None detected None detected None detected Absent Absent
Thin Layer Chromatography (Ph. Eur. 2.2.27)	Compare to reference run at the same time under the same conditions	Complies

***QA APPROVED**

I have conducted the necessary tests as outlined in this document :

Sue-Ann Engelbrecht
Quality Control

07th March 2016
Date

DIRECTOR HU Feiler

| Parceval (Pty) Ltd Pharmaceuticals
| PO Box 158 Wellington 7654
| South Africa
| Phone 021 8733895
| Fax 021 8735955
| e-mail info@parceval.co.za



PARCEVAL

CERTIFICATE OF ANALYSIS

LEONOTIS LEONURUS HERBA ϕ HAB 4A

Packing Code. 09L0069 PHAR001

Packing Batch No: 0213026

Bulk Part no: 04L0022

Bulk Batch no: 0213026

Manufacturing Date: February 2013

Expiry Date: 02/2018

Specification: Parceval v.002

Alcohol content: 62% m/m

	Parameters	Results
Appearance	A greenish liquid.	Complies
Odour & Taste (Ph. Eur. 2.3.4)	Characteristic odour with an intensely bitter taste.	Complies
Relative density (Ph. Eur. 2.2.5)	Between 0.8850 - 0.9050	0.8947
Dry residue (Ph. Eur. 2.8.16)	No less than 1.5% m/m	1.74%
Ethanol Content (Ph.Eur. 2.9.10)	Between 58 - 64% m/m	59.7%
Thin Layer Chromatography (Ph. Eur. 2.2.27)	Compare to reference run at the same time under the same conditions	Complies

I have conducted the necessary tests as outlined in this document :

Sue-Ann Engelbrecht
Quality Control

07th March 2016

Date

DIRECTOR HU Feiler

| Parceval (Pty) Ltd
| PO Box 158 Wellington 7654
| South Africa
| Phone 021 8733895
| Fax 021 8735955
| e-mail info@parceval.co.za

ADDENDUM C

APPARENT PERMEABILITY DATA AS WELL AS *EX VIVO* TRANSPORT DATA OF RHODAMINE 123

Table C.1: Apical-to-basolateral cumulative percentage transport of Lucifer yellow alone across excised pig jejunum tissue to determine integrity

Time (min)	Percentage transport: Chamber 1	Percentage transport: Chamber 2	Percentage transport: Chamber 3	Standard deviation	Mean percentage transport
0	0.000	0.000	0.000	0.000	0.000
20	0.181	0.178	0.206	0.013	0.188
40	0.215	0.233	0.286	0.030	0.245
60	0.238	0.253	0.378	0.063	0.290
80	0.276	0.306	0.463	0.082	0.348
100	0.291	0.364	0.532	0.101	0.396
120	0.332	0.389	0.614	0.122	0.445
P_{app} (x 10⁻⁷)	2.133	2.693	4.465	3.097	

Table C.2: Apical-to-basolateral cumulative percentage transport of Rhodamine 123 in the presence of Verapamil across excised pig jejunum tissue

Time (min)	Percentage transport: Chamber 1	Percentage transport: Chamber 2	Percentage transport: Chamber 3	Standard deviation	Mean percentage transport
0	0.000	0.000	0.000	0.000	0.000
20	0.643	0.576	0.410	0.098	0.543
40	0.684	0.594	0.440	0.101	0.573
60	0.800	0.651	0.471	0.135	0.641
80	0.822	0.720	0.522	0.124	0.688
100	0.984	0.796	0.606	0.154	0.795
120	1.081	0.829	0.639	0.181	0.849
P_{app} (x 10⁻⁷)	6.790	5.105	3.997	1.406	

Table C.3: Basolateral-to-apical cumulative percentage transport of Rhodamine 123 in the presence of Verapamil across excised pig jejunum tissue

Time (min)	Percentage transport: Chamber 1	Percentage transport: Chamber 2	Percentage transport: Chamber 3	Standard deviation	Mean percentage transport
0	0.000	0.000	0.000	0.000	0.000
20	0.075	0.086	0.089	0.006	0.083
40	0.170	0.150	0.113	0.023	0.144
60	0.198	0.189	0.123	0.034	0.170
80	0.202	0.198	0.138	0.029	0.179
100	0.217	0.207	0.143	0.033	0.189
120	0.213	0.213	0.157	0.026	0.194
$P_{app} (x 10^{-7})$	1.595	1.557	1.011	0.327	

Table C.4: Apical-to-basolateral cumulative percentage transport of Rhodamine 123 alone across excised pig jejunum tissue

Time (min)	Percentage transport: Chamber 1	Percentage transport: Chamber 2	Percentage transport: Chamber 3	Standard deviation	Mean percentage transport
0	0.000	0.000	0.000	0.000	0.000
20	0.339	0.142	0.301	0.085	0.261
40	0.346	0.145	0.304	0.087	0.265
60	0.355	0.227	0.472	0.100	0.351
80	0.365	0.229	0.530	0.123	0.374
100	0.379	0.241	0.530	0.118	0.383
120	0.408	0.244	0.562	0.130	0.405
$P_{app} (x 10^{-7})$	2.208	1.695	3.960	1.187	

Table C.5: Basolateral-to-apical cumulative percentage transport of Rhodamine 123 alone across excised pig jejunum tissue

Time (min)	Percentage transport: Chamber 1	Percentage transport: Chamber 2	Percentage transport: Chamber 3	Standard deviation	Mean percentage transport
0	0.000	0.000	0.000	0.000	0.000
20	0.060	0.177	0.179	0.056	0.139
40	0.101	0.346	0.385	0.126	0.277
60	0.134	0.404	0.519	0.162	0.352
80	0.196	0.441	0.570	0.155	0.403
100	0.293	0.475	0.610	0.130	0.459
120	0.334	0.519	0.660	0.134	0.504
$P_{app} (x 10^{-7})$	2.615	3.756	5.060	1.223	

Table C.6: Apical-to-basolateral cumulative percentage transport of Rhodamine 123 in the presence of 0.00396% (w/v) methylsulfonylmethane across excised pig jejunum tissue

Time (min)	Percentage transport: Chamber 1	Percentage transport: Chamber 2	Percentage transport: Chamber 3	Standard deviation	Mean percentage transport
0	0.000	0.000	0.000	0.000	0.000
20	0.251	0.080	0.091	0.078	0.140
40	0.257	0.109	0.104	0.071	0.156
60	0.262	0.142	0.114	0.064	0.173
80	0.247	0.178	0.122	0.051	0.182
100	0.244	0.206	0.136	0.045	0.195
120	0.241	0.279	0.154	0.053	0.225
$P_{app} (x 10^{-7})$	1.172	1.939	0.954	0.518	

Table C.7: Basolateral-to-apical cumulative percentage transport of Rhodamine 123 in the presence of 0.00396% (w/v) methylsulfonylmethane across excised pig jejunum tissue

Time (min)	Percentage transport: Chamber 1	Percentage transport: Chamber 2	Percentage transport: Chamber 3	Standard deviation	Mean percentage transport
0	0.000	0.000	0.000	0.000	0.000
20	0.078	0.608	0.116	0.241	0.268
40	0.204	0.695	0.188	0.235	0.363
60	0.302	0.768	0.234	0.237	0.435
80	0.357	0.871	0.299	0.257	0.509
100	0.391	0.855	0.345	0.231	0.530
120	0.395	0.886	0.428	0.224	0.569
$P_{app} (x 10^{-7})$	3.281	5.564	3.094	1.375	

Table C.8: Apical-to-basolateral cumulative percentage transport of Rhodamine 123 in the presence of 0.0396% (w/v) methylsulfonylmethane across excised pig jejunum tissue

Time (min)	Percentage transport: Chamber 1	Percentage transport: Chamber 2	Percentage transport: Chamber 3	Standard deviation	Mean percentage transport
0	0.000	0.000	0.000	0.000	0.000
20	0.038	0.041	0.095	0.026	0.058
40	0.081	0.043	0.137	0.039	0.087
60	0.098	0.049	0.154	0.043	0.101
80	0.106	0.062	0.157	0.039	0.108
100	0.116	0.067	0.171	0.043	0.118
120	0.128	0.079	0.185	0.043	0.130
$P_{app} (x 10^{-7})$	0.940	0.513	1.215	0.354	

Table C.9: Basolateral-to-apical cumulative percentage transport of Rhodamine 123 in the presence of 0.0396% (w/v) methylsulfonylmethane across excised pig jejunum tissue

Time (min)	Percentage transport: Chamber 1	Percentage transport: Chamber 2	Percentage transport: Chamber 3	Standard deviation	Mean percentage transport
0	0.000	0.000	0.000	0.000	0.000
20	0.443	0.352	0.403	0.037	0.399
40	0.597	0.455	0.728	0.111	0.593
60	0.600	0.507	0.737	0.095	0.615
80	0.683	0.571	0.734	0.068	0.663
100	0.780	0.588	0.866	0.116	0.745
120	0.882	0.651	1.016	0.151	0.850
$P_{app} (x 10^{-7})$	5.700	4.248	6.653	1.211	

Table C.10: Apical-to-basolateral cumulative percentage transport of Rhodamine 123 in the presence of 0.396% (w/v) methylsulfonylmethane across excised pig jejunum tissue

Time (min)	Percentage transport: Chamber 1	Percentage transport: Chamber 2	Percentage transport: Chamber 3	Standard deviation	Mean percentage transport
0	0.000	0.000	0.000	0.000	0.000
20	0.047	0.042	0.084	0.019	0.057
40	0.054	0.048	0.099	0.023	0.067
60	0.056	0.048	0.098	0.022	0.067
80	0.057	0.048	0.106	0.026	0.070
100	0.062	0.052	0.103	0.022	0.072
120	0.074	0.060	0.112	0.022	0.082
$P_{app} (x 10^{-7})$	0.428	0.334	0.638	0.156	

Table C.11: Basolateral-to-apical cumulative percentage transport of Rhodamine 123 in the presence of 0.396% (w/v) methylsulfonylmethane across excised pig jejunum tissue

Time (min)	Percentage transport: Chamber 1	Percentage transport: Chamber 2	Percentage transport: Chamber 3	Standard deviation	Mean percentage transport
0	0.000	0.000	0.000	0.000	0.000
20	1.397	1.190	1.876	0.287	1.488
40	1.517	1.241	2.057	0.339	1.605
60	1.609	1.306	2.100	0.327	1.672
80	1.653	1.331	2.069	0.302	1.684
100	1.710	1.323	2.148	0.337	1.727
120	1.886	1.320	2.158	0.349	1.788
P_{app} (x 10⁻⁷)	10.733	7.216	11.757	2.382	

Table C.12: Apical-to-basolateral cumulative percentage transport of Rhodamine 123 in the presence of 0.000264% (w/v) *Vitis vinifera* seed extract across excised pig jejunum tissue

Time (min)	Percentage transport: Chamber 1	Percentage transport: Chamber 2	Percentage transport: Chamber 3	Standard deviation	Mean percentage transport
0	0.000	0.000	0.000	0.000	0.000
20	0.331	0.186	0.369	0.079	0.296
40	0.350	0.245	0.500	0.104	0.365
60	0.362	0.300	0.512	0.089	0.391
80	0.378	0.375	0.539	0.076	0.431
100	0.451	0.432	0.540	0.047	0.474
120	0.478	0.532	0.549	0.030	0.520
P_{app} (x 10⁻⁷)	2.845	3.711	3.391	0.438	

Table C.13: Basolateral-to-apical cumulative percentage transport of Rhodamine 123 in the presence of 0.000264% (w/v) *Vitis vinifera* seed extract across excised pig jejunum tissue

Time (min)	Percentage transport: Chamber 1	Percentage transport: Chamber 2	Percentage transport: Chamber 3	Standard deviation	Mean percentage transport
0	0.000	0.000	0.000	0.000	0.000
20	0.233	0.318	0.216	0.044	0.256
40	0.255	0.335	0.303	0.033	0.298
60	0.410	0.360	0.377	0.021	0.382
80	0.458	0.375	0.401	0.034	0.411
100	0.469	0.468	0.449	0.009	0.462
120	0.530	0.516	0.529	0.007	0.525
$P_{app} (x 10^{-7})$	3.791	3.159	3.598	0.324	

Table C.14: Apical-to-basolateral cumulative percentage transport of Rhodamine 123 in the presence of 0.00264% (w/v) *Vitis vinifera* seed extract across excised pig jejunum tissue

Time (min)	Percentage transport: Chamber 1	Percentage transport: Chamber 2	Percentage transport: Chamber 3	Standard deviation	Mean percentage transport
0	0.000	0.000	0.000	0.000	0.000
20	1.215	1.736	1.560	0.217	1.504
40	1.360	1.939	1.784	0.244	1.694
60	1.481	2.036	1.853	0.231	1.790
80	1.514	2.080	1.927	0.239	1.840
100	1.560	2.064	1.989	0.222	1.871
120	1.557	2.091	2.008	0.235	1.885
$P_{app} (x 10^{-7})$	9.222	11.822	11.747	1.480	

Table C.15: Basolateral-to-apical cumulative percentage transport of Rhodamine 123 in the presence of 0.00264% (w/v) *Vitis vinifera* seed extract across excised pig jejunum tissue

Time (min)	Percentage transport: Chamber 1	Percentage transport: Chamber 2	Percentage transport: Chamber 3	Standard deviation	Mean percentage transport
0	0.000	0.000	0.000	0.000	0.000
20	0.411	0.467	0.418	0.025	0.432
40	0.484	0.617	0.511	0.057	0.537
60	0.525	0.668	0.550	0.062	0.581
80	0.606	0.740	0.620	0.060	0.655
100	0.618	0.802	0.631	0.084	0.683
120	0.675	0.934	0.684	0.120	0.764
$P_{app} (x 10^{-7})$	4.282	6.008	4.325	0.984	

Table C.16: Apical-to-basolateral cumulative percentage transport of Rhodamine 123 in the presence of 0.0264% (w/v) *Vitis vinifera* seed extract across excised pig jejunum tissue

Time (min)	Percentage transport: Chamber 1	Percentage transport: Chamber 2	Percentage transport: Chamber 3	Standard deviation	Mean percentage transport
0	0.000	0.000	0.000	0.000	0.000
20	2.234	2.982	1.136	0.758	2.117
40	2.279	3.291	1.355	0.791	2.309
60	2.406	3.343	1.468	0.765	2.406
80	2.562	3.287	1.570	0.704	2.473
100	2.592	3.592	1.878	0.703	2.687
120	2.654	3.807	2.178	0.684	2.879
$P_{app} (x 10^{-7})$	14.982	21.127	13.763	3.947	

Table C.17: Basolateral-to-apical cumulative percentage transport of Rhodamine 123 in the presence of 0.0264% (w/v) *Vitis vinifera* seed extract across excised pig jejunum tissue

Time (min)	Percentage transport: Chamber 1	Percentage transport: Chamber 2	Percentage transport: Chamber 3	Standard deviation	Mean percentage transport
0	0.000	0.000	0.000	0.000	0.000
20	1.059	0.947	1.054	0.052	1.020
40	1.146	1.045	1.155	0.050	1.116
60	1.180	1.072	1.184	0.052	1.146
80	1.239	1.084	1.229	0.071	1.184
100	1.269	1.240	1.266	0.013	1.258
120	1.364	1.323	1.272	0.037	1.320
P_{app} (x 10⁻⁷)	7.698	7.682	7.215	0.274	

Table C.18: Apical-to-basolateral cumulative percentage transport of Rhodamine 123 in the presence of 0.00255% (w/v) *Hoodia gordonii* across excised pig jejunum tissue

Time (min)	Percentage transport: Chamber 1	Percentage transport: Chamber 2	Percentage transport: Chamber 3	Standard deviation	Mean percentage transport
0	0.000	0.000	0.000	0.000	0.000
20	0.237	0.197	0.283	0.035	0.239
40	0.262	0.262	0.455	0.091	0.326
60	0.279	0.293	0.520	0.111	0.364
80	0.290	0.337	0.525	0.101	0.384
100	0.302	0.370	0.556	0.107	0.409
120	0.325	0.455	0.562	0.097	0.447
P_{app} (x 10⁻⁷)	1.893	2.986	3.844	0.978	

Table C.19: Basolateral-to-apical cumulative percentage transport of Rhodamine 123 in the presence of 0.00255% (w/v) *Hoodia gordonii* across excised pig jejunum tissue

Time (min)	Percentage transport: Chamber 1	Percentage transport: Chamber 2	Percentage transport: Chamber 3	Standard deviation	Mean percentage transport
0	0.000	0.000	0.000	0.000	0.000
20	0.211	0.225	0.227	0.007	0.221
40	0.242	0.273	0.258	0.013	0.258
60	0.317	0.296	0.279	0.015	0.297
80	0.341	0.321	0.298	0.018	0.320
100	0.360	0.347	0.307	0.023	0.338
120	0.399	0.373	0.331	0.028	0.367
$P_{app} (x 10^{-7})$	2.665	2.354	1.993	0.337	

Table C.20: Apical-to-basolateral cumulative percentage transport of Rhodamine 123 in the presence of 0.0255% (w/v) *Hoodia gordonii* across excised pig jejunum tissue

Time (min)	Percentage transport: Chamber 1	Percentage transport: Chamber 2	Percentage transport: Chamber 3	Standard deviation	Mean percentage transport
0	0.000	0.000	0.000	0.000	0.000
20	0.094	0.101	0.330	0.110	0.175
40	0.172	0.130	0.450	0.142	0.251
60	0.247	0.258	0.555	0.143	0.353
80	0.292	0.291	0.738	0.211	0.440
100	0.351	0.335	0.778	0.205	0.488
120	0.423	0.384	0.788	0.182	0.532
$P_{app} (x 10^{-7})$	3.182	2.979	5.932	1.650	

Table C.21: Basolateral-to-apical cumulative percentage transport of Rhodamine 123 in the presence of 0.0255% (w/v) *Hoodia gordonii* across excised pig jejunum tissue

Time (min)	Percentage transport: Chamber 1	Percentage transport: Chamber 2	Percentage transport: Chamber 3	Standard deviation	Mean percentage transport
0	0.000	0.000	0.000	0.000	0.000
20	0.210	0.101	0.097	0.052	0.136
40	0.230	0.138	0.128	0.046	0.166
60	0.294	0.179	0.135	0.067	0.203
80	0.301	0.224	0.167	0.055	0.231
100	0.345	0.244	0.253	0.046	0.281
120	0.348	0.275	0.274	0.035	0.299
P_{app} (x 10⁻⁷)	2.317	2.002	1.963	0.194	

Table C.22: Apical-to-basolateral cumulative percentage transport of Rhodamine 123 in the presence of 0.255% (w/v) *Hoodia gordonii* across excised pig jejunum tissue

Time (min)	Percentage transport: Chamber 1	Percentage transport: Chamber 2	Percentage transport: Chamber 3	Standard deviation	Mean percentage transport
0	0.000	0.000	0.000	0.000	0.000
20	0.273	0.669	0.599	0.173	0.514
40	0.469	0.711	0.654	0.103	0.611
60	0.650	0.728	0.787	0.056	0.721
80	0.874	0.743	0.799	0.054	0.805
100	0.983	0.749	0.803	0.100	0.845
120	1.006	0.804	0.866	0.085	0.892
P_{app} (x 10⁻⁷)	8.101	4.356	5.268	1.953	

Table C.23: Basolateral-to-apical cumulative percentage transport of Rhodamine 123 in the presence of 0.255% (w/v) *Hoodia gordonii* across excised pig jejunum tissue

Time (min)	Percentage transport: Chamber 1	Percentage transport: Chamber 2	Percentage transport: Chamber 3	Standard deviation	Mean percentage transport
0	0.000	0.000	0.000	0.000	0.000
20	0.120	0.106	0.396	0.133	0.207
40	0.125	0.133	0.418	0.136	0.225
60	0.141	0.120	0.435	0.144	0.232
80	0.169	0.126	0.437	0.138	0.244
100	0.178	0.153	0.442	0.130	0.258
120	0.180	0.188	0.451	0.126	0.273
P_{app} (x 10⁻⁷)	1.171	1.091	2.446	0.600	

Table C.24: Apical-to-basolateral cumulative percentage transport of Rhodamine 123 in the presence of 0.00188% (w/v) *Harpagophytum procumbens* across excised pig jejunum tissue

Time (min)	Percentage transport: Chamber 1	Percentage transport: Chamber 2	Percentage transport: Chamber 3	Standard deviation	Mean percentage transport
0	0.000	0.000	0.000	0.000	0.000
20	0.311	0.194	0.078	0.095	0.194
40	0.342	0.242	0.124	0.089	0.236
60	0.344	0.235	0.146	0.081	0.242
80	0.348	0.229	0.146	0.083	0.241
100	0.355	0.234	0.153	0.083	0.247
120	0.356	0.231	0.161	0.081	0.249
P_{app} (x 10⁻⁷)	1.944	1.270	1.096	0.448	

Table C.25: Basolateral-to-apical cumulative percentage transport of Rhodamine 123 in the presence of 0.00188% (w/v) *Harpagophytum procumbens* across excised pig jejunum tissue

Time (min)	Percentage transport: Chamber 1	Percentage transport: Chamber 2	Percentage transport: Chamber 3	Standard deviation	Mean percentage transport
0	0.000	0.000	0.000	0.000	0.000
20	0.224	0.255	0.356	0.057	0.278
40	0.277	0.316	0.390	0.047	0.328
60	0.320	0.364	0.391	0.029	0.358
80	0.440	0.434	0.412	0.012	0.429
100	0.541	0.526	0.474	0.029	0.514
120	0.588	0.605	0.600	0.007	0.598
$P_{app} (x 10^{-7})$	4.285	4.141	3.439	0.457	

Table C.26: Apical-to-basolateral cumulative percentage transport of Rhodamine 123 in the presence of 0.0188% (w/v) *Harpagophytum procumbens* across excised pig jejunum tissue

Time (min)	Percentage transport: Chamber 1	Percentage transport: Chamber 2	Percentage transport: Chamber 3	Standard deviation	Mean percentage transport
0	0.000	0.000	0.000	0.000	0.000
20	0.186	0.250	0.129	0.049	0.188
40	0.197	0.264	0.165	0.041	0.208
60	0.199	0.268	0.180	0.038	0.216
80	0.203	0.269	0.194	0.034	0.222
100	0.208	0.278	0.204	0.034	0.230
120	0.212	0.283	0.222	0.031	0.239
$P_{app} (x 10^{-7})$	1.148	1.522	1.412	0.192	

Table C.27: Basolateral-to-apical cumulative percentage transport of Rhodamine 123 in the presence of 0.0188% (w/v) *Harpagophytum procumbens* across excised pig jejunum tissue

Time (min)	Percentage transport: Chamber 1	Percentage transport: Chamber 2	Percentage transport: Chamber 3	Standard deviation	Mean percentage transport
0	0.000	0.000	0.000	0.000	0.000
20	0.443	0.258	0.234	0.093	0.312
40	0.522	0.334	0.285	0.102	0.380
60	0.549	0.342	0.312	0.105	0.401
80	0.605	0.421	0.425	0.086	0.484
100	0.654	0.459	0.504	0.083	0.539
120	0.679	0.538	0.609	0.058	0.609
P_{app} (x 10⁻⁷)	4.251	3.513	4.192	0.410	

Table C.28: Apical-to-basolateral cumulative percentage transport of Rhodamine 123 in the presence of 0.188% (w/v) *Harpagophytum procumbens* across excised pig jejunum tissue

Time (min)	Percentage transport: Chamber 1	Percentage transport: Chamber 2	Percentage transport: Chamber 3	Standard deviation	Mean percentage transport
0	0.000	0.000	0.000	0.000	0.000
20	0.062	0.077	0.033	0.019	0.057
40	0.085	0.088	0.042	0.021	0.072
60	0.106	0.099	0.055	0.023	0.087
80	0.125	0.104	0.098	0.012	0.109
100	0.127	0.125	0.121	0.002	0.125
120	0.142	0.130	0.133	0.005	0.135
P_{app} (x 10⁻⁷)	0.997	0.842	1.056	0.111	

Table C.29: Basolateral-to-apical cumulative percentage transport of Rhodamine 123 in the presence of 0.188% (w/v) *Harpagophytum procumbens* across excised pig jejunum tissue

Time (min)	Percentage transport: Chamber 1	Percentage transport: Chamber 2	Percentage transport: Chamber 3	Standard deviation	Mean percentage transport
0	0.000	0.000	0.000	0.000	0.000
20	0.324	0.365	0.349	0.017	0.346
40	0.364	0.448	0.423	0.035	0.412
60	0.452	0.465	0.479	0.011	0.465
80	0.503	0.474	0.516	0.017	0.498
100	0.533	0.546	0.577	0.019	0.552
120	0.623	0.647	0.657	0.014	0.642
P_{app} (x 10⁻⁷)	4.055	3.895	4.213	0.159	

Table C.30: Apical-to-basolateral cumulative percentage transport of Rhodamine 123 in the presence of 0.000755% (w/v) *Leonotis leonurus* across excised pig jejunum tissue

Time (min)	Percentage transport: Chamber 1	Percentage transport: Chamber 2	Percentage transport: Chamber 3	Standard deviation	Mean percentage transport
0	0.000	0.000	0.000	0.000	0.000
20	0.036	0.084	0.158	0.050	0.093
40	0.041	0.106	0.179	0.056	0.109
60	0.045	0.131	0.208	0.066	0.128
80	0.053	0.141	0.246	0.079	0.147
100	0.112	0.235	0.281	0.071	0.209
120	0.115	0.260	0.293	0.078	0.223
P_{app} (x 10⁻⁷)	0.849	1.866	1.996	0.628	

Table C.31: Basolateral-to-apical cumulative percentage transport of Rhodamine 123 in the presence of 0.000755% (w/v) *Leonotis leonurus* across excised pig jejunum tissue

Time (min)	Percentage transport: Chamber 1	Percentage transport: Chamber 2	Percentage transport: Chamber 3	Standard deviation	Mean percentage transport
0	0.000	0.000	0.000	0.000	0.000
20	0.222	0.277	0.293	0.031	0.264
40	0.254	0.321	0.302	0.028	0.292
60	0.293	0.327	0.325	0.016	0.315
80	0.432	0.372	0.358	0.032	0.387
100	0.444	0.377	0.388	0.030	0.403
120	0.530	0.428	0.415	0.052	0.458
P_{app} (x 10⁻⁷)	3.702	2.564	2.493	0.678	

Table C.32: Apical-to-basolateral cumulative percentage transport of Rhodamine 123 in the presence of 0.00755% (w/v) *Leonotis leonurus* across excised pig jejunum tissue

Time (min)	Percentage transport: Chamber 1	Percentage transport: Chamber 2	Percentage transport: Chamber 3	Standard deviation	Mean percentage transport
0	0.000	0.000	0.000	0.000	0.000
20	0.066	0.069	0.092	0.011	0.076
40	0.090	0.075	0.141	0.028	0.102
60	0.097	0.127	0.178	0.033	0.134
80	0.126	0.192	0.221	0.039	0.180
100	0.158	0.234	0.247	0.039	0.213
120	0.279	0.276	0.306	0.013	0.287
P_{app} (x 10⁻⁷)	1.765	2.135	2.187	0.300	

Table C.33: Basolateral-to-apical cumulative percentage transport of Rhodamine 123 in the presence of 0.00755% (w/v) *Leonotis leonurus* across excised pig jejunum tissue

Time (min)	Percentage transport: Chamber 1	Percentage transport: Chamber 2	Percentage transport: Chamber 3	Standard deviation	Mean percentage transport
0	0.000	0.000	0.000	0.000	0.000
20	0.126	0.139	0.151	0.010	0.139
40	0.217	0.174	0.211	0.019	0.201
60	0.256	0.198	0.315	0.048	0.256
80	0.293	0.215	0.380	0.068	0.296
100	0.301	0.220	0.472	0.105	0.331
120	0.316	0.258	0.529	0.116	0.368
$P_{app} (x 10^{-7})$	2.297	1.630	4.009	1.227	

Table C.34: Apical-to-basolateral cumulative percentage transport of Rhodamine 123 in the presence of 0.0755% (w/v) *Leonotis leonurus* across excised pig jejunum tissue

Time (min)	Percentage transport: Chamber 1	Percentage transport: Chamber 2	Percentage transport: Chamber 3	Standard deviation	Mean percentage transport
0	0.000	0.000	0.000	0.000	0.000
20	0.157	0.075	0.096	0.035	0.110
40	0.233	0.137	0.106	0.054	0.159
60	0.265	0.173	0.109	0.064	0.182
80	0.404	0.219	0.137	0.111	0.253
100	0.413	0.246	0.182	0.097	0.281
120	0.425	0.292	0.240	0.078	0.319
$P_{app} (x 10^{-7})$	3.272	2.173	1.543	0.875	

Table C.35: Basolateral-to-apical cumulative percentage transport of Rhodamine 123 in the presence of 0.0755% (w/v) *Leonotis leonurus* across excised pig jejunum tissue

Time (min)	Percentage transport: Chamber 1	Percentage transport: Chamber 2	Percentage transport: Chamber 3	Standard deviation	Mean percentage transport
0	0.000	0.000	0.000	0.000	0.000
20	0.682	0.724	0.630	0.038	0.679
40	0.718	0.758	0.669	0.036	0.715
60	0.732	0.759	0.683	0.032	0.725
80	0.738	0.763	0.707	0.023	0.736
100	0.745	0.764	0.720	0.018	0.743
120	0.758	0.768	0.733	0.014	0.753
P_{app} (x 10⁻⁷)	4.047	3.993	4.041	0.029	

ADDENDUM D

TRANS-EPITHELIAL ELECTRICAL RESISTANCE (TEER) READINGS

Table D.1: Apical-to-basolateral TEER measurements across excised pig jejunum tissue of the positive control (i.e. Rhodamine 123 and Verapamil)

	TEER (kΩ)			
Time (min)	Chamber 1	Chamber 2	Chamber 3	Average
0	15.60	15.90	15.60	15.70
120	14.20	14.60	14.10	14.30
Percentage change	91.03	91.82	90.38	91.08

Table D.2: Basolateral-to-apical TEER measurements across excised pig jejunum tissue of the positive control (i.e. Rhodamine 123 and Verapamil)

	TEER (kΩ)			
Time (min)	Chamber 1	Chamber 2	Chamber 3	Average
0	13.20	10.10	11.00	11.43
120	12.00	9.60	11.20	10.93
Percentage change	90.91	95.05	101.82	95.63

Table D.3: Apical-to-basolateral TEER measurements across excised pig jejunum tissue of the negative control (i.e. Rhodamine 123 alone)

	TEER (kΩ)			
Time (min)	Chamber 1	Chamber 2	Chamber 3	Average
0	12.00	12.00	13.70	12.57
120	12.60	10.80	11.70	11.70
Percentage change	105.00	90.00	85.40	93.10

Table D.4: Basolateral-to-apical TEER measurements across excised pig jejunum tissue of the negative control (i.e. Rhodamine 123 alone)

	TEER (kΩ)			
Time (min)	Chamber 1	Chamber 2	Chamber 3	Average
0	9.80	9.70	12.30	10.60
120	10.40	10.00	10.80	10.40
Percentage change	106.12	103.09	87.80	98.11

Table D.5: Apical-to-basolateral TEER measurements across excised pig jejunum tissue in the presence of 0.00396% (w/v) methylsulfonylmethane

	TEER (kΩ)			
Time (min)	Chamber 1	Chamber 2	Chamber 3	Average
0	14.00	13.70	12.00	13.23
120	12.50	11.70	10.80	11.67
Percentage change	89.29	85.40	90.00	88.16

Table D.6: Basolateral-to-apical TEER measurements across excised pig jejunum tissue in the presence of 0.00396% (w/v) methylsulfonylmethane

	TEER (kΩ)			
Time (min)	Chamber 1	Chamber 2	Chamber 3	Average
0	10.80	11.20	12.00	11.33
120	11.00	11.10	11.80	11.30
Percentage change	101.85	99.11	98.33	99.71

Table D.7: Apical-to-basolateral TEER measurements across excised pig jejunum tissue in the presence of 0.0396% (w/v) methylsulfonylmethane

Time (min)	TEER (k Ω)			
	Chamber 1	Chamber 2	Chamber 3	Average
0	12.40	11.60	10.00	11.33
120	11.00	11.00	10.40	10.80
Percentage change	88.71	94.83	104.00	95.29

Table D.8: Basolateral-to-apical TEER measurements across excised pig jejunum tissue in the presence of 0.0396% (w/v) methylsulfonylmethane

Time (min)	TEER (k Ω)			
	Chamber 1	Chamber 2	Chamber 3	Average
0	11.00	10.00	12.20	11.07
120	9.10	9.20	10.40	9.57
Percentage change	82.73	92.00	85.25	86.45

Table D.9: Apical-to-basolateral TEER measurements across excised pig jejunum tissue in the presence of 0.396% (w/v) methylsulfonylmethane

Time (min)	TEER (k Ω)			
	Chamber 1	Chamber 2	Chamber 3	Average
0	9.80	10.40	9.70	9.97
120	10.40	10.90	10.00	10.43
Percentage change	106.12	104.81	103.09	104.68

Table D.10: Basolateral-to-apical TEER measurements across excised pig jejunum tissue in the presence of 0.396% (w/v) methylsulfonylmethane

	TEER (kΩ)			
Time (min)	Chamber 1	Chamber 2	Chamber 3	Average
0	12.2	10.1	9.1	10.47
120	10	9	10	9.67
Percentage change	81.97	89.11	109.89	92.36

Table D.11: Apical-to-basolateral TEER measurements across excised pig jejunum tissue in the presence of 0.000264% (w/v) *Vitis vinifera* seed extract

	TEER (kΩ)			
Time (min)	Chamber 1	Chamber 2	Chamber 3	Average
0	12.00	11.00	10.10	11.03
120	7.00	6.00	8.00	7.00
Percentage change	58.33	54.55	79.21	63.44

Table D.12: Basolateral-to-apical TEER measurements across excised pig jejunum tissue in the presence of 0.000264% (w/v) *Vitis vinifera* seed extract

	TEER (kΩ)			
Time (min)	Chamber 1	Chamber 2	Chamber 3	Average
0	12.00	11.00	10.10	11.03
120	8.00	6.00	8.00	7.333
Percentage change	72.73	59.41	72.51	66.47

Table D.13: Apical-to-basolateral TEER measurements across excised pig jejunum tissue in the presence of 0.00264% (w/v) *Vitis vinifera* seed extract

Time (min)	TEER (kΩ)			
	Chamber 1	Chamber 2	Chamber 3	Average
0	10.10	11.00	12.20	11.10
120	8.00	7.00	10.00	8.33
Percentage change	79.21	63.64	81.97	75.08

Table D.14: Basolateral-to-apical TEER measurements across excised pig jejunum tissue in the presence of 0.00264% (w/v) *Vitis vinifera* seed extract

Time (min)	TEER (kΩ)			
	Chamber 1	Chamber 2	Chamber 3	Average
0	14.00	11.00	10.00	11.67
120	10.10	8.00	8.00	8.70
Percentage change	72.14	72.73	80.00	74.57

Table D.15: Apical-to-basolateral TEER measurements across excised pig jejunum tissue in the presence of 0.0264% (w/v) *Vitis vinifera* seed extract

Time (min)	TEER (kΩ)			
	Chamber 1	Chamber 2	Chamber 3	Average
0	12.20	11.00	10.00	11.07
120	8.00	7.40	6.00	7.13
Percentage change	65.57	67.27	60.00	64.46

Table D.16: Basolateral-to-apical TEER measurements across excised pig jejunum tissue in the presence of 0.0264% (w/v) *Vitis vinifera* seed extract

	TEER (k Ω)			
Time (min)	Chamber 1	Chamber 2	Chamber 3	Average
0	12.20	11.00	12.00	11.73
120	9.00	9.40	8.00	8.80
Percentage change	73.77	85.45	66.67	75.00

Table D.17: Apical-to-basolateral TEER measurements across excised pig jejunum tissue in the presence of 0.00255% (w/v) *Hoodia gordonii* extract

	TEER (k Ω)			
Time (min)	Chamber 1	Chamber 2	Chamber 3	Average
0	10.00	12.20	10.10	10.77
120	9.40	11.80	9.00	10.07
Percentage change	94.00	96.72	89.11	93.50

Table D.18: Basolateral-to-apical TEER measurements across excised pig jejunum tissue in the presence of 0.00255% (w/v) *Hoodia gordonii* extract

	TEER (k Ω)			
Time (min)	Chamber 1	Chamber 2	Chamber 3	Average
0	11.20	12.10	12.20	11.83
120	9.00	11.00	10.00	10.00
Percentage change	80.36	90.91	81.97	84.51

Table D.19: Apical-to-basolateral TEER measurements across excised pig jejunum tissue in the presence of 0.0255% (w/v) *Hoodia gordonii* extract

Time (min)	TEER (k Ω)			
	Chamber 1	Chamber 2	Chamber 3	Average
0	10.00	10.10	11.00	10.37
120	7.00	9.80	9.00	8.600
Percentage change	70.00	97.03	81.82	82.96

Table D.20: Basolateral-to-apical TEER measurements across excised pig jejunum tissue in the presence of 0.0255% (w/v) *Hoodia gordonii* extract

Time (min)	TEER (k Ω)			
	Chamber 1	Chamber 2	Chamber 3	Average
0	11.2	10	12.1	11.10
120	10.4	9.8	11.6	10.60
Percentage change	92.86	98.00	95.87	95.50

Table D.21: Apical-to-basolateral TEER measurements across excised pig jejunum tissue in the presence of 0.255% (w/v) *Hoodia gordonii* extract

Time (min)	TEER (k Ω)			
	Chamber 1	Chamber 2	Chamber 3	Average
0	11.1	12.2	12.4	11.90
120	6	7.1	9	7.37
Percentage change	54.05	58.20	72.58	61.90

Table D.22: Basolateral-to-apical TEER measurements across excised pig jejunum tissue in the presence of 0.255% (w/v) *Hoodia gordonii* extract

	TEER (k Ω)			
Time (min)	Chamber 1	Chamber 2	Chamber 3	Average
0	12.2	9.8	10.1	9.95
120	10	9.6	9	9.30
Percentage change	81.97	97.96	89.11	93.47

Table D.23: Apical-to-basolateral TEER measurements across excised pig jejunum tissue in the presence of 0.00188% (w/v) *Harpagophytum procumbens* extract

	TEER (k Ω)			
Time (min)	Chamber 1	Chamber 2	Chamber 3	Average
0	12.1	13	11.1	12.07
120	11	12	11	11.33
Percentage change	90.91	92.31	99.10	93.92

Table D.24: Basolateral-to-apical TEER measurements across excised pig jejunum tissue in the presence of 0.00188% (w/v) *Harpagophytum procumbens* extract

	TEER (k Ω)			
Time (min)	Chamber 1	Chamber 2	Chamber 3	Average
0	10.00	9.60	11.00	10.20
120	10.10	9.40	11.20	10.20
Percentage change	101.00	97.92	101.82	100.33

Table D.25: Apical-to-basolateral TEER measurements across excised pig jejunum tissue in the presence of 0.0188% (w/v) *Harpagophytum procumbens* extract

Time (min)	TEER (k Ω)			
	Chamber 1	Chamber 2	Chamber 3	Average
0	11.00	10.00	10.10	10.37
120	10.80	9.40	9.60	9.93
Percentage change	98.18	94.00	95.05	95.82

Table D.26: Basolateral-to-apical TEER measurements across excised pig jejunum tissue in the presence of 0.0188% (w/v) *Harpagophytum procumbens* extract

Time (min)	TEER (k Ω)			
	Chamber 1	Chamber 2	Chamber 3	Average
0	11.60	12.10	12.40	12.03
120	11.40	12.00	12.10	11.83
Percentage change	98.28	99.17	97.58	98.34

Table D.27: Apical-to-basolateral TEER measurements across excised pig jejunum tissue in the presence of 0.188% (w/v) *Harpagophytum procumbens* extract

Time (min)	TEER (k Ω)			
	Chamber 1	Chamber 2	Chamber 3	Average
0	10.00	12.00	11.00	11.00
120	9.80	11.60	11.10	10.83
Percentage change	98.00	96.67	100.91	98.48

Table D.28: Basolateral-to-apical TEER measurements across excised pig jejunum tissue in the presence of 0.188% (w/v) *Harpagophytum procumbens* extract

Time (min)	TEER (kΩ)			
	Chamber 1	Chamber 2	Chamber 3	Average
0	12.10	11.60	10.00	11.23
120	12.00	11.50	10.10	11.20
Percentage change	99.17	99.14	101.00	99.70

Table D.29: Apical-to-basolateral TEER measurements across excised pig jejunum tissue in the presence of 0.000755% (w/v) *Leonotis leonurus* extract

Time (min)	TEER (kΩ)			
	Chamber 1	Chamber 2	Chamber 3	Average
0	10.10	9.60	9.70	9.80
120	10.00	9.80	9.60	9.80
Percentage change	99.01	102.08	98.97	100.00

Table D.30: Basolateral-to-apical TEER measurements across excised pig jejunum tissue in the presence of 0.000755% (w/v) *Leonotis leonurus* extract

Time (min)	TEER (kΩ)			
	Chamber 1	Chamber 2	Chamber 3	Average
0	9.40	11.20	12.20	10.93
120	9.00	10.00	11.00	10.00
Percentage change	95.74	89.29	90.16	91.46

Table D.31: Apical-to-basolateral TEER measurements across excised pig jejunum tissue in the presence of 0.00755% (w/v) *Leonotis leonurus* extract

Time (min)	TEER (kΩ)			
	Chamber 1	Chamber 2	Chamber 3	Average
0	12.20	10.20	11.40	11.27
120	12.10	10.00	11.30	11.13
Percentage change	99.18	98.04	99.12	98.82

Table D.32: Basolateral-to-apical TEER measurements across excised pig jejunum tissue in the presence of 0.00755% (w/v) *Leonotis leonurus* extract

Time (min)	TEER (kΩ)			
	Chamber 1	Chamber 2	Chamber 3	Average
0	12.20	9.40	10.40	10.67
120	10.00	8.00	9.00	9.00
Percentage change	81.97	85.11	86.54	84.38

Table D.33: Apical-to-basolateral TEER measurements across excised pig jejunum tissue in the presence of 0.0755% (w/v) *Leonotis leonurus* extract

Time (min)	TEER (kΩ)			
	Chamber 1	Chamber 2	Chamber 3	Average
0	9.60	11.20	12.10	10.97
120	9.60	11.10	12.00	10.90
Percentage change	100.00	99.11	99.17	99.39

Table D.34: Basolateral-to-apical TEER measurements across excised pig jejunum tissue in the presence of 0.0755% (w/v) *Leonotis leonurus* extract

Time (min)	TEER (k Ω)			
	Chamber 1	Chamber 2	Chamber 3	Average
0	11.40	12.00	11.60	11.67
120	10.00	9.00	9.20	9.40
Percentage change	87.72	75.00	79.31	80.57

ADDENDUM E

EFFLUX RATIOS

Table E.1: Apparent permeability (P_{app}) values and efflux ratios (ER) for methylsulfonylmethane at selected test concentrations

Concentration (%w/v)	Transport direction	P_{app} ($\times 10^{-7}$)	Average P_{app} ($\times 10^{-7}$)	Efflux ratio
0.00396%	Apical-to-basolateral	1.172	1.355	2.938
		1.939		
		0.954		
	Basolateral-to-apical	3.281	3.980	
		5.564		
		3.094		
0.0396%	Apical-to-basolateral	0.940	0.900	6.221
		0.513		
		1.215		
	Basolateral-to-apical	5.700	5.534	
		4.248		
		6.653		
0.396%	Apical-to-basolateral	0.428	0.467	21.221
		0.334		
		0.638		
	Basolateral-to-apical	10.733	9.902	
		7.216		
		11.757		

Table E.2: Apparent permeability (P_{app}) values and efflux ratios (ER) for *Vitis vinifera* seed extract at selected test concentrations

Concentration (%w/v)	Transport direction	P_{app} ($\times 10^{-7}$)	Average P_{app} ($\times 10^{-7}$)	Efflux ratio
0.000264%	Apical-to-basolateral	2.845	3.316	0.958
		3.711		
		3.391		
	Basolateral-to-apical	3.791	3.5167	
		3.159		
		3.598		
0.00264%	Apical-to-basolateral	9.222	10.930	0.446
		11.822		
		11.747		
	Basolateral-to-apical	4.282	4.872	
		6.008		
		4.325		
0.0264%	Apical-to-basolateral	14.982	16.624	0.453
		21.127		
		13.763		
	Basolateral-to-apical	7.698	7.532	
		7.682		
		7.215		

Table E.3: Apparent permeability (P_{app}) values and efflux ratios (ER) for *Hoodia gordonii* at selected test concentrations

Concentration (%w/v)	Transport direction	P_{app} ($\times 10^{-7}$)	Average P_{app} ($\times 10^{-7}$)	Efflux ratio
0.00255%	Apical-to-basolateral	1.893	2.908	0.804
		2.986		
		3.844		
	Basolateral-to-apical	2.665	2.337	
		2.354		
		1.993		
0.0255%	Apical-to-basolateral	3.182	4.031	0.519
		2.979		
		5.932		
	Basolateral-to-apical	2.317	2.094	
		2.002		
		1.963		
0.255%	Apical-to-basolateral	8.101	5.909	0.266
		4.356		
		5.268		
	Basolateral-to-apical	1.171	1.569	
		1.091		
		2.446		

Table E.4: Apparent permeability (P_{app}) values and efflux ratios (ER) for *Harpagophytum procumbens* at selected test concentrations

Concentration (%w/v)	Transport direction	P_{app} ($\times 10^{-7}$)	Average P_{app} ($\times 10^{-7}$)	Efflux ratio
0.00188%	Apical-to-basolateral	1.096	1.437	2.753
		1.944		
		1.270		
	Basolateral-to-apical	4.285	3.955	
		4.141		
		3.439		
0.0188%	Apical-to-basolateral	1.148	1.360	2.929
		1.522		
		1.412		
	Basolateral-to-apical	4.251	3.986	
		3.513		
		4.193		
0.188%	Apical-to-basolateral	0.997	0.965	4.202
		0.842		
		1.056		
	Basolateral-to-apical	4.055	4.055	
		3.895		
		4.213		

Table E.5: Apparent permeability (P_{app}) values and efflux ratios (ER) for *Leonotis leonurus* at selected test concentrations

Concentration (%w/v)	Transport direction	P_{app} ($\times 10^{-7}$)	Average P_{app} ($\times 10^{-7}$)	Efflux ratio
0.000755%	Apical-to-basolateral	0.849	1.570	1.859
		1.866		
		1.996		
	Basolateral-to-apical	3.702	2.919	
		2.564		
		2.493		
0.00755%	Apical-to-basolateral	1.765	2.029	1.304
		2.135		
		2.187		
	Basolateral-to-apical	2.297	2.645	
		1.630		
		4.009		
0.0755%	Apical-to-basolateral	3.272	2.329	1.729
		2.173		
		1.543		
	Basolateral-to-apical	4.047	4.027	
		3.993		
		4.041		

ADDENDUM F

STATISTICAL ANALYSIS

Table F.1 Tukey HSD post hoc multiple comparison of apical-to-basolateral transport of Rhodamine 123 in in the presence of selected herbal extracts and supplements (Marked differences are significant at $p < 0.05000$)

Experiment	Tukey HSD test											
	{1}	{2}	{3}	{4}	{5}	{6}	{7}	{8}	{9}	{10}	{11}	{12}
NC5AB {1}		0.999999	0.698701	0.999997	0.999995	0.999976	0.997737	0.524517	0.954191	0.000152	1.000000	1.000000
NC5BA {2}	0.999999		0.999853	0.854895	0.837622	1.000000	0.518262	0.997909	0.244683	0.000173	1.000000	1.000000
PC5AB {3}	0.698701	0.999853		0.060999	0.055628	0.999988	0.013702	1.000000	0.003413	0.007240	0.983435	0.975953
PC5BA {4}	0.999997	0.854895	0.060999		1.000000	0.756079	1.000000	0.030786	1.000000	0.000152	0.988554	0.992591
MSM0.00396AB {5}	0.999995	0.837622	0.055628	1.000000		0.734103	1.000000	0.027876	1.000000	0.000152	0.985588	0.990486
MSM0.00396BA {6}	0.999976	1.000000	0.999988	0.756079	0.734103		0.397209	0.999658	0.168266	0.000200	1.000000	1.000000
MSM0.0396AB {7}	0.997737	0.518262	0.013702	1.000000	1.000000	0.397209		0.006360	1.000000	0.000152	0.853309	0.881366
MSM0.0396BA {8}	0.524517	0.997909	1.000000	0.030786	0.027876	0.999658	0.006360		0.001540	0.015525	0.937179	0.918112
MSM0.396AB {9}	0.954191	0.244683	0.003413	1.000000	1.000000	0.168266	1.000000	0.001540		0.000152	0.572015	0.615597
MSM0.396BA {10}	0.000152	0.000173	0.007240	0.000152	0.000152	0.000200	0.000152	0.015525	0.000152		0.000154	0.000154
GSE0.000264AB{11}	1.000000	1.000000	0.983435	0.988554	0.985588	1.000000	0.853309	0.937179	0.572015	0.000154		1.000000
GSE0.000264BA{12}	1.000000	1.000000	0.975953	0.992591	0.990486	1.000000	0.881366	0.918112	0.615597	0.000154	1.000000	
GSE0.00264AB {13}	0.000152	0.000152	0.000305	0.000152	0.000152	0.000152	0.000152	0.000547	0.000152	1.000000	0.000152	0.000152
GSE0.00264BA {14}	0.926985	1.000000	1.000000	0.180123	0.166901	1.000000	0.049749	1.000000	0.013821	0.001737	0.999650	0.999317
GSE0.0264AB {15}	0.000152	0.000152	0.000152	0.000152	0.000152	0.000152	0.000152	0.000152	0.000152	0.000153	0.000152	0.000152
GSE0.0264BA {16}	0.002593	0.101098	0.932226	0.000169	0.000166	0.153744	0.000154	0.981567	0.000152	0.880110	0.024916	0.020822
HG0.00255AB {17}	1.000000	1.000000	0.871230	0.999774	0.999662	1.000000	0.979013	0.733438	0.845552	0.000152	1.000000	1.000000
HG0.00255BA {18}	1.000000	0.999876	0.489762	1.000000	1.000000	0.999069	0.999912	0.328401	0.992512	0.000152	1.000000	1.000000
HG0.0255AB {19}	0.999949	1.000000	0.999995	0.721708	0.698710	1.000000	0.363138	0.999818	0.149132	0.000211	1.000000	1.000000
HG0.0255BA {20}	1.000000	0.998028	0.324186	1.000000	1.000000	0.991601	0.999998	0.199063	0.999212	0.000152	0.999998	0.999999
HG0.255AB {21}	0.274825	0.966264	1.000000	0.009524	0.008555	0.988479	0.001804	1.000000	0.000484	0.048162	0.755482	0.716106
HG0.255BA {22}	1.000000	0.929990	0.099273	1.000000	1.000000	0.861160	1.000000	0.052307	1.000000	0.000152	0.997385	0.998511
HP0.00188AB {23}	0.999999	0.878440	0.069779	1.000000	1.000000	0.787152	1.000000	0.035612	1.000000	0.000152	0.992027	0.994996

HP0.00188BA {24}	0.999984	1.000000	0.999982	0.772158	0.750755	1.000000	0.414299	0.999542	0.178235	0.000196	1.000000	1.000000
HP0.0188AB {25}	0.999995	0.840718	0.056536	1.000000	1.000000	0.737998	1.000000	0.028366	1.000000	0.000152	0.986146	0.990885
HP0.0188BA {26}	0.999974	1.000000	0.999989	0.752304	0.730203	1.000000	0.393310	0.999681	0.166027	0.000201	1.000000	1.000000
HP0.188AB {27}	0.998927	0.574435	0.017383	1.000000	1.000000	0.449775	1.000000	0.008148	1.000000	0.000152	0.888840	0.912369
HP0.188BA {28}	0.999928	1.000000	0.999997	0.705421	0.682029	1.000000	0.348038	0.999866	0.140941	0.000217	1.000000	1.000000
LL0.000755AB {29}	1.000000	0.930271	0.099499	1.000000	1.000000	0.861594	1.000000	0.052437	1.000000	0.000152	0.997406	0.998524
LL0.000755BA {30}	0.999824	1.000000	0.999999	0.657739	0.633516	1.000000	0.306931	0.999947	0.119638	0.000237	1.000000	1.000000
LL0.00755AB {31}	1.000000	0.996404	0.285674	1.000000	1.000000	0.986542	1.000000	0.171626	0.999622	0.000152	0.999993	0.999997
LL0.00755BA {32}	0.999911	1.000000	0.999997	0.694697	0.671079	1.000000	0.338424	0.999891	0.135824	0.000221	1.000000	1.000000
LL0.0755AB {33}	1.000000	0.999862	0.483832	1.000000	1.000000	0.998986	0.999922	0.323424	0.992970	0.000152	1.000000	1.000000
LL0.0755BA {34}	0.999961	1.000000	0.999993	0.734894	0.712256	1.000000	0.375838	0.999768	0.156153	0.000207	1.000000	1.000000

Table F.1 continued

Experiment	Tukey HSD test											
	{13}	{14}	{15}	{16}	{17}	{18}	{19}	{20}	{21}	{22}	{23}	{24}
NC5AB {1}	0.00015	0.92698	0.00015	0.00259	1.00000	1.00000	0.99994	1.00000	0.27482	1.00000	0.99999	0.99998
NC5BA {2}	0.00015	1.00000	0.00015	0.10109	1.00000	0.99987	1.00000	0.99802	0.96626	0.92999	0.87844	1.00000
PC5AB {3}	0.00030	1.00000	0.00015	0.93222	0.87123	0.48976	0.99999	0.32418	1.00000	0.09927	0.06977	0.99998
PC5BA {4}	0.00015	0.18012	0.00015	0.00016	0.99977	1.00000	0.72170	1.00000	0.00952	1.00000	1.00000	0.77215
MSM0.00396A	0.00015	0.16690	0.00015	0.00016	0.99966	1.00000	0.69871	1.00000	0.00855	1.00000	1.00000	0.75075
MSM0.00396B	0.00015	1.00000	0.00015	0.15374	1.00000	0.99906	1.00000	0.99160	0.98847	0.86116	0.78715	1.00000

MSM0.0396AB {7}	0.00015	0.04974	0.00015	0.00015	0.97901	0.99991	0.36313	0.99999	0.00180	1.00000	1.00000	0.41429
MSM0.0396BA {8}	0.00054	1.00000	0.00015	0.98156	0.73343	0.32840	0.99981	0.19906	1.00000	0.05230	0.03561	0.99954
MSM0.396AB {9}	0.00015	0.01382	0.00015	0.00015	0.84555	0.99251	0.14913	0.99921	0.00048	1.00000	1.00000	0.17823
MSM0.396BA {10}	1.00000	0.00173	0.00015	0.88011	0.00015	0.00015	0.00021	0.00015	0.04816	0.00015	0.00015	0.00019
GSE0.000264AB{11	0.00015	0.99965	0.00015	0.02491	1.00000	1.00000	1.00000	0.99999	0.75548	0.99738	0.99202	1.00000
GSE0.000264BA{12	0.00015	0.99931	0.00015	0.02082	1.00000	1.00000	1.00000	0.99999	0.71610	0.99851	0.99499	1.00000
GSE0.00264AB		0.00017	0.00027	0.21776	0.00015	0.00015	0.00015	0.00015	0.00178	0.00015	0.00015	0.00015
GSE0.00264BA	0.00017		0.00015	0.71012	0.98528	0.79265	1.00000	0.62532	1.00000	0.26688	0.20120	1.00000
GSE0.0264AB {15}	0.00027	0.00015		0.00015	0.00015	0.00015	0.00015	0.00015	0.00015	0.00015	0.00015	0.00015
GSE0.0264BA {16}	0.21776	0.71012	0.00015		0.00679	0.00102	0.17332	0.00048	0.99924	0.00019	0.00017	0.14485
HG0.00255AB {17}	0.00015	0.98528	0.00015	0.00679		1.00000	1.00000	1.00000	0.45979	0.99998	0.99988	1.00000
HG0.00255BA {18}	0.00015	0.79265	0.00015	0.00102	1.00000		0.99842	1.00000	0.14674	1.00000	1.00000	0.99929
HG0.0255AB {19}	0.00015	1.00000	0.00015	0.17332	1.00000	0.99842		0.98778	0.99211	0.83455	0.75454	1.00000
HG0.0255BA {20}	0.00015	0.62532	0.00015	0.00048	1.00000	1.00000	0.98778		0.07901	1.00000	1.00000	0.99306
HG0.255AB {21}	0.00178	1.00000	0.00015	0.99924	0.45979	0.14674	0.99211	0.07901		0.01701	0.01116	0.98628
HG0.255BA {22}	0.00015	0.26688	0.00015	0.00019	0.99998	1.00000	0.83455	1.00000	0.01701		1.00000	0.87315
HP0.00188AB {23}	0.00015	0.20120	0.00015	0.00017	0.99988	1.00000	0.75454	1.00000	0.01116	1.00000		0.80226
HP0.00188BA {24}	0.00015	1.00000	0.00015	0.14485	1.00000	0.99929	1.00000	0.99306	0.98628	0.87315	0.80226	
HP0.0188AB {25}	0.00015	0.16915	0.00015	0.00016	0.99968	1.00000	0.70277	1.00000	0.00871	1.00000	1.00000	0.75455
HP0.0188BA {26}	0.00015	1.00000	0.00015	0.15585	1.00000	0.99901	1.00000	0.99122	0.98894	0.85830	0.78359	1.00000
HP0.188AB {27}	0.00015	0.06148	0.00015	0.00015	0.98728	0.99997	0.41375	1.00000	0.00232	1.00000	1.00000	0.46788
HP0.188BA {28}	0.00015	1.00000	0.00015	0.18291	0.99999	0.99802	1.00000	0.98562	0.99343	0.82151	0.73895	1.00000
LL0.000755AB {29}	0.00015	0.26736	0.00015	0.00019	0.99998	1.00000	0.83503	1.00000	0.01705	1.00000	1.00000	0.87356
LL0.000755BA {30}	0.00015	1.00000	0.00015	0.21237	0.99999	0.99633	1.00000	0.97778	0.99622	0.78180	0.69288	1.00000
LL0.00755AB {31}	0.00015	0.57686	0.00015	0.00040	1.00000	1.00000	0.98104	1.00000	0.06623	1.00000	1.00000	0.98870
LL0.00755BA {32}	0.00015	1.00000	0.00015	0.18934	0.99999	0.99771	1.00000	0.98406	0.99419	0.81277	0.72865	1.00000

LL0.0755AB {33}	0.00015	0.78768	0.00015	0.00099	1.00000	1.00000	0.99829	1.00000	0.14390	1.00000	1.00000	0.99922
LL0.0755BA {34}	0.00015	1.00000	0.00015	0.16571	1.00000	0.99869	1.00000	0.98936	0.99086	0.84491	0.76709	1.00000

Table F.1 continued

Experiment	Tukey HSD test									
	{25}	{26}	{27}	{28}	{29}	{30}	{31}	{32}	{33}	{34}
NC5AB {1}	0.999995	0.999974	0.998927	0.999928	1.000000	0.999824	1.000000	0.999911	1.000000	0.999961
NC5BA {2}	0.840718	1.000000	0.574435	1.000000	0.930271	1.000000	0.996404	1.000000	0.999862	1.000000
PC5AB {3}	0.056536	0.999989	0.017383	0.999997	0.099499	0.999999	0.285674	0.999997	0.483832	0.999993
PC5BA {4}	1.000000	0.752304	1.000000	0.705421	1.000000	0.657739	1.000000	0.694697	1.000000	0.734894
MSM0.00396AB {5}	1.000000	0.730203	1.000000	0.682029	1.000000	0.633516	1.000000	0.671079	1.000000	0.712256
MSM0.00396BA {6}	0.737998	1.000000	0.449775	1.000000	0.861594	1.000000	0.986542	1.000000	0.998986	1.000000
MSM0.0396AB {7}	1.000000	0.393310	1.000000	0.348038	1.000000	0.306931	1.000000	0.338424	0.999922	0.375838
MSM0.0396BA {8}	0.028366	0.999681	0.008148	0.999866	0.052437	0.999947	0.171626	0.999891	0.323424	0.999768
MSM0.396AB {9}	1.000000	0.166027	1.000000	0.140941	1.000000	0.119638	0.999622	0.135824	0.992970	0.156153
MSM0.396BA {10}	0.000152	0.000201	0.000152	0.000217	0.000152	0.000237	0.000152	0.000221	0.000152	0.000207
GSE0.000264AB{11}	0.986146	1.000000	0.888840	1.000000	0.997406	1.000000	0.999993	1.000000	1.000000	1.000000
GSE0.000264BA{12}	0.990885	1.000000	0.912369	1.000000	0.998524	1.000000	0.999997	1.000000	1.000000	1.000000
GSE0.00264AB {13}	0.000152	0.000152	0.000152	0.000152	0.000152	0.000153	0.000152	0.000153	0.000152	0.000152
GSE0.00264BA {14}	0.169158	1.000000	0.061480	1.000000	0.267363	1.000000	0.576866	1.000000	0.787681	1.000000
GSE0.0264AB {15}	0.000152	0.000152	0.000152	0.000152	0.000152	0.000152	0.000152	0.000152	0.000152	0.000152
GSE0.0264BA {16}	0.000167	0.155854	0.000154	0.182916	0.000193	0.212378	0.000409	0.189346	0.000996	0.165714
HG0.00255AB {17}	0.999685	1.000000	0.987284	0.999999	0.999983	0.999998	1.000000	0.999999	1.000000	1.000000
HG0.00255BA {18}	1.000000	0.999011	0.999971	0.998020	1.000000	0.996339	1.000000	0.997715	1.000000	0.998698
HG0.0255AB {19}	0.702772	1.000000	0.413757	1.000000	0.835036	1.000000	0.981046	1.000000	0.998292	1.000000

HG0.0255BA {20}	1.000000	0.991225	1.000000	0.985622	1.000000	0.977785	1.000000	0.984067	1.000000	0.989361
HG0.255AB {21}	0.008717	0.988945	0.002323	0.993432	0.017058	0.996225	0.066233	0.994191	0.143900	0.990869
HG0.255BA {22}	1.000000	0.858302	1.000000	0.821519	1.000000	0.781804	1.000000	0.812776	1.000000	0.844911
HP0.00188AB {23}	1.000000	0.783590	1.000000	0.738958	1.000000	0.692887	1.000000	0.728654	1.000000	0.767099
HP0.00188BA {24}	0.754554	1.000000	0.467888	1.000000	0.873569	1.000000	0.988709	1.000000	0.999227	1.000000
HP0.0188AB {25}		0.734119	1.000000	0.686155	1.000000	0.637773	1.000000	0.675242	1.000000	0.716261
HP0.0188BA {26}	0.734119		0.445673	1.000000	0.858741	1.000000	0.985999	1.000000	0.998923	1.000000
HP0.188AB {27}	1.000000	0.445673		0.397661	1.000000	0.353596	1.000000	0.387367	0.999974	0.427230
HP0.188BA {28}	0.686155	1.000000	0.397661		0.822016	1.000000	0.978005	1.000000	0.997862	1.000000
LL0.000755AB {29}	1.000000	0.858741	1.000000	0.822016		0.782352	1.000000	0.813285	1.000000	0.845372
LL0.000755BA {30}	0.637773	1.000000	0.353596	1.000000	0.782352		0.967312	1.000000	0.996073	1.000000
LL0.00755AB {31}	1.000000	0.985999	1.000000	0.978005	1.000000	0.967312		0.975839	1.000000	0.983310
LL0.00755BA {32}	0.675242	1.000000	0.387367	1.000000	0.813285	1.000000	0.975839		0.997522	1.000000
LL0.0755AB {33}	1.000000	0.998923	0.999974	0.997862	1.000000	0.996073	1.000000	0.997522		0.998588
LL0.0755BA {34}	0.716261	1.000000	0.427230	1.000000	0.845372	1.000000	0.983310	1.000000	0.998588	

Table F.2 Analysis test of variance for Rhodamine 123 across excised pig jejunum tissue

Analysis of variance								
Marked effects are significant at $p < 0.05000$								
Variabl e	SS effect	df effec	MS effect	SS error	df erro	MS error	F	P
P_{app}	0.00000 0	33	0.00000 0	0.00000 0	68	0.00000 0	21.2921 9	0.00000 0

Table F.3 Brown-Forsythe Test of Homogeneity of Variances for Rhodamine 123 across excised pig jejunum tissue

Brown-Forsythe Test of Homogeneity of Variances								
Marked effects are significant at $p < 0.05000$								
Variabl e	SS effect	df effec	MS effect	SS error	df erro	MS error	F	P
P_{app}	0.00000 0	33	0.00000 0	0.00000 0	68	0.00000 0	0.92600 3	0.58666 6

Table F.4 The 2-Way Tables of Descriptive Statistics for Rhodamine 123 across excised pig jejunum tissue

Experiment	2-Way Tables of Descriptive Statistics (N=102)		
	P _{app} Means	P _{app} N	P _{app} Std. Dev.
NC5AB	0.000000262	3	0.000000119
NC5BA	0.000000381	3	0.000000122
PC5AB	0.000000530	3	0.000000141
PC5BA	0.000000139	3	0.000000033
MSM0.00396AB	0.000000135	3	0.000000052
MSM0.00396BA	0.000000398	3	0.000000138
MSM0.0396AB	0.000000089	3	0.000000035
MSM0.0396BA	0.000000553	3	0.000000121
MSM0.396AB	0.000000047	3	0.000000016
MSM0.396BA	0.000000990	3	0.000000238
GSE0.000264AB	0.000000332	3	0.000000044
GSE0.000264BA	0.000000326	3	0.000000045
GSE0.00264AB	0.000001093	3	0.000000148
GSE0.00264BA	0.000000487	3	0.000000098
GSE0.0264AB	0.000001662	3	0.000000395
GSE0.0264BA	0.000000753	3	0.000000027
HG0.00255AB	0.000000291	3	0.000000098
HG0.00255BA	0.000000234	3	0.000000034
HG0.0255AB	0.000000403	3	0.000000165
HG0.0255BA	0.000000209	3	0.000000019
HG0.255AB	0.000000591	3	0.000000195
HG0.255BA	0.000000157	3	0.000000076
HP0.00188AB	0.000000144	3	0.000000045
HP0.00188BA	0.000000395	3	0.000000045
HP0.0188AB	0.000000136	3	0.000000019
HP0.0188BA	0.000000399	3	0.000000041
HP0.188AB	0.000000096	3	0.000000011
HP0.188BA	0.000000405	3	0.000000016
LL0.000755AB	0.000000157	3	0.000000063
LL0.000755BA	0.000000412	3	0.000000173
LL0.00755AB	0.000000203	3	0.000000023
LL0.00755BA	0.000000407	3	0.000000205
LL0.0755AB	0.000000233	3	0.000000088

LL0.0755BA	0.000000401	3	0.000000003
All Groups	0.000000396	102	0.000000338